VIRTUÁLNÍ XXVIII. 2020
VÝROČNÍ SJEZD ČESKÉ KARDIOLOGICKÉ SPOLEČNOSTI

TO NEJLEPŠÍ Z **ČESKÉ KARDIOLOGIE**
ZA ROK 2019

ČESKÁ KARDIOLOGICKÁ SPOLEČNOST

Nejlepší původní české práce publikované v roce 2019

Tato sekce prezentuje každoročně na výročním sjezdu ČKS **nejlepší původní vědecké práce členů ČKS**, vzniklé na pracovištích v ČR a publikované v předchozím kalendářním roce v mezinárodních časopisech s impakt faktorem >2,0. Tři nejlepší jsou rovněž **oceněny výborem ČKS**. Práce jsou řazeny dle IF.

Podmínky:

- Práce musí být publikována v časopise s impakt faktorem > 2,0 v průběhu posledního kalendářního roku před sjezdem ČKS, na který je přihlášena
- Práce musí vzniknout na pracovišti v České republice
- Prvním autorem musí být člen ČKS
- Musí jít o původní práci, prezentující vlastní výzkumné výsledky (nemůže se jednat o přehledný článek, editorial, abstrakt ani o kasuistiku)
- Nemůže se jednat ani o práci vzniklou v zahraničí (např. při studijním pobytu českého lékaře)
- Současně s přihlášením práce je autor povinen zaslat do sekretariátu ČKS e–mailem PDF verzi originálního článku s přihlášenou prací. Bez tohoto textu „in extenso" nemůže být práce přijata.

Short- and long-term outcomes of alcohol septal ablation for hypertrophic obstructive cardiomyopathy in patients with mild left ventricular hypertrophy: a propensity score matching analysis
J. Veselka a kol.

Non-invasive electromechanical cell-based biosensors for improved investigation of 3D cardiac models
G. Caluori a kol.

Continual measurement of arterial dP/dtmax enables minimally invasive monitoring of left ventricular contractility in patients with acute heart failure
P. Ošťádal a kol.

New Imaging Markers of Clinical Outcome in Asymptomatic Patients with Severe Aortic Regurgitation.
R. Kočková a kol.

The Role of GDF-15 in Heart Failure Patients With Chronic Kidney Disease
J. Beneš a kol.

Alcohol septal ablation in patients with severe hypertrophy
J. Veselka a kol.

Independent effect of atrial fibrillation on natriuretic peptide release.
M. Šramko a kol.

Cardiovascular progenitor cells and tissue plasticity are reduced in a myocardium affected by Becker muscular dystrophy
M. Pešl a kol.

Combination of left ventricular reverse remodeling and brain natriuretic peptide level at one year after cardiac resynchronization therapy predicts long-term clinical outcome
T. Roubíček a kol.

Prognostic Value of MicroRNAs in Patients after Myocardial
M. Hromádka a kol.

Outcome of patients ≥ 60 years of age after alcohol septal ablation for hypertrophic obstructive cardiomyopathy
D. Jindrová a kol.

High-Grade Patent foramen Ovale Is a Risk Factor for Unprovoked Decompression Sickness in Recreational Divers
J. Honěk a kol.

J. Veselka a kol.

Short- and long-term outcomes of alcohol septal ablation for hypertrophic obstructive cardiomyopathy in patients with mild left ventricular hypertrophy: a propensity score matching analysis *(id 20)*

European Heart Journal
Impact Factor: 23,239

rejstřík

ESC European Society of Cardiology

European Heart Journal (2019) **40**, 1681–1687
doi:10.1093/eurheartj/ehz110

CLINICAL RESEARCH
Heart failure/cardiomyopathy

Short- and long-term outcomes of alcohol septal ablation for hypertrophic obstructive cardiomyopathy in patients with mild left ventricular hypertrophy: a propensity score matching analysis

Josef Veselka[1]*, Lothar Faber[2], Max Liebregts[3], Robert Cooper[4], Jaroslav Januska[5], Maksim Kashtanov[6], Maciej Dabrowski[7], Peter Riis Hansen[8], Hubert Seggewiss[2,9], Eva Hansvenclova[1], Henning Bundgaard[10], Jurriën ten Berg[3], Rodney Hilton Stables[4], and Morten Kvistholm Jensen[10]

[1]Department of Cardiology, Second Medical School, Charles University, University Hospital Motol, V Úvalu 84, Prague 15000, Czech Republic; [2]Department of Cardiology, Heart and Diabetes Centre NRW, Ruhr -University Bochum, Georgstraße 11, 32545 Bad Oeynhausen, Germany; [3]Department of Cardiology, St. Antonius Hospital, Koekoekslaan 1, 3435 CM Nieuwegein, the Netherlands; [4]Institute of Cardiovascular Medicine and Science, Liverpool Heart and Chest Hospital, Thomas Dr, Liverpool L14 3PE, England; [5]Cardiocentre Podlesí, Konská 453, 739 61, Třinec, Czech Republic; [6]Sverdlovsk Regional Hospital N1, 185 Volgogradskaya St., Yekaterinburg, 620102, Sverdlovsk, Russian Federation; [7]Department of Interventional Cardiology and Angiology, Institute of Cardiology, Alpejska 42, 04-628 Warsaw, Poland; [8]Department of Cardiology, Gentofte Hospital Copenhagen University Hospital, Kildegårdsvej 28, 2900 Hellerup, Denmark; [9]Department of Internal Medicine, Juliusspital Wuerzburg, Juliuspromenade 19, 97070 Würzburg, Wuerzburg, Germany; and [10]Unit for Inherited Cardiac Diseases, Department of Cardiology, Copenhagen University Hospital, Rigshospitalet, Blegdamsvej 9, 2100 Copenhagen, Denmark

Received 10 October 2018; revised 30 November 2018; editorial decision 12 February 2019; accepted 18 February 2019; online publish-ahead-of-print 30 April 2019

See page 1688 for the editorial comment on this article (doi: 10.1093/eurheartj/ehz312)

Aims Based on European guidelines, alcohol septal ablation (ASA) for hypertrophic obstructive cardiomyopathy (HOCM) is indicated only in patients with interventricular septum (IVS) thickness >16 mm. The aim of this study was to evaluate the short- and long-term outcomes in ASA patients with mild hypertrophy (IVS ≤ 16 mm).

Methods and results We retrospectively evaluated 1505 consecutive ASA patients and used propensity score to match 172 pairs (344 patients) in groups IVS ≤ 16 mm or IVS > 16 mm. There was no occurrence of post-ASA ventriculoseptal defect in the whole cohort ($n = 1505$). Matched patients had 30-day mortality rate 0% in IVS ≤ 16 mm group and 0.6% in IVS > 16 mm group ($P = 1$). Patients in IVS ≤ 16 mm group had more ASA-attributable early complications (16% vs. 9%; $P = 0.049$), which was driven by higher need for pacemaker implantation (13% vs. 8%; $P = 0.22$). The mean follow-up was 5.4 ± 4.3 years and the annual all-cause mortality rate was 1.8 and 3.2 deaths per 100-patient-years in IVS ≤ 16 group and IVS > 16 group, respectively (log-rank test $P = 0.04$). There were no differences in symptom relief and left ventricular (LV) gradient reduction. Patients with IVS ≤ 16 mm had less repeated septal reduction procedures (log-rank test $P = 0.03$).

Conclusion Selected patients with HOCM and mild hypertrophy (IVS ≤ 16 mm) had more early post-ASA complications driven by need for pacemaker implantation, but their long-term survival is better than in patients with IVS >16 mm. While relief of symptoms and LV obstruction reduction is similar in both groups, a need for repeat septal reduction is higher in patients with IVS > 16 mm.

Keywords Alcohol septal ablation • Prognosis • Survival • Hypertrophy

* Corresponding author. Tel: +420 224434900, Fax: +420 2 24434920, Email: veselka.josef@seznam.cz

Introduction

Two-thirds of patients with hypertrophic cardiomyopathy (HCM) have evidence of left ventricular (LV) outflow tract obstruction.[1,2] These patients might be treated conservatively or with septal reduction therapy, which is based on mechanical relief of obstruction using surgical myectomy or alcohol septal ablation (ASA). Both these procedures result in widening of LV outflow tract, reduction or elimination of LV gradient and relief of symptoms.[1–15]

Since both procedures lead to marked thinning of basal interventricular septum (IVS), the current European guidelines caution of a risk of ventriculoseptal defect following ASA in patients with only mild hypertrophy (≤16 mm) at the point of the mitral leaflet-septal contact. The recommendation is to treat them with dual chamber pacing or mitral valve repair/replacement.[1] Very limited evidence is available on occurrence of post-ASA ventriculoseptal defects[16,17] and we are not aware of published reports on outcomes after ASA in a large cohort of patients with mild hypertrophy.

Therefore, we collected patients treated with ASA in experienced centres[11] and assessed the short- and long-term outcomes of carefully selected patients with mild hypertrophy (≤16 mm).

Methods

Patients, diagnosis and interventions

A total of 1505 patients with symptomatic obstructive HCM (HOCM) underwent ASA between 1997 and 2017 and were enrolled in this study. Procedures were performed in tertiary HCM centres with a number of performed ASA > 50 at each site. Some of the patients were included in previous reports.

The diagnosis of HCM was established by experienced cardiologists based on typical clinical, echocardiographic, or magnetic resonance features, with unexplained LV wall thickness of ≥15 mm or ≥13 mm in the presence of a first-degree family member affected by HCM occurring in the absence of any other cardiac or systemic disease that could have been responsible for the hypertrophy. The patients had to have LV outflow tract gradient ≥30 mmHg at rest and/or ≥50 mmHg after provocation was required to proceed to septal reduction.

In all centres, the primary indication for invasive treatment was intractable symptoms despite maximal pharmacotherapy. The decision regarding septal reduction therapy was made after detailed multidisciplinary evaluation and discussions with the patient and his/her family.

All ASA procedures were performed by experienced interventional cardiologists (only one or two cardiologists in each centre). Details of the myocardial contrast echocardiography-guided ASA technique have been published in the past.[13,14] There were no important differences in ASA technique amongst sites.

Study design

Basal IVS diameter was measured on transthoracic or transoesophageal echocardiography. We identified patients with maximum basal IVS thickness ≤16 mm (*Table 1*) and used propensity score to match each patient with basal IVS thickness ≤16 mm to a comparable patient with basal IVS thickness >16 mm in a ratio 1:1. Both short- and long-term outcomes of patients in both groups were compared.

Clinical, demographic, and echocardiographic data and symptoms were recorded at baseline and during follow-up. Most patients had a clinical examination three to six months after ASA and every year thereafter. The follow-up programme included recording of events, symptoms, physical examination, ECG, and echocardiographic examination. All clinical adverse events were confirmed by reviewing the medical records. The survival of patients treated in the Czech Republic and Denmark were continuously checked in the National Database of Deaths. The survival of patients treated in other countries was recently updated by clinical examination, telephone call, or mail communication.

The indication for repeated septal reduction therapy was at the discretion of each participating centre.

The study was performed in compliance with the Helsinki declaration.

Definitions endpoints

Cardiovascular death was defined as death related to any cardiovascular disease, including death of unknown origin and sudden death. Sudden death was defined as instantaneous and unexpected natural death within 1 h after witnessing collapse in a previously stable patient or death during sleep.

We assessed the occurrence of post-ASA ventriculoseptal defects in the whole population. In the matched population, we evaluated (i) 30-day major cardiovascular adverse events (i.e. ASA-attributable early complications) including cardiovascular death, electrical defibrillation for ventricular tachycardia/fibrillation, cardiac tamponade, and pacemaker implantation; (ii) 30-day all-cause mortality rate; (iii) long-term all-cause death; (iv) LV gradient reduction and improvement in functional status (New York Heart Association, NYHA class) at the most recent clinical check-up; and (v) rate of reintervention (re-ASA or myectomy).

Since 161/192 (84%) patients with IVS ≤ 16 mm had thickness of basal IVS 15 or 16 mm, we evaluated the short- and long-term outcomes of this subgroup separately.

Statistical analysis

All data were assessed and edited by two experienced research statisticians. Data are presented as means ± standard deviation or interquartile range for continuous variable and counts and proportions for categorical variable. The Student's *t*-tests or Mann–Whitney tests (where continuous variables had skewed distributions according to Kolmogorov–Smirnov test) were used to assess the difference between continuous variables, and the χ^2 test between categorical variables. In the database, we missed up to 8% of data and therefore we used traditional statistical techniques and imputation techniques were not considered.

Given the inherent differences between patients with IVS ≤ 16 mm and IVS > 16 mm, we calculated a propensity score for following variables: sex, age, LV gradient at baseline, LV end-diastolic diameter at baseline, LV ejection fraction at baseline, NYHA class at baseline, bundle branch block at baseline, implantable cardioverter-defibrillator (ICD) or pacemaker at baseline, and a year of performed ASA (1996–2000 or 2001–2010 or 2011–2017). The propensity score was estimated using a logit model. Matching was performed using 1:1 nearest neighbour method without replacement, which yielded 172 subjects with IVS ≤ 16 mm and matched with 172 subjects with IVS > 16 mm. Cox's proportional hazards model with clustered standard errors was used for the analysis.

To find risk predictors of all-cause mortality and repeated septal therapy in the matched population, the following variables were evaluated in a univariate model: sex, age, LV gradient at baseline, LV end-diastolic diameter at baseline, left atrial diameter at baseline, LV ejection fraction at baseline, NYHA Class 1 or 2 at baseline, NYHA Class 3 or 4 at baseline, bundle branch block at baseline, ICD or pacemaker at baseline, and year of performed ASA (until 2007 vs. later). Subsequently, variables with a *P*-value of 0.15 were then entered into a multivariable analysis, which was performed using a backward stepwise multiple Cox's regression.

Table 1 Clinical and echocardiographic characteristics at baseline and at the last check-up

	Unmatched cohort			Matched cohort		
	IVS ≤16 group (*N* = 192)	IVS >16 group (*N* = 1313)	*P*-value	IVS ≤16 group (*N* = 172)	IVS >16 group (*N* = 172)	*P*-value
Age (years)	59.8 ± 11.9	56.9 ± 14.1	0.008	59.5 ± 11.9	61.1 ± 13.4	0.225
Females, *n* (%)	99 (52)	629 (48)	0.354	86 (50)	83 (48)	0.829
Total alcohol (mL)	2.0 ± 0.7	2.3 ± 1	<0.001	2.0 ± 0.7	2.3 ± 0.9	0.001
Alcohol dose (mL)/basal septum thickness (mm)	0.13 ± 0.05	0.11 ± 0.05	<0.001	0.13 ± 0.05	0.11 ± 0.04	<0.001
Basal septum thickness (mm)						
Baseline	15.2 ± 1.2	21.6 ± 4.0	<0.001	15.3 ± 1.0	20.9 ± 3.9	<0.001
Last clinical check-up	13.4 ± 3.8	16.0 ± 4.5	<0.001	13.3 ± 3.9	15.6 ± 3.5	<0.001
NYHA Class III/IV, *n* (%)						
Baseline	150 (78)	1059 (81)	0.437	133 (77)	139 (81)	0.508
Last clinical check-up	26 (14)	157 (12)	0.554	24 (14)	27 (16)	0.762
Angina, CCS class						
Baseline	1.2 ± 1.2	1.2 ± 1.2	0.679	1.2 ± 1.2	1.0 ± 1.2	0.107
Last clinical check-up	0.5 ± 0.8	0.7 ± 0.8	0.023	0.5 ± 0.8	0.7 ± 0.8	0.158
LV outflow gradient at rest (mmHg)						
Baseline	60.7 ± 38.4	70.4 ± 38.3	0.001	60.3 ± 39.0	60.7 ± 32.6	0.930
Last clinical check-up	14.4 ± 21.3	16.8 ± 21.3	0.153	13.5 ± 20.8	14.5 ± 15.6	0.627
>30 mmHg, n (%)	16 (8)	175 (13)	0.062	12 (7)	20 (12)	0.193
LV diameter (mm)						
Baseline	43.0 ± 6.3	43.2 ± 6.4	0.704	43.6 ± 6.2	43.3 ± 5.7	0.641
Last clinical check-up	44.4 ± 5.9	45.7 ± 6.2	0.014	44.7 ± 5.8	45.5 ± 5.5	0.243
LV ejection fraction (%)						
Baseline	69 ± 9	70 ± 9	0.038	70 ± 9	70 ± 9	0.884
Last clinical check-up	65 ± 11	67 ± 10	0.086	66 ± 11	67 ± 10	0.709
Left atrium diameter (mm)						
Baseline	44.6 ± 6.7	47.3 ± 6.9	<0.001	44.9 ± 6.4	46.7 ± 6.4	0.023
Last clinical check-up	42.8 ± 7.0	46.0 ± 7.2	<0.001	43.1 ± 6.6	45.4 ± 6.3	0.005
Mean follow-up duration (years)	5.6 ± 4.4	5.3 ± 4.2		5.8 ± 4.5	5.0 ± 4.1	

LV, left ventricular; NYHA, New York Heart Association.

Estimates for long-term outcomes were made by the Kaplan–Meier method and differences were assessed by the log-rank test.

P-value <0.05 was considered statistically significant. All reported *P*-values were two-sided. The software GraphPad (release 6.05, GraphPad Software Inc., La Jolla, CA, USA) and Stata (release 14.2, StataCorp LP, College Station, TX, USA) were used for statistical analysis.

Results

A total of 1505 consecutive patients treated with ASA for HOCM were enrolled. In this cohort, the median basal IVS thickness at baseline was 20 mm (interquartile range 18–23 mm) (*Figure 1*).

We identified 192 (13%) patients with IVS ≤ 16 mm and compared them with 1313 patients with IVS > 16 mm (*Table 1*).

The matched cohort analysis comprised 344 patients (172 patients in the IVS ≤ 16 mm group and 172 patients in the IVS > 16 mm group) (*Table 1*). Histograms demonstrating the baseline IVS thickness both in the whole population and the matched population are depicted in *Figures 1* and *2*.

The matched cohort with mild LV hypertrophy was treated with a reduced dose of alcohol (2 ± 0.7 ml in IVS ≤16 mm group vs. 2.3 ± 0.9 mL in IVS >16 mm group), which means 0.13 ± 0.05 mL of alcohol per 1 mm of IVS thickness vs. 0.11 ± 0.04 mL of alcohol per 1 mm of IVS thickness ($P < 0.01$).

Short-term outcome

None of 1505 patients treated with ASA experienced ventriculoseptal defect. Short-term complications, both in matched and unmatched cohorts, are summarized in *Table 2*. Patients in the matched IVS ≤ 16 mm group had significantly more ASA-attributable complications (16% vs. 9%; $P = 0.049$), which were driven by a higher occurrence of conduction disturbances with subsequent need of permanent pacemaker implantation (13% vs. 8%; $P = 0.22$) (*Table 2*).

Two patients (1.2%) in the matched IVS ≤ 16 mm group died during the 30 days post-ASA compared with no deaths in the matched

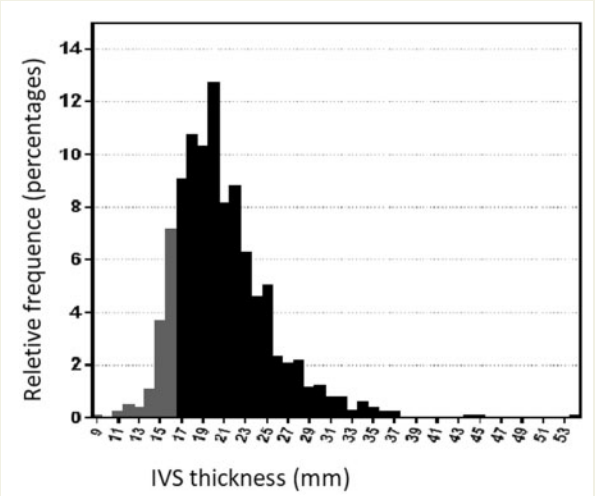

Figure 1 Histogram demonstrating distribution of the basal interventricular septum thickness in the whole population (1505 patients).

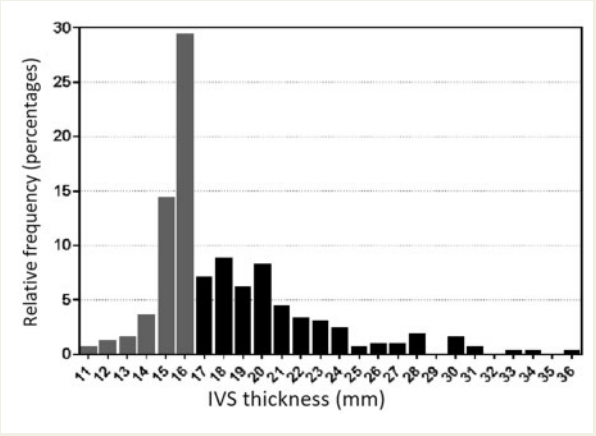

Figure 2 Histogram demonstrating distribution of the basal interventricular septum thickness in the matched population (344 patients).

IVS > 16 mm group ($P = 0.50$; *Table 2*). Causes of deaths are summarized in *Table 3*.

A total of 161 patients with basal IVS thickness of 15 or 16 mm had the 30-day post ASA mortality rate and need of pacemaker implantation 0.6% and 14%, respectively.

Long-term outcome

None of the patients were lost to follow-up. In the matched population, the mean follow-up was 5.4 ± 4.3 years and a total of 46 (13%) deaths occurred during 1869 patient-years, which translates to 1.8 and 3.2 deaths per 100-patient-years in the IVS ≤ 16 mm group and the IVS > 16 mm group, respectively. The survival free of all-cause death in IVS ≤ 16 mm group vs. IVS > 16 mm group at 5 and 10 years were 96% [95% confidence interval (CI) 92–99%] vs. 87% (95% CI 79–92%), and 78% (95% CI 65–86%) vs. 71% (95% CI 59–81%) (log rank $P = 0.04$). The Kaplan–Meier curves of all-cause death are shown in *Take home figure*.

In multivariable analysis, the only predictor of all-cause mortality was patients' age at which ASA was performed [hazard ratio (HR) 1.07, 95% CI 1.03–1.10; $P < 0.01$].

In matched groups, there was no difference in post-ASA level of dyspnoea (NYHA class 1.6 ± 0.7 in IVS ≤ 16 mm group vs. NYHA class 1.8 ± 0.7 in IVS > 16 mm group; $P = 0.10$) or LV gradient (14 ± 21 mmHg in IVS ≤ 16 mm group vs. 15 ± 16 mmHg in IVS > 16 mm group; $P = 0.63$).

A total of 32 (10%) patients underwent 37 repeated septal reduction procedures attributable to insufficient symptomatic relief and persistence of significant LV gradient (11 patients in IVS ≤ 16 mm group vs. 21 patients in IVS > 16 mm group; *Table 4*). The Kaplan–Meier curves describing re-intervention rates are shown in *Figure 3* (log rank $P = 0.03$).

In multivariable analysis, the predictors of repeated septal reduction therapy were LV gradient at baseline (HR 1.01, 95% CI 1.00–1.02; $P = 0.02$) and ASA performed in years 2008–2017 (HR 6.31, 95% CI 2.35–16.91; $P < 0.01$).

In 161 patients with basal IVS thickness 15 or 16 mm, a total of 14 deaths occurred during 881 patient-years, which translates to rate of 1.6 deaths per 100-patient years; LV gradient decreased from 60 ± 36 mmHg to 14 ± 22 mmHg and dyspnoea was reduced from NYHA class 2.8 ± 0.5 to 1.6 ± 0.7 ($P < 0.01$ for both).

Discussion

To our knowledge, this is the first study evaluating short- and long-term outcomes of ASA for HOCM patients with mild LV hypertrophy. This study was designed to test the statement in the current European guidelines suggesting that treating patients with IVS ≤ 16 mm with septal reduction therapy is not recommended due to fear of ventriculoseptal defect. Here, we report the following essential findings: (i) none of 1505 patients treated in this study experienced a post-ASA ventriculoseptal defect including 192 patients with IVS ≤ 16 mm. (ii) Propensity matched patients with IVS ≤ 16 mm had significantly higher occurrence of early post-procedural complications driven by pacemaker implantation rate and (iii) the early post-procedural mortality was very low in both groups. In the long-term follow-up, patients in the IVS ≤ 16 mm group had (iv) a lower all-cause mortality rate, (v) a similar relief to dyspnoea and reduction of LV gradient, and (vi) a significantly lower rate of repeated septal reduction therapy than patients in the IVS > 16 mm group.

The median thickness in our 1505 patients was 20 mm, this is similar to findings reported by Nguyen *et al.*[15] in patients treated with myectomy at the Mayo Clinic. Thus, HOCM patients with mild hypertrophy (≤16 mm) represent only a minority among those who are considered for septal reduction therapy (i.e.13% in this study) and most of these had thickness of IVS 15 or 16 mm. Notably, this subgroup of patients not recommended for ASA, according to current guidelines, had an excellent post-ASA long-term outcome in our study.

Table 2 The non-hierarchical occurrence of cardiovascular adverse events in the first 30 days after ASA

Events	Unmatched cohort			Matched cohort		
	IVS ≤16 group (*N* = 192)	IVS >16 group (*N* = 1313)	*P*-value	IVS ≤16 group (*N* = 172)	IVS >16 group (*N* = 172)	*P*-value
Cardiovascular death, *n* (%)	1 (0.5)	10 (0.76)	1.000	1 (0.6)	0	1.000
Electrical cardioversion for VT/VF or ICD discharge, *n* (%)	3 (1.6)	15 (1.1)	0.493	3 (1.7)	0	0.123
Cardiac tamponade, *n* (%)	3 (1.6)	13 (1.0)	0.446	2 (1.2)	1 (0.6)	1.000
Pacemaker implantation, *n* (%)	24 (12.5)	123 (9.4)	0.192	22 (12.8)	14 (8.1)	0.217
Total, *n* (%)	31 (16.1)	161 (12.3)	0.133	28 (16.3)	15 (8.7)	0.049

ICD, implantable cardioverter-defibrillator; VT/VF, ventricular fibrillation or tachycardia.

Table 3 Causes of all-cause deaths during the 30 days after ASA

Causes	Unmatched cohort			Matched cohort		
	IVS ≤16 group (*N* = 192)	IVS >16 group (*N* = 1313)	*P*-value	IVS ≤16 group (*N* = 172)	IVS >16 group (*N* = 172)	*P*-value
Cardiac tamponade, n (%)	1 (0.5)	2 (0.2)	0.336	1 (0.6)	0	1.000
Carcinoma, *n* (%)	1 (0.5)	0	0.128	1 (0.6)	0	1.000
Ventricular fibrillation, *n* (%)	0	3 (0.2)	1.000	0	0	1.000
Pulmonary embolism, *n* (%)	0	3 (0.2)	1.000	0	0	1.000
Stroke, cerebral bleeding, *n* (%)	0	1 (0.1)	1.000	0	0	1.000
Heart failure, *n* (%)	0	1 (0.1)	1.000	0	0	1.000
Total, *n* (%)	2 (1.0)	10 (0.8)	0.658	2 (1.2)	0	0.499

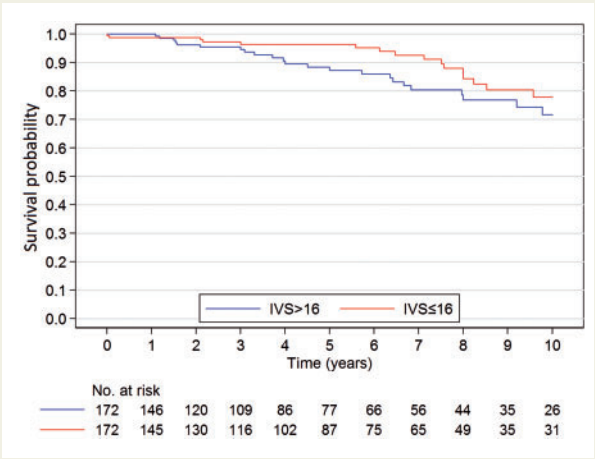

Take home figure Selected patients treated with alcohol septal ablation for hypertrophic obstructive cardiomyopathy with mild left ventricular hypertrophy (septum thickness ≤16 mm) had higher rate of early post-procedural complications, but their long-term survival was better than for those with septum thickness >16 mm.

Based on an expert consensus, the most imminent complication of injection of desiccated alcohol in mildly hypertrophied septum might be a subsequent ventriculoseptal defect.[1] Although this complication may be underreported, we found only two cases in the literature reporting ventriculoseptal defect potentially attributable to previous ASA.[16,17] Similarly, Nagueh *et al.*[4] did not report any post-ASA septal defect in the Multicenter North American Registry (*n* = 874 patients). Thus, post-ASA ventriculoseptal defect seems to be a rare complication of ASA and based on the existing observations it is unclear if mild LV hypertrophy is a risk factor for its occurrence.

We found that post-ASA mortality rate was very low (<1%) regardless of IVS thickness. On the other hand, matched patients with IVS ≤ 16 mm had significantly higher occurrence of early post-procedural complications than those with IVS > 16 mm (16% vs. 9%; *P* = 0.049), this was driven by conduction disturbances requiring implantation of permanent pacemaker (13% vs. 8%; *P* = 0.22). Based on results of the Euro-ASA registry,[18] we speculate that although the matched cohort with mild LV hypertrophy was treated with a reduced dose of alcohol this dose was still relatively high and likely led to higher rate of complete heart block. Reduction of alcohol dose in the IVS ≤ 16 mm group might favourably influence the occurrence of post-ASA complete heart block. However, this hypothesis should be tested in further ASA studies.

The most important goals of cardiac interventions are the improvement of patient's long-term prognosis and quality of life. This study demonstrated that quality of life with regard to dyspnoea and angina pectoris was similar regardless of the IVS thickness of the treated patients. However, the long-term survival was significantly

Table 4 Repeated interventions

	Matched cohort	
	IVS ≤16 group (*N* = 172)	IVS >16 group (*N* = 172)
Repeated ASA, *n* (%)	9 (5.2)	19 (11.0)
Myectomy after ASA, *n* (%)	5 (2.9)	4 (2.3)
Patients with reASA + myectomy, *n* (%)	3 (1.7)	2 (1.2)
Patients with any repeated interventions, *n* (%)	11 (6.4)	21 (12.2)

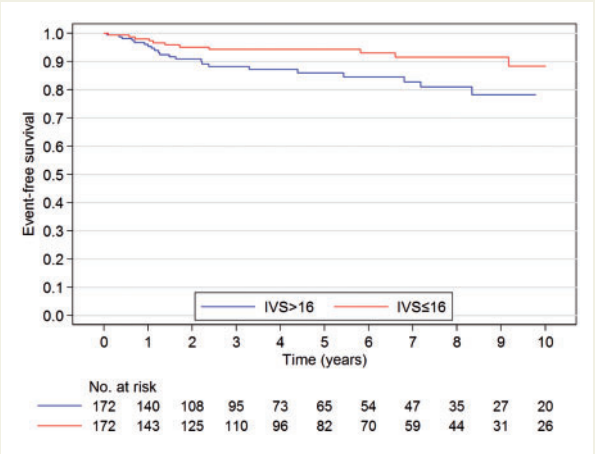

Figure 3 The Kaplan–Meier survival curves describing freedom from repeated septal reduction therapy in the interventricular septum ≤16 vs. interventricular septum >16 group ($P = 0.03$).

better in patients with mild hypertrophy. This finding is not surprising because several studies in the past demonstrated that a thicker IVS in HCM patients is not only a risk factor of sudden cardiac death,[19–21] but also for a long-term post-ASA survival rate. Indeed, in a Scandinavian/German study patients with IVS thickness >25 mm had five times increased risk of all-cause mortality compared to patients with IVS thickness <20 mm in the long-term follow-up.[20] Thus, we can assume that LV hypertrophy plays a key role in the prognosis of HCM patients and that this inherent risk factor determines prognosis more than the slightly higher risk of periprocedural ASA complications that are usually clinically manageable in hands of experienced cardiologists. Additionally, patients with mild hypertrophy had only half the risk of repeated septal reduction therapy than patients traditionally referred for ASA (IVS ≥ 16 mm). Interestingly, a risk factor for repeated septal reduction therapy was a procedure performed in the last decade. We speculate that accumulating favourable results of repeated septal reduction procedures, with a low procedural risk and ultimate reduction of LV obstruction followed by symptom relief, led to more liberal indication for repeated procedures within the last few years. Moreover, recently it has been shown that residual LV gradient ≥30 mmHg was associated with significantly higher occurrence of subsequent cardiovascular mortality events, which suggests that complete elimination of obstruction should be pursued.[22]

This study has several limitations. First, a retrospective, multicentre and multinational design has some limitations including slight differences in indications, interventions and patients follow-up. Second, we have to be aware that these patients were treated by tertiary centre cardiologists specializing in HCM, and therefore, these results cannot simply be generalized to all patients with mild LV hypertrophy treated in all interventional centres.[8,11] Moreover, it is unknown how many patients were discouraged from the interventional therapy because of a thin basal IVS, and therefore, we cannot assess our selection bias. Third, propensity score matching estimates an average therapeutic effect from observational data, which has its own inherent limitations.[23] Therefore, randomized trials would be necessary to ultimately determine whether patients with mild hypertrophy should be treated with ASA or not. However, more retrospective data such as presented here could challenge the prevailing cautionary view of current guidelines on performance of ASA in HOCM patients with mild hypertrophy. Since most patients in IVS ≤ 16 mm group had basal IVS thickness 15 or 16 mm, it might be considered to change the indication for ASA in carefully selected HOCM patients to this reduced value of basal IVS thickness, which was shown to be safe and effective in this study.

Conclusions

Selected patients with HOCM and mild LV hypertrophy (IVS ≤ 16 mm) had higher rate of early post-ASA complications, but no post-ASA ventriculoseptal defect was observed. Their long-term survival was better than for those with IVS > 16 mm. While relief of symptoms and reduction of LV obstruction was similar in both groups, need for repeat septal reduction therapy was higher in patients with more marked LV hypertrophy.

Acknowledgements

The authors are grateful to Dr Marek Maly for his assistance with statistical analysis. The authors also thank colleagues responsible for the HCM clinics in all participated centres.

Conflict of interest: none declared.

References

1. Elliott PM, Anastakis A, Borger MA, Borggrefe M, Cecchi F, Charron P, Hagege AA, Lafont A, Limongelli G, Mahrholdt H, McKenna WJ, Mogensen J, Nihoyannopoulos P, Nistri S, Pieper PG, Pieske B, Rapezzi C, Rutten FH, Tillmanns C, Watkins H. 2014 ESC Guidelines on diagnosis and management of hypertrophic cardiomyopathy. *Eur Heart J* 2014;**35**:2733–2779.
2. Gersh BJ, Maron BJ, Bonow RO, Dearani JA, Fifer MA, Link MS, Naidu SS, Nishimura RA, Ommen SR, Rakowski H, Seidman CE, Towbin JA, Udelson JE, Yancy CW. 2011 ACCF/AHA guideline for the diagnosis and treatment of hypertrophic cardiomyopathy. *Circulation* 2011;**124**:e783–e831.
3. Fifer MA, Sigwart U. Controversies in cardiovascular medicine. Hypertrophic obstructive cardiomyopathy: alcohol septal ablation. *Eur Heart J* 2011;**32**:1059–1064.
4. Nagueh SF, Groves BM, Schwartz L, Smith KM, Wang A, Bach RG, Nielsen C, Leya F, Buergler JM, Rowe SK, Woo A, Maldonado YM, Spencer WH. Alcohol septal ablation for the treatment of hypertrophic obstructive cardiomyopathy: a Multicenter North American registry. *J Am Coll Cardiol* 2011;**58**:2322–2328.

5. Sorajja P, Ommen SR, Holmes DR Jr, Dearani JA, Rihal CS, Gersh BJ, Lennon RJ, Nishimura RA. Survival after alcohol septal ablation for obstructive hypertrophic cardiomyopathy. *Circulation* 2012;**16**:2374–2380.
6. Veselka J, Lawrenz T, Stellbrink C, Zemanek D, Branny M, Januska J, Sitar J, Dimitrow P, Krejci J, Dabrowski M, Mizera S, Bartel T, Kuhn H. Early outcomes of alcohol septal ablation for hypertrophic obstructive cardiomyopathy: a European multicenter and multinational study. *Catheter Cardiovasc Interv* 2014;**84**:101–107.
7. Veselka J, Tomasov P, Zemanek D. Long-term effects of varying alcohol dosing in percutaneous septal ablation for obstructive hypertrophic cardiomyopathy: a randomized study with a follow-up up to 11 years. *Can J Cardiol* 2011;**27**: 763–767.
8. Kim LK, Swaminathan RV, Looser P, Minutello RM, Wong SC, Bergman G, Naidu SS, Gade CLF, Charitakis K, Singh HS, Feldman DN. Hospital volume outcomes after septal myectomy and alcohol septal ablation for treatment of obstructive hypertrophic cardiomyopathy: US nationwide inpatient database, 2003–2011. *JAMA Cardiol* 2016;**1**:324.
9. Ferrazzi P, Spirito P, Iacovoni A, Calabrese A, Migliorati K, Simon C, Pentiricci S, Poggio D, Grillo M, Amigoni P, Iascone M, Mortara A, Maron BJ, Senni M, Bruzzi P. Transaortic chordal cutting: mitral valve repair for obstructive hypertrophic cardiomyopathy with mild septal hypertrophy. *J Am Coll Cardiol* 2015;**66**: 1687–1696.
10. Schaff HV, Dearani JA, Ommen SR, Sorajja P, Nishimura RA. Expanding the indications for septal myectomy in patients with hypertrophic cardiomyopathy: results of operation in patients with latent obstruction. *J Thorac Cardiovasc Surg* 2012;**143**:303–309.
11. Veselka J, Faber L, Jensen MK, Cooper R, Januska J, Krejci J, Bartel T, Dabrowski M, Hansen PR, Almaas VM, Seggewiss H, Horstkotte D, Adlova R, Bundgaard H, ten Berg J, Liebregts M. Effects of institutional experience on outcomes of alcohol septal ablation for hypertrophic obstructive cardiomyopathy. *Can J Cardiol* 2018;**34**:16–22.
12. Veselka J, Anavekar N, Charron P. Hypertrophic obstructive cardiomyopathy. *Lancet* 2017;**389**:1253–1267.
13. Rigopoulos AG, Sakellaropoulos S, Ali M, Mavrogeni S, Manginas A, Pauschinger M, Noutsias M. Transcatheter septal ablation in hypertrophic cardiomyopathy: a technical guide and review of published studies. *Heart Fail Rev* 2018; doi: 10.1007/s10741-018-9706-z [Epub ahead of print].
14. Veselka J, Duchoňová R, Procházková Š, PálenícKová J, Sorajja P, Tesař D. Effects of varying ethanol dosing in percutaneous septal ablation for obstructive hypertrophic cardiomyopathy on early hemodynamic changes. *Am J Cardiol* 2005;**95**: 675–678.
15. Nguyen A, Schaff HV, Nishimura RA, Dearani JA, Geske JB, Lahr BD, Ommen SR. Does septal thickness influence outcome of myectomy for hypertrophic obstructive cardiomyopathy? *Eur J Cardiothorac Surg* 2018;**53**:582–589.
16. Liebregts M, Bol GM, Groen JW, Lieuw-A-Fa M, Heijmen RH, ten Berg JM. FOLFOX chemotherapy as a cause of ventricular septal rupture after alcohol septal ablation for obstructive hypertrophic cardiomyopathy? *Intern J Cardiol* 2016;**207**:208–210.
17. Aroney CN, Goh TH, Hourigan LA, Dyer W. Ventricular septal rupture following nonsurgical septal reduction for hypertrophic cardiomyopathy: treatment with percutaneous closure. *Catheter Cardiovasc Interv* 2004;**61**:411–414.
18. Veselka J, Jensen MK, Liebregts M, Januska J, Krejci J, Bartel T, Dabrowski M, Hansen PR, Almaas VM, Seggewiss H, Horstkotte D, Tomasov P, Adlova R, Bundgaard H, Steggerda R, ten Berg J, Faber L. Long-term clinical outcome after alcohol septal ablation for obstructive hypertrophic cardiomyopathy: results from the Euro-ASA registry. *Eur Heart J* 2016;**37**:1517–1523.
19. Spirito P, Bellone P, Harris KM, Bernabo P, Bruzzi P, Maron BJ. Magnitude of left ventricular hypertrophy and risk of sudden death in hypertrophic cardiomyopathy. *N Engl J Med* 2000;**342**:1778–1785.
20. Jensen MK, Jacobsson L, Almaas V, van Buuren F, Hansen PR, Hansen TF, Aakhus S, Eriksson MJ, Bundgaard H, Faber L. Influence of septal thickness on the clinical outcome after alcohol septal ablation in hypertrophic cardiomyopathy. *Circ Cardiovasc Interv* 2016;**9**:e003214.
21. ÓMahony C, Jichi F, Pavlou M, Monserrat L, Anastakis A, Rapezzi C, Biagini E, Gimeno JR, Limongelli G, McKenna WJ, Omar RZ, Elliott PM. A novel clinical risk prediction model for sudden cardiac death in hypertrophic cardiomyopathy (HCM risk-SCD). *Eur Heart J* 2014;**35**:2010–2020.
22. Veselka J, Tomasov P, Januska J, Krejci J, Adlova R. Obstruction after alcohol septal ablation is associated with cardiovascular mortality events. *Heart* 2016;**102**: 1793–1796.
23. Garrido MM, Kelley AS, Paris J, Roza K, Meier DE, Morrison RS, Aldridge MD. Methods for constructing and assessing propensity scores. *Health Serv Res* 2014; **46**:1701–1172.

G. Caluori a kol.

Non-invasive electromechanical cell-based biosensors for improved investigation of 3D cardiac models *(id 1389)*

Biosensors and Bioelectronics
Impact Factor: 9,518

rejstřík

Biosensors and Bioelectronics 124–125 (2019) 129–135

Contents lists available at ScienceDirect

Biosensors and Bioelectronics

journal homepage: www.elsevier.com/locate/bios

Non-invasive electromechanical cell-based biosensors for improved investigation of 3D cardiac models

Guido Caluori[a,b,c], Jan Pribyl[a], Martin Pesl[b,d,e], Sarka Jelinkova[d], Vladimir Rotrekl[d], Petr Skladal[a,*], Roberto Raiteri[c,*]

[a] Central European Institute of Technology, Masaryk University, Kamenice 5, 62500 Brno, Czech Republic
[b] International Clinical Research Centre of Saint Anne Hospital Brno, Pekarska 53, 60200 Brno, Czech Republic
[c] Department of Informatics, Bioengineering Robotics and Systems Engineering, University of Genova, Via All'Opera Pia, 13, 16145 Genova, Italy
[d] Department of Biology, Faculty of Medicine, Masaryk University, Kamenice 5, 62500 Brno, Czech Republic
[e] 1st Department of Cardiovascular Diseases, St. Anne's University Hospital and Masaryk University, Pekarska 53, Brno, Czech Republic

ARTICLE INFO

Keywords:
Excitation-contraction coupling
Human pluripotent stem cells
Cardiomyocytes
Atomic force microscopy
Microelectrode array
Drug testing

ABSTRACT

Cardiomyocytes (CM) placed on microelectrode array (MEA) were simultaneously probed with cantilever from atomic force microscope (AFM) system. This electric / nanomechanical combination in real time recorded beating force of the CMs cluster and the triggering electric events. Such "organ-on-a-chip" represents a tool for drug development and disease modeling. The human pluripotent stem cells included the WT embryonic line CCTL14 and the induced dystrophin deficient line reprogrammed from fibroblasts of a patient affected by Duchenne Muscular Dystrophy (DMD, complete loss of dystrophin expression). Both were differentiated to CMs and employed with the AFM/MEA platform for diseased CMs' drug response testing and DMD characterization. The dependence of cardiac parameters on extracellular Ca^{2+} was studied. The differential evaluation explained the observed effects despite variability of biological samples. The β-adrenergic stimulation (isoproterenol) and antagonist trials (verapamil) addressed ionotropic and chronotropic cell line-dependent features. For the first time, a distinctive beating-force relation for DMD CMs was measured on the 3D cardiac in vitro model.

1. Introduction

In the field of cell-based biosensors, cardiomyocytes (CM) are often used as models to study heart related diseases. The monitoring of electric activities of CMs is typically chosen; (multi)electrode transducers seem well established and widely available as microelectrode arrays (MEA) (Rothermel et al., 2005). The beating of CMs can be followed relatively easily (e.g. by video microscopy, Laurila et al., 2015), though in many situations the missing information on the associated beating force is of paramount importance in heart remodeling pathologies, such as dystrophinopathies and cardiomyopathies (Vatta et al., 2005). Beating force is associated with pathophysiological electro-mechanical coupling, and its alterations result often in mechanical heart failure (Pesl et al., 2016a). Such biomechanical measurements investigating the dilated cardiomyopathy were previously done on CMs using the stretcher device (Knoll et al., 2002). More detailed investigations were later done using cantilevers as nanomechanical transducers and atomic force microscope (AFM) as the evaluation system in real time with individual cardiomyocyte cells (Liu et al., 2012a,2012b) or cell clusters (Pesl et al., 2016a). Thus, combination of AFM for biomechanical changes with MEA sensing electric signals described here seems naturally promising for elucidating complex events in cardiomyocytes obtained from patient derived stem cells. This approach provides a robust and convenient example of the organ-on-a-chip system demonstrating its capabilities on disease related CMs.

Supplementary material related to this article can be found online at doi:10.1016/j.bios.2018.10.021.

The introduction of human pluripotent stem cells (hPSC, either embryonic, hESC, or induced pluripotent, hiPSC) and cardiac differentiation protocols allowed almost two decades of study on the cardiac organogenesis and functionality. In particular, patient-specific hiPSC representing a direct supply of healthy and mutation-carrying samples (Sinnecker et al., 2014) allow for description of the diseases progression involved in heart failure (Moretti et al., 2013). To improve the comparison between in vitro models, CRISPR-Cas9 technology has recently gained an outstanding popularity for its efficiency and flexibility in inducing precise mutations in cell lines, providing researchers with isogenic controls (Motta et al., 2017). hPSC-derived cardiomyocytes

* Corresponding authors.
E-mail addresses: skladal@chemi.muni.cz (P. Skladal), roberto.raiteri@unige.it (R. Raiteri).

https://doi.org/10.1016/j.bios.2018.10.021
Received 1 July 2018; Received in revised form 11 October 2018; Accepted 11 October 2018
Available online 16 October 2018
0956-5663/

and models recapitulate the morphological, genetic and functional characteristics of the heart muscle, specifically the subcellular cascade known as cardiac excitation-contraction coupling (cECC), responsible for heart pumping function (Bers, 2002). Cardiomyocytes from hPSC can be derived as 2D or 3D stem cell cultures. However, the 3D models seem to be superior and more physiologically relevant compared to the 2D ones (Regmi and Jeong, 2016). For monolayer culture, the multiple existing protocols with high differentiation efficiency involve modulation of the canonical Wnt/β-catenin pathway (Lian et al., 2012; Burridge et al., 2014), with high differentiation efficiency. For 3D cultures, the protocols exploit the spontaneous differentiation triggered from the aggregation of hPSC into embryoid bodies, which is driven to cardiac phenotypes using hypoxia and small molecules cocktails (Pesl et al., 2014). The efficiency of differentiation and grade of maturation can vary according to protocol and cell lines, and can be improved by physical methods, as in electro-mechanical stimulation (Bauwens et al., 2016). Purified hPSC-CMs can be further reassembled in precise geometries, such as in the engineered heart tissue (Tzatzalos et al., 2016). From gene expression to functionality, hPSC-CMs present an embryonic-like cardiac phenotype, with immature sarcomeres, sarcoplasmic reticulum and calcium cycling (Mummery et al., 2012; Acimovic et al., 2014). An immature phenotype has also been proven for embryoid body-derived cardiac models (Doevendans et al., 2000). Nevertheless, hPSC-CMs play a key role in future drug development with reduced attrition rate (Liang et al., 2013; Zheng et al., 2013), in cardiotoxicity assays (Takeda et al., 2018), disease modeling (Dell'Era et al., 2015) and in cell-based regenerative therapies (Doppler et al., 2013), and further studies to achieve cardiac maturation are ongoing. This aspect is also investigated by our proposed approach, to assess its robustness.

The hPSC-derived cardiac models can be characterized by functional (or phenotypic) properties though multiple in vitro assays, reviewed in another work from our group (Pesl et al., 2016b). Among these, atomic force microscopy has in the past three decades achieved remarkable role in the evaluation of biological samples mechanics and topography (Alonso and Goldmann, 2003; Kilpatrick et al., 2015) in native culture environment. In particular, it has been employed in important studies on single CMs (Liu et al., 2012a). A combination of AFM and 3D cardiac models has already been proposed as cell-based biosensor (CBB) in our previous work (Pesl et al., 2016a). Most AFM systems are now currently integrated with optical and confocal microscopy, which allows the implementation of combined measures of AFM and calcium imaging (Liu et al., 2012b; Caluori et al., 2018), but further systems can be included if properly miniaturized. Small biosensors, such as microelectrode arrays (MEA), can be engineered to comply with AFM and optical microscopy systems for cardiac investigation (Cogollo et al., 2011). The attractiveness of MEA-based electrophysiology resides in its ability to multiprobe extracellular field potentials (EFP) of electroactive cells in a non-destructive fashion, which allows for prolonged and complex measurements of cells and tissues (Spira and Hai, 2013).

In this work, we present an electromechanical in vitro system for the combined study of cECC on 3D cardiac models, employing both AFM and MEA platforms together. The aim of this work is to provide an improved method for cardiac models characterization and drug testing in the format of an organ (heart)-on-a-chip. For this reason, we have confronted a model of cardiac maturation with respect to its control, and employed a disease model of Duchenne muscular dystrophy (DMD), a progressively invalidating pathology of the striated muscle, including the myocardium (Finsterer and Stöllberger, 2003).

2. Materials and methods

2.1. hPSC culture and cardiac differentiation

The cardiac cells clusters were obtained using the hESC line CCTL14 (Adewumi et al., 2007) and one hiPSC line reprogrammed from fibroblasts of a patient affected by Duchenne Muscular Dystrophy (DMD). The patient carries a deletion of exons 45–50 of the DMD gene causing a complete loss of dystrophin expression. The line has been fully characterized for pluripotency markers (https://hpscreg.eu/cell-line/MUNIi001-A) and the differentiated CMs were tested for presence of striated pattern of sarcomeres labeled with cardiac troponin T (sc-8121, Santa Cruz), and cytoplasmic presence of dystrophin (NCL-DYSB, Leica) (see Supplementary material, SFig. 1). Pluripotent cells were firstly thawed and seeded on mitotically-inactivated mouse embryonic fibroblasts (feeder cells). The hPSC colonies were cultivated in DMEM-F12 (Thermofisher, Waltham, MA, USA) supplemented with 15% KnockOut fetal bovine serum Serum Replacement (FBS, Life Technologies, Carlsbad, CA, USA), 1% L-glutamine (Thermofisher), 0.5% penicillin/streptomycin (Thermofisher), 1% 2-mercaptoethanol (Thermofisher), 1% non-essential amino acids (Life Technologies), and 4 ng ml^{-1} and 10 ng ml^{-1} human fibroblast growth factor 2 (hFGF2, Peptrotech, London, UK) for hESC and hiPSC, respectively. Medium was changed daily and colonies were propagated for at least 5 passages, by manual fractioning. hESC cells were divided in a control group (CTRL) and another group (DORSO) undergoing an exposure to 500 nM of dorsomorphin (Sigma Aldrich, St. Louis, MO, USA) 4 days to the differentiation protocol, to improve cardiac commitment (Hao et al., 2008).

Cardiac differentiation was started by embryoid body formation, as described elsewhere (Pesl et al., 2013). Briefly, compact, round colonies were manually cut and scratched from the culture surface. For DMD iPSC, the colonies were kept intact, carefully detached from the culturing surface as a whole. The cell leaflets were transferred in hypoxic incubation atmosphere (5% O_2) and underwent a sequential cytokine modulation in KnockOut DMEM (Life Technologies), supplemented with 10% FBS, 1% L-glutamine, 1% PS, 1% 2-mercapthoethanol, 1% non-essential amino acids (further referred simply as culture medium). Beating cardiac clusters (BCC, Supplementary Fig. 1) were visible from day 14 and were transferred into normoxic atmosphere. After day 22, they were kept in the culture medium with 10 μg ml^{-1} ascorbic acid (Sigma Aldrich).

2.2. Microelectrode arrays cleaning and coating

Before beating CMs cluster plating, 60 channel MEAs (60MEA200/30iR-Ti/ITO, Multichannel Systems, Reutlingen, Germany) were cleaned using a 0.1% w/v solution of Tergazyme detergent (Alconox, White Plains, NY, US) in MilliQ water for at least 8 h. The culture well (i.e. the area inside the plastic ring) was then thoroughly washed with MilliQ water to remove the excess detergent. The preparation of the device was moved to a UV-sterilized clean box (Biosan, Riga, Latvia). Each MEA was placed in 100 mm sterile Petri dish (TPP, Trasadingen, Switzerland), and the MEA culture well was sterilized by filling it with 70% ethanol solution. After 30 min, the sterilizing solution was removed, the culture well on MEA was rinsed twice with 0.2 μm-filtered MilliQ water and let dry. The sensing area (i.e. the electrode array area) was then coated with 20–50 μl of 0.1 mg ml^{-1} laminin (Sigma Aldrich) and fibronectin (Sigma Aldrich) mixture, 1:1 ratio, to promote cell adhesion. The MEAs were put in a cell incubator at 37 °C, 5% CO_2, overnight. The next day, MEAs were rinsed twice with filtered MilliQ water to remove excess of adhesion factor from the surface.

2.3. BCCs plating on MEA chips

Suspended BCCs were collected and plated on MEA sensing area with 30 μl droplet of the culture medium. This amount of medium was a safe tradeoff between sample wobbling limitation and the need of hydrated environment. Samples were manually placed on top of electrode array, then put in standard cell incubator and kept in this overnight (with loosely fitted lid and additional droplets were placed separately around the well to prevent evaporation). The following day, medium

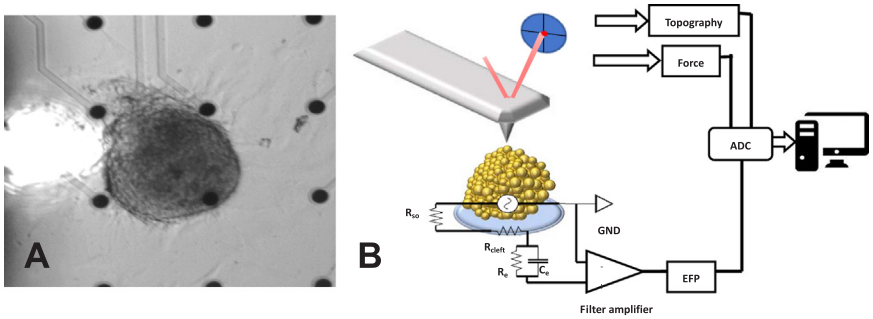

Fig. 1. Real case and schematic of the proposed electromechanical cell-based system. A) A beating cardiac cluster (BCC) placed on a microelectrode array (MEA) sensing area. The bright spot on the left side represents the AFM laser reflecting from the cantilever. Scale bar is 200 μm. B) Schematic representation of the implemented setup. The BCC acts as a periodic micro-voltage generator sensed by the planar electrode, while the AFM measures the topographical displacement and the exerted force. The synchronous acquisition is guaranteed by the common acquisition board and computer.

was gently added atop up to 1 ml. The BCCs were allowed to stabilize up to 3 days in vitro to ensure appropriate adhesion, spreading and formation of cell-electrode contacts. Fig. 1A and Supplementary Fig. 3 show typical BCCs properly placed on MEA, before beginning the experiments. Supplementary video recording presents movements of the adhered BCC clearly demonstrating the regular beating events.

2.4. Setup preparation and experimental protocols

The MEA chip containing the samples was housed in a customized holder made of an aluminum plate with adhesive heating pads and Pt100 temperature probe (RS Components, Corby, UK), and an electronic board with contacts to interface with the MEA electrodes. The electronic board was equipped with 60-channels unity-gain amplifiers to provide low impedance tracks and noise shielding. A second filtering-amplifying stage provides a pass-band of 10–3000 Hz and a total gain of 60 dB. The described holder was then fixed on the motorized stage of an inverted microscope (Olympus IX-81S1F-3, Tokyo, Japan). An AFM scanner head with 15 μm vertical range (BioAFM NanoWizard 3, JPK, Berlin, Germany) was placed above the sample. A soft silicon nitride cantilever SNL-10-D (Bruker, Billerica, MA, USA; nominal spring constant 30 pN m^{-1}) was used as nanomechanical probe to ensure stable contact without applying disruptive forces on the sample. The cantilever spring constant was calibrated before each experiment using the thermal noise method (Butt and Jaschke, 1995). A contact force of 5 nN was found optimal compromise between baseline stability and absence of visible adverse effects on the sample, as previously showed (Pesl et al., 2016a). Each experiment was performed in Tyrode solution (135 mM NaCl, 10 mM HEPES, 5.4 mM KCl, 0.9 mM $MgCl_2$, pH 7.4) supplemented with 10 mM glucose and 1.8 mM $CaCl_2$. After solution exchange, the calibrated cantilever was immersed in liquid and put in contact with the sample several times to identify the superficial center of contraction (i.e. the point with highest vertical positive displacement). Once the center of contraction was found, the drug trials started at an interval of 5 min of recording and 10 min settling time after drug administration or washout (a schematic is provided in Supplementary Fig. 4).

Calcium chloride solution was obtained in Tyrode buffer to give a stepwise increment of 1.1 mM after each addition. Isoproterenol stock solution (30 μM) was made in sterilized MilliQ water to prevent it from quenching: the selected step increment was 300 nM. Finally, Verapamil hydrochloride (Lekoptin, Lek Pharmaceuticals, Ljubljana, Slovinia) stock solutions (127.5 μM) were made in Tyrode, for a step increment of 255 nM. The added volume of drug solution never exceeded 5% of the basal volume in the MEA chip (2 ml).

2.5. Data recording and evaluation

All the presented protocols were repeated on 3 biological replicates of each cell line. Electromechanical recordings were acquired at 5 kHz sampling frequency through a LabVIEW virtual instrument and a proprietary data acquisition board PCI6071E (National Instruments, Austin, TX, USA). Fig. 1B shows a schematic of the acquisition system. Cell mechanocardiogram (MCG) comprehends the time-dependent topographical changes (i.e. the vertical displacement of the AFM piezo actuator, in μm) and the uncompensated force (in nN). The cell-cantilever contact was never lost during drug injections or medium washout. The obtained data were post-processed and analyzed using a Matlab R2016b (Natwick, MA, USA) GUI, using state of the art algorithms. From each recording, the parameters listed in Table 1 and defined in Supplementary Fig. 5 were determined. Statistical analysis was performed in Prism 5.0 (GraphPad Software, La Jolla, CA, USA) and numerical results are presented as mean ± SEM, after passing normality test. Datasets were compared for statistical significance using 1-way analysis of variance (ANOVA) with Bonferroni post-test, or repeated measures 2-way ANOVA with matching on drug concentration levels. Statistical significance was accepted with p-values below 0.05.

3. Results and discussion

3.1. Simultaneous electromechanical recording

The implemented setup allowed the simultaneous visualization, synchronous recording and coupled analysis of the electromechanical features of the cECC (Fig. 2A). The lowest observable noise level in the MEA-EP traces was 33.3 μVpp, whereas the average noise in the force and in the Z height traces were 18.3 pN and 24.5 nm respectively. Online and post-processing digital filtration allowed the analysis of

Table 1
Description of extracted parameters.

Parameter name	Description
Beating rate	Reciprocal of time distance between two adjacent events
Electro mechanical delay	Time between the electrical event and 10% of the next contraction maximum amplitude
Contraction time	Time between 10% of the peak amplitude and the peak, on the rising side
Relaxation time	Time between the event peak and the point corresponding to 10% of the peak amplitude on the falling side
Duration time	The sum of contraction and relaxation times
Average speed of contraction	Mean of the first derivative of the rising part of contraction
Time constant	Time parameter obtained by fitting the relaxation time interval with a decreasing exponential function
Force	The uncompensated force peak-to-peak during the contraction
Z height	The peak excursus of the AFM Z-piezo following the contraction

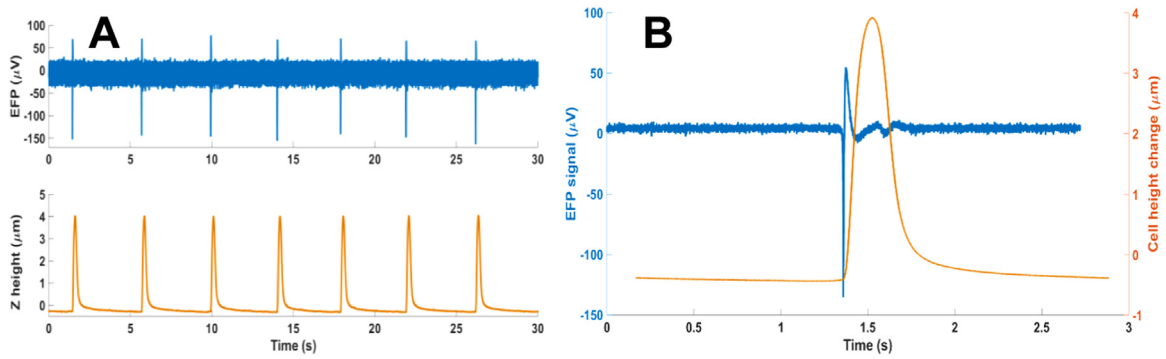

Fig. 2. Representative recording obtained with the implemented electromechanical system, and its post-processed part. A) Simultaneously and synchronously acquired extracellular field potential (top) and mechanical contraction (bottom). B) Averaged curves from the same recording; it is possible to appreciate the noise reduction due to filtering. The two traces are separated by the mean calculated delay.

EFPs with signal-to-noise ratio even close to 0 dB. Nevertheless, approximately half of the plated samples were able to produce a visible EFP trace, while mechanically beating. This issue is most probably due to scarcely-conductive coupling between the MEA planar electrodes and the BCC. Extracellular biopotentials morphology is fundamentally dependent on the conductive sample/electrode proximity and high resistance cleft (Spira and Hai, 2013). As BCC present a mixed cell population of cardiomyocytes and fibroblast-like cells (Supplementary Fig. 1A), as also previously reported (Ma et al., 2011); it is plausible that a non-conductive patch might adhere to the electrode area. In fact, fibroblast-like cells are found to be dedicated into BCC adhesion and spreading (Supplementary Fig. 2). This drawback is easily amendable, since it is possible to remove gently and re-plate BCCs in sterile conditions.

Each measurement lasted between 4 and 5 h, without any remarkable alteration of cardiac activity, if not due to drug stimulation. This can be also seen in the absence of morphological alteration between beginning and end of protocol (Supplementary Fig. 3). Although probed in not completely sterile conditions, it was found that if refilled with antibiotics-containing medium, at the end of the experiments, the samples can keep on without visible contamination up to 4 days. This is particularly useful when testing overnight or realizing several-day treatments. Such evidence shows, like previously reported, how the adopted BCC model presents an outstanding resilience. Since an applied force of 5 nN did not elicit any spontaneous change in the measured parameters, in time, one can infer that the implemented CBBs are really following alteration of cECC and not mechano-electric feedback from stretch-induced depolarization (Zhang et al., 2008).

An accurate peak detection and averaging period selection allowed the reconstruction of important physiological parameters described in Table 1, namely beating rate, contraction speed, cardiac cycle duration and, most importantly, a coupled parameter such as the electro-mechanical delay (EMD). To our best knowledge, this is the first time that such parameter is measured on 3D cardiac in vitro model. Fig. 2B shows the obtainable averaged electromechanical events, corrected by the calculated EMD.

3.2. Differential drug response and correlation analysis is indispensable to distinguish cell-type dependency of cardiac parameters

Once the feasibility and features of the implemented electromechanical CBBs were assessed, we firstly asked whether basal conditions would be sufficient to distinguish diseased and healthy hPSC derived BCC. The baseline beating frequency for all the cell lines tested was not significantly different (0.327 ± 0.023 Hz for CTRL, 0.325 ± 0.062 Hz for DORSO and 0.468 ± 0.103 Hz for DMD). The same evidence was found for other important functional parameters, such as the basal force (2.1 ± 1.9 nN for CTRL, 12.0 ± 4.7 nN for DORSO and 0.89 ± 0.46 nN for DMD) and EMD (23.0 ± 1.3 ms for CTRL, 22.0 ± 3.0 ms for DORSO and 25.6 ± 5.3 ms for DMD). Therefore, different stimulation / inhibition drug protocols were tested to validate the adopted models versus the expected cardiac response and assess the presence of cell type-dependent differences.

3.3. Calcium trials

Initially, the dependence of cardiac parameters on extracellular Ca^{2+} concentration was tested. This ion and its extracellular availability are in fact of primary importance for cECC, particularly for the hPSC-derived CMs, which possess an immature calcium handling toolkit (Keung et al., 2014) and rely mostly on membrane transport (Youm, 2016). Cell type-dependency was found by 2-way ANOVA for beating rate ($p = 0.007$), contraction duration ($p = 0.0003$), time decay ($p < 0.0001$) and EMD ($p = 0.026$). A difference close to significance was reached for the average speed of contraction ($p = 0.069$). The effect of the Ca^{2+} concentration was found significant only in relationship to the beating rate ($p < 0.0001$). All cell lines experienced a decrease in beating rate proportional to Ca^{2+} concentration. The CTRL and DORSO groups plateaued around ¾ of the basal rate (67 ± 10% and 68.6 ± 5.1%, respectively), while the DMD group decreased to 89.5 ± 3.2% of its basal rate. The beating rate phenotype of mutation-carrying cell line correlates with previously described pre-existing calcium stress impairing inward ion flux (Fanchaouy et al., 2009). This frequency decrease was paralleled by an increase of exerted force in all the cell lines (120.3 ± 9.4% for the CTRL group, 110 ± 14% for DORSO and 112 ± 19% for DMD). This phenomenon is due to the immature contractile phenotype of hPSC-derived CMs, which possess negative frequency-force relationship (Pesl et al., 2016b). The observed change of contractile events was found as an increase of the relaxation period, expressed by the decay time constant for the CTRL and DORSO groups (108.1 ± 3.5% and 110.5 ± 4.2%, respectively) and a decrease for DMD (84.3 ± 5.2%). The Ca^{2+} dependent decay time decrease in dystrophin mutation-carrying line is in correlation with previously described pre-existing calcium overload (Fanchaouy et al., 2009), which may limit the contraction dilation due to saturated sarcomere, probably resulting in limited ability of the DMD CBB to employ force imposed reaction during cluster stretch as imposed in healthy tissue by Frank Starling mechanisms. The EMD, a parameter directly connected to electromechanical coupling, did prove statistically significant for cell-type. CTRL did not show a dose-dependent relation with the Ca^{2+} concentration (109–99% variation range); DORSO showed a similar trend with only non-significant increase with respect to CTRL (142–131%), validating the CBB's robustness toward line specific variability in differentiation efficiency. Conversely, the DMD group showed a dose-dependent trend (up to 257 ± 71% of the basal delay); it is possible that increasing calcium levels are gradually

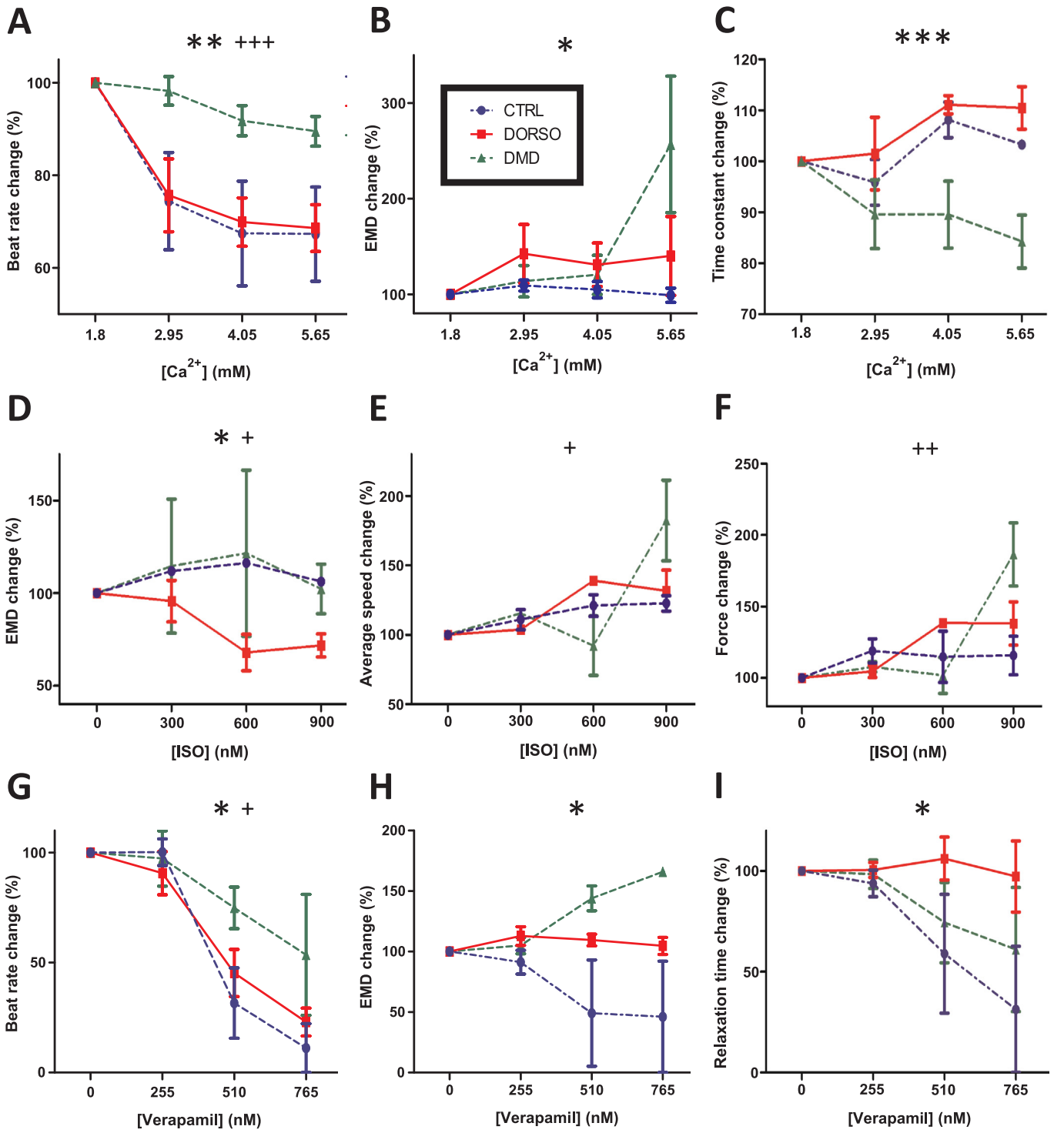

Fig. 3. Selected results of drug trials performed with the presented electrochemical cell-based biosensor. The top row (A-B-C) represents extracellular calcium concentration trials. The middle row (D-E-F) β-adrenergic stimulation trials (Isoproterenol). The bottom row (G-H-I) represent class IV antiarrhythmic / calcium channel blocker trial (Verapamil). The * symbol indicates statistically significant difference according to the beating cardiac cluster type. The + symbol indicates statistically significant difference due to the chemical concentration. One symbol indicates a p-value < 0.05, two symbols < 0.01, three symbols < 0.001. All the comparisons are carried on with repeated measurements 2-way ANOVA with row matching (drug concentration).

impairing the already elevated activity of an altered ryanodine receptor to coordinate the calcium-induced calcium release (Fauconier et al., 2010). The previous results are summarized in Fig. 3A-C.

3.4. Isoproterenol trials

The β-adrenergic stimulation was performed via increasing isoproterenol concentration to assess the ionotropic and chronotropic cell line-dependent features. Surprisingly, no extracted parameter showed significant dependency over the cell type, except for the EMD ($p = 0.0130$), which was also significantly concentration dependent ($p = 0.012$). Other concentration-dependent parameters were the average speed of contraction ($p = 0.031$) and the exerted force ($p = 0.006$), with DMD group showing marked increase at end

concentration (182 ± 29% and 186 ± 22% respectively). In contrast, DORSO experienced roughly 1/3 increase of these parameters (132 ± 15% for average speed and 138 ± 15% for force) and CTRL only 1/5 increase (122.7 ± 5.5% and 116 ± 14% respectively). Isoproterenol effect appears to have a threshold concentration between 300 and 600 nM. After this threshold, the CTRL and DMD groups slightly altered EMD (101.0 ± 6.0% and 96.6 ± 2.7%, respectively), whereas the DORSO group decreased its measured EMD to 73.0 ± 7.6% of the baseline value. This difference might be explained with better differentiation grade of dorsomorphin-treated groups, since dorsomorphin is an inhibitor of BMP signaling and promotes cardiac differentiation (Kattman et al., 2011). It is therefore plausible that an improved differentiation guarantees a better BCC syncytium, able to improve cECC timing in response to adrenergic stimulation. The notable results are shown in Fig. 3D-F. The same negative beating rate/force relationship was also noticed for all the cell lines, except when an arrhythmic behavior (e.g. multiple beating modes) was induced.

3.5. Verapamil trials

The antagonist trials were carried on L-type calcium channels to observe the reaction of different BCCs to class IV antiarrhythmics. Verapamil, as an example of this class, was shown to improve skeletal muscle force in DMD patients but led also to adverse cardiac side effect. However, no data on mechanism of such adverse effect exists (Nascimento Osorio et al., 2018). Previously, the growing CMs were coupled to RTCA impedance system, which allowed to quantify only beat rate effects of Verapamil (Wang et al., 2013). Here, the beat rate influence of drug showed to be cell type-dependent ($p = 0.019$) and dose dependent ($p = 0.001$). The EMD parameter was found to be only cell-type dependent ($p = 0.0316$), together with the relaxation time ($p = 0.030$). The measured exerted force and Z height change were found solely dose-dependent ($p = 0.015$ and $p = 0.019$ respectively). The DMD cells showed decrease in beating rate down to 53 ± 27% of baseline, compared to 11 ± 11% of CTRL and 23.0 ± 6.3% of DORSO groups. The EMD shows different trends for each cell line: for the CTRL groups, the delay drops to 46 ± 46% of the baseline; DORSO group upped to 112% of the baseline and ended the trial at 104.0 ± 7.1%; the DMD group showed an increase of 143% to finish the trial at 111 ± 55%. These distinct trends can be due to the different biological backgrounds of the BCC models: CTRL group may respond to L-type channel inhibition by referring to the inositol-3-phosphate complex, which spontaneously produces calcium influx in embryonic cardiac phenotype (Youm, 2016); dorsomorphin-treated BCC might express higher number of functional L-type calcium channels, therefore being more resilient to the same drug concentration and present delayed coupling, with stable force level. DMD samples can present calcium leaking at the membrane level (Burr and Molkentin, 2015), although cECC delay is linearly increasing, which together with the decreasing force suggests impairment of the contractile machinery (Li et al., 2014). The mentioned notable results are shown in Fig. 3G-I.

4. Conclusions

We have successfully implemented and tested the electro-mechanical cell-based biosensor for the simultaneous and synchronous probing of cardiac excitation-contraction coupling. The system allows the characterization of cardiac models through differential drug trials and sample-type discrimination. For the first time, to our knowledge, a distinctive beating-force relation was shown for Duchenne muscular dystrophy cardiac models. The bioelectromechanical parameters derived from the cardiomyocyte cluster based models provide important insights into heart pathologies and sometimes (such as in β-adrenergic stimulation assays) serve as the only discriminant between different models.

Current limitations of the systems regard the non-sterility of the measurement environment, and the localized probing of a 3D model with a single MEA electrode and AFM cantilever. The system also suffers from a substantial biological sample variability, which requires more experimental repetitions to achieve better accuracy of results; this can be overcome by suitable choice of drug treatment regimens to focus the data collection toward the desired disease phenotype. Future improvement with higher-density electrode arrays and tip-less cantilevers providing a wider surface contact should provide a higher information content and improve stability of models, respectively.

Acknowledgments

This research has been financially supported by the Ministry of Education, Youth and Sports of the Czech Republic under the project CEITEC 2020 (LQ1601) and ICRC (LQ1605), the CIISB research infrastructure project LM2015043 supported the AFM measurements at the Core Facility Nanobiotechnology, and the Grant Agency of the Czech Republic (GACR) provided support through grant no. P302/12/G157.

Conflict of interest

The authors declare no conflict of interest.

Appendix A. Supporting information

Supplementary data associated with this article can be found in the online version at doi:10.1016/j.bios.2018.10.021.

References

Acimovic, I., Vilotic, A., Pesl, M., Lacampagne, A., Dvorak, P., Rotrekl, V., Meli, A.C., 2014. Biomed. Res. Int. 2014, 512831.
Adewumi, O., Aflatoonian, B., Ahrlund-Richter, L., Amit, M., Andrews, P.W., Beighton, G., Bello, P.A., Benvenisty, N., Berry, L.S., et al., 2007. International stem cell initiative. Nat. Biotechnol. 25, 803–816.
Alonso, L., Goldmann, W.H., 2003. Life Sci. 72, 2553–2560.
Bauwens, C.L., Toms, D., Ungrin, M., 2016. J. Vis. Exp. 115, e54308.
Bers, D.M., 2002. Cardiac excitation–contraction coupling. Nature 415, 198–205.
Burr, A.R., Molkentin, J.D., 2015. Cell Death Differ. 22, 1402–1412.
Burridge, P.W., Matsa, E., Shukla, P., Lin, Z.C., Churko, J.M., Ebert, A.D., Lan, F., Diecke, S., Huber, B., Mordwinkin, N.M., Plews, J.R., Abilez, O.J., Cui, B., Gold, J.D., Wu, J.C., 2014. Nat. Methods 11, 855–860.
Butt, H.-J., Jaschke, M., 1995. Nanotechnology 6, 1–7.
Caluori, G., Pribyl, J., Cmiel, V., Pesl, M., Potocnak, T., Provaznik, I., Skladal, P., Rotrekl, V., 2018. Simultaneous study of mechanobiology and calcium dynamics on hESC-derived cardiomyocytes clusters. J. Mol. Recognit. e2760.
Cogollo, J.F.S., Tedesco, M., Martinoia, S., Raiteri, R., 2011. Biomed. Microdevice 13, 613–621.
Dell'Era, P., Benzoni, P., Crescini, E., Valle, M., Xia, E., Consiglio, A., Memo, M., 2015. World J. Stem Cells 7, 329–342.
Doevendans, P.A., Kubalak, S.W., An, R.-H., Becker, D.K., Chien, K.R., Kass, R.S., 2000. J. Mol. Cell. Cardiol. 32, 839–851.
Doppler, S.A., Deutsch, M.A., Lange, R., Krane, M., 2013. J. Thorac. Dis. 5, 683–697.
Fanchaouy, M., Polakova, E., Jung, C., Ogrodnik, J., Shirokova, N., Niggli, E., 2009. Cell Calcium 46, 114–121.
Finsterer, J., Stöllberger, C., 2003. Cardiology 99, 1–19.
Hao, J., Daleo, M.A., Murphy, C.K., Yu, P.B., Ho, J.N., Hu, J., Peterson, R.T., Hatzopoulos, A.K., Hong, C.C., 2008. PLOS One 3, e2904.
Kattman, S.J., Witty, A.D., Gagliardi, M., Dubois, N.C., Niapour, M., Hotta, A., Ellis, J., Keller, G., 2011. Cell Stem Cell 18, 228–240.
Keung, W., Boheler, K.R., Li, R.A., 2014. Stem Cell Res. Ther. 5, 17.
Kilpatrick, J.I., Revenko, I., Rodriguez, B.J., 2015. Adv. Healthc. Mater. 4, 2456–2474.
Knoll, R., Hoshijima, M., Hoffman, H.M., Person, V., Lorenzen-Schmidt, I., Bang, M.L., Hayashi, T., Shiga, N., Yasukawa, H., Schaper, W., McKenna, W., Yokoyama, M., Schork, N.J., Omens, J.H., McCulloch, A.D., Kimura, A., Gregorio, C.C., Poller, W., Schultheiss, P., Chien, K.R., 2002. Cell 111, 943–955.
Laurila, E., Ahola, A., Hyttinen, J., Aalto-Setälä, K., 2015. Biochim Biophys. Acta 1863-7B, 1864–1872.
Lian, X., Zhang, J., Azarin, S.M., Zhu, K., Hazeltine, L.B., Bao, X., Hsiao, C., Kamp, T.J., Palecek, S.P., 2012. Nat. Protoc. 8, 162–175.
Li, Y., Zhang, S., Zhang, X., Li, J., Ai, X., Zhang, L., Yu, D., Yu, D., Ge, S., Peng, Y., Chen, X., 2014. Cardiovasc. Res. 103, 60–71.
Liang, P., Lan, F., Lee, A.S., Gong, T., Sanchez-Freire, V., Wang, Y., Diecke, S., Sallam, K., Knowles, J.W., Wang, P.J., Nguyen, P.K., Bers, D.M., Robbins, R.C., Wu, J.C., 2013. Circulation 127, 1677–1691.
Liu, J., Sun, N., Bruce, M.A., Wu, J.C., Butte, M.J., 2012a. PLoS One 7, e37559.

Liu, Y., Feng, J., Shi, L., Niu, R., Sun, Q., Liu, H., Li, J., Guo, J., Zhu, J., Han, D., 2012b. Nanoscale 4, 99–102.
Ma, J., Guo, L., Fiene, S.J., Anson, B.D., Thomson, J.A., Kamp, T.J., Kolaja, K.L., Swanson, B.J., January, C.T., 2011. Am. J. Physiol. Hear. Circ. Physiol 301, H2006–H2017. https://doi.org/10.1152/ajpheart.00694.2011.
Moretti, A., Laugwitz, K.L., Dorn, T., Sinnecker, D., Mummery, C., 2013. Cold Spring Harb. Perspect. Med. 3.
Motta, B.M., Pramstaller, P.P., Hicks, A.A., Rossini, A., 2017. Stem Cells Int. 2017, 8960236.
Mummery, C.L., Zhang, J., Ng, E.S., Elliott, D.A., Elefanty, A.G., Kamp, T.J., 2012. Circ. Res. 111, 344–358.
Nascimento Osorio, A., Medina Cantillo, J., Camacho Salas, A., Madruga Garrido, M., Vilchez Padill, J.J., 2018. Neurologia. https://doi.org/10.1016/j.nrleng.2018.01.001. (In press).
Pesl, M., Acimovic, I., Pribyl, J., Hezova, R., Vilotic, A., Fauconnier, J., Vrbsky, J., Kruzliak, P., Skladal, P., Kara, T., Rotrekl, V., Lacampagne, A., Dvorak, P., Meli, A.C., Fauconnier, J., Vrbsky, J., Kruzliak, P., Skladal, P., Kara, T., Rotrekl, V., Lacampagne, A., Dvorak, P., Meli, A.C., 2013. Heart Vessels 29, 834–846.
Pesl, M., Ivana, A., Pribyl, J., Hezova, R., Vilotic, A., Aimond, F., Fauconnier, J., Vrbsky, J., Kruzliak, P., Skladal, P., Kara, T., Rotrekl, V., Lacampagne, A., Dvorak, P., Meli, A.C., 2014. Biophys. J. 106 (565A–565A).
Pesl, M., Pribyl, J., Acimovic, I., Vilotic, A.A., Jelinkova, S., Salykin, A., Lacampagne, A., Dvorak, P., Meli, A.C., Skladal, P., Rotrekl, V., 2016a. Biosens. Bioelectron. 85, 751–757.
Pesl, M., Pribyl, J., Caluori, G., Cmiel, V., Acimovic, I., Jelinkova, S., Dvorak, P., Starek, Z., Skladal, P., Rotrekl, V., 2016b. J. Mol. Recognit. 30, e2602.
Regmi, S., Jeong, J.H., 2016. Macromol. Res. 24, 1037–1046.
Rothermel, A., Kurz, R., Ruffer, M., Weigel, W., Jahnke, H.G., Sedello, A.K., Stepan, H., Faber, R., Schulze-Forster, K., Robitzki, A.A., 2005. Cell. Physiol. Biochem. 16, 51–58.
Sinnecker, D., Laugwitz, K.-L.L., Moretti, A., 2014. Pharmacol. Ther. 143, 246–252.
Spira, M.E., Hai, A., 2013. Nat. Nanotechnol. 8, 83–94.
Takeda, M., Miyagawa, S., Fukushima, S., Saito, A., Ito, E., Harada, A., Sawa, Y., 2018. Tissue Eng. C Meth. 24, 56–67.
Tzatzalos, E., Abilez, O.J., Shukla, P., Wu, J.C., 2016. Adv. Drug Deliv. Rev. 96, 234–244.
Vatta, M., Sinagra, G., Brunelli, L., Faulkner, G., 2005. J. Cardiovasc. Med. 10, 149–156.
Wang, T., Hu, N., Cao, J., Wu, J., Su, K., Wang, P., 2013. Biosens. Bioelectron. 49, 9–13.
Youm, J.B., 2016. Integr. Med. Res. 5, 3–10.
Zhang, Y., Sekar, R.B., McCulloch, A.D., Tung, L., 2008. Prog. Biophys. Mol. Biol. 97, 367–382.
Zheng, W., Thorne, N., McKew, J.C., 2013. Drug Discov. Today 18, 1067–1073.

P. Ošťádal a kol.

Continual measurement of arterial dP/dtmax enables minimally invasive monitoring of left ventricular contractility in patients with acute heart failure
(id 647)

Critical Care
Impact Factor: 6,959

Ostadal et al. Critical Care (2019) 23:364
https://doi.org/10.1186/s13054-019-2654-8

Critical Care

RESEARCH Open Access

Continual measurement of arterial dP/dt$_{max}$ enables minimally invasive monitoring of left ventricular contractility in patients with acute heart failure

Petr Ostadal*, Dagmar Vondrakova, Andreas Krüger, Marek Janotka and Jan Naar

Abstract

Background: Continuous, reliable evaluation of left ventricular (LV) contractile function in patients with advanced heart failure requiring intensive care remains challenging. Continual monitoring of dP/dt$_{max}$ from the arterial line has recently become available in hemodynamic monitoring. However, the relationship between arterial dP/dt$_{max}$ and LV dP/dt$_{max}$ remains unclear. This study aimed to determine the relationship between arterial dP/dt$_{max}$ and LV dP/dt$_{max}$ assessed using echocardiography in patients with acute heart failure.

Methods: Forty-eight patients (mean age 70.4 years [65% male]) with acute heart failure requiring intensive care and hemodynamic monitoring were recruited. Hemodynamic variables, including arterial dP/dt$_{max}$, were continually monitored using arterial line pressure waveform analysis. LV dP/dt$_{max}$ was assessed using continuous-wave Doppler analysis of mitral regurgitation flow.

Results: Values from continual arterial dP/dt$_{max}$ monitoring were significantly correlated with LV dP/dt$_{max}$ assessed using echocardiography ($r = 0.70$ [95% confidence interval (CI) 0.51–0.82]; $P < 0.0001$). Linear regression analysis revealed that LV dP/dt$_{max}$ = 1.25 × (arterial dP/dt$_{max}$) ($P < 0.0001$). Arterial dP/dt$_{max}$ was also significantly correlated with stroke volume (SV) ($r = 0.63$; $P < 0.0001$) and cardiac output (CO) ($r = 0.42$; $P = 0.0289$). In contrast, arterial dP/dt$_{max}$ was not correlated with SV variation, dynamic arterial elastance, heart rate, systemic vascular resistance (SVR), or mean arterial pressure. Markedly stronger agreement between arterial and LV dP/dt$_{max}$ was observed in subgroups with higher SVR ($N = 28$; $r = 0.91$; $P < 0.0001$), lower CO ($N = 26$; $r = 0.81$; $P < 0.0001$), and lower SV ($N = 25$; $r = 0.60$; $P = 0.0014$). A weak correlation was observed in the subjects with lower SVR ($N = 20$; $r = 0.61$; $P = 0.0004$); in the subgroups with higher CO ($N = 22$) and higher SV ($N = 23$), no significant correlation was found.

Conclusion: Our results suggest that in patients with acute heart failure requiring intensive care with an arterial line, continuous calculation of arterial dP/dt$_{max}$ may be used for monitoring LV contractility, especially in those with higher SVR, lower CO, and lower SV, such as in patients experiencing cardiogenic shock. On the other hand, there was only a weak or no significant correlation in the subgroups with higher CO, higher SV, and lower SVR.

Keywords: Left ventricle, Contractility, dP/dt, Systemic vascular resistance, Cardiac output, Stroke volume, Acute heart failure

* Correspondence: ostadal.petr@gmail.com
Cardiovascular Center, Na Homolce Hospital, Roentgenova 2, 150 00 Prague, Czech Republic

Background

Left ventricular (LV) contractility is one of the most important parameters determining LV performance and cardiac function and, therefore, directly influences global hemodynamic status [1]. Clinical conditions with impaired LV contractility, such as heart failure or septic cardiomyopathy, are frequent subjects of intensive and acute cardiology care [1]. There is, therefore, an apparent clinical need for bedside measurement or even monitoring of contractility. However, current options for the assessment of LV contractility are significantly limited. The reference method for the measurement of LV contractility (i.e., LV end-systolic elastance [2]) cannot be used in routine clinical practice due to invasiveness and technical issues [3, 4]. The maximum rate of LV pressure rise during ventricular contraction (LV dP/dt_{max}) has been adopted as a surrogate marker of LV inotropic state and contractility [5]. This parameter is determinable in clinical settings; however, it requires direct LV pressure measurement, which is impractical and too invasive for LV contractility monitoring. LV dP/dt_{max} can also be estimated non-invasively using echocardiographic techniques [6, 7]. However, although this measurement can be performed repeatedly, it is not feasible for continuous monitoring and is frequently limited by low-quality signal.

Recently, a new surrogate has been proposed—arterial dP/dt_{max}. This parameter can be calculated from the arterial pressure waveform, obtained minimally invasively from a peripheral arterial line [8–10] or even non-invasively [11]. Arterial dP/dt_{max} is, therefore, available bedside and in patients with an arterial line already used for pressure monitoring and blood gas analyses; it does not require any additional invasive access. Moreover, arterial dP/dt_{max} can be measured on a beat-by-beat basis and, therefore, continually monitored. On the other hand, arterial dP/dt_{max} is not only determined by LV contraction but is also influenced by various peripheral arterial factors and load conditions [8–11]. Recently, several experimental studies demonstrating a significant relationship between arterial dP/dt_{max} and LV contractility have been published [8–10]. To date, however, clinical studies focusing on the relationship between arterial and LV dP/dt_{max} in patients with acute heart failure requiring intensive care and an arterial line are lacking. The aim of our study was, therefore, to assess the relationship between arterial and LV dP/dt_{max} in this patient population.

Methods

Study population

Consecutive patients admitted between January and September 2018 to the cardiology intensive care unit due to acute heart failure requiring an arterial line for invasive blood pressure monitoring and central venous catheter were eligible for the study. Patients with moderate to severe aortic stenosis, those who required mechanical circulatory support, and those with absence of mitral regurgitation enabling measurement of LV dP/dt_{max} were excluded. All patients have to be at the time of measurement on stable doses of inotropes/vasopressors, on stable ventilation support, and with regular cardiac rhythm.

Hemodynamic measurement

Arterial blood pressure (mean), central venous pressure (mean), heart rate, cardiac output (CO), stroke volume (SV), dynamic arterial elastance, and systemic vascular resistance (SVR) were measured using a clinical monitoring platform (EV1000, equipped with HPI software, Edwards Lifesciences, Irvine, CA, USA) connected to the arterial and central venous lines. SVR was calculated using the formula: $SVR = 80 \times (MAP - CVP)/CO$. The dynamic arterial elastance was defined as the ratio of pulse pressure variation and stroke volume variation. All parameters were calculated in the 20-s interval that contains few respiratory cycles. An arterial catheter was inserted into the left or right radial artery, and the left or right jugular vein was used for central venous access, with the tip of catheter in the superior vena cava.

dP/dt_{max} measurement

Arterial dP/dt_{max} was measured from the arterial pressure curve by the EV1000 system and HPI software. The system calculates dP/dt_{max} for each beat in a 20-s cycle, then the median value of all the dP/dt_{max} values in the 20-s interval is displayed; values obtained at the time of LV dP/dt_{max} were used in the analysis. LV dP/dt_{max} was measured at the end of expiration using transthoracic echocardiography (Phillips CX50, Amsterdam, The Netherlands) from the analysis of the mitral regurgitation jet by continuous-wave Doppler; calculation was based on the time interval (T) between blood flow of 1 m/s and 3 m/s using the formula: LV $dP/dt_{max} = 32/T$ [6, 7]. Three measurements were performed at one time, and the mean values were used for analysis. The echocardiographic measurements were performed by an experienced physician who was blinded to the arterial dP/dt_{max} values.

Statistical analysis

Gaussian distribution of the measurement data was tested using the Shapiro-Wilk normality test. Correlation was tested using the Spearman test by calculating the Spearman correlation coefficient. LV and arterial dP/dt_{max} were compared using the Bland-Altman analysis. Linear regression was used to derive the equation representing the relationship between LV and arterial dP/dt_{max}. The analyses were performed using GraphPad Prism version 7 (GraphPad

Software, Inc., La Jolla, CA, USA) and MedCalc (MedCalc Software, Ostend, Belgium); $P < 0.05$ was considered to be statistically significant.

Results

Forty-eight patients were enrolled in the study; baseline characteristics of the study population are summarized in Table 1. The mean age was 70.4 years, the majority were males (65%), and the main cause of acute heart failure was ischemic cardiomyopathy (65%). Eighty-five percent of patients were treated with intravenous inotropes, and the majority required vasopressors (73%).

The values from continual arterial dP/dt_{max} monitoring were significantly correlated with LV dP/dt_{max} assessed using echocardiography ($r = 0.70$ [95% confidence interval (CI) 0.51–0.82]; $P < 0.0001$) (Fig. 1). Linear regression revealed that LV $dP/dt_{max} = 1.25 \times$ (arterial dP/dt_{max}) ($P < 0.0001$). Arterial dP/dt_{max} was significantly correlated with SV ($r = 0.63$ [95% CI 0.41–0.78]; $P < 0.0001$) and CO ($r = 0.42$ [95% CI 0.14–0.63]; $P = 0.003$). In contrast, arterial dP/dt_{max} was not correlated with SV variation, dynamic arterial elastance, heart rate, SVR, or mean arterial pressure (Table 2).

The correlation between arterial and LV dP/dt_{max} was calculated also in subgroups above and below the mean value of the recorded variables. Marked differences in the correlation between arterial and LV dP/dt_{max} were observed in the subgroups based on the mean SVR, CO, and SV; on the other hand, similar correlation was observed in the subgroups based on SV variation ($r = 0.54$ vs. $r = 0.59$), dynamic arterial elastance ($r = 0.70$ vs. $r = 0.73$), heart rate (0.68 vs. 0.72), and mean arterial pressure ($r = 0.80$ vs. $r = 0.76$).

Table 1 Baseline characteristics ($n = 48$)

Characteristics	Value
Male sex	31 (65)
Age (years, mean ± SD)	70.4 ± 8.1
Decompensated CHF	31 (65)
De novo AHF	17 (35)
Ischemic cardiomyopathy	31 (65)
Dilated cardiomyopathy	7 (15)
Acute myocardial infarction	15 (31)
Severe mitral regurgitation	19 (40)
Left ventricular ejection fraction (%, mean ± SD)	28 ± 10
Mechanical ventilation	17 (35)
Inotropes (dobutamine, milrinone)	41 (85)
Vasopressors (norepinphrine, vasopressin)	35 (73)
Heart rate (beats/min, mean ± SD)	92.7 ± 11.7
Mean arterial pressure (mmHg, mean ± SD)	74.0 ± 5.2
Cardiac output (L/min, mean ± SD)	6.0 ± 1.2
Stroke volume (mL, mean ± SD)	65.5 ± 10.1
Systemic vascular resistance (dyn·s/cm^5, mean ± SD)	891.5 ± 236.3

Data presented as *n* (%) unless otherwise indicated. *CHF* chronic heart failure, *AHF* acute heart failure

SVR subgroups

The study population was divided into two groups according to the mean level of SVR (> or < 900 dyn·s/cm^5). In the subgroup of patients with lower SVR (< 900 dyn·s/cm^5 [$n = 28$]), a statistically significant correlation between arterial dP/dt_{max} and LV dP/dt_{max} was found ($r = 0.61$ [95% CI 0.31 to 0.80]; $P = 0.0004$). However, in the subgroup with higher SVR (> 900 dyn·s/cm^5 [$n = 20$]), the correlation between arterial and LV dP/dt_{max} was markedly stronger and highly statistically significant ($r = 0.91$ [95% CI 0.78 to 0.97]; $P < 0.0001$) (Fig. 2). Linear regression analysis revealed that in subgroup with higher SVR, LV dP/dt_{max} could be calculated according to the equation: LV $dP/dt_{max} = 1.08 \times$ (arterial dP/dt_{max}).

CO subgroups

In the subgroup of patients with lower CO (< 6 L/min [$n = 26$]), a strong and highly statistically significant correlation between arterial dP/dt_{max} and LV dP/dt_{max} was found ($r = 0.81$ [95% CI 0.60 to 0.91]; $P < 0.0001$). In contrast, in the subgroup with higher CO (> 6 L/min [$n = 22$]), the correlation between arterial and LV dP/dt_{max} was not statistically significant ($r = 0.29$ [95% CI − 0.16 to 0.64]; $P = 0.18$) (Fig. 3). Linear regression revealed that in the subgroup with lower CO, LV dP/dt_{max} could be calculated according to the equation: LV $dP/dt_{max} = 1.21 \times$ (arterial dP/dt_{max}).

SV subgroups

In the subgroup of patients with lower SV (< 65 mL [$n = 25$]), a statistically significant correlation between arterial dP/dt_{max} and LV dP/dt_{max} was found ($r = 0.60$ [95% CI 0.26 to 0.81]; $P = 0.0014$). In contrast, in the subgroup with higher SV (> 65 mL [$n = 23$]), the correlation of between arterial and LV dP/dt_{max} was not statistically significant ($r = 0.38$ [95% CI − 0.05 to 0.69]; $P < 0.07$) (Fig. 4). Linear regression revealed that in the subgroup with lower SV, LV dP/dt_{max} could be calculated according to the equation: LV $dP/dt_{max} = 1.33 \times$ (arterial dP/dt_{max}).

Discussion

Our results demonstrate that in adult patients with acute heart failure, the values of arterial dP/dt_{max}, which can be continuously monitored by analysis of the pressure waveform, were significantly correlated with LV dP/dt_{max}. An even better agreement between arterial dP/dt_{max} and LV dP/dt_{max} was observed in subgroups with higher SVR, lower CO, and lower SV. This observation is particularly important because monitoring LV contractility is most desirable in patients with heart failure with critical hemodynamic

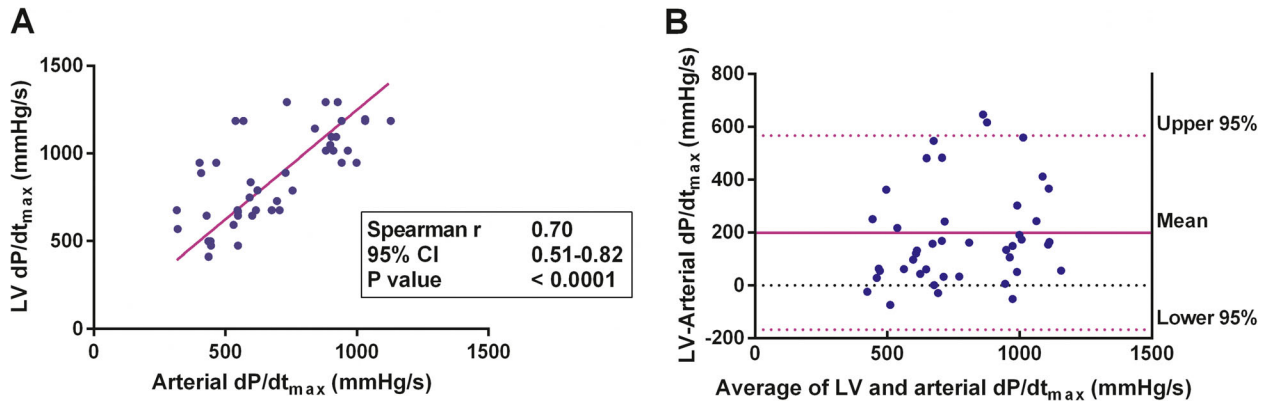

Fig. 1 Arterial and left ventricular (LV) dP/dt_{max}. **a** Correlation between arterial and LV dP/dt_{max} with linear regression curve. **b** The Bland-Altman plot of agreement between arterial and LV dP/dt_{max}

collapse, such as in cardiogenic shock, characterized by increased SVR and decreased CO and SV. In contrast, in the subgroups with lower SVR, higher CO, and higher SV, the correlation was weak or even absent.

Acute heart failure is a critical condition in which LV contractility is commonly depressed, and therapeutic strategies are frequently based on increasing inotropy [12]. Although LV contractility status can be routinely and intermittently assessed using echocardiography in patients with acute heart failure, even with the use of new techniques, the measurement can be inaccurate and interpretation difficult [13–17]. There are currently highly limited options for continuous LV contractility monitoring. In contrast to echocardiographic techniques, the maximal rate of arterial pressure increases during systole (arterial dP/dt_{max}) can be easily and continuously calculated from the pressure waveform. It has been shown in animal studies that arterial dP/dt_{max} may correlate with LV contractility status under various hemodynamic conditions. In a porcine model of endotoxin-induced shock and catecholamine infusion, Morimont et al. [8] observed that arterial dP/dt_{max} was significantly correlated with LV contractility measured by LV end-systolic elastance (Ees) or LV dP/dt_{max}. The authors also found a better correlation when adequate vascular filling according to the arterial pulse pressure variation was achieved. These results are consistent with our observations. We have demonstrated a strong relationship between arterial and LV dP/dt_{max} under higher SVR, which could be also a result of increased vascular filling. Monge Garcia et al. [10] analyzed the relationship among arterial dP/dt_{max}, LV dP/dt_{max}, and Ees in sequential changes of afterload, preload, and contractility in pigs. In this study, arterial dP/dt_{max} enabled the tracking of Ees changes, especially during the modification of afterload and contractility, and changes in cardiac contractility (i.e., Ees) were the main determinants of arterial dP/dt_{max} changes. Moreover, these observations are in good agreement with our results; Monge Garcia et al. recorded higher values of LV dP/dt_{max} in comparison with arterial dP/dt_{max}, similar to our study. A good correlation between arterial dP/dt_{max} and LV dP/dt_{max} in heart failure patients was also reported in the study by Tartiere et al. [11], in which the dP/dt_{max} from the radial artery was assessed noninvasively using applanation tonometry and LV dP/

Table 2 Correlation between arterial dP/dt_{max} and other recorded hemodynamic variables

Variable	Spearman's *r*	95% confidence interval	*P* value
Stroke volume	0.6297	0.4137 to 0.7786	< 0.0001
Cardiac output	0.419	0.1446 to 0.6336	0.003
Stroke volume variation	− 0.2635	− 0.5159 to 0.03099	0.0703
Dynamic arterial elastance	0.06733	− 0.2293 to 0.3525	0.6493
Heart rate	− 0.06501	− 0.3505 to 0.2315	0.6607
Systemic vascular resistance	− 0.1734	− 0.4431 to 0.1251	0.2385
Mean blood pressure	0.345	− 0.02172 to 0.6298	0.0574

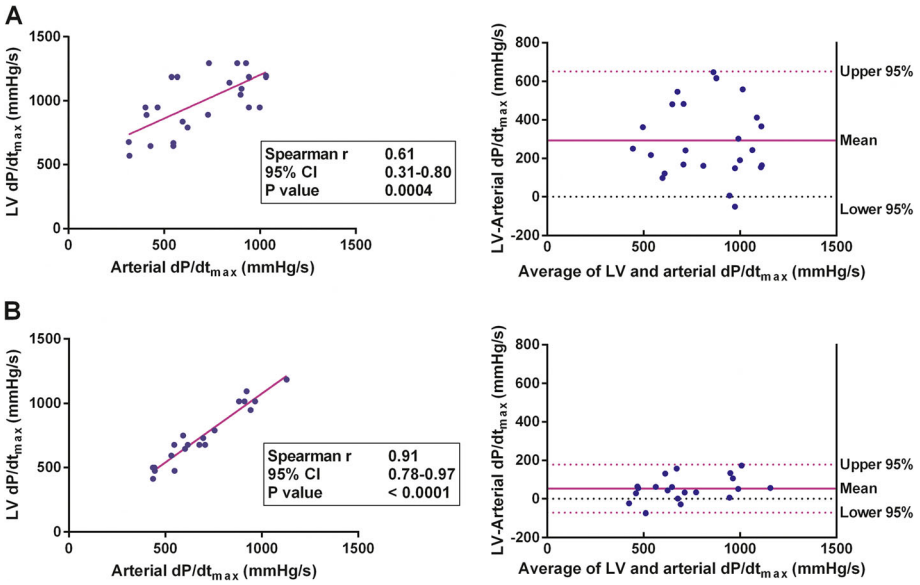

Fig. 2 Arterial and left ventricular (LV) dP/dt_{max} in subgroups according to systemic vascular resistance (SVR). **a** Subgroup with lower SVR (< 900 dyn·s/cm^5, *N* = 20)—correlation between arterial and LV dP/dt_{max} with linear regression curve (left), and the Bland-Altman plot of the agreement between arterial and LV dP/dt_{max} (right). **b** Subgroup with higher SVR (> 900 dyn·s/cm^5, *N* = 28)—correlation between arterial and LV dP/dt_{max} with linear regression curve (left), and the Bland-Altman plot of the agreement between arterial and LV dP/dt_{max} (right)

dt_{max}. Our results are also consistent with the observation by Scolletta et al. [18] who reported significant correlation between arterial dP/dt_{max} and LV dP/dt_{max} in a group of critically ill patients. Furthermore, and again similar to our results, a very close linear relationship was found between arterial dP/dt_{max} from the femoral artery and invasively measured LV dP/dt_{max} (with a catheter in the LV) in patients scheduled for coronary artery bypass surgery [9]; arterial dP/dt_{max} also underestimated LV dP/dt_{max} in this study.

In contrast, Kim et al. [19] studied the relationship between arterial dP/dt_{max} from the radial artery, aortic dP/

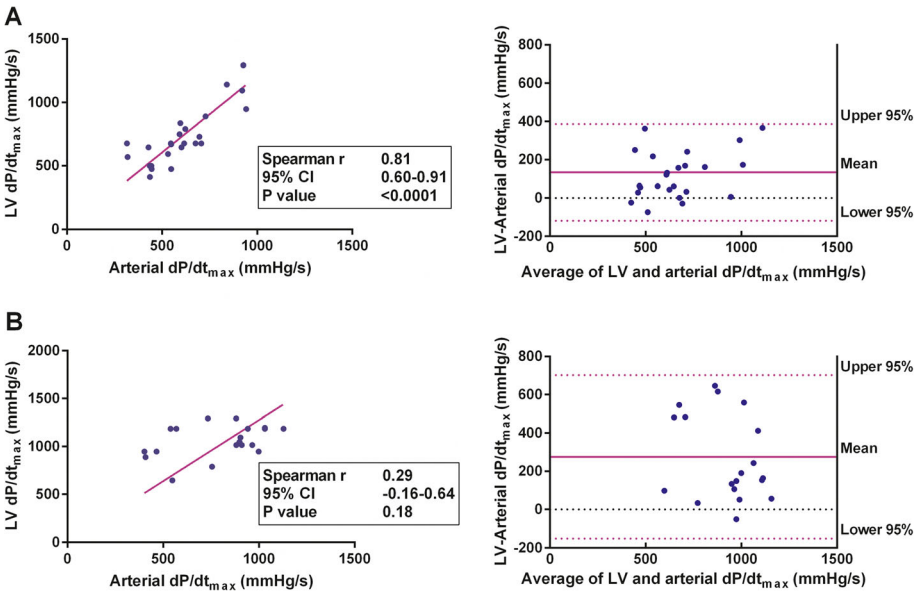

Fig. 3 Arterial and left ventricular (LV) dP/dt_{max} in subgroups according to cardiac output (CO). **a** Subgroup with lower CO (< 6 L/min, *N* = 26)—correlation between arterial and LV dP/dt_{max} with linear regression curve (left), and the Bland-Altman plot of the agreement between arterial and LV dP/dt_{max} (right). **b** Subgroup with higher CO (> 6 L/min, *N* = 22)—correlation between arterial and LV dP/dt_{max} with linear regression curve (left), and the Bland-Altman plot of the agreement between arterial and LV dP/dt_{max} (right)

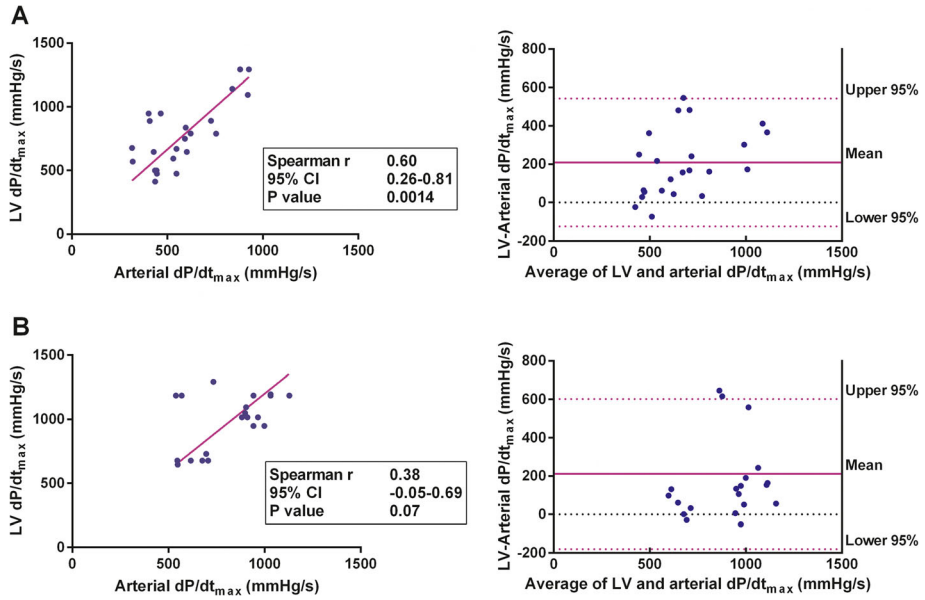

Fig. 4 Arterial and left ventricular (LV) dP/dt_{max} in subgroups according to stroke volume (SV). **a** Subgroup with lower SV (< 65 mL, $N = 25$)—correlation between arterial and LV dP/dt_{max} with linear regression curve (left), and the Bland-Altman plot of the agreement between arterial and LV dP/dt_{max} (right). **b** Subgroup with higher SV (> 65 mL, $N = 23$)—correlation between arterial and LV dP/dt_{max} with linear regression curve (left), and the Bland-Altman plot of the agreement between arterial and LV dP/dt_{max} (right)

dt_{max}, and selected echocardiographic variables such as LV ejection fraction or LV fractional shortening in children undergoing congenital heart disease surgery. They did not find a significant correlation between arterial dP/dt_{max} and the other variables, and these observations were explained by differences between radial artery and aortic pressure waveforms. The discrepancy with our results can be elucidated by the other measured parameters in Kim et al.'s study. While we used LV dP/dt_{max} as a surrogate parameter of LV contractility, Kim et al. measured LV ejection fraction and LV fractional shortening, which are not the accepted markers of LV contractility, because they are influenced by many other factors (e.g., preload, mitral regurgitation). The observations in the study by Kim et al. could be also influenced by CO or SVR (or vascular filling), which were not recorded. Recently, Vaquer et al. [20] published a study focused on femoral arterial dP/dt_{max} in critically ill patients, predominantly with septic shock. They observed increase in arterial dP/dt_{max} after administration of dobutamine and norepinephrine but not after volume expansion. The changes in arterial dP/dt_{max} were strongly correlated with the changes in pulse pressure and systolic arterial pressure in all interventions including volume expansion. Vaquer et al. conclude that femoral arterial dP/dt_{max} is, therefore, an unreliable estimate of LV systolic function [20]. Our study was not designed to evaluate the relationship between dP/dt_{max} and LV systolic function; we focused on the comparison of the arterial dP/dt_{max} and the LV dP/dt_{max}, as a surrogate marker of LV contractility. Although the study group characteristics are different, the observation of increase in arterial dP/dt_{max} after administration of agents with inotropic effect (dobutamine, norepinephrine) in the study by Vaquer et al. [20] is in a good agreement with our results showing significant correlation between arterial and LV dP/dt_{max}. Our observation that correlation between arterial and LV dP/dt_{max} depends on SVR is also consistent with the results by Vaquer et al. [20] describing that femoral dP/dt_{max} is influenced by LV preload and afterload.

Several authors reported that the arterial dP/dt_{max} is significantly influenced by vascular filling conditions [8, 10, 20]. We observed in our study that the correlation between arterial and LV dP/dt_{max} was influenced by SVR, which reflects loading conditions; however, SV variation or dynamic arterial elastance had no effect on the relationship between arterial and LV dP/dt_{max}. This contrast can be at least partly explained by the fact that in our study, the measurement was done in a single time point, while in the other studies, serial measurements were performed enabling evaluation of dynamic changes. In addition, we included entirely patients with acute left heart failure, where the LV preload is usually increased that may or may not be accompanied by changes in other indirect markers of vascular filling. Our study had several limitations, the first of which was possible bias caused by the small sample size. We designed only a pilot study focusing primarily on feasibility; however, a larger trial should be performed to confirm our results. We also acknowledge that arterial dP/dt_{max} is not only a function of

LV contractility but is influenced by many other factors, at least by arterial vessel wall characteristics (e.g., arterial elasticity and stiffness), which was not assessed in the present study. We did not record pulse pressure enabling to calculate arterial elastance. It can be assumed that there can be marked individual differences in arterial system properties in heart failure patients, who often present with other diseases and various degrees of peripheral atherosclerosis. Patients with moderate to severe aortic stenosis were ineligible for this study; however, we cannot exclude the possibility that even mild aortic stenosis may have influenced the results. Moreover, in our study, we have performed only single measurements at one time point in each patient. Our study, therefore, was not designed to evaluate the trends in arterial dP/dt_{max} changes. In addition, while the LV dP/dt_{max} values were obtained at the end of expiration, the arterial dP/dt_{max} were calculated as a median value from 20-s interval, therefore not at the same period of respiratory cycle. Finally, LV dP/dt_{max} is only a surrogate marker of LV contractility and measurement of this parameter using echocardiography can be inaccurate.

Conclusions

Our results suggest that in patients with acute heart failure requiring intensive care with an arterial line, continuous calculation of arterial dP/dt_{max} may be used for monitoring LV contractility, especially in those with higher SVR, lower CO, and lower SV, such as in patients experiencing cardiogenic shock. On the other hand, there was only a weak or no significant correlation in the subgroups with higher CO, higher SV, and lower SVR.

Abbreviations

CO: Cardiac output; Ees: End-systolic elastance; LV: Left ventricular; SV: Stroke volume; SVR: Systemic vascular resistance; T: Time interval

Authors' contributions

PO and DV conceived and designed the study. DV, AK, MJ, and JN contributed to the recruitment of trial participants and were responsible for the acquisition of data and their integrity. PO, MJ, and JN did the statistical analysis and prepared the figures and tables. All authors participated in the interpretation of the results. PO wrote the first draft of the manuscript. DV, AK, MJ, and JN critically reviewed and revised the manuscript for important intellectual content. All authors approved the final version for publication.

Funding

The study was supported by an institutional grant MH CZ-DRO (Nemocnice Na Homolce-NNH, 00023884), IG150501.

Availability of data and materials

The datasets used and/or analyzed during the current study are available from the corresponding author on reasonable request.

Ethics approval and consent to participate

The present study was performed in accordance with the principles of the Declaration of Helsinki, and the study protocol was approved by the Institutional Ethics Committee of the Na Homolce Hospital (Prague, Czech Republic). Informed consent was obtained from conscious patients before measurements. In unconscious subjects at the time of measurement, informed consent was obtained retrospectively. In two deceased patients, informed consent was obtained from next of kin.

Consent for publication

Not applicable

Competing interests

PO received speaker's fee from Edwards Lifesciences. The other authors declare that they have no competing interests.

Received: 6 July 2019 Accepted: 21 October 2019
Published online: 21 November 2019

References

1. Cecconi M, De Backer D, Antonelli M, Beale R, Bakker J, Hofer C, Jaeschke R, Mebazaa A, Pinsky MR, Teboul JL, et al. Consensus on circulatory shock and hemodynamic monitoring. Task force of the European Society of Intensive Care Medicine. Intensive Care Med. 2014;40(12):1795–815.
2. Dewilde WJ, Oirbans T, Verheugt FW, Kelder JC, De Smet BJ, Herrman JP, Adriaenssens T, Vrolix M, Heestermans AA, Vis MM, et al. Use of clopidogrel with or without aspirin in patients taking oral anticoagulant therapy and undergoing percutaneous coronary intervention: an open-label, randomised, controlled trial. Lancet. 2013;381(9872):1107–15.
3. Suga H, Sagawa K. Instantaneous pressure-volume relationships and their ratio in the excised, supported canine left ventricle. Circ Res. 1974; 35(1):117–26.
4. Sagawa K. The end-systolic pressure-volume relation of the ventricle: definition, modifications and clinical use. Circulation. 1981;63(6):1223–7.
5. Wallace AG, Skinner NS Jr, Mitchell JH. Hemodynamic determinants of the maximal rate of rise of left ventricular pressure. Am J Phys. 1963;205:30–6.
6. Bargiggia GS, Bertucci C, Recusani F, Raisaro A, de Servi S, Valdes-Cruz LM, Sahn DJ, Tronconi L. A new method for estimating left ventricular dP/dt by continuous wave Doppler-echocardiography. Validation studies at cardiac catheterization. Circulation. 1989;80(5):1287–92.
7. Chung N, Nishimura RA, Holmes DR Jr, Tajik AJ. Measurement of left ventricular dp/dt by simultaneous Doppler echocardiography and cardiac catheterization. J Am Soc Echocardiogr. 1992;5(2):147–52.
8. Morimont P, Lambermont B, Desaive T, Janssen N, Chase G, D'Orio V. Arterial dP/dtmax accurately reflects left ventricular contractility during shock when adequate vascular filling is achieved. BMC Cardiovasc Disord. 2012;12:13.
9. De Hert SG, Robert D, Cromheecke S, Michard F, Nijs J, Rodrigus IE. Evaluation of left ventricular function in anesthetized patients using femoral artery dP/dt (max). J Cardiothorac Vasc Anesth. 2006;20(3):325–30.
10. Monge Garcia MI, Jian Z, Settels JJ, Hunley C, Cecconi M, Hatib F, Pinsky MR. Performance comparison of ventricular and arterial dP/dtmax for assessing left ventricular systolic function during different experimental loading and contractile conditions. Crit Care. 2018;22(1):325.
11. Tartiere JM, Logeart D, Beauvais F, Chavelas C, Kesri L, Tabet JY, Cohen-Solal A. Non-invasive radial pulse wave assessment for the evaluation of left ventricular systolic performance in heart failure. Eur J Heart Fail. 2007;9(5): 477–83.
12. Mebazaa A, Tolppanen H, Mueller C, Lassus J, DiSomma S, Baksyte G, Cecconi M, Choi DJ, Cohen Solal A, Christ M, et al. Acute heart failure and cardiogenic shock: a multidisciplinary practical guidance. Intensive Care Med. 2016;42(2):147–63.
13. Robotham JL, Takata M, Berman M, Harasawa Y. Ejection fraction revisited. Anesthesiology. 1991;74(1):172–83.
14. Boissier F, Razazi K, Seemann A, Bedet A, Thille AW, de Prost N, Lim P, Brun-Buisson C, Mekontso Dessap A. Left ventricular systolic dysfunction during septic shock: the role of loading conditions. Intensive Care Med. 2017;43(5):633–42.
15. Cikes M, Solomon SD. Beyond ejection fraction: an integrative approach for assessment of cardiac structure and function in heart failure. Eur Heart J. 2016;37(21):1642–50.
16. Burns AT, La Gerche A, D'Hooge J, MacIsaac AI, Prior DL. Left ventricular strain and strain rate: characterization of the effect of load in human subjects. Eur J Echocardiogr. 2010;11(3):283–9.
17. Nafati C, Gardette M, Leone M, Reydellet L, Blasco V, Lannelongue A, Sayagh F, Wiramus S, Antonini F, Albanese J, et al. Use of speckle-tracking strain in preload-dependent patients, need for cautious interpretation! Ann Intensive Care. 2018;8(1):29.

18. Scolletta S, Bodson L, Donadello K, Taccone FS, Devigili A, Vincent JL, De Backer D. Assessment of left ventricular function by pulse wave analysis in critically ill patients. Intensive Care Med. 2013;39(6):1025–33.
19. Kim JW, Bang JY, Park CS, Gwak M, Shin WJ, Hwang GS. Usefulness of the maximum rate of pressure rise in the central and peripheral arteries after weaning from cardiopulmonary bypass in pediatric congenital heart surgery: a retrospective analysis. Medicine (Baltimore). 2016;95(49):e5405.
20. Vaquer S, Chemla D, Teboul JL, Ahmad U, Cipriani F, Oliva JC, Ochagavia A, Artigas A, Baigorri F, Monnet X. Influence of changes in ventricular systolic function and loading conditions on pulse contour analysis-derived femoral dP/dtmax. Ann Intensive Care. 2019;9(1):61.

Publisher's Note

R. Kočková a kol.

New Imaging Markers of Clinical Outcome in Asymptomatic Patients with Severe Aortic Regurgitation.
(id 417)

Journal of Clinical Medicine
Impact Factor: 5,688

Journal of
Clinical Medicine

MDPI

Article

New Imaging Markers of Clinical Outcome in Asymptomatic Patients with Severe Aortic Regurgitation

Radka Kočková [1,2,*], Hana Línková [3], Zuzana Hlubocká [4], Alena Pravečková [1], Andrea Polednová [1], Lucie Súkupová [1], Martin Bláha [1], Jiří Malý [5], Eva Honsová [6], David Sedmera [7] and Martin Pěnička [8]

1 Department of Cardiology, Institute for Clinical and Experimental Medicine, Prague 14021, Czech Republic; alena.praveckova@ikem.cz (A.P.); andrea.polednova@ikem.cz (A.P.); lucie.sukupova@gmail.com (L.S.); martin.blaha@ikem.cz (M.B.)
2 Faculty of Medicine in Hradec Králové, Charles University, Šimkova 870, Hradec Králové 500 03, Czech Republic
3 Department of Cardiology, Royal Vinohrady University Hospital, Prague 10034, Czech Republic; hana.linkova@fnkv.cz
4 Department of Cardiology, General University Hospital, Prague 12808, Czech Republic; zuzana.hlubocka@vfn.cz
5 Department of Cardiothoracic surgery, Institute for Clinical and Experimental Medicine, Prague 14021, Czech Republic; jiri.maly@ikem.cz
6 Institute for Clinical and Experimental Medicine, Clinical and Transplant Pathology Centre, Prague 14021, Czech Republic; eva.honsova@ikem.cz
7 First Faculty of Medicine, Institute of Anatomy, Charles University in Prague, Prague 12800, Czech Republic; david.sedmera@lf1.cuni.cz
8 Cardiovascular Center Aalst, OLV Clinic, 9300, Belgium; martin.penicka@olvz-aalst.be
* Correspondence: radka.kockova@ikem.cz; Tel.: +420-606-483-586

Received: 23 September 2019; Accepted: 6 October 2019; Published: 11 October 2019

Abstract: *Background:* Determining the value of new imaging markers to predict aortic valve (AV) surgery in asymptomatic patients with severe aortic regurgitation (AR) in a prospective, observational, multicenter study. *Methods:* Consecutive patients with chronic severe AR were enrolled between 2015–2018. Baseline examination included echocardiography (ECHO) with 2- and 3-dimensional (2D and 3D) vena contracta area (VCA), and magnetic resonance imaging (MRI) with regurgitant volume (RV) and fraction (RF) analyzed in CoreLab. *Results:* The mean follow-up was 587 days (interquartile range (IQR) 296–901) in a total of 104 patients. Twenty patients underwent AV surgery. Baseline clinical and laboratory data did not differ between surgically and medically treated patients. Surgically treated patients had larger left ventricular (LV) dimension, end-diastolic volume (all $p < 0.05$), and the LV ejection fraction was similar. The surgical group showed higher prevalence of severe AR (70% vs. 40%, $p = 0.02$). Out of all imaging markers 3D VCA, MRI-derived RV and RF were identified as the strongest independent predictors of AV surgery (all $p < 0.001$). *Conclusions:* Parameters related to LV morphology and function showed moderate accuracy to identify patients in need of early AV surgery at the early stage of the disease. 3D ECHO-derived VCA and MRI-derived RV and RF showed high accuracy and excellent sensitivity to identify patients in need of early surgery.

Keywords: aortic regurgitation; echocardiography; magnetic resonance imaging; vena contracta area; longitudinal strain; T1 mapping

1. Introduction

Chronic aortic regurgitation (AR) is the third most common valvular heart disease in Western countries, with a prevalence of 0.1% to 2.0%. Degenerative etiology on tricuspid or bicuspid aortic valves and annuloaortic ectasia are the most common causes of chronic AR. Rheumatic fever remains a frequent cause of chronic AR in developing countries [1–4]. In chronic AR, progressive left ventricular (LV) dilatation compensates for the increase of LV end-diastolic pressure. Left ventricular dilatation enables the preservation of cardiac output despite the large regurgitant volume of blood returning to the LV in diastole. Increased afterload in chronic AR is compensated by eccentric LV hypertrophy. This complex volume and pressure compensatory mechanisms explain the long asymptomatic course of the disease.

A combination of several clinical and imaging characteristics makes the timing of aortic valve (AV) intervention challenging. Patients with severe AR are often middle-aged males with a long asymptomatic course [1,2,5]. Furthermore, current indications for AV intervention (i.e., two-dimensional (2D) echocardiography (ECHO)-derived assessment of AR severity and left ventricular (LV) remodeling), appear to be rather specific but less sensitive [1,2,6–10]. This may lead to late AV intervention resulting in irreversible myocardial damage and impaired outcome [1–3,11,12]. Thus, a more a sensitive and accurate imaging marker to trigger early AV intervention may be of crucial importance.

Several promising imaging approaches to assess AR or its impact on LV structure and function have emerged recently [13–20]. For instance, three-dimensional (3D) ECHO- or magnetic resonance (MRI)-derived evaluation of AR severity may increase the accuracy of AR classification [16,19,20]. Assessment of LV myocardial fibrosis, strain or work may be more sensitive than LV diameters or ejection fraction (LVEF) to detect irreversible myocardial damage at an early stage [13–15,17,18,21]. Therefore, in a multicenter study, we thought to determine the value of new imaging markers to predict AV surgery in asymptomatic patients with severe AR and preserved LVEF. Imaging markers from all participating centers were analyzed centrally by a CoreLab.

2. Experimental Section

2.1. Design

A prospective, observational and multicenter study was conducted in three tertiary cardiology centers. All imaging markers were evaluated centrally in a CoreLab (Institute of Clinical and Experimental Medicine, Prague), which holds the European Association of Cardiovascular Imaging (EACVI) Laboratory accreditation and individual certification for both ECHO and MRI.

2.2. Patients

The study population consisted of all consecutive patients (age 44.4 ± 13.2 years, 85.4% males) with chronic severe AR and no indication for AV intervention who were referred to participating heart valve centers for AR assessment between March 2015 and September 2018. To be eligible for the study patients had to fulfil the following inclusion criteria: (1) severe AR defined by using the integrative 2D ECHO approach [10]; (2) absence of symptoms validated using bicycle ergometry; (3) preserved LVEF (>50%); (4) non-dilated LV end-diastolic diameter (≤70 mm) and LV end-systolic diameter index (≤25 mm/m^2); and (5) sinus rhythm. Patients with guideline indications for AV intervention, acute AR, aortic dissection, endocarditis, irregular heart rate, associated with more than mild valvular disease, complex congenital heart disease, intracardiac shunt, creatinine clearance <30 mL/min, pregnancy, or contra indication for MRI were excluded [1,2]. The study protocol and informed consent was approved by the ethics committees of all participating institutions. All patients had to sign informed consent prior to the enrollment. The study was registered in ClinicalTrials.gov under a unique identifier NCT02910349.

2.3. Protocol

An initial assessment was performed by specialized heart valve cardiologist in all participating centers. It included a history, clinical examination, Electrocardiography (ECG), bicycle ergometry, blood sampling, and comprehensive 2D and 3D ECHO. A cardiac MRI was performed in the center where the CoreLab was based for all participants. Patients from this particular center underwent MRI on the day of enrollment while patients from other two centers underwent an MRI within 2 weeks after the enrollment. Analysis of all ECHO- and MRI-derived markers were centralized in the CoreLab.

2.4. Follow-Up and Study Endpoints

After enrollment, patients were followed in participating heart valve centers every 6 months till 30 September 2018. The decision-making on conservative versus surgical treatment was left at the discretion of a particular heart valve team. In patients undergoing AV surgery, a perioperative biopsy was performed at the level of basal interventricular septum to assess the extent of myocardial fibrosis as previously described in our pilot study [14]. The follow-up data on AV interventions, mortality, and cardiac hospitalizations were obtained in all patients (100%) using population registry, medical files, and contact with referring physicians or family. Baseline clinical and imaging characteristics were analyzed to identify independent predictors of AV surgery. A prespecified study endpoint was cumulative of the indication for aortic valve intervention, ventricular arrhythmia occurrence (non-sustained or sustained ventricular tachycardia, ventricular ectopic beats >10%), hospitalization for heart failure, Brain natriuretic peptide (BNP) elevation >150 ng/L or cardiovascular death.

2.5. Doppler ECHO

A comprehensive 2D and 3D transthoracic ECHO was performed using a Vivid 7 and Vivid 9 (GE HealthCare, Horten, Norway) ultrasound system equipped with 4-dimensional active matrix 4-D volume phased array probe. Several 3D ECHO loops in each view were recorded using ECG-gated full-volume acquisition over four (LV function) to six (color Doppler) cardiac cycles during end-expiratory apnea. Images were optimized by adjusting the depth, sector size, gain, number of frames per second (FPS), the number of heart beats, and breath hold. All acquired images were digitally stored, anonymized, and analyzed using the commercially available software EchoPac BT 202, GE HealthCare. An average of at least 3 beats was taken for each measurement. Blood pressure and heart rate was recorded during each examination.

LV internal diameters were derived from an LV internal cavity using M-mode whenever possible. The biplane Simpson method was used to assess 2D LV volumes and Ejection fraction (EF) [21]. A semi-automatic contouring method with manual correction was used to measure 3D LV volumes and EF [21]. Global longitudinal strain (GLS) was assessed using a semi-automatic speckle tracking method with manual adjustment with frame rate of >60 FPS for 2D GLS (Figure 1B) and LV twist, and >25 FPS for 3D GLS [21]. Myocardial work was derived from 2D GLS, brachial blood pressure, and the timing of valvular events as described previously [18,22]. The severity of AR was assessed using the recommended approach integrating valve morphology, vena contracta width, the size of regurgitant jet in LV cavity and its width in LVOT, the jet pressure half time, the velocity of the diastolic flow reversal in the descending aorta, and the size of the proximal isovelocity surface area (PISA) [7,10]. Given the high prevalence of bicuspid valves in the study population and eccentric jets, the calculation of regurgitant volume (RV) using the PISA method was not consistently feasible. Therefore, the RV and regurgitant fraction (RF) of AR was assessed using the Doppler volumetric method, which uses the differences between the mitral and aortic stroke volumes (SV) to calculate RV and RF of AR [7,10]. Moderate-to-severe AR was defined by the presence of 2–3 specific criteria and RV of 45–59 mL or RF of 40%–49% [7,10]. Severe AR was defined by the presence of ≥4 specific criteria or by the presence of 2–3 specific criteria and RV ≥60 mL or RF ≥50% [10]. Moreover, 3D ECHO derived vena contracta area (VCA) was assessed in zoomed parasternal long-axis view (Figure 1A). In brief, the narrowest

sector possible and multibeat acquisition was used to maximize the frame rate. To identify VCA, the 3D dataset was rotated to bisect the regurgitant color jet at the level of the leaflet coaptation zone perpendicularly to its long axis in 2 orthogonal planes. The image was cropped along the jet direction to visualize the cross-sectional area at the level of the vena contracta. Low velocity peripheral signals of the color spectrum were rejected. The VCA was defined as the high velocity core of the color spectrum [20].

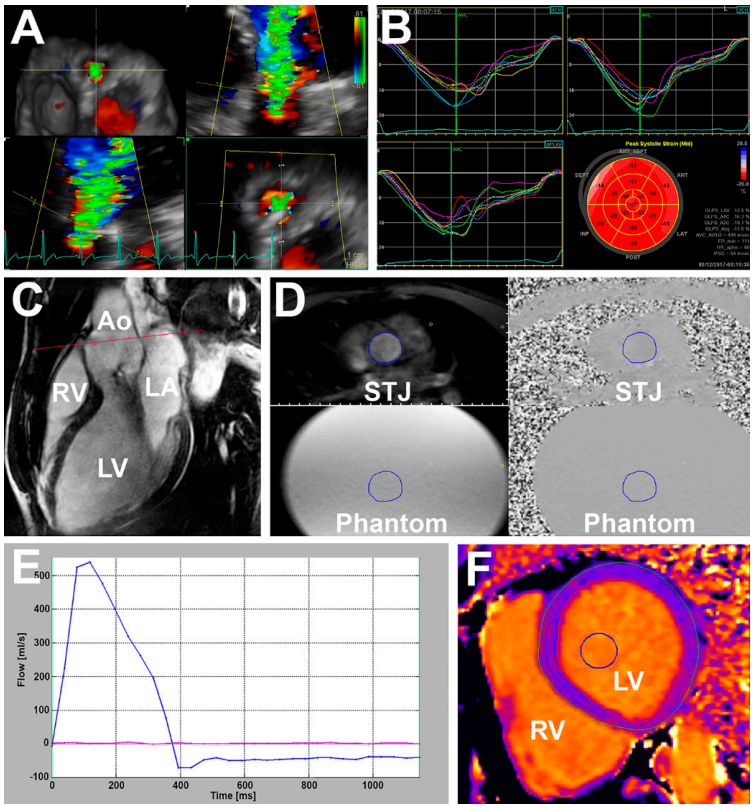

Figure 1. Imaging markers. (**A**) Echocardiography derived three-dimensional vena contracta area; (**B**) echocardiography two-dimensional global longitudinal strain; (**C**) magnetic resonance—the left ventricular outflow tract (cine), red line—through-plane flow sequence slice position displayed on, Ao—aorta, LA—left atrium, LV—left ventricle, RV—right ventricle; (**D**) through-plane flow sequence at sinotubular junction level (STJ) of the aorta (displayed on (**C**)), the blue circle is a manually drawn region of interest where the blood flow and regurgitant volume and fraction are calculated. The exact copy of the region interest is in all four images, phantom—stationary phantom used for flow measurement correction; (**E**) flow-time curve based on (**D**)—blue line shows blood flow at STJ and red line show flow in stationary phantom; (**F**) native T1 mapping from modified Look–Locker Inversion recovery sequence (MOLLI) sequence, blue circle—a semi-automatically drawn region of interest within the blood pool, blue ellipsoid—a manually drawn region of interest within the myocardium at the level of the interventricular septum utilized for myocardial fibrosis calculation.

2.6. Cardiac MRI

An examination was performed using a 1.5T scanner (Magnetom Avanto fit, Siemens, Munich, Germany). The protocol consisted of pilots, T2 weighted dark blood, cine with 2-, 4-, 3-chambers, and short axis (SA) images covering the entire end-diastolic ventricular length, through-plane phase-contrast velocity mapping at the level of the aortic root, contrast late gadolinium enhancement (LGE), and modified Look–Locker Inversion recovery sequence (MOLLI) [14,23]. Analysis was performed using a commercially available software (Segment CMR, Medviso AB 2018, Lund, Sweden). Blood pressure and heart rate was recorded during each examination.

LV volumes and LVEF were calculated using the steady state free precession cine imaging in short-axis stack (slice thickness 8 mm, slice spacing 0) with correction for the valve position in long-axis planes. LV radial, circumferential and longitudinal strain were assessed in the short axis and apical views. Native T1 relaxation time and extracellular volume fraction (ECV) were evaluated using the MOLLI sequence as previously described [14]. The T1 relaxation time measurement was performed in basal-to-mid short-axis slice 15 min pre and 15 min post contrast administration (Figure 1F). Parameters of the MOLLI sequence were as follows: field of view (FoV) 360 × 301 mm, matrix 118 × 256, slice thickness 8 mm, voxel size 1.4 mm × 1.4 mm × 8 mm, echo time 1.1 ms, repetition time 359 ms, flip angle 35°, bandwidth 1.085 Hz/Pixel.

Aortic forward and regurgitation flow were obtained by using the through-plane phase-contrast velocity mapping during breath-hold over 10–20 ms with retrospective ECG gating (Figure 1D). Parameters were as follows: temporal resolution 25–55 ms; echo time 2.7 ms; repetition time 46.8 ms, FoV 300 × 200 mm; matrix size 192 × 132; velocity window 1.5 to 4.0 m/s. Several image slices were prescribed at the level of the aortic root in end-diastole starting from 0.5 cm above AV annulus to 0.5 cm above the sinotubular junction (slice thickness 6 mm, spacing 0). Care was taken to align the slices perpendicularly to the direction of blood flow in two orthogonal imaging planes (Figure 1C). The lowest velocity encoding without flow aliasing was chosen for the analysis. Background velocity offset errors were corrected by using flow stationary phantom and post-processing correction. It has been shown previously that the ascending aorta slice location with the most accurate measurement of RV is between annulus and coronary ostia [24]. To reduce underestimation of RV and RF of AR, the closest slice to the AV without interference of turbulent flow was selected for the analysis [16,19]. Flow measurements from 3 acquisitions were averaged. Aortic forward volume (SV) and RV were derived by integration of the flow curve over 1 cardiac cycle. RF was calculated as RV/(SV * 100%) (Figure 1E).

2.7. New Imaging Markers

Apart from conventional clinical and imaging parameters, the value of the following new imaging markers to predict AV surgery was tested: 2D GLS, 2D myocardial work, 3D GLS, 3D VCA, MRI-derived native T1 relaxation time and ECV, MRI-derived GLS and circumferential strain, and MRI-derived RV and RF.

2.8. Statistical Analysis

Data are expressed as mean ± SD for continuous variables and as counts or percentages for categorical variables. Unpaired Student *t*-test, Pearson χ^2 or Fisher exact tests were used as appropriate. Receiver-operating characteristic curve analysis was used to identify imaging markers to predict future AV surgery. The optimal cutoff value for sensitivity and specificity was calculated according to the Youden's index and according to the clinical relevance. Several Cox proportional hazard models were used to identify independent predictors of aortic valve surgery (AVR). The selection of variables for the models was based on clinical relevance. Care was taken to avoid overfitting and to avoid combining mutually dependent variables in one analysis. Results were reported as hazard ratios (HRs) with the 95% of confidence interval (95% CI) of probability values. The Kaplan–Meier method and log-rank test was used for temporal analysis of differences in AV surgery between groups. For all tests, values of $p < 0.05$ were considered significant. Statistical analysis was performed using the SPSS version 20 (SPSS Inc, Chicago, IL, USA) and the GraphPad Prism version 6.0 (GraphPad Software, San Diego, CA, USA).

3. Results

3.1. Baseline Clinical and Imaging Characteristics

Tables 1 and 2 show baseline clinical and imaging characteristics, respectively. A two-dimensional ECHO study with satisfactory image quality was successfully completed in all patients. Feasibility of 3D ECHO was 99% for LV volumes, 89% for 3D GLS, and 100% for VCA. Three patients (3%) failed to complete the cardiac MRI because of claustrophobia ($n = 2$) or severe spine deformity ($n = 1$). Feasibility of MRI-derived T1 mapping and LV strain was 96% and 95%, respectively. Blood pressure and heart rate was similar during ECHO and MRI examination. The majority of patients were middle-aged males (86%) with bicuspid AV (76%). The most prevalent risk factor for coronary artery disease was hypertension (47%) with corresponding medication. Per study inclusion criteria, all patients were asymptomatic, in sinus rhythm, with normal LV dimensions, and LVEF. A total of 56 (54%) individuals had moderate-to-severe AR while the remaining 48 (46%) showed severe AR. During median follow-up of 587 days (interquartile range (IQR) 296–901 days), no patient died. A total of 20 (19%) individuals underwent AV surgery (surgical group) while the remaining patients were treated conservatively (conservative group). Median time to AV surgery was 236 days (IQR 125–460 days). Clinical characteristics, BNP, and creatinine values were similar between groups (Table 1).

Table 1. Baseline clinical characteristics.

	Total ($n = 104$)	Conservative ($n = 84$)	Surgical ($n = 20$)	p-Value
Age, years	44 ± 13	44 ± 13	45 ± 14	0.922
Male gender, N (%)	89 (86)	72 (86)	17 (85)	0.292
Hypertension, N (%)	50 (48)	40 (48)	10 (50)	0.801
Diabetes mellitus, N (%)	6 (6)	5 (6)	1 (5)	1.000
Hyperlipidemia, N (%)	29 (28)	24 (29)	5 (25)	0.773
Smoker, N (%)	14 (13)	11 (13)	3 (15)	1.000
Coronary artery disease, N (%)	4 (4)	3 (4)	1 (5)	0.542
Previous cardiac surgery, N (%)	4 (4)	3 (4)	1 (5)	1.000
Stroke, N (%)	1 (1)	0 (0)	1 (5)	0.175
Aspirin, N (%)	10 (10)	7 (8)	3 (15)	0.686
Oral anticoagulants, N (%)	5 (5)	3 (4)	2 (10)	0.542
ACEI/ARBs, N (%)	54 (52)	44 (52)	10 (50)	0.607
Beta-blockers, N (%)	25 (24)	21 (25)	4 (20)	0.231
Calcium channel blockers, N (%)	20 (19)	16 (19)	4 (20)	0.759
Diuretics, N (%)	15 (14)	9 (11)	6 (30)	0.261
Statins, N (%)	22 (21)	18 (21)	4 (20)	1.000
NYHA Class I, N (%)	104 (100)	84 (100)	20 (100)	1.000
Height, cm	180 ± 9	180 ± 9	181 ± 8	0.752
Weight, kg	85 ± 14	84 ± 14	86 ± 14	0.744
Systolic blood pressure, mmHg	136 ± 16	135 ± 16	139 ± 18	0.334
Diastolic blood pressure, mmHg	70 ± 12	71 ± 12	68 ± 12	0.292
Heart rate, beats per min	64 ± 10	63 ± 10	64 ± 13	0.965
Sinus rhythm, N (%)	104 (100)	84 (100)	20 (100)	1.000
B-natriuretic peptide, ng/L	27 (42)	24 (36)	34 (117)	0.054
Creatinine Clearance mL/min	118 ± 31	120 ± 32	107 ± 28	0.110
Aortic valve morphology				0.551
Trileaflet, N (%)	14 (13.6)	11 (12.9)	3 (16.7)	
Bicuspid, N (%)	79 (76.7)	65 (76)	14 (70)	
Unicuspid/quadricuspid, N (%)	4 (4)	4 (5)	0 (0)	
Unknown, N (%)	6 (6)	4 (5)	2 (10)	

Values are means ± standard deviations, median (interquartile range) or numbers (percentage). ACEI/ARB, angiotensin converting enzyme inhibitor/angiotensin receptor blocker; NYHA, New York Heart Association.

Table 2. Baseline imaging characteristics.

	Total (n = 104)	Medical (n = 84)	Surgical (n = 20)	p-Value
LV assessment				
2D ECHO end-diastolic diameter, mm	58 ± 6	58 ± 6	61 ± 4	0.031
2D ECHO end-systolic diameter, mm	37 ± 5	37 ± 5	40 ± 4	0.006
2D ECHO end-systolic diameter index, mm/m^2	18 ± 3	18 ± 3	20 ± 3	0.019
2D ECHO end-diastolic volume, mL	158 ± 68.0	156 ± 58	194 ± 60	0.008
2D ECHO end-diastolic volume index, mL/m^2	77 ± 31	76 ± 26	89 ± 32	0.019
2D ECHO end-systolic volume, mL	56 ± 32	56 ± 29	70 ± 39	0.069
2D ECHO end-systolic volume index, mL/m^2	28 ± 15.0	26 ± 14	33 ± 18	0.072
2D ECHO ejection fraction, %	64 ± 6	64 ± 6	64 ± 6	0.695
3D ECHO end-diastolic volume, mL	177 ± 51	175 ± 46	196 ± 68	0.125
3D ECHO end-diastolic volume index, mL/m^2	86 ± 23	85 ± 21	94.9 ± 28	0.108
3D ECHO end-systolic volume, mL	69 ± 24	68 ± 21	78 ± 34	0.12
3D ECHO end-systolic volume index, mL/m^2	33 ± 11	33 ± 10	38 ± 15	0.095
3D ECHO ejection fraction, %	62 ± 5	62 ± 5	61 ± 6	0.678
MRI end-diastolic volume, mL	234 ± 81	223 ± 80	293 ± 76	<0.001
MRI end-diastolic volume index, mL/m^2	118 ± 30	114 ± 27	142 ± 34	<0.001
MRI end-systolic volume, mL	88 ± 51	86 ± 41	124 ± 68	0.005
MRI end-systolic volume index, mL/m^2	43 ± 23	41 ± 20	60 ± 28	0.003
MRI ejection fraction, %	61 ± 6	61 ± 6	60 ± 5	0.248
MRI native T1 relaxation time, ms	1023 ± 30	1023 ± 30	1022 ± 29	0.934
MRI extracellular volume fraction, %	24 ± 3	24 ± 3	24 ± 2	0.819
2D ECHO global longitudinal strain, %	−18 ± 2	−19 ± 2	−17 ± 3	0.07
2D ECHO TWIST	14 ± 4	13 ± 4	14 ± 4	0.496
3D ECHO global longitudinal strain, %	−15 ± 4	−15 ± 4	−15 ± 4	0.518
MRI global longitudinal strain, %	−15 ± 2	−15 ± 2	−14 ± 3	0.62
MRI global circumferential strain, %	−22 ± 3	−22 ± 3	−21 ± 2	0.54
MRI global radial strain, %	31 ± 7	31 ± 7	31 ± 6	0.55
AR assessment				
Integrative approach				0.02
Moderate-to-severe AR, N (%)	56 (54)	50 (60)	6 (30)	
Severe AR, N (%)	48 (46)	34 (40)	14 (70)	
2D ECHO vena contracta width, mm	6.5 ± 1.5	6.3 ± 1.5	6.9 ± 1.6	0.118
Diastolic flow reversal velocity, cm/s	19.4 ± 4.3	18.8 ± 4.0	22.8 ± 4.0	<0.001
2D ECHO regurgitant volume, mL	52 ± 48	52 ± 47	69 ± 63	0.041
2D ECHO regurgitant fraction, %	36 ± 18	34 ± 18	45 ± 17	0.017
3D ECHO vena contracta area, mm^2	29 ± 13	26 ± 11	38 ± 15	<0.001
MRI regurgitation volume, mL	50 ± 28	44 ± 25	73 ± 30	<0.001
MRI regurgitation fraction, %	38 ± 17	36 ± 17	49 ± 11	0.001

Values are means ± standard deviations or numbers (percentage). 2D, two-dimensional; 3D, three dimensional; AR, aortic regurgitation; ECHO, echocardiography; MRI, magnetic resonance imaging; TWIST, left ventricular torsion.

3.2. Assessment of LV Morphology and Function

At 2D ECHO, patients who underwent AV surgery had significantly larger LV dimensions, end-diastolic volume (LVEDV) (all $p < 05$) and tended to have larger end-systolic volume (LVESV) than patients treated conservatively (Table 2). MRI-derived LV volumes showed a similar trend with significantly larger volumes in the surgical versus the conservative group (all $p < 0.01$). In contrast, LVEF derived by using whatever method was similar. Imaging markers of subtle myocardial damage (i.e., the MRI-derived T1 relaxation time or ECV, 2D-, 3D-, or MRI-derived LV strain), did not show statistically significant differences between groups, although 2D GLS tended to be lower in the surgical versus the conservative group (p = 0.07). Average myocardial fibrosis on perioperative myocardial biopsy (n = 14) was 15 ± 20%. The degree of myocardial fibrosis correlated significantly with MRI-derived LV mass (r = 0.66), native T1 relaxation time (r = 0.56), ECV (r = 0.31), and 2D ECHO-derived GLS (0.46).

3.3. Assessment of AR Severity

Using the integrative approach, the surgical group showed a significantly higher prevalence of severe AR than the conservative group (70% vs. 40%, $p = 0.02$). Accordingly, we observed significantly larger velocity of the diastolic flow reversal in the descending aorta, 2D ECHO RV and RF of AR, and 3D ECHO VCA in patients treated surgically versus conservatively (all $p < 0.05$) (Table 2). In contrast, 2D vena contracta width was similar between groups. MRI-derived RV and RF were significantly larger in patients undergoing surgery than in patients treated conservatively (both $p < 0.01$).

3.4. Prediction of AV Surgery

Table 3 and Figure 2 show accuracy of selected imaging markers to identify patients who underwent AV surgery. The integrative 2D ECHO approach had high negative predictive value (89%), but low positive predictive value (29%) to identify future AV surgery. All the ECHO- and MRI-derived indices of LV remodeling and function had an area under the curve (AUC) <0.7. Out of the ECHO-derived parameters, end-systolic diameter (LVESD), with an optimal cutoff value of >37 mm, its index (LVESDi), with an optimal cutoff value of >18 mm/m^2, had the largest AUC. Higher cutoff values of LVESD (>45 mm) or LVESDi (>22 mm/m^2), approaching the guideline recommendations, were highly specific (>90%) but lacked the sensitivity (<20%). The MRI-derived volumes and their indexed values were also rather specific than sensitive. Out of the ECHO-derived indices of AR severity, the largest AUC was observed for velocity of diastolic flow reversal in aorta descendens and 3D VCA. The optimal cutoff value of 3D VCA ≥30 mm^2 had a sensitivity of 80% and a specificity of 63% to identify future AV surgery (Figure 3A). A total of 31 patients treated conservatively had VCA ≥30 mm^2 (false positive). Combining VCA with LVESD or LVESDi increased the specificity up to 97% depending on the cutoff (Table 3). Out of all tested imaging markers, the MRI-derived RV, with a cutoff value ≥45 mL (Figure 3B), and the MRI-derived RF, with a cutoff value ≥34% (Figure 3C), showed the largest AUC (>0.75) with very high sensitivity (≥90%). A total of 33 out of 36 patients in the conservative group had RV ≥45 mL and RF ≥34%, respectively (false positive). Combining RV and RF with LV end-diastolic or end-systolic volume index increased the specificity up to 78% and 89%, respectively (Table 3). In Cox regression analysis, 3D VCA, MRI-derived RV and RF were identified as strongest independent predictors of AV surgery (Table 4). In contrast, LV strain, T1 time or ECV were not independent predictors.

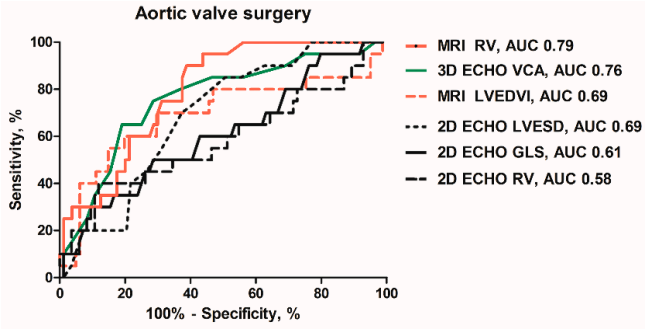

Figure 2. Receiver-operating characteristics curves of the MRI-derived: regurgitant volume (RV) and left ventricular end-diastolic volume index (LVEDVI); the 3D ECHO-derived: vena contracta area (VCA); 2D ECHO-derived: left ventricular end-systolic diameter (LVESD); RV and global longitudinal strain (GLS) to predict AV surgery.

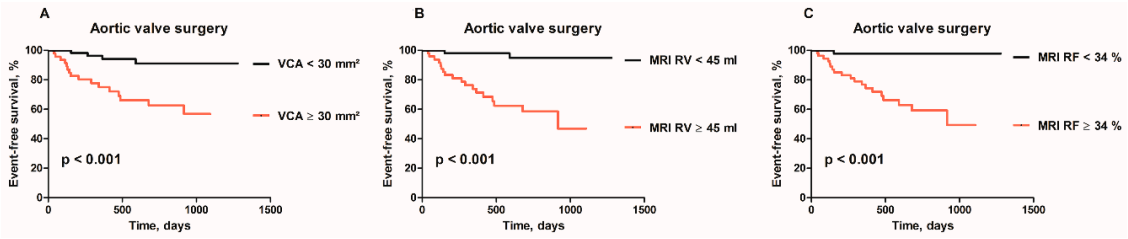

Figure 3. (**A**) Kaplan–Meier curves for aortic valve surgery (AVR) in patients with 3D ECHO-derived VCA ≥30 mm^2 vs. <30 mm^2, (**B**) MRI-derived RV ≥45 mL vs. <45 mL; and (**C**) MRI-derived RF ≥34% vs. <34%.

Table 3. Predictive accuracy of selected imaging markers to identify patients undergoing AV surgery.

	AUC (95% CI)	Cutoff Value	Sensitivity (%)	Specificity (%)
Markers of LV remodeling				
2D ECHO LVESD, mm	0.69 (0.57–0.80)	37 40 45	85 55 15	56 69 94
2D ECHO LVESDi, mm/m^2	0.66 (0.54–0.78)	18 20 22	80 30 15	53 75 90
MRI LVEDV, mL	0.68 (0.53–0.83)	281	50	84
MRI LVEDVi, mL/m^2	0.69 (0.54–0.84)	110 124 139	80 70 55	53 70 85
MRI LVESV, mL	0.64 (0.48–0.80)	121	50	84
MRI LVESVi, mL/m^2	0.65 (0.49–0.81)	42 56 58	70 60 50	53 77 81
2D ECHO GLS, %	0.61 (0.47–0.70)	−17.5	50	71
Markers of AR severity				
Diastolic flow reversal velocity, cm/s	0.72 (0.59–0.85)	22	65	78
2D ECHO RV, mL	0.58 (0.43–0.74)	93	40	88
2D ECHO RF, %	0.61 (0.47–0.76)	47	50	73
3D VCA (mm^2)	0.76 (0.64–0.88)	29 31 36	80 75 65	63 71 81
MRI RV, mL	0.79 (0.70–0.88)	41 45	95 90	56 61
MRI RF, %	0.77 (0.68–0.86)	34	95	55
Integrative approach				
2D ECHO integrative approach	0.65 (0.52–0.78)	Severe AR	70	60
3D ECHO VCA ≥30 mm^2 and 2D ECHO LVESD or LVESDi	NA	LVESD >40 mm LVESD >45 mm LVESDi >20 mm/m^2 LVESDi >22 mm/m^2	80 80 80 80	71 97 77 87
MRI regurgitant volume ≥45 mL and MRI LVEDVi or LVESVi	NA	LVEDVi >139 mL/m^2 LVESVI >62 mL/m^2	90 90	78 78
MRI regurgitant fraction ≥34% and MRI LVEDVi or LVESVi	NA	LVEDVi >139 mL/m^2 LVESVI >62 mL/m^2	95 95	89 89

2D, two-dimensional; 3D, three dimensional, AUC, area under curve; ECHO, echocardiography; GLS, global longitudinal strain; LV, left ventricle; LVEDV, left ventricular end-diastolic volume; LVEDVi, left ventricular end-diastolic volume index; LVESD, left ventricular end-systolic diameter; LVESDi, left ventricular end-systolic diameter index; LVESV, left ventricular end-systolic volume; LVESVi, left ventricular end-systolic volume index; MRI, magnetic resonance imaging; RF, regurgitant fraction; RV, regurgitant volume; VCA, vena contracta area.

Table 4. Independent predictors of aortic valve surgery.

	Univariable Analysis		Multivariable Analysis	
	HR (95% CI)	***p*-Value**	**HR (95% CI)**	***p*-Value**
2D ECHO LVEDD	1.08 (0.99–1.18)	0.084		
2D ECHO LVESD	1.12 (1.02–1.23)	0.014	1.12 (1.02–1.23)	0.018 *
2D ECHO LVESDi	1.18 (1.02–1.37)	0.031	1.18 (1.01–1.38)	0.042 *
MRI LVEDV	1.01 (1.00–1.02)	0.004	1.01 (1.00–1.01)	0.036 †
MRI LVEDVi	1.02 (1.00–1.03)	0.004	1.01 (1.00–1.03)	0.033 †
MRI LVESV	1.02 (1.00–1.03)	0.017		
MRI LVESVi	1.03 (1.01–1.06)	0.014		
2D ECHO RV	1.01 (1.00–1.02)	0.011	1.01 (1.00–1.02)	0.035 ‡
2D ECHO RF	1.03 (1.01–1.06)	0.018	1.03 (1.00–1.06)	0.020 ‡
3D VCA	1.07 (1.04–1.10)	<0.001	1.06 (1.03–1.10)	<0.001 ‡
MRI RV	1.03 (1.02–1.05)	<0.001	1.03 (1.01–1.04)	<0.001 §
MRI RF	1.05 (1.03–1.08)	<0.001	1.05 (1.02–1.08)	<0.001 §

CI, confidence interval; HR, hazard ratio; for other abbreviations see previous tables. * LVESD and LVESDi remained significant predictors of aortic valve (AV) surgery after adjustment for ECHO RV and ECHO RF but they lost predictive significance in combination with 3D VCA. † MRI LVEDV and LVEDVi showed borderline significance to predict AV surgery after adjustment with MRI RF but they lost predictive significance in combination with MRI RV. ‡ 2D ECHO RV, 2D ECHO RF and 3D VCA consistently retained their independent predictive value after adjustment for ECHO-derived LV diameters or their indices, 3D VCA was the strongest predictor. § MRI RV and RF were strong independent predictors after adjustment for MRI-derived LV volumes or their indices.

4. Discussion

The present study included asymptomatic patients with normal LVEF and non-dilated LV. Compared with the previous reports in asymptomatic AR patients, individuals included in the present study were younger, had less dilated LV, lower BNP, higher magnitude of GLS, and experienced less endpoints during follow-up [6,8,13,15,19,25]. This suggests the very early stage of AR disease. The findings of the present study can be summarized as follows: (1) AR severity seemed to be the major determinant of early disease progression while indices of LV morphology and function showed lower predictive accuracy; (2) new imaging markers of AR severity (i.e., 3D VCA, MRI-derived RV and RF), showed higher sensitivity than those derived using 2D Doppler ECHO; (3) integrating a sensitive with a specific parameter, for instance ECHO-derived VCA with LVESDi, or MRI-derived RV or RF with LVEDVi or LVESVi showed higher discriminative power than 2D ECHO integrative approach to identify patients undergoing early AV surgery.

4.1. LV Morphology and Function

Chronic AR leads to LV volume and pressure overload with subsequent hypertrophy, dilatation, systolic dysfunction, and heart failure. LV dimensions (LVESD >50 mm or LVESDi >25 mm/m^2), and LVEF (LVEF <50%) are currently used as indications for AV intervention [1]. Several recent studies demonstrated low sensitivity of these cutoffs by showing improved outcome in patients who had been operated on before the onset of these triggers [6,8]. In the present study, the optimal cutoff of LVEDSi (>18 mm/m^2), with acceptable sensitivity (80%), was lower than previously proposed [1,6,8]. Using higher cutoff of 20 or 22 mm/m^2 increased specificity (75%–93%) at the expense of unacceptably low sensitivity (15%–30%). MRI-derived volumes were rather specific but had lower sensitivity. It is of note, that a considerable proportion of patients (38%) showed increased LV volumes at MRI despite normal 2D ECHO dimensions. Nevertheless, the predictive accuracy of LV dimensions or volumes, derived by either technique, were moderate with an area under the curve <0.7 in all cases. Several new markers describing subtle myocardial damage or dysfunction have emerged recently [13–20]. MRI-derived native T1 mapping and ECV are accurate and validated markers of diffuse myocardial fibrosis [14,23,26]. ECHO-derived GLS has been introduced as a sensitive marker of early systolic dysfunction and potentially of clinical outcome in different valvular diseases [1,21]. Several studies reported independent association between speckle-tracking-derived GLS and the need

for AV surgery [13,15,17]. In the present study, only 2D GLS tended to be lower in the surgical versus the conservative group while 3D GLS or MRI-derived strains, T1 relaxation time, and ECV were similar. The explanation of different findings can be that previous studies included more advanced disease as documented by a higher prevalence of endpoints, older age, more dilated LV or lower magnitude of GLS compared with our data [13,15]. Of interest, in the surgical group, we observed increased myocardial fibrosis (median 15%) at perioperative biopsy. These values are clearly elevated as a normal range between 1%–4.5% [27,28]. Both T1 relaxation time, ECV, and GLS showed significant correlation with the extent of fibrosis in histological samples. Moreover, T1 relaxation time was significantly longer (1022 ± 30 ms vs. 980 ± 22 ms, $p < 0.01$) and 2D GLS significantly lower (−18 ± 2% vs. −22.5 ± 2%, $p < 0.01$) compared with 30 healthy controls. Yet, these parameters failed to identify patients with early disease progression. This suggests that at the early stage of AR disease, the parameters reflecting subtle myocardial damage may not be accurate enough to predict early disease progression.

4.2. Assessment of AR Severity

The majority of recommended indices to assess AR are semiquantitative, lack the sensitivity or their accuracy is hampered by jet eccentricity [7,9,10]. Accordingly, in the present study with high prevalence bicuspid AV and eccentric jets, the consistent measurement of PISA-derived effective regurgitant orifice (ERO) and RV was not possible. It might have been for the same reasons that 2D vena contracta width did not show significant differences between groups. In contrast, 3D data can be rotated perpendicular to the jet direction in several planes to avoid the limitation introduced by jet eccentricity. The vena contracta area is a 3D-derived area of the vena contracta without any geometric assumption. VCA has been shown to be highly accurate, reproducible, and superior to the PISA method in different native valve regurgitations [20,29–31]. In the present study, 3D VCA had the highest accuracy out of all ECHO markers of AR severity to identify patients in need for early AV surgery. A combination of sensitive VCA with specific LVEDSi showed the optimal discriminative power. MRI-derived assessment of blood flow at the level of the aortic root is a highly reproducible and quantitative technique, which allows for direct assessment of RV of AR [16,19]. In the present study, MRI-derived RV and RF showed the largest accuracy out of all the imaging parameters to predict AV surgery. Our cutoff values of RV (≥45 mL) and RF (≥34%) were similar to values (RV >42 mL, RF >33%) published previously in more advanced AR disease [19]. In our study, both RV and RF were highly sensitive but less specific. In contrast, Myerson observed balanced high sensitivity (92%–85%) and specificity (85%–92%) for both indices [19]. This difference in specificity may be related to the very early stage of AR disease in our study while Myerson included older patients with more a dilated LV [19]. In the present study, combining sensitive RV or RF with specific LV volumes or their indices increased the specificity to identify future AV surgery. Of note, 2D ECHO integrative approach showed lower predictive accuracy. This suggests that, in asymptomatic patients with severe AR, both 3D ECHO-derived VCA and MRI-derived RV and RF may be clinically useful to increase sensitivity and accuracy of the recommended approach.

5. Conclusions

The present study assessed the clinical value of new imaging markers in asymptomatic patients with chronic severe AR at the early stage of the disease. Parameters related to LV morphology and function showed moderate accuracy to identify patients in need for early AV surgery. This suggests their limited accuracy at the early stage of AR disease while they may become useful later in the disease course with ongoing LV remodeling. In contrast, 3D ECHO-derived VCA and MRI-derived RV and RF showed the highest accuracy and excellent sensitivity to identify patients in need for early AV surgery. This suggests their clinical potential since the recommended integrative approach is rather specific than sensitive.

Author Contributions: Conceptualization, R.K. and M.P.; investigation, L.S., M.B., J.M., and E.H.; project administration, A.P. (Andrea Polednová); validation, H.L., Z.H. and A.P. (Alena Pravečková); writing—review and editing, D.S.

Funding: This study was supported by the Ministry of Health of the Czech Republic 17-28265A. No potential conflict of interest was reported by the authors.

Acknowledgments: We are grateful to Marek Maly at the National Institute of Public Health, Prague, Czech Republic, for his invaluable statistical analysis.

Conflicts of Interest: The authors declare no conflicts of interest.

References

1. Baumgartner, H.; Falk, V.; Bax, J.J.; Bonis, M.; Hamm, C.; Holm, P.J.; Iung, B.; Lancelloti, P.; Lansac, E.; Rodriguez Munoz, D.; et al. ESC Scientific Document Group. 2017 ESC/EACTS Guidelines for the management of valvular heart disease. *Eur. Heart J.* **2017**, *38*, 2739–2791. [CrossRef]
2. Nishimura, R.A.; Otto, C.M.; Bonow, R.O.; Carabello, B.A.; Erwin, J.P., 3rd; Fleisher, L.A.; Jneid, H.; Mack, M.J.; McLeod, C.J.; O'Gara, P.T.; et al. 2017 AHA/ACC Focused Update of the 2014 AHA/ACC Guideline for the Management of Patients with Valvular Heart Disease: A Report of the American College of Cardiology/American Heart Association Task Force on Clinical Practice Guidelines. *J. Am. Coll. Cardiol.* **2017**, *70*, 252–289. [CrossRef] [PubMed]
3. Iung, B.; Baron, G.; Butchart, E.G.; Delahaye, F.; Gohlke-Barwolf, C.; Levang, O.W.; Tornos, P.; Vanoverschelde, J.L.; Vermeer, F.; Boersma, E.; et al. A prospective survey of patients with valvular heart disease in Europe: The Euro Heart Survey on Valvular Heart Disease. *Eur. Heart J.* **2003**, *24*, 1231–1243. [CrossRef]
4. Nkomo, V.T.; Gardin, J.M.; Skelton, T.N.; Gottdiener, J.S.; Scott, C.G.; Enriquez-Sarano, M. Burden of valvular heart diseases: A population-based study. *Lancet* **2006**, *368*, 1005–1011. [CrossRef]
5. Klodas, E.; Enriquez-Sarano, M.; Tajik, A.J.; Mullany, C.J.; Bailey, K.R.; Seward, J.B. Surgery for aortic regurgitation in women. Contrasting indications and outcomes compared with men. *Circulation* **1996**, *94*, 2472–2478. [CrossRef] [PubMed]
6. de Meester, C.; Gerber, B.L.; Vancraeynest, D.; Pouleur, A.C.; Noirhomme, P.; Pasquet, A.; Gerber, B.L.; Vanoverschelde, J.L. Do Guideline-Based Indications Result in an Outcome Penalty for Patients with Severe Aortic Regurgitation? *JACC Cardiovasc. Imaging* **2019**, *12*, 2880. [CrossRef] [PubMed]
7. Lancellotti, P.; Tribouilloy, C.; Hagendorff, A.; Popescu, B.A.; Edvardsen, T.; Pierard, L.A.; Badano, L.; Zamorano, J.L.; Scientific Document Committee of the European Association of Cardiovascular Imaging. Recommendations for the echocardiographic assessment of native valvular regurgitation: an executive summary from the European Association of Cardiovascular Imaging. *Eur. Heart J. Cardiovasc. Imaging* **2013**, *14*, 611–644. [CrossRef] [PubMed]
8. Mentias, A.; Feng, K.; Alashi, A.; Rodriguez, L.L.; Gillinov, A.M.; Johnston, D.R.; Sabik, J.F.; Svensson, L.G.; Grimm, R.A.; Griffin, B.P.; et al. Long-Term Outcomes in Patients with Aortic Regurgitation and Preserved Left Ventricular Ejection Fraction. *J. Am. Coll. Cardiol.* **2016**, *68*, 2144–2153. [CrossRef] [PubMed]
9. Messika-Zeitoun, D.; Detaint, D.; Leye, M.; Tribouilloy, C.; Michelena, H.I.; Pislaru, S.; Brochet, E.; Iung, B.; Vahanian, A.; Enriquez-Sarano, M. Comparison of semiquantitative and quantitative assessment of severity of aortic regurgitation: clinical implications. *J. Am. Soc. Echocardiogr.* **2011**, *24*, 1246–1252. [CrossRef] [PubMed]
10. Zoghbi, W.A.; Adams, D.; Bonow, R.O.; Enriquez-Sarano, M.; Foster, E.; Grayburn, P.A.; Hahn, R.T.; Han, Y.; Hung, J.; Lang, R.M.; et al. Recommendations for Noninvasive Evaluation of Native Valvular Regurgitation: A Report from the American Society of Echocardiography Developed in Collaboration with the Society for Cardiovascular Magnetic Resonance. *J. Am. Soc. Echocardiog.* **2017**, *30*, 303–371. [CrossRef]
11. Krayenbuehl, H.P.; Hess, O.M.; Monrad, E.S.; Schneider, J.; Mall, G.; Turina, M. Left ventricular myocardial structure in aortic valve disease before, intermediate, and late after aortic valve replacement. *Circulation* **1989**, *79*, 744–755. [CrossRef] [PubMed]
12. Pizarro, R.; Bazzino, O.O.; Oberti, P.F.; Falconi, M.L.; Arias, A.M.; Krauss, J.G.; Cagide, A.M. Prospective validation of the prognostic usefulness of B-type natriuretic peptide in asymptomatic patients with chronic severe aortic regurgitation. *J. Am. Coll. Cardiol.* **2011**, *58*, 1705–1714. [CrossRef] [PubMed]

13. Ewe, S.H.; Haeck, M.L.; Ng, A.C.; Witkowski, T.G.; Auger, D.; Leong, D.P.; Abate, E.; Ajmone Marsan, N.; Holman, E.R.; Schalij, M.J.; et al. Detection of subtle left ventricular systolic dysfunction in patients with significant aortic regurgitation and preserved left ventricular ejection fraction: speckle tracking echocardiographic analysis. *Eur. Heart J. Cardiovasc. Imaging* **2015**, *16*, 992–999. [CrossRef] [PubMed]
14. Kockova, R.; Kacer, P.; Pirk, J.; Maly, J.; Sukupova, L.; Sikula, V.; Kotrc, M.; Barciakova, L.; Honsova, E.; Maly, M.; et al. Native T1 Relaxation Time and Extracellular Volume Fraction as Accurate Markers of Diffuse Myocardial Fibrosis in Heart Valve Disease- Comparison with Targeted Left Ventricular Myocardial Biopsy. *Circ. J.* **2016**, *80*, 1202–1209. [CrossRef] [PubMed]
15. Kusunose, K.; Agarwal, S.; Marwick, T.H.; Griffin, B.P.; Popovic, Z.B. Decision making in asymptomatic aortic regurgitation in the era of guidelines: incremental values of resting and exercise cardiac dysfunction. *Circ. Cardiovasc. Imaging* **2014**, *7*, 352–362. [CrossRef] [PubMed]
16. Lee, J.C.; Branch, K.R.; Hamilton-Craig, C.; Krieger, E.V. Evaluation of aortic regurgitation with cardiac magnetic resonance imaging: A systematic review. *Heart* **2018**, *104*, 103–110. [CrossRef]
17. Lee, J.K.T.; Franzone, A.; Lanz, J.; Siontis, G.C.M.; Stortecky, S.; Gräni, C.; Roost, E.; Windecker, S.; Pilgrim, T. Early Detection of Subclinical Myocardial Damage in Chronic Aortic Regurgitation and Strategies for Timely Treatment of Asymptomatic Patients. *Circulation* **2018**, *137*, 184–196. [CrossRef]
18. Manganaro, R.; Marchetta, S.; Dulgheru, R.; Ilardi, F.; Sugimoto, T.; Robinet, S.; Cimino, S.; Go, Y.Y.; Bernard, A.; Kacharava, G.; et al. Echocardiographic reference ranges for normal non-invasive myocardial work indices: Results from the EACVI NORRE study. *Eur. Heart J. Cardiovasc. Imaging* **2019**, *20*, 582–590. [CrossRef]
19. Myerson, S.G.; d'Arcy, J.; Mohiaddin, R.; Greenwood, J.P.; Karamitsos, T.D.; Francis, J.M.; Banning, A.P.; Christiansen, J.P.; Neubauer, S. Aortic regurgitation quantification using cardiovascular magnetic resonance: Association with clinical outcome. *Circulation* **2012**, *126*, 1452–1460. [CrossRef]
20. Vecera, J.; Bartunek, J.; Vanderheyden, M.; Kotrc, M.; Kockova, R.; Penicka, M. Three-dimensional echocardiography-derived vena contracta area at rest and its increase during exercise predicts clinical outcome in mild-moderate functional mitral regurgitation. *Circ. J.* **2014**, *78*, 2741–2749. [CrossRef]
21. Lang, R.M.; Badano, L.P.; Mor-Avi, V.; Afilalo, J.; Armstrong, A.; Emande, L.; Flachskampf, F.A.; Foster, E.; Goldstein, S.A.; Kuznetsova, T.; et al. Recommendations for cardiac chamber quantification by echocardiography in adults: An update from the American Society of Echocardiography and the European Association of Cardiovascular Imaging. *J. Am. Soc. Echocardiogr.* **2015**, *28*, 1–39. [CrossRef] [PubMed]
22. Russell, K.; Eriksen, M.; Aaberge, L.; Wilhelmsen, N.; Skulstad, H.; Remme, E.W.; Haugaa, K.H.; Opdahl, A.; Fjeld, J.G.; Gjesdal, O.; et al. A novel clinical method for quantification of regional left ventricular pressure-strain loop area: A non-invasive index of myocardial work. *Eur. Heart J.* **2012**, *33*, 724–733. [CrossRef] [PubMed]
23. Messroghli, D.R.; Radjenovic, A.; Kozerke, S.; Higgins, D.M.; Sivananthan, M.U.; Ridgway, J.P. Modified Look-Locker inversion recovery (MOLLI) for high-resolution T1 mapping of the heart. *Magn. Reson. Med.* **2004**, *52*, 141–146. [CrossRef] [PubMed]
24. Chatzimavroudis, G.P.; Walker, P.G.; Oshinski, J.N.; Franch, R.H.; Pettigrew, R.I.; Yoganathan, A.P. Slice location dependence of aortic regurgitation measurements with MR phase velocity mapping. *Magn. Reson. Med.* **1997**, *37*, 545–551. [CrossRef] [PubMed]
25. Detaint, D.; Messika-Zeitoun, D.; Maalouf, J.; Tribouilloy, C.; Mahoney, D.W.; Tajik, A.J.; Enriquez-Sarano, M. Quantitative echocardiographic determinants of clinical outcome in asymptomatic patients with aortic regurgitation: A prospective study. *JACC Cardiovasc. Imaging* **2008**, *1*, 1–11. [CrossRef] [PubMed]
26. Messroghli, D.R.; Moon, J.C.; Ferreira, V.M.; Frosse-Wortmann, L.; He, T.; Kellman, P.; Mascherbauer, J.; Nezafat, R.; Salerno, M.; Schelbert, E.B.; et al. Clinical recommendations for cardiovascular magnetic resonance mapping of T1, T2, T2* and extracellular volume: A consensus statement by the Society for Cardiovascular Magnetic Resonance (SCMR) endorsed by the European Association for Cardiovascular Imaging (EACVI). *J. Cardiovasc. Magn. Reson.* **2017**, *19*, 75. [CrossRef] [PubMed]
27. Meckel, C.R.; Wilson, J.E.; Sears, T.D.; Rogers, J.G.; Goaley, T.J.; McManus, B.M. Myocardial fibrosis in endomyocardial biopsy specimens: Do different bioptomes affect estimation? *Am. J. Cardiovasc. Pathol.* **1989**, *2*, 309–313. [PubMed]

28. Tanaka, M.; Fujiwara, H.; Onodera, T.; Wu, D.J.; Hamashima, Y.; Kawai, C. Quantitative analysis of myocardial fibrosis in normals, hypertensive hearts, and hypertrophic cardiomyopathy. *Br. Heart J.* **1986**, *55*, 575–581. [CrossRef]
29. Abudiab, M.M.; Chao, C.J.; Liu, S.; Naqvi, T.Z. Quantitation of valve regurgitation severity by three-dimensional vena contracta area is superior to flow convergence method of quantitation on transesophageal echocardiography. *Echocardiography* **2017**, *34*, 992–1001. [CrossRef]
30. Sato, H.; Ohta, T.; Hiroe, K.; Okada, S.; Shimizu, K.; Murakami, R.; Tanabe, K. Severity of aortic regurgitation assessed by area of vena contracta: A clinical two-dimensional and three-dimensional color Doppler imaging study. *Cardiovasc. Ultrasound.* **2015**, *5*, 13–24. [CrossRef]
31. Zeng, X.; Levine, R.A.; Hua, L.; Morris, E.L.; Kang, Y.; Flaherty, M.; Morgan, N.V.; Hung, J. Diagnostic value of vena contracta area in the quantification of mitral regurgitation severity by color Doppler 3D echocardiography. *Circ. Cardiovasc. Imaging* **2011**, *4*, 506–513. [CrossRef] [PubMed]

J. Beneš a kol.

The Role of GDF-15 in Heart Failure Patients With Chronic Kidney Disease
(id 877)

Canadian Journal of Cardiology
Impact Factor: 5,592

rejstřík

Canadian Journal of Cardiology 35 (2019) 462–470

Clinical Research

The Role of GDF-15 in Heart Failure Patients With Chronic Kidney Disease

Jan Benes, MD, PhD,[a] Martin Kotrc, MD,[a] Peter Wohlfahrt, MD, PhD,[a,b] Michael J. Conrad, MLA,[c] Janka Franekova, MD, PhD,[d,e] Antonin Jabor, MD, PhD,[d,e] Petr Lupinek, MD, PhD,[a] Josef Kautzner, MD, PhD,[a] Vojtech Melenovsky, MD, PhD,[a] and Petr Jarolim, MD, PhD[c]

[a] *Department of Cardiology, Institute for Clinical and Experimental Medicine-IKEM, Prague, Czech Republic*

[b] *Center for Cardiovascular Prevention of the First Faculty of Medicine, Charles University and Thomayer Hospital, Prague, Czech Republic*

[c] *Department of Pathology, Brigham and Women's Hospital, Harvard Medical School, Boston, Massachusetts, USA*

[d] *Department of Laboratory Methods, Institute for Clinical and Experimental Medicine-IKEM, Prague, Czech Republic*

[e] *Third Faculty of Medicine, Charles University, Prague, Czech Republic*

ABSTRACT

Background: Growth differentiation factor-15 (GDF-15) is a stress-inducible cytokine and member of the transforming growth factor-β cytokine superfamily that refines prognostic assessment in subgroups of patients with heart failure (HF). We evaluated its role in HF patients with chronic kidney disease (CKD, estimated glomerular filtration rate <60 mL/min/1.73 m^2).

Methods: A total of 358 patients with stable systolic HF were followed for a median of 1121 (interquartile range, 379-2600) days. Comprehensive evaluation including B-type natriuretic peptide (BNP) and GDF-15 testing was performed at study entry; the analysis was stratified according to kidney function.

Results: Patients with CKD (33.8%) were older, had more often diabetes, and were less often treated with angiotensin converting enzyme inhibitors (ACEi)/angiotensin receptor blockers (ARB). GDF-15 was associated with estimated glomerular filtration rate, whereas BNP was associated with left ventricular-end diastolic diameter and ejection fraction ($P < 0.01$). During follow-up, 244 patients (68.2%)

RÉSUMÉ

Contexte : Le facteur de croissance et de différenciation cellulaire 15 (GDF-15) est une cytokine pouvant être induite par le stress. Elle fait partie d'une superfamille de cytokines, les facteurs de croissance transformant β, qui permet de raffiner l'établissement d'un pronostic chez des sous-groupes de patients atteints d'insuffisance cardiaque. Nous avons étudié son rôle chez des patients atteints d'insuffisance cardiaque et d'une néphropathie chronique (débit de filtration glomérulaire estimé : < 60 ml/min/1,73 m^2).

Méthodologie : Au total, 358 patients atteints d'une forme stable d'insuffisance cardiaque systolique ont été suivis pendant une période médiane de 1 121 jours (intervalle interquartile : de 379 à 2 600 jours). Une évaluation exhaustive comprenant, entre autres, des dosages du peptide natriurétique de type B (BNP) et du GDF-15 a été réalisée au moment de l'admission des patients à l'étude; les données analysées ont été stratifiées d'après la qualité de la fonction rénale.

Résultats : Les patients affligés d'une néphropathie chronique (33,8 %) étaient plus âgés, plus souvent atteints de diabète et moins souvent

Growth differentiation factor-15 (GDF-15) is a stress-inducible cytokine and member of the transforming growth factor-β cytokine superfamily. Plasma levels of GDF-15 are increased in response to multiple pathologic conditions such as inflammation, tissue injury, and oxidative stress.[1] Consequently, higher GDF-15 levels are associated with increased frequency of adverse events and higher mortality.[2] The source of GDF-15 in patients with heart failure (HF) has not been completely elucidated; however, it appears to be produced predominantly by peripheral tissues.[3] Previous studies in HF[4-6] showed that GDF-15 concentrations increase both with increasing HF severity and with various comorbidities. By reflecting several pathophysiological processes, GDF-15 functions as an integrator of both cardiac and noncardiac processes and may therefore serve as a biomarker in various clinical scenarios.[7,8] The exact role of GDF-15 in HF is still being investigated.

B-type natriuretic peptide (BNP) is a well-established biomarker of HF with excellent diagnostic and prognostic

Received for publication January 8, 2018. Accepted December 16, 2018.

Corresponding author: Dr Petr Jarolim, Department of Pathology, Brigham and Women's Hospital, 75 Francis Street, Boston, Massachusetts 02115, USA. Tel. +1-617-732-6672; fax: +1-617-731-4872.

E-mail: pjarolim@bwh.harvard.edu

See page 469 for disclosure information.

https://doi.org/10.1016/j.cjca.2018.12.027

experienced an adverse outcome (death, urgent transplantation, implantation of mechanical circulatory support). In patients with HF and CKD, the Cox proportional hazard model identified BNP, GDF-15, sex, systolic blood pressure, sodium, total cholesterol, and ACEi/ARB treatment as significant variables associated with an adverse outcome ($P < 0.05$). In multivariable analysis, BNP was replaced by GDF-15. Net reclassification improvement confirmed prognostic superiority of the model encompassing GDF-15 (GDF-15, sodium, total cholesterol, ACEi/ARB treatment) compared with the model without GDF-15 (BNP, sex, sodium, ACEi/ARB treatment), net reclassification improvement 0.62, $P = 0.005$. In contrast, in patients with HF and normal kidney function, BNP remained superior to GDF-15 in a multivariable model.

Conclusions: In patients with systolic HF and CKD, GDF-15 is more strongly associated with adverse outcomes than the conventionally used BNP.

traités par des inhibiteurs de l'enzyme de conversion de l'angiotensine (ECA) et des antagonistes des récepteurs de l'angiotensine (ARA). Nous avons établi un parallèle entre le GDF-15 et le débit de filtration glomérulaire estimé et constaté que le BNP avait plutôt un lien avec le diamètre télédiastolique du ventricule gauche et la fraction d'éjection ($p < 0{,}01$). Pendant la période de suivi, 244 patients (68,2 %) ont été victimes de complications (décès, transplantation effectuée en urgence, implantation d'un dispositif d'assistance circulatoire mécanique). Chez les patients atteints d'insuffisance cardiaque et d'une néphropathie chronique, le modèle des risques proportionnels de Cox a permis de déterminer que le BNP, le GDF-15, le sexe, la pression artérielle systolique, le sodium, le cholestérol total et le traitement par un inhibiteur de l'ECA et par un ARA sont des variables importantes quant aux issues défavorables ($p < 0{,}05$). Lors d'une analyse multivariée, le BNP a été remplacé par le GDF-15. Une reclassification nettement améliorée a confirmé la supériorité pronostique du modèle tenant compte du GDF-15 (GDF-15, sodium, cholestérol total, traitement par un inhibiteur de l'ECA et par un ARA) comparativement au modèle ne le prenant pas en compte (BNP, sexe, sodium, traitement par un inhibiteur de l'ECA et par un ARA) (amélioration nette de la classification : 0,62; $p = 0{,}005$). En revanche, un modèle d'analyse multivariée a révélé que le BNP conservait sa supériorité sur le GDF-15 chez les patients atteints d'insuffisance cardiaque ayant une fonction rénale normale.

Conclusions : Chez les patients atteints d'insuffisance cardiaque systolique et d'une néphropathie chronique, le lien entre le GDF-15 et une issue défavorable est plus fort que celui observé avec le BNP, le marqueur qui est habituellement utilisé.

power. However, in a disease as complex as HF, prognosis is estimated using multiple types of predictor variables (laboratory, clinical, imaging, therapeutic) that are integrated into validated models (eg, Seattle HF model [SHFM]) rather than relying on a single parameter.

Chronic kidney disease (CKD) is a condition leading to increased oxidative stress and to multiple systemic sequelae[9] that confound some of the variables used (BNP, haemoglobin, creatinine). In patients with HF and CKD, additional laboratory biomarkers reflecting different pathophysiological pathways may thus refine the outcome prediction even when compared with a multimarker model.[10]

We hypothesized that in patients with HF and CKD, GDF-15 may improve prognostic utility of a multimarker model that already included BNP such as SHFM. The goal of the study was to identify variables associated with BNP and GDF-15 levels and to examine the association between BNP, GDF-15, and outcome in HF patients with CKD.

Methods

Study subjects

Patients with stable HF of at least 6-month duration resulting from left ventricular (LV) systolic dysfunction (LV ejection fraction [LVEF] < 40%), hospitalized at the Institute for Clinical and Experimental Medicine in Prague for elective percutaneous coronary intervention, radiofrequency ablation, device implantation, or transplant eligibility evaluation, were screened. Those receiving stable medical therapy were enrolled into the study. Patients with recent HF decompensation (ie, diuretics in the previous month) or reversible LV dysfunction (planned valve surgery, revascularization, or tachycardia-induced cardiomyopathy) were excluded. Patients were prospectively followed for adverse outcome defined as the combined endpoint of death, urgent heart transplantation (patients with United Network for Organ Sharing [UNOS] status 1a/1b), or ventricular assist device implantation. Because the time to nonurgent transplantation (patients with UNOS status 2) reflects donor availability rather than the recipient's condition, patients who received a nonurgent heart transplant were censored as having no adverse outcome event at the day of transplantation.[11]

At the study enrollment, patients completed a Minnesota Living with Heart Failure Questionnaire and had anthropometric tests and echocardiographic study (Vivid-7; General Electric, Milwaukee, WI). LV function and dimensions were measured according to published recommendations.[12] A subgroup of 174 patients underwent right-heart catheterization at discretion of the examining cardiologist to help decide further therapeutic strategy. The investigation conforms with the principles outlined in the Declaration of Helsinki, the study protocol was approved by the Institutional Ethics Committee, and all subjects signed an informed consent.

Laboratory assessment

Blood was collected into ethylenediaminetetraacetic acid (EDTA)-anticoagulated tubes on patient enrollment. Basic biochemical parameters were assessed at the Institute for Clinical and Experimental Medicine. Sodium was measured by an indirect ion-specific electrode (ISE) method; creatinine (traceable to

the isotope dilution mass spectrometry (IDMS), Standard Reference Material (SRM) 967) and total cholesterol were measured by enzymatic methods (Abbott Architect; Abbott Laboratories Inc, Abbott Park, IL). Estimated glomerular filtration rate (eGFR) was calculated by the Modification of Diet in Renal Disease (MDRD) equation, based on serum creatinine levels, age, ethnicity, and sex.[13] BNP was measured on the ARCHITECT analyzer (Abbott Diagnostics, Abbott Park, IL) using a chemiluminescent immunoassay with a reportable range 10-25,000 ng/L. Intermediate precision was 6.8%, 5.6%, and 5.6% at 69.0, 286.0, and 1381.0 ng/L, respectively. GDF-15 was measured in the Biomarker Research and Clinical Trials Laboratory at Brigham and Women's Hospital. Patient specimens were diluted 4 times and 50 μL aliquots were tested in duplicates using the Quantikine Human GDF-15 Immunoassay (R&D Systems Inc, Minneapolis, MN). The reportable range was 94-6000 pg/mL and total imprecision was 8.3% at 162 pg/mL, 7.6% at 414 pg/mL, and 12.0% at 797 pg/mL.

Parameters used for an outcome analysis

In addition to BNP and GDF-15, we used the SHFM-derived set of validated variables to assess the prognosis of patients with HF: age, HF duration, sex, HF etiology, body mass index, systolic blood pressure, New York Heart Association (NYHA) functional class, heart rate, eGFR, sodium level, lymphocyte percentage, total cholesterol, uric acid, haemoglobin, Hb1Ac, LVEF, furosemide daily dose, use of angiotensin converting enzyme inhibitors (ACEi) or angiotensin receptor blockers (ARB), use of β-blockers, and presence of an implantable cardioverter defibrillator (ICD).[14,15]

Statistical analysis

The unpaired *t* test and/or Mann-Whitney *U* test was used to determine differences between parameters in patients with normal renal function and kidney disease. The Kolmogorov-Smirnov test was used to evaluate the Gaussian distribution. The χ^2 test was used to compare categorical variables. The association between variables was determined by linear regression. The effect of biomarker concentration on prognosis was tested using the univariate and multivariable Cox model; the forward Wald method was used for multivariable analysis. Because both BNP and GDF-15 showed markedly skewed distribution, log-normal values were used. Event-free survival of patients was analysed by Kaplan-Meier analysis with log-rank test comparison between groups. Calculations were performed using JMP 11 (SAS Institute Inc, Cary, NC) and SPSS version 19 software (Chicago, IL). Receiver operating characteristic (ROC) curves were analysed calculating C-statistics improvement using the method proposed by DeLong et al.[16] Net reclassification improvement was calculated by the method described by Pencina et al.[17]

Results

Patient characteristics

A total of 358 patients with systolic HF (LVEF 24.7% ± 5.0%, NYHA 2.8 ± 0.6) were followed for 1121 (interquartile range, 379-2600) days. During follow-up, 244 patients (68.2%) experienced an adverse outcome. Basic patient characteristics are summarized in Table 1.

Kidney function

Patients with CKD (eGFR < 60 mL/min/1.73 m^2, n = 121, 33.8% of total) were older, and had more often diabetes and ischemic etiology of HF and higher NYHA class. They were less often treated with ACEi or ARB but more frequently with cardiac resynchronization therapy. They also had borderline higher furosemide dose. No significant differences in any echocardiographic parameter were observed between the 2 groups. Patients with CKD had higher levels of both BNP and GDF-15 (Table 1). Patients with lower eGFR had significantly shorter event-free survival than those with normal kidney function (Supplemental Fig. S1).

Association of BNP and GDF-15 with clinical variables

There was a statistically significant but weak association between BNP and GDF-15 ($r = 0.49$, $P < 0.0001$). Both BNP and GDF-15 were negatively associated with systolic blood pressure and positively with NYHA class. There was a strong negative association between eGFR and GDF-15, whereas the association between eGFR and BNP was not significant ($P = 0.28$). Similarly, furosemide daily dose was associated with GDF-15 but not with BNP. BNP but not GDF-15 was associated with LVEF, LV end-diastolic diameter, and degree of mitral regurgitation (Table 2).

A subgroup of 174 patients underwent invasive haemodynamic assessment. Right atrial pressure, mean pulmonary pressure, and pulmonary capillary wedge pressure were associated with both BNP and GDF-15. In contrast, measured cardiac output was associated with BNP but not with GDF-15 (Table 2).

Outcome analysis

ROC analysis. Among patients with CKD, the ROC area under the curve (AUC) for GDF-15 (AUC 0.731, $P = 0.002$) was significantly higher (difference between areas 0.120, standard error 0.0548, $P = 0.03$, Fig. 1A) as compared with BNP (AUC 0.612, $P = 0.06$), which showed only a borderline association with the risk of adverse events. On the other hand, the ROC curves for GDF-15 (AUC 0.700, $P < 0.0001$) and BNP (AUC 0.705, $P < 0.0001$) did not differ in patients with normal kidney function (difference between areas 0.005, standard error 0.036, $P = 0.89$, Fig. 1B).

Kaplan-Meier analysis. We have further used ROC curve–derived cutoff values to stratify the cohort. For patients with CKD, BNP and GDF-15 levels of 652.7 ng/L and 1646.0 ng/L, respectively, were identified as optimal cutoffs. In patients with normal kidney function, the respective values were 264.0 ng/L for BNP and 1204.0 ng/L for GDF-15.

In patients with low BNP (both in patients with CKD and normal kidney function), those with high GDF-15 had substantially worse outcomes compared with those with low GDF-15 values (Fig. 2). In contrast, in patients with high BNP values, the difference between subjects with low and high GDF-15 was only small and did not reach statistical significance for patients with CKD (Supplemental Fig. S2). GDF-15 thus strengthens

Table 1. Basic characteristics of patients stratified according to the estimated glomerular filtration rate

Anthropometry	Total cohort (n = 358)	eGFR < 60 (n = 121)	eGFR > 60 (n = 237)	*P* value
Age (y)	58.92 ± 10.72	63.60 ± 8.85	56.53 ± 10.83	**< 0.0001**
Male gender	303 (84.6%)	103 (85.1%)	200 (84.4%)	0.85
BMI (kg/m^2)	27.7 ± 4.76	28.03 ± 4.89	27.60 ± 4.69	0.41
Heart failure and comorbidities				
Ischemic etiology	196 (54.7%)	78 (64.5%)	118 (49.8%)	**0.008**
HF duration (y)	8.25 ± 7.09	10.10 ± 8.08	7.28 ± 6.31	**0.0008**
NYHA functional class (1-4)	2.79 ± 0.55	2.88 ± 0.55	2.73 ± 0.55	**0.02**
Diabetes	122 (34.1%)	55 (45.5%)	67 (28.3%)	**0.001**
Obesity	102 (28.5 %)	34 (28.1%)	68 (28.7%)	0.91
Hb (g/L)	140.45 ± 16.63	137.12 ± 17.94	142.50 ± 15.59	**0.004**
eGFR (mL/min/1.73 m^2)	69.68 ± 22.91	47.22 ± 9.71	81.15 ± 18.85	**< 0.0001**
Hb1Ac (mmol/mol)	49.78 ± 16.11	51.90 ± 18.48	48.69 ± 14.67	0.07
Asthma/COPD	57 (15.9%)	21 (17.4%)	36 (15.2%)	0.60
BNP (ng/L)	562 (278; 1208)	653 (345; 1397)	515 (236; 1102)	**0.02**
GDF-15 (ng/L)	1503 (956; 2323)	2094 (1553; 3059)	1204 (835; 2641)	**< 0.0001**
Cardiac function				
Heart rate (min^{-1})	77.68 ± 9.09	77.26 ± 16.03	77.02 ± 14.14	0.89
Systolic blood pressure (mm Hg)	114.64 ± 18.91	114.51 ± 18.96	114.71 ± 18.93	0.93
LVEF (%)	24.68 ± 5.00	24.98 ± 5.44	24.54 ± 4.76	0.43
LV end-diastolic diameter (mm)	70.68 ± 9.09	70.52 ± 9.14	70.76 ± 9.08	0.82
RV dysfunction grade (0-3)	2 (1; 2)	2 (1; 2)	1 (1; 2)	0.16
Mitral regurgitation (0-2)	1 (0; 2)	1 (0; 1)	1 (0; 2)	0.13
Tricuspid regurgitation (0-2)	0 (0; 1)	0 (0; 1)	0 (0; 1)	0.49
IVC (mm)	20.03 ± 5.95	19.94 ± 6.26	20.08 ± 5.79	0.84
Medication				
Furosemide use (daily dose, mg)	96.55 ± 81.60	107.85 ± 85.04	90.56 ± 79.27	0.07
β-Blocker use	333 (93.0%)	110 (90.9%)	223 (94.1%)	0.27
ACEi/ARB use	310 (86.6%)	96 (79.3%)	214 (90.3%)	**0.005**
Aldosterone antag. use	282 (78.8%)	100 (82.6%)	182 (76.8%)	0.19
Triple therapy	228 (63.7%)	72 (59.5%)	156 (65.8%)	0.24
Devices				
ICD	239 (66.8%)	80 (66.1%)	159 (67.1%)	0.85
CRT	161 (45.0%)	64 (52.9%)	97 (40.9%)	**0.03**
Follow-up				
Follow-up length (d)	1121 (379; 2600)	802 (296; 2115)	1435 (470; 2740)	**0.002**
Survival	92 (25.7%)	20 (16.5%)	72 (30.4%)	–
Death	159 (44.4%)	68 (56.2%)	91 (38.4%)	–
Urgent HTx	54 (15.1%)	20 (16.5%)	34 (14.4%)	–
Normal HTx (%)	22 (6.1%)	7 (5.8%)	15 (6.3%)	–
LVAD implantation (%)	31 (8.7%)	6 (5.0%)	25 (10.5%)	–

Data are presented as means ± standard deviation or medians and interquartile ranges (if appropriate). Obesity was defined as BMI > 30. Triple therapy was defined as the therapy with β-blockers, ACEi/ARB, and aldosterone antagonist.

ACEi, angiotensin converting enzyme inhibitors; ARB, angiotensin receptor blockers; BMI, body mass index; BNP, B-type natriuretic peptide; COPD, chronic obstructive pulmonary disease; CRT, cardiac resynchronization therapy; eGFR, estimated glomerular filtration rate; GDF-15, growth differentiation factor-15; HF, heart failure; HTx, heart transplantation; ICD, implantable cardioverter defibrillator; IVC, inferior vena cava; LVAD, left ventricle assist device; LVEF, left ventricle ejection fraction; NYHA, New York Heart Association functional class; RV, right ventricle.

the association with adverse outcomes in patients with HF, in particular those with low BNP.

Cox proportional hazard model—patients with normal kidney function. In the Cox univariate analysis, BNP, GDF-15, sex, systolic blood pressure, sodium, furosemide daily dose, lymphocyte percentage in complete blood count, total cholesterol, the use of ACEi/ARB, uric acid, NYHA functional class, Hb1Ac level, LVEF, body mass index, and HF etiology were significantly associated with an adverse outcome in patients with HF and normal kidney function (Table 3). In contrast, heart rate, age, eGFR, haemoglobin, HF duration, the presence of ICD, and β-blocker therapy were not statistically significant. Multivariable analysis with BNP but without GDF-15 identified BNP, sex, sodium, and the presence of ACEi/ARB as significant predictors of an adverse outcome. The addition of GDF-15 into the model did not change the results (Table 3).

Cox proportional hazard model—patients with CKD. In patients with HF and CKD, BNP, GDF-15, sex, systolic blood pressure, sodium, total cholesterol, and the treatment with ACEi/ARB were significantly associated with an adverse outcome, whereas other variables were not (Table 4). Multivariable analysis using BNP but not GDF-15 identified BNP, sodium, and ACEi/ARB treatment as variables associated with an adverse outcome. When GDF-15 was added into the model, it replaced BNP that was no longer significant (Table 4).

Net reclassification improvement analysis. We used net reclassification improvement (NRI) analysis to compare both models (BNP, Na, ACEi/ARB treatment vs GDF-15, Na, total cholesterol, ACEi/ARB treatment). Among patients with CKD, an addition of GDF-15 to the model led to a significant NRI by 62% at *P* level = 0.005 (6.4% for event NRI and 55.6% for nonevent NRI). We thus conclude that in patients with HF and CKD, GDF-15 is not only an additive but also a superior variable associated with an adverse outcome compared with BNP.

Table 2. Association of clinical, echocardiographic, and haemodynamic variables with GDF-15 and BNP

	GDF-15		BNP	
n = 358	*r*	*P* value	*r*	*P* value
SBP (mm Hg)	−0.10	**0.048**	−0.27	**< 0.0001**
Age (y)	+ 0.24	**< 0.0001**	+ 0.02	0.78
NYHA (II-IV)	+ 0.54	**0.0012**	+ 0.13	**0.01**
Heart rate (min^{-1})	+ 0.08	0.13	+ 0.19	**0.0003**
BMI (kg/m^2)	−0.037	0.47	−0.31	**< 0.0001**
eGFR (mL/min/1.73 m^2)	−0.40	**< 0.0001**	−0.06	0.28
FSM daily dose (mg)	+ 0.23	**< 0.0001**	+ 0.07	0.23
Echocardiography (n = 358)				
LVEF (%)	−0.09	0.08	−0.25	**< 0.0001**
LVEDd (mm)	+ 0.03	0.54	+ 0.14	**0.0057**
MiR (0-2)	+ 0.096	0.33	+ 0.2	**< 0.0001**
TriR (0-2)	+ 0.28	**< 0.0001**	+ 0.28	**< 0.0001**
RV dysfunction grade (0-3)	+ 0.23	**< 0.0001**	+ 0.3	**< 0.0001**
IVC (mm)	+ 0.99	**0.02**	+ 0.29	**< 0.0001**
Haemodynamics (n = 174)				
RAP (mm Hg)	+ 0.45	**< 0.0001**	+ 0.30	**< 0.0001**
MAP (mm Hg)	+ 0.17	**0.02**	+ 0.32	**< 0.0001**
PCWP (mm Hg)	+ 0.2	**0.01**	+ 0.35	**< 0.0001**
TPG (mm Hg)	+ 0.08	0.31	+ 0.13	0.09
CO (mm Hg)	+ 0.11	0.14	−0.29	**< 0.0001**

BMI, body mass index; BNP, B-type natriuretic peptide; CO, cardiac output; eGFR, estimated glomerular filtration rate; FSM, furosemide; GDF-15, growth differentiation factor-15; IVC, inferior vena cava; LVEDd, left-ventricle diameter in end-diastole; LVEF, left-ventricle ejection fraction; MAP, mean pulmonary artery pressure; MiR, mitral regurgitation; NYHA, New York Heart Association functional class; PCWP, pulmonary capillary wedge pressure; RAP, right atrial pressure; RV, right ventricle; SBP, systolic blood pressure; TPG, transpulmonary gradient; TriR, tricuspid regurgitation.

Discussion

Our study compared association of BNP and GDF-15 with adverse outcomes in HF population. When taking into account kidney function, the main conclusion is that the addition of GDF-15 refines prognosis of patients with low BNP. In addition, in patients with systolic HF and CKD, GDF-15 is more strongly associated with adverse outcomes than the conventionally used BNP. Both biomarkers were associated with distinct clinical variables; BNP was associated with parameters of LV function, whereas GDF-15 was more strongly associated with glomerular filtration.

Therapy of patients with HF and CKD

CKD is a common comorbidity in patients with HF with a prevalence of approximately 40%,[18] which is similar to the CKD prevalence observed in our patient cohort (33.8%). Patients with CKD are less often treated with HF medication,[18] which was confirmed in our study as well; patients with CKD had a significantly lower prevalence of ACEi/ARB therapy. However, ACEi/ARB treatment was an important factor related to the prognosis of patients regardless of kidney function. Importantly, patients with CKD were reported to derive similar benefit from ACEi/ARB therapy as those with normal kidney function.[19]

Association of biomarkers with clinical variables

The study showed that BNP and GDF-15 were associated with distinct clinical variables likely reflecting different pathophysiological mechanisms responsible for their release. BNP is produced by ventricular and atrial cardiomyocytes on mechanical stress that is believed to be the main stimulus for its biosynthesis and release.[20] Consistently, we observed a significant association between BNP and LV diameter and ejection fraction. Compared with BNP, the stimuli for GDF-15 production are more diverse. Cardiac myocytes produce and secrete large amounts of GDF-15 in response to oxidative stress and ischemia,[21] but considerable amount of GDF-15 is also produced by other tissues such as macrophages,[22] vascular smooth muscle cells,[23] adipocytes,[24] and endothelial cells.[25] Although the main source of GDF-15 in patients with HF is less clear, it seems that the majority is produced by noncardiac tissues.[3] Accordingly, we documented no relation between GDF-15 and LV size or function but a significant association with GFR. Similarly, GDF-15 was associated with tricuspid regurgitation severity, right ventricle dysfunction grade, and inferior vena cava diameter (but not mitral

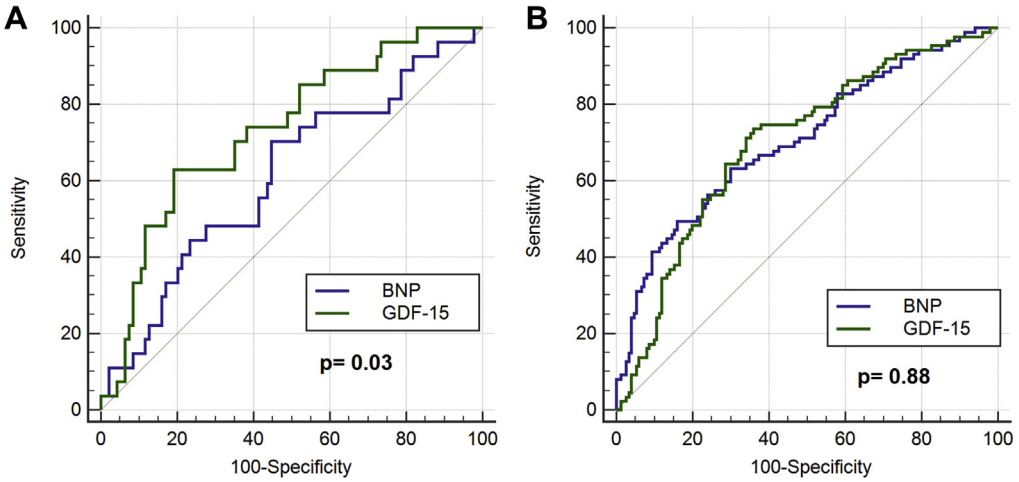

Figure 1. Receiver operating characteristic curve based on B-type natriuretic peptide (BNP) and growth differentiation factor-15 (GDF-15) in patients with chronic kidney disease (**A**) and in patients with normal kidney function (**B**).

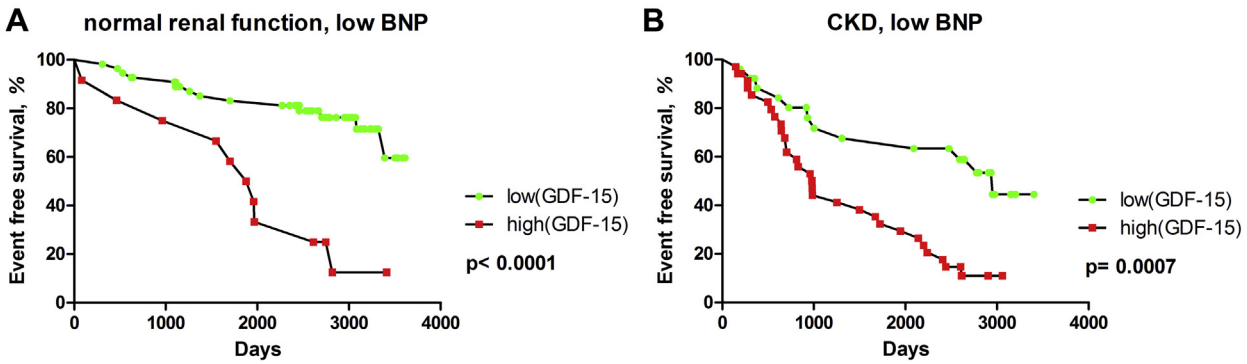

Figure 2. Kaplan-Meier analysis showing an outcome of patients with low B-type natriuretic peptide (BNP)/low growth differentiation factor-15 (GDF-15) compared with those with low BNP/high GDF-15 in patients with normal renal function (**A**) and chronic kidney disease (CKD) (**B**). Cutoff values to discriminate between high and low BNP and GDF-15 are based on receiver operating characteristic curve analysis and are as follows: BNP of 264.0 and 652.7 ng/L for patients with normal kidney function and CKD, respectively; GDF-15 of 1204.0 and 1646.0 ng/L for patients with normal kidney function and CKD, respectively.

regurgitation severity nor cardiac output), which likely reflects the degree of congestion and is thus related to renal function.

Patients with CKD had a higher level of both BNP and GDF-15. CKD is known to be associated with elevated levels of natriuretic peptides,[26] which can be only partially explained by decreased kidney clearance.[27,28] The association between increased GDF-15 levels and decreased kidney function is likely due to either increased production or decreased clearance. Kidneys produce GDF-15 in response to injury or metabolic stress, and increased concentration of GDF-15 in urine of patients with diabetic nephropathy has been described.[29]

The higher level of GDF-15 in HF patients with CKD thus probably reflects not only decreased clearance of GDF-15 but also increased production likely related to increased oxidative stress and inflammation.[4,30] A strong association between renal function and GDF-15 levels is in agreement with previous observations.[4,5,30]

Table 3. Variables associated with an adverse outcome in patients with HF and normal renal function

N = 237, 150 events	Univariate analysis			Multivariable analysis (excluding GDF-15)			Multivariable analysis (including GDF-15)		
Variable	HR	95% CI	*P* value	HR	95% CI	*P* value	HR	95% CI	*P* value
BNP (1 ln, ng/L)	1.82	1.55-2.16	**< 0.0001**	1.50	1.26-1.79	**< 0.0001**	1.50	1.26-1.79	**< 0.0001**
GDF-15 (1 ln, ng/L)	2.28	1.72-3.01	**< 0.0001**		**not included**				
Sex (males vs females)	3.37	1.91-6.62	**< 0.0001**	2.20	1.10-4.39	**0.025**	2.20	1.10-4.39	**0.025**
Systolic blood pressure (5 mm Hg)	0.88	0.84-0.93	**< 0.0001**						
Na (mmol/L)	0.89	0.86-0.93	**< 0.0001**	0.91	0.87-0.96	**< 0.0001**	0.91	0.87-0.96	**< 0.0001**
Furosemide daily dose (10 mg)	1.03	1.01-1.05	**0.001**						
Lymphocyte percentage (1%)	0.98	0.96-0.99	**0.009**						
Total cholesterol (mmol/L)	0.82	0.70-0.96	**0.02**						
ACEi or ARB (present vs absent)	0.32	0.20-0.54	**< 0.0001**	0.44	0.26-0.75	**0.002**	0.44	0.26-0.75	**0.002**
Uric acid (100 µmol/L)	1.27	1.10-1.46	**0.001**						
NYHA (I+II vs III+IV)	0.60	0.41-0.86	**0.005**						
Hb1Ac (mmol/mol)	1.02	1.008-1.025	**0.0002**						
LVEF (5%)	0.73	0.60-0.88	**0.0008**						
BMI (kg/m^2)	0.94	0.91-0.98	**0.002**						
Heart rate (min^{-1})	1.01	0.999-1.02	0.051						
Age (5 y)	0.99	0.92-1.08	0.90						
eGFR (mL/min/1.73 m^2)	0.99	0.99-1.004	0.34						
Haemoglobin (10 g/L)	1.05	0.95-1.17	0.35						
HF etiology (CAD vs non-CAD)	1.47	1.06-2.04	**0.02**						
HF duration (y)	1.01	0.98-1.03	0.53						
ICD (present vs absent)	0.98	0.70-1.39	0.89						
β-Blockers (present vs absent)	0.77	0.43-1.58	0.45						

Note that both models excluding and including GDF-15 are identical indicating that the inclusion of GDF-15 in the model has not changed the results of the model based on BNP.

ACEi, angiotensin converting enzyme inhibitors; ARB, angiotensin receptor blockers; BMI, body mass index; BNP, B-type natriuretic peptide; CAD, coronary artery disease; CI, confidence interval; eGFR, estimated glomerular filtration rate; GDF-15, growth differentiation factor-15; HF, heart failure; HR, hazard ratio; LVEF, left-ventricle ejection fraction; NYHA, New York Heart Association functional class.

Table 4. Variables associated with an adverse outcome in patients with HF and CKD

N = 121, 94 events	Univariate analysis			Multivariable analysis (excluding GDF-15)			Multivariable analysis (including GDF-15)		
Variable	HR	95% CI	*P* value	HR	95% CI	*P* value	HR	95% CI	*P* value
BNP (1 ln, ng/L)	1.65	1.31-2.07	**< 0.0001**	1.45	1.15-1.83	**0.002**			
GDF-15 (1 ln, ng/L)	2.87	1.90-4.30	**< 0.0001**	**not included**			2.05	1.29-3.26	**0.002**
Sex (males vs females)	2.20	1.17-4.73	**0.01**						
Systolic blood pressure (5 mm Hg)	0.92	0.87-0.98	**0.005**						
Na (mmol/L)	0.90	0.85-0.96	**0.001**	0.92	0.86-0.98	**0.009**	0.93	0.87-0.99	**0.02**
Furosemide daily dose (10 mg)	1.02	0.996-1.04	0.10						
Lymphocyte percentage (1%)	0.98	0.96-1.003	0.11						
Total cholesterol (mmol/L)	0.61	0.47-0.79	**< 0.0001**				0.76	0.59-0.98	**0.034**
ACEi or ARB (present vs absent)	0.32	0.20-0.52	**< 0.0001**	0.48	0.27-0.83	**0.008**	0.51	0.29-0.87	**0.014**
Uric acid (100 µmol/L)	1.04	0.90-1.22	0.53						
NYHA (I+II vs III+IV)	0.77	0.44-1.28	0.32						
Hb1Ac (mmol/mol)	1.00	0.996-1.02	0.18						
LVEF (5%)	0.94	0.78-1.12	0.50						
BMI (kg/m^2)	0.98	0.93-1.02	0.36						
Heart rate (min^{-1})	1.00	0.99-1.01	0.88						
Age (5 y)	0.96	0.86-1.07	0.42						
eGFR (mL/min/1.73 m^2)	0.98	0.96-1.30	0.15						
Haemoglobin (10 g/L)	0.97	0.86-1.09	0.60						
HF etiology (CAD vs non-CAD)	0.92	0.60-1.44	0.72						
HF duration (y)	1.00	0.98-1.03	0.76						
ICD (present vs absent)	1.06	0.70-1.64	0.79						
β-Blockers (present vs absent)	0.72	0.40-1.44	0.33						

ACEi, angiotensin converting enzyme inhibitors; ARB, angiotensin receptor blockers; BMI, body mass index; BNP, B-type natriuretic peptide; CAD, coronary artery disease; CI, confidence interval; CKD, chronic kidney disease; eGFR, estimated glomerular filtration rate; GDF-15, growth differentiation factor-15; HF, heart failure; HR, hazard ratio; LVEF, left-ventricle ejection fraction; NYHA, New York Heart Association functional class.

The role of GDF-15 in outcome prediction of patients with HF

GDF-15 is elevated in many states reflecting primarily cardiac but also noncardiac pathology[31] and thus integrates multiple pathophysiological pathways.[30] GDF-15 captures different aspects of cardiovascular disease pathology that are not represented by established HF biomarkers that are related to outcome in HF. Although HF with reduced ejection fraction is caused primarily by a cardiac pathology, it is truly a syndrome rather than a disease and has many distinct subtypes.[1] Considering that HF affects multiple organ systems, biomarkers reflecting cardiac and extracardiac abnormalities may provide incremental information beyond purely cardiac markers such as natriuretic peptides in distinct HF subtypes. CKD is a condition accompanied by inflammation and increased oxidative stress; we have therefore hypothesized that an addition of GDF-15 (reflecting extracardiac component) to BNP (assessing cardiac component) would provide additional information compared with BNP alone. In our cohort, GDF-15 further stratified the outcome of patients with low BNP (< 264 ng/L in patients with normal kidney function and < 652.7 ng/L in patients with CKD). In patients with CKD, its association with an adverse outcome was superior to conventionally used BNP; such a strong role of GDF-15 was not observed in patients with HF and normal kidney function. Although we have observed a strong association between GDF-15 and eGFR, it was GDF-15 but not eGFR that was most tightly related to a poor outcome. GDF-15 thus seems to reflect qualitatively broader information beyond kidney function.

The fact that the majority of GDF-15 is produced outside the heart may explain why it adds so potently to a biomarker such as BNP that is produced exclusively in the cardiac tissue. Although the prognostic role of GDF-15 in patients with HF was already described in previous studies,[4,5,30] we believe that this is the first study specifically describing the role of GDF-15 in patients with HF and CKD.

Relationship to previous studies of GDF-15 in HF

Our study has several unique features. First, it had a long follow-up (upper quartile range 2600 days) during which more than two-thirds of patients (68.6%) experienced an outcome. Second, our cohort of patients had a considerably higher level of guideline-recommended HF therapy (93% β-blockers, 87% ACEi/ARB, 79% mineralocorticoid receptor antagonist, 67% ICD) than previously published studies. Kempf et al.[4] described that GDF-15 remained an independent predictor of mortality even after adjustment for clinical variables and established biomarkers of adverse prognosis including N-terminal type BNP. This study did not specifically focus on refinement of prognosis in certain HF subtypes and investigated a cohort with a lower level of guideline-recommended HF therapy (58.6% β-blocker, 23.7% spironolactone, no information about device therapy was provided). In a subanalysis of the **Val**sartan **He**art **F**ailure **T**rial (Val-HeFT) trial, GDF-15 predicted mortality independently of a comprehensive set of established prognostic variables including NYHA class, LVEF, renal function, haemoglobin, sodium, uric acid, HF medication, and prognostic biomarkers, including BNP, high-sensitivity troponin T, and C-reactive protein.[5] However, only 34.5% of patients were treated with β-blockers in the Val-HeFT trial compared with 67.1% treated with digoxin.[9] With the exception of neprilysin inhibitor therapy, BNP levels decrease with adequate HF pharmacotherapy (β-blockers, ACEi/ARB, mineralocorticoid receptor antagonist).[32] Additional biomarkers may therefore

refine the information about prognosis in patients treated with these agents. In comparison with previous studies,[4,5,30] our results thus provide an insight into the role of GDF-15 in an HF cohort treated according to the HF guidelines.

Study limitations

Our study was performed in a heart centre offering a complex cardiovascular program including ventricular assist device implantation and heart transplantation. Because this could introduce bias related to the analysis of prognostic value, urgent heart transplantation and LV assist device implantation were considered adverse outcomes,[11] whereas the patients receiving nonurgent heart transplant were censored as having no adverse outcome on the day of transplantation. In addition, it was a single-centre study with a substantial predominance of male patients. Because some of the patients were evaluated for heart transplant eligibility, this study cohort overall included patients with rather advanced HF. However, the prevalence of kidney disease was similar to other community-based cohorts.[18] Consequently, the results might not be fully applicable to patients with milder HF. Data about HF rehospitalizations were not available in all patients; this endpoint thus could not have been included in the analysis.

Conclusions

GDF-15 is strongly associated with adverse outcomes in patients with stable HF and optimized drug and device therapy. Regardless of kidney function, it refines risk stratification in subjects with low BNP. In patients with systolic HF and CKD, GDF-15 is more strongly related to an adverse outcome than conventionally used BNP.

Funding Sources

This work was supported by Ministry of Health, Czech Republic—conceptual development of research organization (Institute for Clinical and Experimental Medicine—IKEM) [IN 00023001] and by grant [17-28784A]; by the grant agency of the Czech Republic—grant [15-14200], and by fund [103517] of the Biomarker Research and Clinical Trials Laboratory at Brigham and Women's Hospital.

Disclosures

Josef Kautzner is a member of Advisory Boards for Bayer, Boehringer Ingelheim, Daiichi Sankyo, Biosense Webster, Boston Scientific, Medtronic, LivaNova, and St Jude Medical. He has received speaker honoraria from the above-mentioned companies and Biotronik. Petr Jarolim received research support from Abbott Laboratories, Amgen Inc, AstraZeneca LP, Beckman Coulter, Daiichi Sankyo Inc, GlaxoSmithKline, Merck & Co, Inc, Roche Diagnostics Corporation, Takeda Global Research and Development Center, and Waters Technologies Corporation; and speaker honoraria from Roche Diagnostics Corporation. The remaining authors have no conflicts of interest to disclose.

References

1. Wollert KC, Kempf T. Growth differentiation factor 15 in heart failure: an update. Curr Heart Fail Rep 2012;9:337-45.
2. Rohatgi A, Patel P, Das SR, et al. Association of growth differentiation factor-15 with coronary atherosclerosis and mortality in a young, multiethnic population: observations from the Dallas Heart Study. Clin Chem 2012;58:172-82.
3. Lok SI, Winkens B, Goldschmeding R, et al. Circulating growth differentiation factor-15 correlates with myocardial fibrosis in patients with non-ischaemic dilated cardiomyopathy and decreases rapidly after left ventricular assist device support. Eur J Heart Fail 2012;14:1249-56.
4. Kempf T, von Haehling S, Peter T, et al. Prognostic utility of growth differentiation factor-15 in patients with chronic heart failure. J Am Coll Cardiol 2007;50:1054-60.
5. Anand IS, Kempf T, Rector TS, et al. Serial measurement of growth-differentiation factor-15 in heart failure: relation to disease severity and prognosis in the Valsartan Heart Failure Trial. Circulation 2010;122:1387-95.
6. Izumiya Y, Hanatani S, Kimura Y, et al. Growth differentiation factor-15 is a useful prognostic marker in patients with heart failure with preserved ejection fraction. Can J Cardiol 2014;30:338-44.
7. Corre J, Hebraud B, Bourin P. Concise review: growth differentiation factor 15 in pathology: a clinical role? Stem Cells Transl Med 2013;2:946-52.
8. Retnakaran R. Novel biomarkers for predicting cardiovascular disease in patients with diabetes. Can J Cardiol 2018;34:624-31.
9. Di Lullo L, House A, Gorini A, et al. Chronic kidney disease and cardiovascular complications. Heart Fail Rev 2015;20:259-72.
10. Santema BT, Kloosterman M, Van Gelder IC, et al. Comparing biomarker profiles of patients with heart failure: atrial fibrillation vs. sinus rhythm and reduced vs. preserved ejection fraction. Eur Heart J 2018;39:3867-75.
11. Aaronson KD, Schwartz JS, Chen TM, et al. Development and prospective validation of a clinical index to predict survival in ambulatory patients referred for cardiac transplant evaluation. Circulation 1997;95:2660-7.
12. Lang RM, Bierig M, Devereux RB, et al. Recommendations for chamber quantification. Eur J Echocardiogr 2006;7:79-108.
13. National Kidney Foundation. K/DOQI clinical practice guidelines for chronic kidney disease: evaluation, classification, and stratification. Am J Kidney Dis 2002;39:S1-266.
14. Mozaffarian D, Anker SD, Anand I, et al. Prediction of mode of death in heart failure: the Seattle Heart Failure Model. Circulation 2007;116:392-8.
15. May HT, Horne BD, Levy WC, et al. Validation of the Seattle Heart Failure Model in a community-based heart failure population and enhancement by adding B-type natriuretic peptide. Am J Cardiol 2007;100:697-700.
16. DeLong ER, DeLong DM, Clarke-Pearson DL. Comparing the areas under two or more correlated receiver operating characteristic curves: a nonparametric approach. Biometrics 1988;44:837-45.
17. Pencina MJ, D'Agostino RB Sr, D'Agostino RB Jr, Vasan RS. Evaluating the added predictive ability of a new marker: from area under the ROC curve to reclassification and beyond. Stat Med 2008;27:157-72 [discussion: 207-12].
18. van Deursen VM, Urso R, Laroche C, et al. Co-morbidities in patients with heart failure: an analysis of the European Heart Failure Pilot Survey. Eur J Heart Fail 2014;16:103-11.

19. Gurwitz JH, Magid DJ, Smith DH, et al. Treatment effectiveness in heart failure with comorbidity: lung disease and kidney disease. J Am Geriatr Soc 2017;65:2610-8.

20. Daniels LB, Maisel AS. Natriuretic peptides. J Am Coll Cardiol 2007;50:2357-68.

21. Kempf T, Eden M, Strelau J, et al. The transforming growth factor-beta superfamily member growth-differentiation factor-15 protects the heart from ischemia/reperfusion injury. Circ Res 2006;98:351-60.

22. Schlittenhardt D, Schober A, Strelau J, et al. Involvement of growth differentiation factor-15/macrophage inhibitory cytokine-1 (GDF-15/MIC-1) in oxLDL-induced apoptosis of human macrophages in vitro and in arteriosclerotic lesions. Cell Tissue Res 2004;318:325-33.

23. Bermudez B, Lopez S, Pacheco YM, et al. Influence of postprandial triglyceride-rich lipoproteins on lipid-mediated gene expression in smooth muscle cells of the human coronary artery. Cardiovascular research 2008;79:294-303.

24. Ding Q, Mracek T, Gonzalez-Muniesa P, et al. Identification of macrophage inhibitory cytokine-1 in adipose tissue and its secretion as an adipokine by human adipocytes. Endocrinology 2009;150:1688-96.

25. Nickel N, Jonigk D, Kempf T, et al. GDF-15 is abundantly expressed in plexiform lesions in patients with pulmonary arterial hypertension and affects proliferation and apoptosis of pulmonary endothelial cells. Respir Res 2011;12:62.

26. Vickery S, Price CP, John RI, et al. B-type natriuretic peptide (BNP) and amino-terminal proBNP in patients with CKD: relationship to renal function and left ventricular hypertrophy. Am J Kidney Dis 2005;46:610-20.

27. van Kimmenade RR, Januzzi JL Jr, Bakker JA, et al. Renal clearance of B-type natriuretic peptide and amino terminal pro-B-type natriuretic peptide a mechanistic study in hypertensive subjects. J Am Coll Cardiol 2009;53:884-90.

28. deFilippi CR, Christenson RH. B-type natriuretic peptide (BNP)/NT-proBNP and renal function: is the controversy over? Clin Chem 2009;55:1271-3.

29. Simonson MS, Tiktin M, Debanne SM, et al. The renal transcriptome of db/db mice identifies putative urinary biomarker proteins in patients with type 2 diabetes: a pilot study. Am J Physiol Renal Physiol 2012;302:F820-9.

30. Chan MM, Santhanakrishnan R, Chong JP, et al. Growth differentiation factor 15 in heart failure with preserved vs. reduced ejection fraction. Eur J Heart Fail 2016;18:81-8.

31. Dostalova I, Roubicek T, Bartlova M, et al. Increased serum concentrations of macrophage inhibitory cytokine-1 in patients with obesity and type 2 diabetes mellitus: the influence of very low calorie diet. Eur J Endocrinol 2009;161:397-404.

32. Fung JW, Yu CM, Yip G, et al. Effect of beta blockade (carvedilol or metoprolol) on activation of the renin-angiotensin-aldosterone system and natriuretic peptides in chronic heart failure. Am J Cardiol 2003;92:406-10.

Supplementary Material

To access the supplementary material accompanying this article, visit the online version of the *Canadian Journal of Cardiology* at www.onlinecjc.ca and at https://doi.org/10.1016/j.cjca.2018.12.027.

J. Veselka a kol.

Alcohol septal ablation in patients with severe hypertrophy *(id 41)*

Heart failure and cardiomyopathies
Impact Factor: 5,082

rejstřík

ORIGINAL RESEARCH ARTICLE

Alcohol septal ablation in patients with severe septal hypertrophy

Josef Veselka,[1] Morten Jensen,[2] Max Liebregts,[3] Robert M Cooper,[4] Jaroslav Januska,[5] Maksim Kashtanov,[6,7] Maciej Dabrowski,[8] Peter Riis Hansen,[9] Hubert Seggewiss,[10,11] Eva Hansvenclova,[1] Henning Bundgaard,[2] Jurrien ten Berg,[3] Rodney Hilton Stables,[4] Lothar Faber[11]

For numbered affiliations see end of article.

Correspondence to
Dr Josef Veselka, Dpt. of Cardiology, University Hospital Motol, Prague 15000, Czech Republic;
veselka.josef@seznam.cz

Received 17 May 2019
Revised 30 July 2019
Accepted 5 August 2019

To cite: Veselka J, Jensen M, Liebregts M, *et al*. *Heart* Epub ahead of print: [*please include* Day Month Year]. doi:10.1136/heartjnl-2019-315422

ABSTRACT

Objective The current guidelines suggest alcohol septal ablation (ASA) is less effective in hypertrophic obstructive cardiomyopathy (HOCM) patients with severe left ventricular hypertrophy, despite acknowledging that systematic data are lacking. Therefore, we analysed patients in the Euro-ASA registry to test this statement.

Methods We compared the short-term and long-term outcomes of patients with basal interventricular septum (IVS) thickness <30 mm Hg to those with ≥30 mm Hg treated using ASA in nine European centres.

Results A total of 1519 patients (57±14 years, 49% women) with symptomatic HOCM were treated, including 67 (4.4%) patients with IVS thickness ≥30 mm. The occurrence of short-term major adverse events were similar in both groups. The mean follow-up was 5.4±4.3 years and 5.1±4.1 years, and the all-cause mortality rate was 2.57 and 2.94 deaths per 100 person-years of follow-up in the IVS <30 mm group and the IVS ≥30 mm group (p=0.047), respectively. There were no differences in dyspnoea (New York Heart Association class III/IV 12% vs 16%), residual left ventricular outflow tract gradient (16±20 vs 16±16 mm Hg) and repeated septal reduction procedures (12% vs 18%) in the IVS <30 mm group and IVS ≥30 mm group, respectively (p=NS for all).

Conclusions The short-term results and the long-term relief of dyspnoea, residual left ventricular outflow obstruction and occurrence of repeated septal reduction procedures in patients with basal IVS ≥30 mm is similar to those with IVS <30mm. However, long-term all-cause and cardiac mortality rates are worse in the ≥30 mm group.

INTRODUCTION

Symptomatic patients with hypertrophic obstructive cardiomyopathy (HOCM) have been successfully treated with alcohol septal ablation (ASA) for years.[1–5] The current European guidelines on hypertrophic cardiomyopathy caution that ASA is less effective in patients with severe hypertrophy (≥30 mm), while acknowledging that systematic data are lacking.[6] US guidelines also note that the effectiveness of ASA is uncertain in patients with marked septal hypertrophy (>30 mm) and that the procedure is generally discouraged in this group.[7] Therefore, we analysed the as yet largest reported cohort of HOCM patients treated with ASA and compared the short-term and long-term outcomes of patients with basal interventricular septum (IVS) thickness ≥30 mm to those with an IVS <30 mm.

METHODS

The study is based on an international, multicentre ASA registry (Euro-ASA registry) collecting 1519 patients who underwent ASA in nine European centres between 1997 and 2018. These patients were prospectively collected in institutional registries and retrospectively reviewed. Some results from this registry were published in the past.[8–10] All centres were experienced with the performance of ASA[11 12] and provided complex care of HOCM patients. Diagnosis of HCM was based on previously reported echocardiographic and magnetic resonance descriptions of a hypertrophied and non-dilated left ventricle (LV) (wall thickness ≥15 mm) in the absence of other cardiac or systemic diseases that could explain the magnitude of LV hypertrophy.[6 7] Maximum IVS thickness was measured in the basal segment. Left ventricular obstruction was considered significant when the maximum gradient estimated by continuous wave Doppler was ≥30 mm Hg at rest or ≥50 mm Hg after provocation.

All ASA procedures were performed by experienced invasive cardiologists (one or two in each centre). The technique details of ASA have been published previously.[1–5 8–21] All patients underwent clinical and echocardiographic follow-ups 1–6 months after the procedure and every year thereafter.

We hypothesised that HOCM patients with severe hypertrophy (≥30 mm) treated with ASA have an outcome similar to those with IVS <30 mm.

Patients were divided in two groups with the basal IVS thickness <30 mm and ≥30 mm, and we assessed: (1) the 30-day rate of cardiovascular adverse events (cardiovascular death, electrical defibrillation for ventricular tachycardia/fibrillation, cardiac tamponade and pacemaker implantation) after first ASA in patients with an IVS thickness of <30 mm versus patients with an IVS thickness ≥30 mm and the long-term (2) all-cause mortality, (3) cardiovascular mortality events (defined as cardiovascular death occurrence, first appropriate implantable cardioverter-defibrillator (ICD) discharge or resuscitation), (4) appropriate ICD discharges, (5) LV outflow gradient changes, (6) changes in severe dyspnoea (NYHA class III/

IV) and (7) repeated septal reduction procedure (re-ASA or myectomy).

This study was conducted in accordance with the Declaration of Helsinki principles.

Statistical analysis

Two experienced statisticians edited and evaluated collected data that are presented as mean±SD or counts and proportions. Student's t-test or Mann-Whitney test were used to evaluate the difference between continuous variables and the Fisher's exact test between categorical variables. The data distribution was evaluated by the Kolmogorov-Smirnov test. Comparison of mortality rates was done using Poisson regression and adjusted for age. Two following variables were prespecified—the age of the patients when ASA was performed and presence of IVS thickness ≥30 mm—and entered as independent variables into an analysis that was performed using a Cox's regression with calculation of HRs and 95% CIs. Estimates for long-term outcomes were based on the Kaplan-Meier method, and differences were compared using the Cox's regression. Kaplan-Meier curves were adjusted to age of 55 years using the Cox's model. P value<0.05 was considered statistically significant. All reported p values were two sided. The software GraphPad (release 6.05, GraphPad Software Inc, La Jolla, California, USA) and Stata (release V.14.2) were used for statistical analysis.

RESULTS

A total of 1519 patients with symptomatic HOCM were treated with ASA, including 67 (4.4%) patients with maximum IVS thickness ≥30 mm. We compared their baseline characteristics and outcomes with patients with maximum IVS thickness <30 mm. (table 1). Patients in the IVS ≥30 mm group were significantly younger, less symptomatic, had a lower LV diameter and a greater proportion had ICDs implanted prior to ASA. The group with IVS ≥30 mm received a higher dose of alcohol at ASA.

Short-term major adverse events in both groups are summarised in table 2. There were no differences in the occurrence of major adverse events between both groups.

None of the patients were lost to follow-up. The mean follow-up was 5.4±4.3 years (7841 patient-years) and 5.1±4.1 years (342 patient-years), and the all-cause mortality rate was 2.57 and 2.94 deaths per 100 person-years of follow-up in the IVS <30 mm group and the IVS ≥30 mm group, respectively (p=0.047).

The age-adjusted estimate for 10-year survival from all-cause death was 0.82 and 0.76 in the IVS <30 mm group and in the IVS ≥30 mm group, respectively. The age-adjusted Kaplan-Meier curves for all-cause mortality are shown in figure 1. In multivariable analysis, all-cause mortality was associated with a higher age at which ASA was performed (HR 1.06 per year; 95% CI 1.05 to 1.07; p<0.01) and baseline IVS thickness ≥30 mm (HR 2.07; 95% CI 1.09 to 4.00; p=0.03).

The occurrence of cardiovascular mortality events is summarised in table 3. The age-adjusted Kaplan-Meier curves for cardiovascular mortality events are demonstrated in figure 2.

In multivariable analysis, the cardiovascular mortality events were associated with a higher age at which ASA was performed (HR 1.03 per year; 95% CI 1.02 to 1.04; p<0.01) and baseline IVS thickness ≥30 mm (HR 3.07; 95% CI 2.25 to 4.18; p<0.01).

The occurrence of appropriate ICD discharges was very low in both groups of patients (table 3).

Table 1 Clinical and echocardiographic characteristics at baseline and at the last follow-up

	IVS <30 mm group (n=1452)	IVS ≥30 mm group (n=67)	P value
Basal IVS thickness, mm			
Baseline	20.2±3.5	32.9±3.9	<0.001
Last clinical check-up	15.4±4.2	21.1±7.2	<0.001
Age, years	57.8±13.7	47.1±13.4	<0.001
Females, n (%)	705 (48.6)	32 (47.8)	1.000
Alcohol at first ASA	2.2±0.9	2.7±1.3	<0.001
Total volume of alcohol, mL	2.3±1.1	3.2±1.9	<0.001
NYHA class III/IV			
Baseline, n (%)	1165 (80)	43 (64)	0.003
Last clinical check-up, n (%)	171 (12)	11 (16)	0.249
Angina, CCS class III/IV			
Baseline, n (%)	266 (18)	6 (9)	0.051
Last clinical check-up, n (%)	9 (1)	0 (0)	1.000
LV outflow gradient at rest, mm Hg			
Baseline	69.2±38.6	73.3±38.9	0.248
Last clinical check-up	16.3±21.2	15.9±15.8	0.127
>30 mm Hg, n (%)	221 (15)	12 (18)	0.602
Change in gradient (%)	72.8±39.7	74.4±22.4	0.829
Diastolic LV diameter, mm			
Baseline	43.4±6.3	39.5±5.8	<0.001
Last clinical check-up	45.7±6.1	43.6±8.4	0.039
LV ejection fraction, %			
Baseline	70±9	70±10	0.989
Last clinical check-up	66±10	67±10	0.666
Left atrial diameter, mm			
Baseline	47.0±6.8	47.4±8.3	0.526
Last clinical check-up	45.7±7.3	45.7±8.1	0.944
ICD, n (%)			
Baseline	51 (4)	15 (22)	<0.001
Last clinical check-up	104 (7)	23 (34)	<0.001
Mean follow-up duration, years	5.4±4.3	5.1±4.1	

ASA, alcohol septal ablation; CCS, Canadian Cardiovascular Society; ICD, Implantable cardioverter-defibrillator; IVS, interventricular septum; LV, left ventricular; NYHA, New York Heart Association.

A total of 168 (11%) patients underwent 187 repeated septal reduction procedures attributable to insufficient symptomatic relief and persistence of significant LV outflow gradient. Kaplan-Meier curves describing reintervention rates are shown

Table 2 Thirty-day non-hierarchical occurrence of major cardiovascular adverse events

Event	IVS <30 mm group (n=1452)	IVS ≥30 mm group (n=67)	P value
Cardiovascular death, n (%)	11 (0.8)	0	1.000
Electrical cardioversion for VT/VF or ICD discharge, n (%)	21 (1.4)	1 (1.5)	1.000
Cardiac tamponade, n (%)	16 (1.1)	0	1.000
Permanent PM after ASA, n (%)	150 (10.3)	3 (4.5)	0.146
Total number of events, n (%)	198 (13.6)	4 (6.0)	0.095

ASA, alcohol septal ablation; ICD, implantable cardioverter-defibrillator;IVS, interventricular septum; PM, permanent pacemaker; VT/VF, ventricular tachycardia/fibrillation.

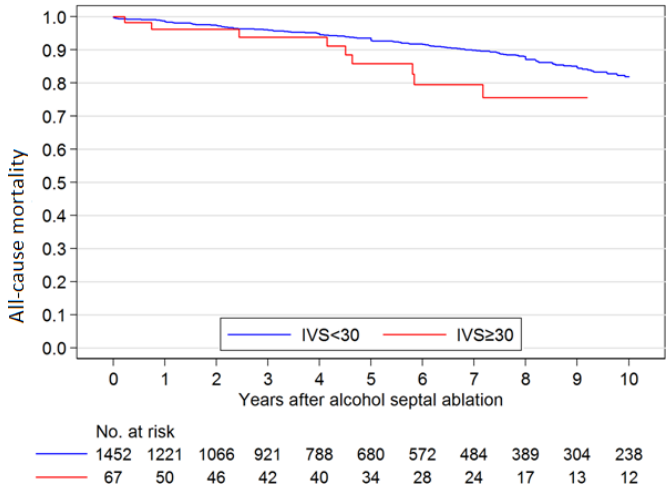

Figure 1 Kaplan-Meier survival curves describing the age-adjusted (55 years) freedom from all-cause mortality in the IVS <30 mm versus IVS ≥30 mm group (p=0.03). IVS, interventricular septum.

in figure 3. In multivariable analysis, repeated septal reduction procedures were associated with a lower age at which ASA was performed (HR 0.98; 95% CI 0.97 to 0.99; p<0.01).

Thinning of IVS diameter after ASA is shown in figure 4.

DISCUSSION

As far as we know, this is the largest study demonstrating short-term and long-term outcomes of ASA for HOCM patients with severe septal hypertrophy. The essential findings are as follows: (1) patients with severe IVS thickness (≥30 mm) had acceptable 30-day post-ASA results that were comparable with patients with less thickened septum (IVS <30 mm); (2) improvement in the long-term decrease of LV gradient and New York Heart Association (NYHA) class was similar in both IVS groups; (3) the long-term cardiovascular mortality event rates and all-cause mortality, respectively, were higher in patients with severe septal hypertrophy; (4) the occurrence of appropriate ICD discharges was very low in both groups; and (5) the occurrence of repeated septal reduction procedures was similar in both groups.

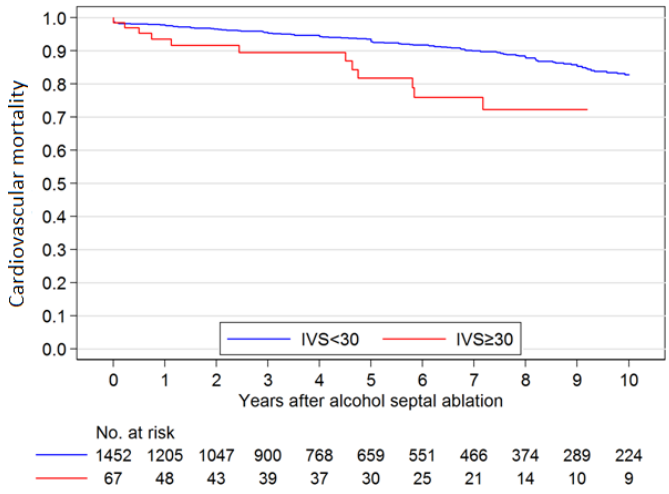

Figure 2 Kaplan-Meier survival curves describing the age-adjusted (55 years) freedom from cardiovascular mortality events in the IVS <30 mm vs IVS ≥30 mm group (p<0.01). IVS, interventricular septum.

Table 3 The occurrence of cardiovascular mortality events per 100 person-years within 5 years after ASA

	IVS <30 group (n=1452)	IVS ≥30 group (n=67)	P value
Cardiovascular death, n (%)	1.14	2.26	0.025
Appropriate ICD discharge, n (%)	0.34	1.41	0.025
Resuscitation, n (%)	0.49	0.46	0.952

ASA, alcohol septal ablation; ICD, implantable cardioverter-defibrillator; IVS, interventricular septum.

The current approach to risk stratification recommended by European and US guidelines on HCM[6 7] is based on several consistent observations demonstrating that severe LV hypertrophy and/or severe LV outflow obstruction are associated with higher risk of sudden cardiac death and diminished long-term survival.[22–27] Therefore, these high-risk patients should be considered candidates for ICD implantation and relief of LV outflow obstruction to decrease the overall risk burden.[6 7 12] However, there is an ongoing debate as to whether ASA-induced scar of the basal IVS is an appropriate therapy for these patients.[28–30] There are at least two uncertainties concerning ASA that should be considered. First, will injection of alcohol followed by infarction and shrinkage of the massively thickened IVS be sufficient to achieve a clinically important reduction of LV outflow obstruction? Second, could the large resultant scar in IVS be associated with a higher risk of ventricular arrhythmias or LV dysfunction? The prior evidence is very limited, but both a Chinese study (n=17) and a multinational European study (n=26) suggested that short-term post-ASA outcomes in patients with severe hypertrophy might be acceptable.[16 21]

Taking into account the limitations of the present study we demonstrated that reduction of dyspnoea and LV outflow gradient were similar in both groups regardless of IVS thickness above or below 30 mm, and long-term occurrence of appropriate ICD discharges was low. Nevertheless, long-term all-cause mortality and cardiovascular mortality event rates were significantly higher in patients with severe IVS hypertrophy which, however, is in line with previous evidence in HCM patients not treated with ASA,[22–26] that is, the increased mortality was more likely related to the severity of the disease rather than to the ASA

Figure 3 Kaplan-Meier survival curves describing the age-adjusted (55 years) freedom from repeated septal reduction procedures in the IVS <30 mm versus IVS ≥30 mm group (p=0.11). IVS, interventricular septum.

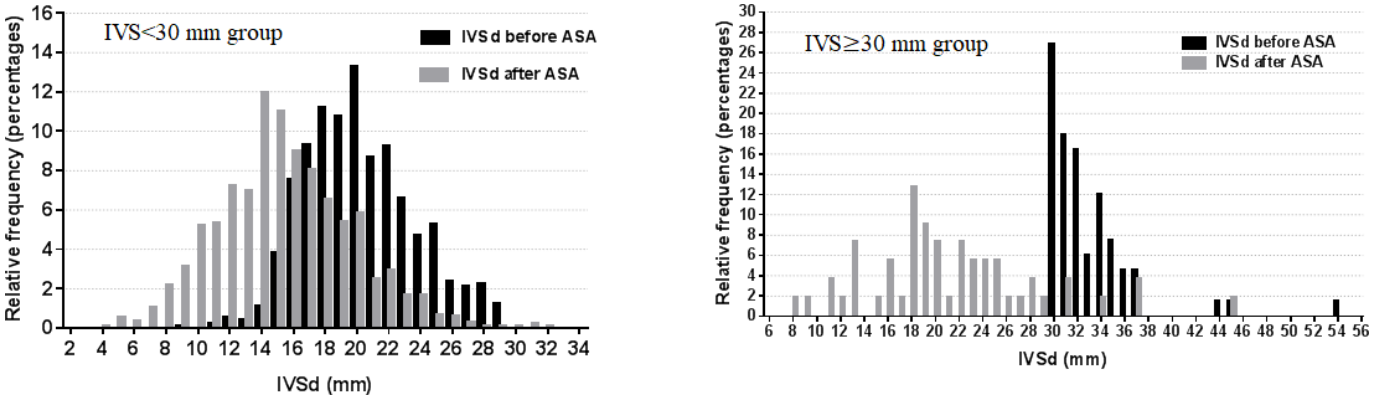

Figure 4 Histograms showing distribution of basal IVS thickness before ASA and at the last echocardiographic check-up in the IVS <30 mm group (A) and in the IVS ≥30 mm group (B). ASA, alcohol septal ablation; IVS, interventricular septum.

procedure. Notably, this study was not designed to evaluate the impact of ASA on long-term prognosis of patients with severe LV hypertrophy, and only randomised trials could ultimately determine whether HOCM patients with severe LV hypertrophy should be treated with ASA. However, these data are the first to challenge the cautionary view of European and US guidelines on performance of ASA in HOCM patients with severe IVS hypertrophy.[6 7]

This retrospective, observational and multinational study has its own inherent limitations that should be considered prior to generalisation of the results. It is not known how many patients with severe hypertrophy were sent to surgery or were discouraged from ASA, and therefore we cannot evaluate our selection bias. Also, only a relatively small number (n=67) of patients with IVS ≥30 mm were included. However, severe LV hypertrophy is relatively rare even in large HCM cohorts. Two important studies published by Elliott *et al*[25] and Spirito *et al*[22] demonstrated this finding only in approximately 10% of HCM patients, and only 20%–30% of these subjects had significant resting LV outflow obstruction (Elliott *et al*,[25] LV outflow obstruction and IVS ≥30 mm, n=23 patients; Spirito *et al*,[22] LV outflow obstruction and IVS ≥30 mm, n=9 patients). Therefore, we believe that our current data carry considerable weight and they challenge the view of current European and US guidelines not to treat patients with severe IVS hypertrophy with ASA.[6 7]

CONCLUSIONS

The short-term results and the long-term relief of dyspnoea, residual left ventricular outflow obstruction and occurrence of repeated septal reduction procedures in patients with basal IVS ≥30 mm is similar to those with IVS <30 mm. However, long-term all cause and cardiac mortality rates are worse in the ≥30 mm group.

Author affiliations
[1]Department of Cardiology, Second Medical School, Charles University, University Hospital Motol, Prague, Czech Republic
[2]Unit for Inherited Cardiac Diseases, Department of Cardiology, Copenhagen University Hospitalet Rigshospitalet, Copenhagen, Denmark
[3]Department of Cardiology, St. Antonius Hospitalen Nieuwegein, Nieuwegein, The Netherlands
[4]Institute of Cardiovascular Medicine and Science, Liverpool Heart and Chest Hospital, Liverpool, UK
[5]Cardiocentre Podlesi, Trinec, Czech Republic
[6]Ural Federal University, Sverdlovsk, Russian Federation
[7]Yekaterinburg Regional Hospital No.1, Yekaterinburg, Russian Federation
[8]Department of Interventional Cardiology and Angiology, Institute of Cardiology, Warsaw, Poland
[9]Department of Cardiology, Gentofte Hospital, Copenhagen University Hospital, Hellerup, Denmark
[10]Department of Internal Medicine, Juliusspital Wuerzburg, Wuerzburg, Germany
[11]Clinic for General and Interventional Cardiology, Heart and Diabetes Centre NRW Ruhr-University Bochum, Bad Oeynhausen, Germany

Acknowledgements The authors are grateful to statistician Dr. Marek Maly for his assistance with statistical analysis. The authors also thank colleagues responsible for the HCM clinics at all participating centres.

Contributors JV drafted the MS, performed statistical analysis, conceived and designed the research and acquired the data; MKJ, ML, RC, JJ, MK, MD, PRH, HS, EH, HB, JB RHS, LF collected data and made criticalrevision of the MS.

Funding The authors have not declared a specific grant for this research from any funding agency in the public, commercial or not-for-profit sectors.

Competing interests None declared.

Patient consent for publication Not required.

Key messages

What is already known on this subject?

- Severe left ventricular hypertrophy (≥30 mm) is associated with both increased risk of sudden death and all-cause mortality in patients with hypertrophic cardiomyopathy. The current guidelines suggest alcohol septal ablation is less effective in hypertrophic obstructive cardiomyopathy (HOCM) patients with severe left ventricular hypertrophy, despite acknowledging that systematic data are lacking.

What might this study add?

- This is the largest study to demonstrate that patients with basal interventricular septal thickness ≥30 mm have acceptable short-term postablation outcome compared with patients with less severe hypertrophy (<30 mm). They also have a similar improvement in the long-term reduction in left ventricular outflow gradient and dyspnoea. However, the long-term cardiovascular mortality event rates and all-cause mortality are significantly higher.

How might this impact on clinical practice?

- The results of this study suggest that alcohol septal ablation in selected patients with HOCM and severe septal hypertrophy is clinically and haemodynamically effective. This finding might challenge the current guidelines on indication for alcohol septal ablation in these patients.

Ethics approval Multicentre Ethical Committee Motol, Prague, approved the protocol.

Provenance and peer review Not commissioned; externally peer reviewed.

Data availability statement All data relevant to the study are included in the article or uploaded as supplementary information.

REFERENCES

1 Cooper RM, Stables RH. Non-Surgical septal reduction therapy in hypertrophic cardiomyopathy. *Heart* 2018;104:73–83.
2 Pelliccia F, Niccoli G, Gragnano F, *et al*. Alcohol septal ablation for hypertrophic obstructive cardiomyopathy: a contemporary reappraisal. *EuroIntervention* 2019. doi:10.4244/EIJ-D-18-00959. [Epub ahead of print: 12 Mar 2019].
3 Fifer MA. Septal reduction therapy for hypertrophic obstructive cardiomyopathy. *J Am Coll Cardiol* 2018;72:3095–7.
4 Veselka J. Alcohol septal ablation for hypertrophic obstructive cardiomyopathy: a review of the literature. *Med Sci Monit* 2007;13:RA62–8.
5 Rigopoulos AG, Sakellaropoulos S, Ali M, *et al*. Transcatheter septal ablation in hypertrophic obstructive cardiomyopathy: a technical guide and review of published results. *Heart Fail Rev* 2018;23:907–17.
6 Elliott PM, Anastasakis A, Borger MA, *et al*. 2014 ESC guidelines on diagnosis and management of hypertrophic cardiomyopathy: the task force for the diagnosis and management of hypertrophic cardiomyopathy of the European Society of cardiology (ESC). *Eur Heart J* 2014;35:2733–79.
7 Gersh BJ, Maron BJ, Bonow RO, *et al*. 2011 ACCF/AHA guideline for the diagnosis and treatment of hypertrophic cardiomyopathy: a report of the American College of cardiology Foundation/American heart association Task force on practice guidelines. *Circulation* 2011;124:e783–831.
8 Veselka J, Jensen MK, Liebregts M, *et al*. Long-Term clinical outcome after alcohol septal ablation for obstructive hypertrophic cardiomyopathy: results from the Euro-ASA registry. *Eur Heart J* 2016;37:1517–23.
9 Liebregts M, Faber L, Jensen MK, *et al*. Validation of the HCM Risk-SCD model in patients with hypertrophic cardiomyopathy following alcohol septal ablation. *Europace* 2018;20:f198–203.
10 Jensen MK, Faber L, Liebregts M, *et al*. Effect of impaired cardiac conduction after alcohol septal ablation on clinical outcomes: insights from the Euro-ASA registry. *Eur Heart J Qual Care Clin Outcomes* 2019;5:252–8.
11 Veselka J, Faber L, Jensen MK, *et al*. Effect of institutional experience on outcomes of alcohol septal ablation for hypertrophic obstructive cardiomyopathy. *Can J Cardiol* 2018;34:16–22.
12 Veselka J, Anavekar NS, Charron P. Hypertrophic obstructive cardiomyopathy. *Lancet* 2017;389:1253–67.
13 Batzner A, Pfeiffer B, Neugebauer A, *et al*. Survival after alcohol septal ablation in patients with hypertrophic obstructive cardiomyopathy. *J Am Coll Cardiol* 2018;72:3087–94.
14 Nagueh SF, Groves BM, Schwartz L, *et al*. Alcohol septal ablation for the treatment of hypertrophic obstructive cardiomyopathy. A multicenter North American registry. *J Am Coll Cardiol* 2011;58:2322–8.
15 Rigopoulos AG, Seggewiss H. A decade of percutaneous septal ablation in hypertrophic cardiomyopathy. *Circ J* 2011;75:28–37.
16 Veselka J, Lawrenz T, Stellbrink C, *et al*. Early outcomes of alcohol septal ablation for hypertrophic obstructive cardiomyopathy: a European multicenter and multinational study. *Catheter Cardiovasc Interv* 2014;84:101–7.
17 Veselka J, Tomašov P, Januška J, *et al*. Obstruction after alcohol septal ablation is associated with cardiovascular mortality events. *Heart* 2016;102:1793–6.
18 Veselka J, Duchonová R, Páleníckova J, *et al*. Impact of ethanol dosing on the long-term outcome of alcohol septal ablation for obstructive hypertrophic cardiomyopathy: a single-center prospective, and randomized study. *Circ J* 2006;70:1550–2.
19 Veselka J, Zemánek D, Jahnlová D, *et al*. Risk and causes of death in patients after alcohol septal ablation for hypertrophic obstructive cardiomyopathy. *Can J Cardiol* 2015;31:1245–51.
20 Sorajja P, Ommen SR, Holmes DR, *et al*. Survival after alcohol septal ablation for obstructive hypertrophic cardiomyopathy. *Circulation* 2012;126:2374–80.
21 Yang Y-J, Fan C-M, Yuan J-Q, *et al*. Effectiveness of alcohol septal ablation in obstructive hypertrophic cardiomyopathy with versus without extreme septal hypertrophy. *J Invasive Cardiol* 2016;28:99–103.
22 Spirito P, Bellone P, Harris KM, *et al*. Magnitude of left ventricular hypertrophy and risk of sudden death in hypertrophic cardiomyopathy. *N Engl J Med* 2000;342:1778–85.
23 O'Mahony C, Jichi F, Pavlou M, *et al*. A novel clinical risk prediction model for sudden cardiac death in hypertrophic cardiomyopathy (HCM Risk-SCD). *Eur Heart J* 2014;35:2010–20.
24 Christiaans I, van Engelen K, van Langen IM, *et al*. Risk stratification for sudden cardiac death in hypertrophic cardiomyopathy: systematic review of clinical risk markers. *Europace* 2010;12:313–21.
25 Elliott PM, Gimeno Blanes JR, Mahon NG, *et al*. Relation between severity of left-ventricular hypertrophy and prognosis in patients with hypertrophic cardiomyopathy. *Lancet* 2001;357:420–4.
26 Romeo F, Pelliccia F, Cristofani R, *et al*. Hypertrophic cardiomyopathy: is a left ventricular outflow tract gradient a major prognostic determinant? *Eur Heart J* 1990;11:233–40.
27 Jensen MK, Jacobsson L, Almaas V, *et al*. Influence of septal thickness on the clinical outcome after alcohol septal ablation in hypertrophic cardiomyopathy. *Circ Cardiovasc Interv* 2016;9:e003214.
28 Fifer MA. Choice of septal reduction therapies and alcohol septal ablation. *Cardiol Clin* 2019;37:83–93.
29 Panza JA, Naidu SS. Historical perspectives in the evolution of hypertrophic cardiomyopathy. *Cardiol Clin* 2019;37:1–10.
30 Burghardt A, van Buuren F, Dimitriadis Z, *et al*. Risk marker profiles in patients treated with percutaneous septal ablation for symptomatic hypertrophic obstructive cardiomyopathy. *Clin Res Cardiol* 2018;107:479–86.

M. Šramko a kol.

Independent effect of atrial fibrillation on natriuretic peptide release.
(id 262)

Clinical Research in Cardiology
Impact Factor: 4,9

rejstřík

Clinical Research in Cardiology (2019) 108:142–149
https://doi.org/10.1007/s00392-018-1332-1

ORIGINAL PAPER

Independent effect of atrial fibrillation on natriuretic peptide release

Marek Sramko[1] · Dan Wichterle[1] · Vojtech Melenovsky[1] · Janka Franekova[2] · Marcell Clemens[1] · Masato Fukunaga[1] · Josef Kautzner[1]

Received: 16 May 2018 / Accepted: 16 July 2018 / Published online: 26 July 2018

Abstract

Background We investigated whether the increase of plasma natriuretic peptides (NPs) in atrial fibrillation (AF) is independent of the effect of AF on the left atrial (LA) hemodynamics.

Methods Hemodynamically stable patients scheduled for AF ablation underwent assessment of B-type natriuretic peptide (BNP) and mid-regional pro-atrial natriuretic peptide (MR-proANP), echocardiography, and direct measurement of left atrial (LA) pressure. Concentrations of the NPs were compared between patients in AF ($n=31$) and controls in sinus rhythm (SR; $n=31$) who were matched for age, gender, heart rate, left ventricular ejection fraction, LA volume index, and directly measured mean LA pressure. Eighteen patients underwent serial measurement of NPs and LA pressure during native SR and after 20 min of pacing-induced AF.

Results Compared to the patients in SR, the patients in AF had 2.6 times higher unadjusted BNP [median (inter-quartile range), 101 (63, 129) vs. 38 (26, 79) ng/L] and two times higher unadjusted MR-proANP [183 (140, 230) vs. 91 (67, 135) pmol/L; both $p<0.001$]. Concentrations of both NPs correlated with mean LA pressure in the patients in SR ($r=0.75$ for BNP and 0.62 for MR-proANP, both $p<0.001$) but not in the patients in AF ($r=0.18$ and 0.04, respectively, both $p>0.3$). Both NPs increased significantly during induced AF [adjusted median (IQR) relative change, BNP: 27 (22; 40)%, MR-proANP: 75 (64; 99)%, both $p<0.001$] without a significant change in the LA pressure.

Conclusions The increase of NPs in AF was independent of its effect on the LA hemodynamics.

Keywords Atrial fibrillation · Natriuretic peptide · Atrial pressure · Heart failure with preserved ejection fraction

Introduction

Plasma concentrations of natriuretic peptides (NPs) are usually increased in patients in atrial fibrillation (AF) compared to patients in sinus rhythm (SR) [1]. It is still unclear whether this phenomenon is caused by AF itself or whether it is related to hemodynamic overload and cardiac remodeling induced by AF. Previous studies were inconclusive in clarifying the mechanisms behind the increase of NPs in AF because they either used non-invasive methods [2–9] or they focused on patients with heart failure [4, 10]. However, a better understanding of how AF affects the release of NPs may have important clinical implications, especially for the diagnosis of early stages of heart failure with preserved ejection fraction (HFpEF). In these patients, symptoms and clinical findings are often ambiguous but AF is highly prevalent [1, 10].

The present study aimed to determine whether the effect of AF on the release of NPs is independent of its effect on the LA hemodynamics. To this end, plasma concentrations of B-type natriuretic peptide (BNP) and mid-regional pro-atrial natriuretic peptide (MR-proANP) were compared between hemodynamically stable patients in AF and a control group of patients in SR who were matched for directly measured LA pressure and key clinical and structural variables. In addition, a subset of the patients underwent measurement of the NPs along with assessment of the LA hemodynamics during SR and after inducing AF. At last, the study investigated whether the presence of AF would affect the

✉ Marek Sramko
marek.sramko@ikem.cz

[1] Department of Cardiology, Institute for Clinical and Experimental Medicine (IKEM), Videnska 1958/9, 14021 Prague, Czech Republic

[2] Department of Laboratory Methods, Institute for Clinical and Experimental Medicine (IKEM), Prague, Czech Republic

relationship between NPs' plasma concentrations and mean LA pressure.

Methods

Study population and protocol

This was a prospective, single-center study. The study protocol was approved by our institutional ethical committee in accordance with the standards of the Declaration of Helsinki, and all patients signed a consent to the investigation. The initial study population included 106 hemodynamically stable patients scheduled for catheter ablation of AF who were either in AF ($n=32$) or in SR ($n=74$) on admission. Excluded were patients with dilated, hypertrophic or restrictive cardiomyopathy, patients with significant valvular heart disease (previous valve surgery, or more than a moderate degree of stenosis or insufficiency of any valve), and patients with congenital heart disease.

On the day before ablation, all patients underwent a thorough clinical evaluation and transthoracic echocardiography. Heart rhythm was monitored by Holter ECG from admission throughout the entire study protocol for at least 18 h. Patients in whom the heart rhythm alternated during this period were excluded. At the beginning of the ablation procedure, after obtaining transseptal access, all patients underwent direct measurement of LA pressure and blood sampling for assessment of BNP and MR-proANP. In 18 consecutive patients, the blood sampling and measurement of the LA pressure were performed during native SR and after 20 min of interrupted AF, which was induced by rapid pacing from the coronary sinus.

Because in the initial non-selected population the patients who presented in AF differed in some characteristics from the patients in SR (Tables 1, 2), they were matched with the patients in SR using propensity-score matching (described in detail below). The final study population consisted of 31 patients who presented with AF and a control group of 31 patients in SR who had similar clinical, structural, and hemodynamic characteristics (Tables 1, 2).

Table 1 Baseline clinical characteristics by AF status

Variable	Non-matched population			Matched population		
	SR ($n=74$)	AF ($n=32$)	SMD	SR ($n=31$)	AF ($n=31$)	SMD
Age (years)	58 ± 12	61 ± 8	0.26	60 ± 10	61 ± 9	0.11
Male gender	58 (78)	19 (59)	0.41*	24 (77)	19 (61)	0.35
Body mass index (kg/m^2)	29 ± 5	29 ± 4	0.09	29 ± 4	29 ± 4	0
Body surface area (m^2)	2.1 ± 0.2	2.1 ± 0.2	0.13	2.1 ± 0.2	2.1 ± 0.2	0.19
History of heart failure	2 (3)	2 (6)	0.17	2 (7)	2 (7)	0
Arterial hypertension	39 (53)	16 (50)	0.05	17 (55)	15 (48)	0.13
Diabetes mellitus	9 (12)	4 (12)	0.01	7 (23)	4 (13)	0.25
Coronary artery disease	5 (7)	1 (3)	0.17	2 (7)	1 (3)	0.15
Peripheral artery disease	9 (12)	2 (9)	0.09	7 (23)	3 (10)	0.35
TIA/stroke	6 (8)	2 (6)	0.07	5 (16)	2 (7)	0.4
CHA2DS2-VASc (0–9)	1 (1–2)	2 (1–3)	0.4	2 (1–3)	2 (1–3)	0.16
Paroxysmal form of AF	64 (86)	6 (19)	1.82***	23 (74)	6 (19)	1.29***
AF symptom duration (years)	3 (1–5)	2 (1–3)	0.19	2 (1–5)	2 (1–4)	0.03
Lone AF	20 (27)	7 (22)	0.12	7 (23)	7 (23)	0
Betablockers	47 (64)	24 (75)	0.25	19 (61)	24 (77)	0.35
ACEI/ARB	27 (36)	11 (34)	0.04	12 (39)	10 (32)	0.13
Loop/nonloop diuretics	12 (16)	10 (31)	0.35	6 (19)	10 (32)	0.29
GFR (ml/min)	82 ± 18	81 ± 14	0.05	80 ± 17	81 ± 14	0.08
BNP (ng/L)	33 (19–62)	103 (65–134)	0.88***	38 (26–79)	101 (63–129)	0.51**
MR-proANP (pmol/L)	83 (62–127)	184 (143 − 234)	1.29***	91 (67–135)	183 (140–230)	1.0***

Values are mean ± standard deviation, median (interquartile range), and count (percentage)

AF atrial fibrillation, *ACEI/ARB* angiotensin-converting enzyme inhibitor/angiotensin receptor blocker, *BNP* B-type natriuretic peptide, *GFR* glomerular filtration rate (CKD-EPI formula), *MR* mid-regional pro-atrial natriuretic peptide, *SR* sinus rhythm, *SMD* standard mean difference, *TIA* transient ischemic attack

*/**/***p value < 0.05/<0.01/<0.001 by logistic regression

Table 2 Cardiac structure, function, and hemodynamics by AF status

Variable	Non-matched population			Matched population		
	SR ($n=74$)	AF ($n=32$)	SMD	SR ($n=31$)	AF ($n=31$)	SMD
Systolic blood pressure (mmHg)	135 ± 19	133 ± 21	0.14	137 ± 19	133 ± 21	0.21
Heart rate (beats/min)	66 ± 15	79 ± 16	0.89***	75 ± 16	79 ± 16	0.29
LV enddiastolic diameter (mm)	53 ± 6	54 ± 7	0.09	54 ± 7	53 ± 7	0.05
LV ejection fraction (%)	57 ± 5	54 ± 7	0.54*	56 ± 7	54 ± 7	0.24
IVS thickness (mm)	9 ± 1	9 ± 1	0.13	10 ± 1	9 ± 1	0.44
E-wave velocity (cm/s)	71 ± 22	84 ± 18	0.69***	75 ± 22	84 ± 18	0.47*
E/*E*′ ratio	7.7 ± 3.2	8.7 ± 2.7	0.33	8.3 ± 3.8	8.6 ± 2.7	0.08
Mitral regurgitation (0–4)	1.1 ± 0.4	1.1 ± 0.3	0.12	1.1 ± 0.6	1.1 ± 0.3	0.07
RV dimension at base (mm)	38 ± 5	37 ± 6	0.16	38 ± 5	37 ± 6	0.11
RV tissue Doppler (cm/s)	13 ± 2	12 ± 2	0.41	12 ± 1	12 ± 2	0.07
Tricuspid regurgitation (0–4)	1 ± 0.2	1.1 ± 0.2	0.1	1.1 ± 0.3	1.1 ± 0.2	0.02
Right atrial pressure (mmHg)	5 ± 3	3 ± 1	0.43	4 ± 3	3 ± 2	0.25
Left atrial volume index (ml/m^2)	37 ± 9	41 ± 9	0.44*	38 ± 9	41 ± 9	0.31
LA mean pressure (mmHg)	9 ± 5	10 ± 4	0.29	10 ± 6	10 ± 4	0.01
LA pulse pressure (mmHg)	17 ± 7	18 ± 7	0.18	19 ± 8	18 ± 7	0.15
LA pressure V-wave (mmHg)	16 ± 8	18 ± 8	0.26	19 ± 9	18 ± 8	0.07
LA wall stress (kdynes/cm^2)	55 ± 28	68 ± 34	0.42	63 ± 35	68 ± 34	0.14
LA stiffness index	0.6 ± 0.3	0.8 ± 0.6	0.5*	0.6 ± 0.4	0.8 ± 0.6	0.38

Data reported as in Table 1

IVS interventricular septum, *LA* left atrial, *LV* left ventricular, *RV* right ventricular

*/**/***p value < 0.05/<0.01/<0.001 by logistic regression

Assessment of cardiac function and hemodynamics

Transthoracic echocardiography was performed by experienced operators (Vivid 7, GE Healthcare, UK). In case of present AF, all measurements were obtained by averaging of at least five consecutive beats.

LA pressure was measured before the LA mapping through an 8-F fluid-filled transseptal sheath placed in the LA cavity. The pressure transducer was zeroed at the midthoracic level. Mean LA pressure was calculated from the electronic mean of the pressure curve over at least three complete breath cycles. The height of the V-wave and LA pulse pressure (V-wave to Y-nadir) were measured manually at end-expirium, using the Prucka CardioLab System (GE Healthcare). LA meridional wall stress and LA diastolic stiffness were calculated as previously described [11]. The minimal and maximal LA volumes for calculation of the LA stiffness were obtained by echocardiography using the area–length method [12]. Central venous pressure was measured via femoral venous sheath. Exact LA volume and relative extent of low LA bipolar voltage (using 0.15 mV cut-off) were determined by point-by-point electroanatomic mapping (CARTO-3, Biosense Webster, Israel) as previously described [13].

Assessment of natriuretic peptides

EDTA-anticoagulated peripheral blood plasma was obtained immediately before the hemodynamic assessment. The samples were stored at − 70 °C until batch analysis. BNP was assessed by a chemiluminescent immunoassay (Architect, Abbott Diagnostics, USA) with a sensitivity of 10 ng/L. MR-proANP was assessed by a luminometric immunoassay (Kryptor, BRAHMS, Germany) with a sensitivity of 2.1 pmol/L. The coefficient of variation was < 10% for both assays. BNP < 35 ng/L and MR-proANP < 116 pmol/L were regarded normal [14, 15].

Statistical analysis

Initially, factors associated with increased NP concentrations were identified in the non-matched population by stepwise multivariable linear regression analysis. The covariates in the models were selected by backward elimination of all significant univariable predictors. The NP values were log-transformed before the analysis because of a right-skewed distribution [16]. The identified independent factors included age, female gender, presence of AF, mean LA pressure, LV ejection fraction (LVEF), LA volume (for both NPs), and

glomerular filtration rate (only for MR-proANP). These factors, along with the patient's heart rate, were subsequently used for propensity-score matching of the patients in AF with the patients in SR (using the nearest neighbor matching with the ratio of 1:1).

Because of the different size of the matched and the non-matched study populations, the differences between the patients in AF and SR were expressed by standardized mean difference, and between-group comparisons were performed by logistic regression. Factors associated with increased NPs were identified by linear regression, similarly as in the non-matched population. The effect of AF on the relationship between LA pressure and NP concentrations was evaluated by linear regression with an interaction term (log(NP) = AF present + LA mean pressure + AF present * LA mean pressure). Other baseline comparisons were performed by the Student's *t* test, Mann–Whitney *U* test, χ^2 test, Fisher's test, or Pearson's correlation, as appropriate. Serial change in the NP concentrations and LA hemodynamic variables was compared by paired *t* test and by multivariable linear regression. p value < 0.05 was considered significant. All analyses were conducted in R 3.2 (R-Foundation, Vienna, Austria) with the use of the MatchIt 3.0 package [17].

Results

Characteristics of the study population

The matched study population ($n = 62$) consisted of mostly mid-age men with paroxysmal AF and a relatively short history of AF-related symptoms (Table 1). Four patients (6%) had a previous history of decompensated heart failure, but all the episodes occurred > 3 months before the study. The patients had overall preserved LVEF and all were euvolemic at the time of the study, which was documented by the low right atrial pressure (Table 2). In the patients who presented with AF, the arrhythmia persisted for a median of 3 months [inter-quartile range (IQR) 1–9 months] before inclusion into the study.

Factors associated with increased plasma NPs

Table 3 shows multivariable analysis of independent factors of increased NPs identified in the matched population. For both NPs, the presence of AF emerged as the strongest factor, accounting for ~25% of the NPs' variance. Other factors which were significantly associated with increased NPs in univariable but not in multivariable analysis included higher age, CHA2DS2-VASc score, *E*/*E*′ ratio, E-wave velocity, mitral insufficiency grade, LA wall stress, and right atrial pressure. In addition, BNP was associated with greater LA pulse pressure, V-wave height, and LA wall stress; and MR-proANP was associated with greater LA volume. No association was found between NP concentrations and heart rate. Within the whole matched population, the concentrations of both NPs correlated with the relative extent of LA low bipolar voltage [$r = 0.2$, $p = 0.02$ for log(BNP), and $r = 0.4$, $p < 0.001$, for log(MR-proANP)], but no correlation was found between the NPs and low LA voltage extent when the SR and AF patients were analyzed separately.

Relationship between plasma NPs and mean LA pressure in AF

Importantly, while in the patients in SR there was a strong correlation between mean LA pressure and log-transformed BNP and MR-proANP concentrations ($r = 0.75$ and 0.62, respectively, both $p < 0.001$), no correlation was found between the NPs and the mean LA pressure in the patients in AF ($r = 0.18$ and 0.04, respectively, both $p > 0.3$; Fig. 1). Moreover, in multivariable analysis, the presence of AF

Table 3 Independent factors of increased natriuretic peptide plasma concentrations

$N = 62$	Beta-coefficient (95% confidence interval)	
	Log(BNP)	Log(MR-proANP)
Presence of AF	0.5 (0.14, 0.8)**	0.5 (0.3, 0.7)***
Mean LA pressure, per 1 mmHg	0.05 (0.01, 0.09)**	0.04 (0.01, 0.06)**
Female gender	0.5 (0.1, 0.9)*	–
LV ejection fraction, per %	–	−0.01 (0.002, -0.03)
LA volume, per 10 ml	0.1 (0.02, 0.2)*	–

Abbreviations as in Tables 1, 2

*/**/***p value < 0.05/<0.01/<0.001. The table shows results of multivariable regression analysis of independent factors of increased NPs in the matched patient population. The covariates in the models were selected by stepwise elimination of all significant univariable predictors. The following candidate variables were considered in the models: age, CHA2DS2-VASc score, persistent AF, non-lone AF, *E*/*E*′ ratio, mitral regurgitation grade, LA pulse pressure, LA wall stress, LA V-wave height, and RA pressure. The parameters of the models were for BNP: intercept = 2.4, $F(4, 56) = 12$, $R^2 = 0.46$, $p < 0.001$ and for MR-proANP: intercept = 4.1, $F(3, 58) = 12$, $R^2 = 0.4$, $p < 0.001$

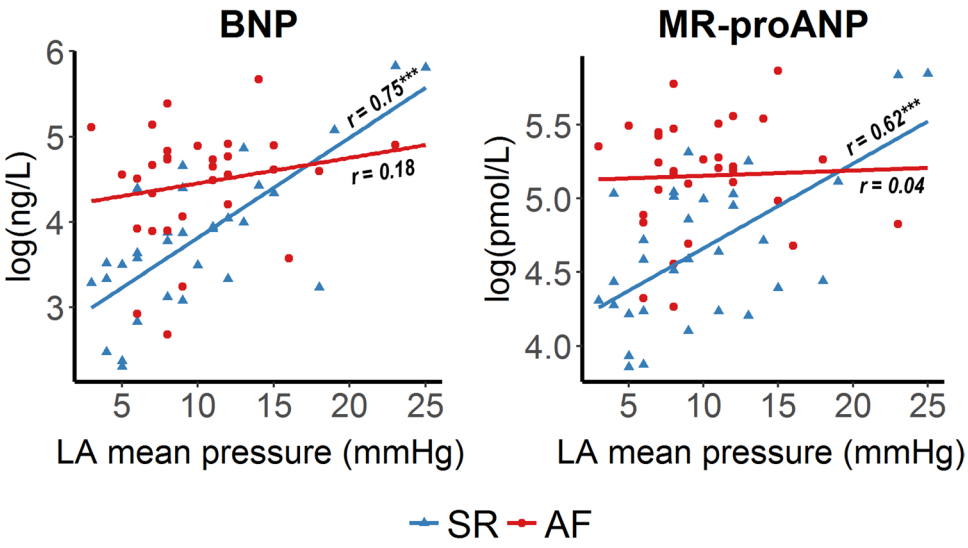

Fig. 1 Correlation of mean left atrial pressure and natriuretic peptide plasma concentrations according to the presence of atrial fibrillation. The figure shows good correlation of unadjusted plasma B-type natriuretic peptide (BNP) and mid-regional pro-atrial natriuretic peptide (MR-proANP) and mean left atrial (LA) pressure in the patients in sinus rhythm (SR; blue triangles) but lacking correlation in the patients in atrial fibrillation (AF; red circles)

caused a significant interaction effect on the relationship between NPs and mean LA pressure (p value for interaction = 0.01 for both NPs).

Comparison between patients in AF and SR

Tables 1 and 2 show comparison between the patients in AF and the matched controls in SR. By design, both groups did not differ in age, gender, key comorbidities, heart rate, LVEF, LV diastolic characteristics, LA volume, or LA hemodynamics, though the patients who presented in AF had expectedly more often persistent than paroxysmal form of AF and higher E-wave velocity.

Despite the similar clinical and hemodynamic profile, the patients in AF had on average 2.6 times higher BNP and 2 times higher MR-pro ANP unadjusted concentrations than the patients in SR (Table 1; Fig. 2). Concentrations of both NPs remained significantly increased in the patients in AF even after adjusting the NP values for all other independent confounders. Median BNP adjusted for gender, mean LA pressure, and LA volume was 78 (63, 112) ng/L in AF vs. 47 (35, 69) ng/L in SR ($p < 0.001$); median MR-proANP adjusted for LVEF and mean LA pressure was 172 (155, 186) pmol/L in AF vs. 101 (88, 117) pmol/L in SR ($p < 0.001$). Unadjusted BNP and MR-proANP, respectively, were in normal range only in 3 (10%) and 5 (16%) of the patients in AF vs. in 14 (45%) and 21 (67%) of the patients in SR ($p < 0.01$ for both).

Change in plasma NPs after induction of AF

Eighteen patients underwent serial assessment of the NPs and hemodynamics during native SR and after 20 min of sustained pacing-induced AF. While there was no

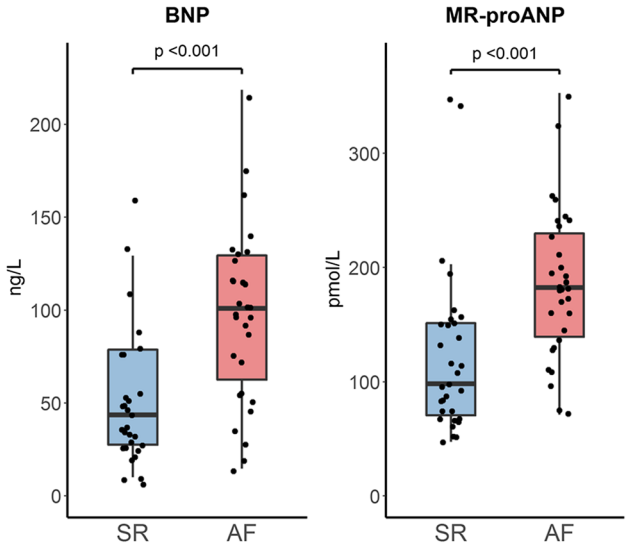

Fig. 2 Comparison of natriuretic peptide concentrations between patients in atrial fibrillation and matched patients in sinus rhythm. The figure shows comparison of unadjusted plasma B-type natriuretic peptide (BNP) and mid-regional pro-atrial natriuretic peptide (MR-proANP) between patients in atrial fibrillation (AF) and matched controls in sinus rhythm (SR). Four data points with BNP values between 330 and 395 ng/l are not shown for visualization purpose. The p values were calculated by Mann–Whitney U test

significant change in the central venous pressure or mean LA pressure, plasma concentrations of both NPs increased significantly during AF (Fig. 3). The elevation of NPs remained significant even after adjusting for CVP, heart rate, mean LAP, and baseline NP concentrations [adjusted median (IQR) relative change for BNP: 27 (22; 40) %; NT-proBNP: 13 (9; 15) %; MR-proANP: 75 (64; 99) %; all $p < 0.001$ by Wilcoxon signed-rank test].

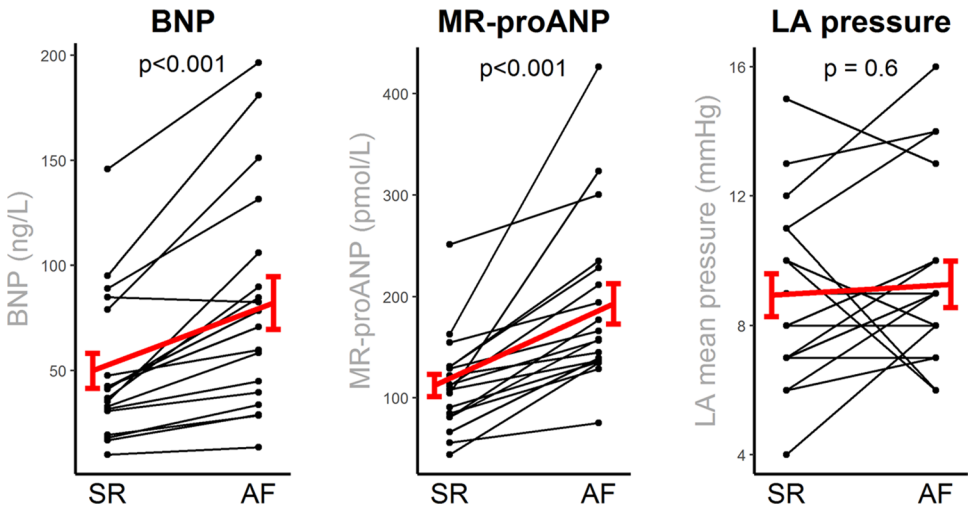

Fig. 3 Change in the natriuretic peptide concentrations after inducing atrial fibrillation. The figure shows paired measurements of BNP, MR-proANP and mean left atrial (LA) pressure during native sinus rhythm (SR) and after 20 min of uninterrupted pacing-induced atrial fibrillation (AF). The thick red lines represent mean values with standard error. The *p* values were calculated by paired *t* test. The graphs highlight significant increase in both natriuretic peptides during AF that was not explained by an increase in the LA pressure

Discussion

This study found 2.6 times higher BNP and 2 times higher MR-pro ANP in stable patients with preserved LVEF who were in AF than in matched controls in SR. More importantly, the study demonstrated that the increase of the NPs in AF was not related to alteration in the LA hemodynamics, as both patient groups had comparable LA pressure, LA volume, and LA meridional wall stress. These observations were further supported by showing that NP concentrations but not LA pressure increased significantly after experimental induction of AF. Lastly, the increase of NPs in AF seemed not to be related to chronic histopathological changes in the LA tissue, which was indicated by the lack of correlation between NP concentrations and LA low-voltage area, and by the comparable LA stiffness between the AF and SR groups.

From a clinical perspective, the most important finding was that plasma concentrations of both NPs correlated well with invasively measured mean LA pressure in the patients in SR, but no such correlation was found in the patients in AF. This finding has implications for clinical use of NPs as a surrogate of left-sided pressure overload, particularly in the diagnosis of latent heart failure with preserved LVEF (HFpEF) [18]. AF occurs in 25–60% of these patients [1, 19, 20] and it is difficult to distinguish whether the patient's symptoms are related to the heart failure or to AF alone [1, 21]. The lack of a correlation between NPs and LA pressure in AF suggests that the diagnostic performance would unlikely improve by applying higher concentration cut-offs. Moreover, the intrinsic increase of NPs in AF not reflecting the hemodynamics implies that clinical trials on HFpEF should be careful with including patients based on increased NPs [22], as this could lead to enrollment of disproportionately more patients with AF [1]. The higher prevalence of AF in such a trial could, in turn, translate to unsatisfactory response to the tested therapy, and it could bias the study results if the NPs represented an outcome measure [23].

Previous studies could not determine conclusively whether the increase of NPs in AF is independent of the impaired LA hemodynamics because they employed only non-invasive methods [2–9]. The only study investigating this phenomenon invasively enrolled unselected patients with established HFpEF. Nevertheless, the study found that the relationship between NT-proBNP and AF was independent of pulmonary capillary wedge pressure [10]. The original feature of our study was that the patients in AF and SR were matched according to the same level of LA pressure which was measured directly in the LA cavity. Our study was also the first to perform serial assessment of NPs in parallel with invasive hemodynamic assessment. While previous studies evaluated decrease of NPs after restoring SR [24–26], our study was the first to demonstrate an actual increase of NPs after the onset of AF.

Evidence from experimental studies indicates that the primary trigger for the release of NPs from myocytes is cellular stretch, which is partially mediated by mechanoreceptors and mechano-sensitive ion channels [27–30]. This likely explains the intrinsic acute release of NPs in AF, as cellular stretch will increase even without an increase in atrial pressure. Although the underlying cellular signaling has not yet been fully elucidated, it may involve activation of the CaMII kinase or calcineurin/NFAT pathways [27, 28]. It is conceivable that chronic activation of these pathways during AF could cause a relative depletion of intracellular calcium, which in turn might explain the blunted release of NPs in response to the increase of LA pressure in patients with AF [29]. At last, the increase of NPs in AF might be related to the heart rhythm irregularity and ensuing greater cyclic rises in LA hemodynamic stress, which could stimulate the NP release more potently than a gradual elevation of the mean LA pressure [31]. On the other hand, the hypothesis would

partially contradict to the fact that the average LA pulse pressure and V-wave height did not differ between AF and SR patients. Further research is needed to clarify the mechanisms responsible for the increase of NPs in AF.

Limitations

Our study did not reevaluate the relationship between NPs and LA pressure after restoring the SR. This would have required a prolonged waiting period after the ablation procedure with a catheter inserted in the LA until the concentration of NPs stabilizes. Serial measurement of NPs and hemodynamics were performed only in a subset of the patient and only after 20-min AF. The main reason was to avoid unnecessary prolongation of the ablation procedure. The LA voltage is incomparable between AF and SR, as it is affected by the LA cycle length [32]. Therefore, the relationship between the LA voltage and NPs could be evaluated only separately within the AF and SR groups. Our study included only hemodynamically stable patients with overall preserved LVEF. While this had the advantage in that the study population was homogeneous and well defined, our results cannot be fully extrapolated to patients with decompensated heart failure with reduced LVEF.

Conclusions

In hemodynamically stable patients with preserved LVEF, the presence of AF was associated with significant increase in plasma concentrations of BNP and MR-proANP. This association was independent of the LA structure and hemodynamics. Moreover, the presence of AF disturbed the relationship between NP concentrations and mean LA pressure. The latter has implications for the use of NPs for diagnosis of latent HFpEF in patients with AF.

Funding This study was funded by the grant of the Ministry of Health of the Czech Republic—"Conceptual development of a research organization (IKEM IN 00023001)". MS was supported by a research fellowship grant from the European Society of Cardiology and a research grant of the Czech Society of Cardiology.

Compliance with ethical standards

Conflict of interest JK served as an advisory board member for Biosense Webster, Boston Scientific, Medtronic, Liva Nova and St. Jude Medical. Other authors have nothing to declare.

References

1. Kotecha D, Lam CS, Van Veldhuisen DJ, Van Gelder IC, Voors AA, Rienstra M (2016) Heart failure with preserved ejection fraction and atrial fibrillation: vicious twins. J Am Coll Cardiol 68(20):2217–2228. https://doi.org/10.1016/j.jacc.2016.08.048
2. Bai M, Yang J, Li Y (2009) Serum N-terminal-pro-brain natriuretic peptide level and its clinical implications in patients with atrial fibrillation. Clin Cardiol 32(12):E1–E5. https://doi.org/10.1002/clc.20478
3. Bakowski D, Wozakowska-Kaplon B, Opolski G (2009) The influence of left ventricle diastolic function on natriuretic peptides levels in patients with atrial fibrillation. Pacing Clin Electrophysiol 32(6):745–752. https://doi.org/10.1111/j.1540-8159.2009.02360.x
4. Corell P, Gustafsson F, Kistorp C, Madsen LH, Schou M, Hildebrandt P (2007) Effect of atrial fibrillation on plasma NT-proBNP in chronic heart failure. Int J Cardiol 117(3):395–402. https://doi.org/10.1016/j.ijcard.2006.03.084
5. Lee SH, Jung JH, Choi SH, Lee N, Park WJ, Oh DJ, Rhim CY, Lee KH (2006) Determinants of brain natriuretic peptide levels in patients with lone atrial fibrillation. Circ J 70(1):100–104
6. Letsas KP, Filippatos GS, Pappas LK, Mihas CC, Markou V, Alexanian IP, Efremidis M, Sideris A, Maisel AS, Kardaras F (2009) Determinants of plasma NT-pro-BNP levels in patients with atrial fibrillation and preserved left ventricular ejection fraction. Clin Res Cardiol 98(2):101–106. https://doi.org/10.1007/s00392-008-0728-8
7. Rossi A, Enriquez-Sarano M, Burnett JC Jr, Lerman A, Abel MD, Seward JB (2000) Natriuretic peptide levels in atrial fibrillation: a prospective hormonal and Doppler-echocardiographic study. J Am Coll Cardiol 35(5):1256–1262
8. Silvet H, Young-Xu Y, Walleigh D, Ravid S (2003) Brain natriuretic peptide is elevated in outpatients with atrial fibrillation. Am J Cardiol 92(9):1124–1127
9. Ulimoen SR, Enger S, Tveit A (2009) Impact of atrial fibrillation on NT-proBNP levels in a 75-year-old population. Scand J Clin Lab Invest 69(5):579–584. https://doi.org/10.1080/00365510902853305
10. Lam CS, Rienstra M, Tay WT, Liu LC, Hummel YM, van der Meer P, de Boer RA, Van Gelder IC, van Veldhuisen DJ, Voors AA, Hoendermis ES (2017) Atrial fibrillation in heart failure with preserved ejection fraction: association with exercise capacity, left ventricular filling pressures, natriuretic peptides, and left atrial volume. JACC Heart Fail 5(2):92–98. https://doi.org/10.1016/j.jchf.2016.10.005
11. Melenovsky V, Hwang SJ, Redfield MM, Zakeri R, Lin G, Borlaug BA (2015) Left atrial remodeling and function in advanced heart failure with preserved or reduced ejection fraction. Circ Heart Fail 8(2):295–303. https://doi.org/10.1161/CIRCHEARTFAILURE.114.001667
12. Degiovanni A, Boggio E, Prenna E, Sartori C, De Vecchi F, Marino PN, From the Novara Atrial Fibrillation Study G (2018) Association between left atrial phasic conduit function and early atrial fibrillation recurrence in patients undergoing electrical cardioversion. Clin Res Cardiol 107(4):329–337. https://doi.org/10.1007/s00392-017-1188-9
13. Sramko M, Wichterle D, Melenovsky V, Clemens M, Fukunaga M, Peichl P, Aldhoon B, Cihak R, Kautzner J (2017) Resting and exercise-induced left atrial hypertension in patients with atrial fibrillation: the causes and implications for catheter ablation. J Am Coll Cardiol EP. https://doi.org/10.1016/j.jacep.2016.12.010
14. Ponikowski P, Voors AA, Anker SD, Bueno H, Cleland JG, Coats AJ, Falk V, Gonzalez-Juanatey JR, Harjola VP, Jankowska EA, Jessup M, Linde C, Nihoyannopoulos P, Parissis JT, Pieske B, Riley JP, Rosano GM, Ruilope LM, Ruschitzka F, Rutten FH, van der Meer P (2016) 2016 ESC Guidelines for the diagnosis and treatment of acute and chronic heart failure: the Task Force for the diagnosis and treatment of acute and chronic heart failure of the European Society of Cardiology (ESC)Developed with the

special contribution of the Heart Failure Association (HFA) of the ESC. Eur Heart J 37(27):2129–2200. https://doi.org/10.1093/eurheartj/ehw128
15. Tzikas S, Keller T, Wild PS, Schulz A, Zwiener I, Zeller T, Schnabel RB, Sinning C, Lubos E, Kunde J, Munzel T, Lackner KJ, Blankenberg S (2013) Midregional pro-atrial natriuretic peptide in the general population/Insights from the Gutenberg Health Study. Clin Chem Lab Med 51(5):1125–1133. https://doi.org/10.1515/cclm-2012-0541
16. Ballo P, Betti I, Barchielli A, Balzi D, Castelli G, De Luca L, Gheorghiade M, Zuppiroli A (2016) Prognostic role of N-terminal pro-brain natriuretic peptide in asymptomatic hypertensive and diabetic patients in primary care: impact of age and gender: results from the PROBE-HF study. Clin Res Cardiol 105(5):421–431. https://doi.org/10.1007/s00392-015-0937-x
17. Ho D, Imai K, King G, Stuart EA (2011) MatchIt: Nonparametric preprocessing for parametric causal inference. J Stat Softw. https://doi.org/10.18637/jss.v042.i08
18. Francis GS, Felker GM, Tang WH (2016) A test in context: critical evaluation of natriuretic peptide testing in heart failure. J Am Coll Cardiol 67(3):330–337. https://doi.org/10.1016/j.jacc.2015.10.073
19. Miro O, Gil VI, Martin-Sanchez FJ, Jacob J, Herrero P, Alquezar A, Llauger L, Aguilo S, Martinez G, Rios J, Dominguez-Rodriguez A, Harjola VP, Muller C, Parissis J, Peacock WF, Llorens P, Research Group on Acute Heart Failure of the Spanish Society of Emergency Medicine R (2018) Short-term outcomes of heart failure patients with reduced and preserved ejection fraction after acute decompensation according to the final destination after emergency department care. Clin Res Cardiol. https://doi.org/10.1007/s00392-018-1237-z
20. Riedel O, Ohlmeier C, Enders D, Elsasser A, Vizcaya D, Michel A, Eberhard S, Schlothauer N, Berg J, Garbe E (2018) The contribution of comorbidities to mortality in hospitalized patients with heart failure. Clin Res Cardiol 107(6):487–497. https://doi.org/10.1007/s00392-018-1210-x
21. Tschope C, Birner C, Bohm M, Bruder O, Frantz S, Luchner A, Maier L, Stork S, Kherad B, Laufs U (2018) Heart failure with preserved ejection fraction: current management and future strategies: expert opinion on the behalf of the Nucleus of the "Heart Failure Working Group" of the German Society of Cardiology (DKG). Clin Res Cardiol 107(1):1–19. https://doi.org/10.1007/s00392-017-1170-6
22. Morbach C, Buck T, Rost C, Peter S, Gunther S, Stork S, Prettin C, Erbel R, Ertl G, Angermann CE, Handheld BNPRN (2018) Point-of-care B-type natriuretic peptide and portable echocardiography for assessment of patients with suspected heart failure in primary care: rationale and design of the three-part handheld-BNP program and results of the training study. Clin Res Cardiol 107(2):95–107. https://doi.org/10.1007/s00392-017-1181-3
23. Greene SJ, Fonarow GC, Solomon SD, Subacius HP, Ambrosy AP, Vaduganathan M, Maggioni AP, Bohm M, Lewis EF, Zannad F, Butler J, Gheorghiade M (2016) Influence of atrial fibrillation on post-discharge natriuretic peptide trajectory and clinical outcomes among patients hospitalized for heart failure: insights from the ASTRONAUT trial. Eur J Heart Fail. https://doi.org/10.1002/ejhf.674
24. Wozakowska-Kaplon B (2010) Changes in plasma natriuretic peptide levels in patients with atrial fibrillation after cardioversion. Int J Cardiol 144(3):436–437. https://doi.org/10.1016/j.ijcard.2009.03.085
25. Charitakis E, Walfridsson H, Alehagen U (2016) Short-term influence of radiofrequency ablation on NT-proBNP, MR-proANP, copeptin, and MR-proADM in patients with atrial fibrillation: data from the observational SMURF Study. J Am Heart Assoc. https://doi.org/10.1161/JAHA.116.003557
26. Vinch CS, Rashkin J, Logsetty G, Tighe DA, Hill JC, Meyer TE, Rosenthal LS, Aurigemma GP (2004) Brain natriuretic peptide levels fall rapidly after cardioversion of atrial fibrillation to sinus rhythm. Cardiology 102(4):188–193. https://doi.org/10.1159/00008100981009
27. Schotten U, Verheule S, Kirchhof P, Goette A (2011) Pathophysiological mechanisms of atrial fibrillation: a translational appraisal. Physiol Rev 91(1):265–325. https://doi.org/10.1152/physrev.00031.2009
28. Heijman J, Voigt N, Nattel S, Dobrev D (2014) Cellular and molecular electrophysiology of atrial fibrillation initiation, maintenance, and progression. Circ Res 114(9):1483–1499. https://doi.org/10.1161/CIRCRESAHA.114.302226
29. Zhang YH, Youm JB, Earm YE (2008) Stretch-activated nonselective cation channel: a causal link between mechanical stretch and atrial natriuretic peptide secretion. Prog Biophys Mol Biol 98(1):1–9. https://doi.org/10.1016/j.pbiomolbio.2008.05.005
30. De Jong AM, Maass AH, Oberdorf-Maass SU, Van Veldhuisen DJ, Van Gilst WH, Van Gelder IC (2011) Mechanisms of atrial structural changes caused by stretch occurring before and during early atrial fibrillation. Cardiovasc Res 89(4):754–765. https://doi.org/10.1093/cvr/cvq357
31. Edwards BS, Zimmerman RS, Schwab TR, Heublein DM, Burnett JC Jr (1988) Atrial stretch, not pressure, is the principal determinant controlling the acute release of atrial natriuretic factor. Circ Res 62(2):191–195
32. Fiala M, Wichterle D, Chovancik J, Bulkova V, Wojnarova D, Nevralova R, Januska J (2010) Left atrial voltage during atrial fibrillation in paroxysmal and persistent atrial fibrillation patients. Pacing Clin Electrophysiol 33(5):541–548. https://doi.org/10.1111/j.1540-8159.2009.02646.x

M. Pešl a kol.

Cardiovascular progenitor cells and tissue plasticity are reduced in a myocardium affected by Becker muscular dystrophy *(id 1294)*

Orphanet Journal of Rare Diseases
Impact Factor: 3,687

‹ rejstřík

Pesl et al. Orphanet Journal of Rare Diseases (2020) 15:65
https://doi.org/10.1186/s13023-019-1257-4

Orphanet Journal of Rare Diseases

RESEARCH Open Access

Cardiovascular progenitor cells and tissue plasticity are reduced in a myocardium affected by Becker muscular dystrophy

Martin Pesl[1,2,3], Sarka Jelinkova[1,2], Guido Caluori[2,4], Maria Holicka[5], Jan Krejci[3], Petr Nemec[6], Aneta Kohutova[1,2], Vita Zampachova[7], Petr Dvorak[1] and Vladimir Rotrekl[1,2*]

Abstract: We describe the association of Becker muscular dystrophy (BMD) derived heart failure with the impairment of tissue homeostasis and remodeling capabilities of the affected heart tissue. We report that BMD heart failure is associated with a significantly decreased number of cardiovascular progenitor cells, reduced cardiac fibroblast migration, and ex vivo survival.

Background: Becker muscular dystrophy belongs to a class of genetically inherited dystrophin deficiencies. It affects male patients and results in progressive skeletal muscle degeneration and dilated cardiomyopathy leading to heart failure. It is a relatively mild form of dystrophin deficiency, which allows patients to be on a heart transplant list. In this unique situation, the explanted heart is a rare opportunity to study the degenerative process of dystrophin-deficient cardiac tissue. Heart tissue was excised, dissociated, and analyzed. The fractional content of c-kit$^+$/CD45$^-$ cardiovascular progenitor cells (CVPCs) and cardiac fibroblast migration were compared to control samples of atrial tissue. Control tissue was obtained from the hearts of healthy organ donor's during heart transplantation procedures.

Results: We report significantly decreased CVPCs (c-kit$^+$/CD45$^-$) throughout the heart tissue of a BMD patient, and reduced numbers of phase-bright cells presenting c-kit positivity in the dystrophin-deficient cultured explants. In addition, ex vivo CVPCs survival and cardiac fibroblasts migration were significantly reduced, suggesting reduced homeostatic support and irreversible tissue remodeling.

Conclusions: Our findings associate genetically derived heart failure in a dystrophin-deficient patient with decreased c-kit$^+$/CD45$^-$ CVPCs and their resilience, possibly hinting at a lack of cardioprotective capability and/or reduced homeostatic support. This also correlates with reduced plasticity of the explanted cardiac tissue, related to the process of irreversible remodeling in the BMD patient's heart.

Keywords: Becker muscular dystrophy, Dystrophin, Cardiovascular progenitor cells, C-kit, Cardiomyopathy, Heart failure

Background

Dystrophinopathies are a class of inherited X-linked genetic disorders that impair the proper synthesis of dystrophin, a scaffolding protein found in skeletal and cardiac muscle [1]. More than 70% of patients suffering from Becker muscular dystrophy (BMD), a mild form of dystrophin deficiency, are diagnosed with dilated cardiomyopathy (DCM) [2, 3], which is uncorrelated with skeletal muscle degeneration [4]. Heart failure is the most common cause of death in those with BMD [5], and patients are, in individual cases, referred for heart transplantation [6].

The cellular dynamics of DCM development in dystrophinopathies are still unclear. Although this condition involves mostly cardiomyocytes, increasing attention has been directed at understanding the features and progression of DCM in the non-muscular cell fractions. These mainly include cardiac fibroblasts [7–9] and endothelial

* Correspondence: vrotrekl@med.muni.cz
[1]Department of Biology, Faculty of Medicine, Masaryk University, Kamenice 5, Brno 62500, Czech Republic
[2]International Clinical Research Center, (ICRC), St. Anne's University Hospital, Pekarska 53, Brno 65691, Czech Republic
Full list of author information is available at the end of the article

cells [10–13], which are, in part, known to affect extracellular matrix and vascular remodeling. Other stromal cells possibly involved in cardiac homeostasis, survival, and disease dynamics are cardiovascular progenitor cells (CVPC) [14], which include the $CD117^+$ (or c-kit)/$CD45^-$ fraction, and has been the main focus of several recent studies [15, 16]. Currently, the evidence shows that c-kit^+/$CD45^-$ are activated by cardiac injury [17] supporting the hypothesis of paracrine regulation of cardiac function under pathophysiological conditions [16, 18, 19]; however, their role and fate in the human heart remains to be elucidated.

Here we describe the first comparative characterization of c-kit^+/$CD45^-$ CVPC occurrence and tissue plasticity in myocardium obtained during a rare case of a BMD heart transplant in our center, and only the third such transplantation in the Czech Republic during the past three decades of the transplantation program [20]. This unique sample from our BMD patient was compared to healthy control cardiac samples from healthy heart donors for cardiac transplantation.

Results

Patients' history

A patient with muscular dystrophy developed mild disease-related symptoms at the age 9 yrs. and Gowers' sign was pronounced by the age 15; additionally, there was calf pseudohypertrophy. To this day (age 48), the patient does not require a wheelchair and has no signs of intellectual impairment (for recent neurological report, see Additional file 1: Supplementary materials). Slowly progressing cardiomyopathy was detected in 2004 (age 33) and an internal cardiac defibrillator (ICD) was implanted in 2012 (the ICD was magnetic resonance incompatible, and no MRI scans could be performed). In 2014, the patient presented with heart failure. A cardiac evaluation found a reduced left ventricular ejection fraction (15%) with severe mitral regurgitation (3rd degree, hemodynamically graded as moderate for echo visualization; for a detailed description see Additional file 1: Supplementary materials and Additional file 2: Video 1; Additional file 3: Video 3; Additional file 4: Video 4), and borderline pulmonary hypertension, all of which responded to pharmacological intervention. Ischemic cardiomyopathy was excluded using coronary angiography (see Additional file 1: Supplementary materials). Due to progressive worsening of dyspnea up to the point of pulmonary edema, which required repeated hospital admissions, the patient was put on the non-urgent heart transplantation waiting list. The prescribed heart failure medication included beta-blockers, loop and mineralocorticoid diuretics, digoxin, angiotensin-converting enzyme (ACE) inhibitors, and proton pump inhibitors. A bicaval orthotropic cardiac transplantation took place shortly before the patient turned 44. He was discharged to out-patient care and follow-up 18 days post-transplantation. During the patient's procedure and the five subsequent heart transplant procedures, surgically available left atrial (LA) tissue, from LA reductions (i.e., surgically required LA shaping and reductions in order to fit the transplant to the left atria of the recipient), were collected for use as healthy controls for this study.

The patient had been screened for genetic mutations, in his twenties, i.e., exon sequencing of the *DMD* gene, but no known mutations were found. Due to the evident clinical presentation, other genes were not screened. A single point mutation c.3328 G > T, (p. Glu1110X) in exon 25, causing a stop codon, was later identified in a sample from the patient's first-degree cousin, which was done as part of a family pedigree (see Fig. 1). The patient was subsequently diagnosed with the same mutation. This mutation would normally result in a DMD phenotype. Nevertheless the BMD phenotype of our patient, with a similar stop codon mutation in exon 25, was explained by the presence of alternatively spliced mRNA, in which a deletion bridges the non-sense mutation and thus partially suppresses its effect [21]. The patient has

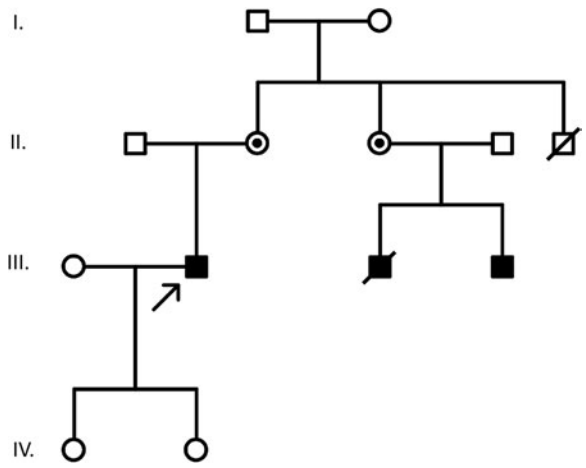

Fig. 1 Family history and pedigree. Proband has no siblings, his father has no signs of muscular dystrophy nor cardiovascular disease and is 70 years old. Mother of patient is alive, with no cardiac involvement, genetic analysis was not performed. Mother's sister, aunt of the proband, was diagnosed as a carrier of an identified mutation, has limited contact with the family, but no cardiac involvement could be traced. Her sons, proband's first cousins, were both confirmed to carry the mutation. The older one (born 1971) died from heart failure in his early thirties, suffering frequent epileptic seizures, aggravating an already unfavorable status, with dystrophy signs since the age of 10. More detailed data could not be retrieved since he was more than 10 years deceased during manuscript preparation. The younger cousin, born 1982 is alive, in his late thirties, with severe myopathy, loss of ambulation since age 14 and was diagnosed with dilated cardiomyopathy. Mother's brother died at 40 years, further details could not be retrieved from the family. The proband has two healthy daughters. Otherwise, the traceable family cardiac history was irrelevant

daughters, however, cascade mutation screening was not performed among female relatives, based on their preference. Creatine kinase (CK) levels before transplantation were only mildly increased, oscillating between 20 and 30 μkat/l (reference value under 3.17 μkat/l); the CK muscle brain (CK-MB) fraction was increased between 0.8–0.9 μkat/l, which normalized after transplantation (under 0.4 μkat/l). A skeletal muscle biopsy was not performed since the diagnosis was genetically verified.

Gross pathologic description of BMD heart

The heart explant (size 150 × 120 × 70 mm) presented bilateral atrial and ventricular dilatation. Both coronary arteries showed sporadic fibrous and atheromatic plaques, without stenosis, and without perivascular inflammation. The wall thickness of the right ventricle (RV) was 4 mm along the anterior basal side and 3 mm along the posterior apical side. RV outflow was partially obstructed by a left ventricle (LV) septal mass. The ventricle walls presented with irregular fibrosis, a thinned or absent myocardial layer, and thickened or prevalent adipose tissue. The LV posterior wall, in particular, was irregularly thick, with the subvalvular wall being 5 mm with a non-compaction appearance (the non-compacted/spongiotic layer: compacted layer ratio was approximately 1). The middle part of the LV posterior wall had a thickness of 8 mm, with fibrosis and thinning toward the apex. The anterior LV wall was irregularly thick (5–10 mm) with focal fibrosis. The IVS thickness was 12 mm. A myxoid transformation of the tricuspid and mitral valves was observed. Histologically, there were partial and non-specific myocardial changes, i.e., dilated cardiomyopathy with hypertrophic cardiomyocytes and interstitial fibrosis. The free LV wall had foci of non-compaction, prominent adipose tissue, and small residual groups of cardiomyocytes. Similar changes were seen in the LV papillary muscles and the RV outflow tract. Laminar fibrosis was present mostly in the subepicardial and middle layers of the compact myocardium regions. Cardiomyocytes showed no signs of acute regressive changes, nor the pathologic changes typical of storage disorders. A slight focal intimal thickening with sporadic incipient atheromatic plaques was found in the coronary arteries.

BMD samples were compared with myocardial samples from hearts explanted due to ischemic heart disease. The controls showed more or less diffuse membranous dystrophin staining. The BMD patient's samples showed a mosaic pattern with an absence of membranous staining and only sporadic isolated myocytes (< 0.1‰) with partial and weak membranous staining. These immunohistopathological findings are shown in Fig. 2.

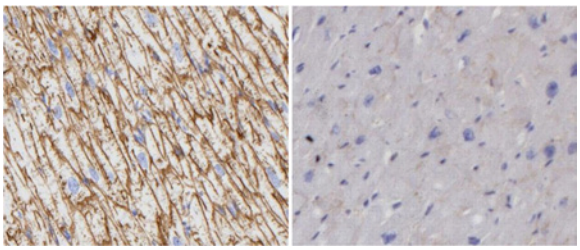

Fig. 2 Immunohistopathology of human myocardium stained for presence of dystrophin. Left image: healthy ventricular myocardium showing membranous aggregation of dystrophin. Right image: Becker muscular dystrophy-affected ventricular myocardium, showing weak membranous distribution of dystrophin. Magnification 400X

C-kit$^+$ /CD45$^-$ cells are depleted in BMD-affected myocardium

We quantified the number of c-kit$^+$/CD45$^-$ cells to detect significant alterations in the cardiac c-kit$^+$/CD45$^-$ population fraction in heart tissue affected by BMD-DCM. Tissue samples from myocardium were dissociated, and single-cell suspensions were quantified with anti-CD117 (c-kit) and anti-CD45 fluorophore-conjugated antibodies. Tissue samples were excised from the whole myocardium of the explanted BMD heart (i.e., LA, right atrium (RA), LV, RV, and intraventricular septum (IVS)) and compared to LA samples of healthy heart donors (HD). While the HD atrial samples contained an average of 1.54% (1.39; 1.62, and 1.62% for each HD sample) c-kit$^+$/CD45$^-$ cells, samples from the BMD myocardium contained 0.28 and 0.35% c-kit$^+$/CD45$^-$ cells (RA and LA, respectively; see Fig. 3a top row), which was less than a quarter of the HD average. The BMD ventricular samples contained 0.42, 0.58, and 0.13% c-kit$^+$ /CD45$^-$ cells (RV, LV, and IVS, respectively; see Fig. 3a bottom row). The BMD c-kit$^+$/CD45$^-$ mean fraction was significantly lower with respect to the mean value of the HD atrial samples ($p = 0.036$, calculated using the Mann-Whitney statistical test, Fig. 3b).

BMD heart tissue shows ex vivo reduced plasticity and phase-bright cells resilience

We evaluated the ability of mildly dissociated tissue explants (< 1 mm^3 pieces) to adhere to culture dishes, in order to prove their ability to retain tissue plasticity. While BMD explants samples required 7 days of ex-vivo cultivation before starting to attach, the HD samples started to attach within 4 days. We then observed and evaluated cardiac fibroblast cell migration from 19 HD and 13 BMD explants-derived samples to estimate the remodeling capacity of the original tissue. The maximal migration distance of fibroblasts from the explant border after 9 days in vitro was 1031.2 ± 351.2 μm in HD samples, but only 330.9 ± 224.4 μm in BMD ($p < 0.001$, Mann-Whitney, Fig. 3c and d top row). We later observed phase-bright

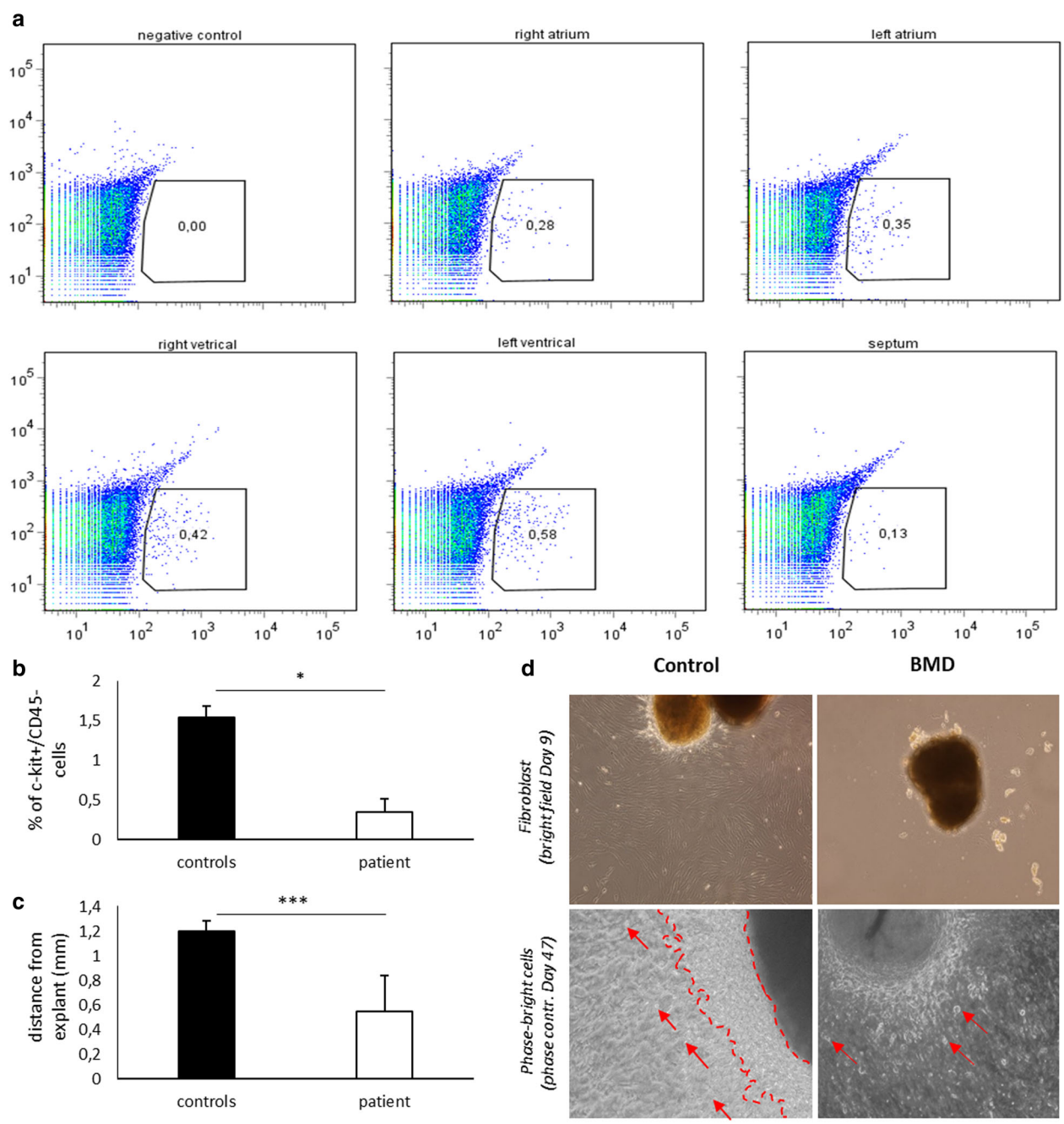

Fig. 3 Results on the cardiac tissue analysis. **a** FACS analysis of c-kit^{+}/CD45^{-} cells from dystrophin-deficient regions in different areas of the organ. **b** Comparison of c-kit^{+}/CD45^{-} cells percentage fractions among negative controls (HD, left atrium) and the dystrophin-deficient heart (indicated parts), * = $p < 0.05$. **c** Maximum distance reached by fibroblasts at the end of the migration assay, statistical difference was assessed using Mann-Whitney test. (*** = $p < 0.001$, **d** Tissue sample images on an optical microscope: top row, bright field images show migrating fibroblasts from healthy samples, while few cells migrated from dystrophin-deficient samples; bottom row shows phase-contrast close-ups of the explants. HD fibroblast layers are covered by phase-bright cells (left, dashed area + red arrows), while dystrophin-deficient layers show only sparse migration of these cells (right, red arrows show examples)

cells on fibroblasts. Phase-bright cells have been previously reported to contain a c-kit^{+} fraction [22]. These loosely adherent cells were thus stained for the presence of the c-kit marker, which revealed a 61 ± 20% positive fraction (6 explant samples analyzed, see Additional file 1: Supplementary materials). Phase-bright cells in HD samples started to appear on the fibroblast layer after 9 days in vitro. In contrast, phase-bright cells in BMD samples

only appeared on fibroblasts after 28 days. BMD explants showed few isolated phase-bright cells on the surrounding fibroblast layer, while HD sample had a dense covering on the surrounding explant tissue (Fig. 3D bottom row). Overall, 32.45% (37/114) of the HD explants showed phase-bright cells, while only 15.64% (23/147) of BMD samples showed phase-bright cells. After 90 days, the HD phase-bright cells had grown enough to allow immunolabelling. The BMD phase-bright cells started to disappear before reaching the quantity necessary for immunolabeling and were no longer observable after 51 days of cultivation, which impaired the comparative analysis.

Discussion

Heart failure due to DCM is a common clinical manifestation in patients with BMD [5]. It has been shown that CVPCs, including c-kit$^+$/CD45$^-$ cells, are involved in cardiac injury and degeneration [17, 23], resulting, for example, in capillary rarefaction, fibrosis, and other pathogeneses of an affected heart [24, 25]. The pathogenesis of dystrophinopathy was previously linked to increased DNA damage and to increased mutagenesis in pluripotent stem cells reprogrammed from DMD patients and lacking dystrophin, as we showed previously [26]. This could affect different organ tissue stem cells or niche supporting cells similar to satellite cells [27]. In this study, we investigated the presence of CVPCs in one model BMD-affected myocardium, as well as tissue remodeling capabilities. We observed that the CVPC fraction found in the dystrophic LA was more than four times lower than the average found in HD samples. The detected values of BMD c-kit$^+$/CD45$^-$ fractions were also comparable to previously reported numbers in idiopathic DCM [28]. This CVPCs depletion resembles DCM associated with accelerated aging [29] and can be caused by an increased turnover concomitant with cell damage. These mechanisms of depletion have been shown, for instance, in hematopoietic stem cells with mutated Sirt1 [30], or dystrophin-deficient ckit$^+$/CD45$^-$ in the GRMD dog model [31]. The reduced tissue plasticity in our model, observed through decreased adherence and cell migration from diseased tissue, also might point to impaired remodeling properties of the BMD-DCM heart. In concert with this hypothesis, only one-tenth of the BMD tissue fragments adhered to gelatin-coated culture dishes, which was almost three-times less than for HD tissue. Dystrophic samples also required nearly twice as much time to attach. Decreased culture dish adherence of BMD heart explanted tissue was accompanied by reduced migration ability of the outgrowing cells. Such behavior could originate in the presence of an activated myofibroblast subpopulation, due to a chronic state of myocardial injury and inflammation [32] with progressive fibrosis [33, 34]. Myofibroblasts are a specialized cell type in between the phenotype of cardiac fibroblasts and smooth muscle myocytes that express α-smooth muscle actinin (SMA) and play an important role in cardiac remodeling [35, 36]. Their motility is reduced due to overexpression of focal adhesion proteins [37] and reduced production of collagen VIII, the lack of which has been associated with decreased migratory abilities [38]. Thus, the presence of terminally differentiated myofibroblasts might explain the reduced adhesion and migration of the cells in vitro.

Ultimately, impaired survival rate of phase-bright cells in BMD samples was observed, while these cells appeared and persisted in the HD fibroblast layer. Moreover, in the BMD samples they were only sparsely identifiable and prematurely disappeared from the BMD fibroblast layer. Their limited in vitro survival in dystrophin-deficient heart explants might hint at altered c-kit$^+$/CD45$^-$ cell resilience also in vitro and subsequently could promote BMD-DCM progression.

The main limitation of the study is the unique characteristic of the human BMD heart sample since only one specimen was available and opportunities to study a heart affected by dystrophinopathy are extremely rare. A comparable sampling of healthy human ventricular tissue was impossible and clearly unethical; thus, atrial tissue controls came from transplants, considered healthy from a cardiac point of view and thus suitable for heart transplantation. We chose donors of similar age to the BMD patient to remove the age bias; with one exception, all were males. Still, tissue availability was limited with only minimal information regarding the medical backgrounds of the donors and families.

In non-ischemic DCM, LA remodeling was observed in functional and morphological changes [39], making this heart area a valid control source. The wide age interval of the donor cohort (see Additional file 1: Supplementary materials) is common in other similar studies [28], and was not significantly different from the age of the BMD patient, as shown using the one-sample t-test ($p = 0.625$). To the best knowledge of the authors, this analysis is the first to directly quantify c-kit$^+$/CD45$^-$ cells from BMD-DCM heart tissue. It contributes to the present understanding of the occurrence and role of c-kit$^+$/CD45$^-$ cells by showing a comparative reduction in this cell fraction, which can be correlated with reduced plasticity and cellular resilience in the BMD heart.

Conclusions

Our findings give further insights into the correlation between c-kit$^+$/CD45$^-$ CVPCs levels, irreversible remodeling, and heart failure in BMD. Future studies aimed at describing c-kit$^+$/CD45$^-$ mechanisms of activation, paracrine modulation, and genetic impairment can provide new therapeutic perspectives into the management of cardiomyopathies. The analysis of c-kit$^+$/CD45$^-$ cells or possibly their secretome might serve as a helpful biomarker for early

stages of cardiomyopathy, possibly not limited only to BMD patients.

Methods

Flow cytometry assay

Tissue samples were excised (in BMD) or extracted during a left atrial biopsy (from heart donors HD). Reduced dystrophin expression was confirmed by immunohistochemistry of myocardial samples. BMD samples were taken from different sections of the heart (left and right atrium, left and right ventricle, and the interventricular septum). As for the healthy donors, only adult patients were included (age 24–62 years, variance statistically insignificant $p = 0.625$) to exclude the bias of pediatric patients that have increased CVPC levels [23]. Due to the unavailability of ventricular samples, only atrial samples, which were obtained from surgical reduction before placing the healthy heart into the chest cavity during transplantations, were used. No other differences in CVPC levels were reported. Samples were treated as previously described by Messina et al. [22]. Briefly, tissue samples were immersed in a 60 mm Petri dish (TPP, Trasadingen, CH) filled with 1xPBS + 2% Pen/Strep (BioSera, Nuaille, France) and cut into 1–2 mm^3 pieces with scissors. Tissue fragments were digested in a dissociating solution composed of 0.1% Collagenase IV in DMEM-F12 (both from Life Technologies, Carlsbad, CA, USA). Dissociation was carried out for 2 h at 37 °C with gentle manual agitation every 15 mins. The dissociation was stopped by adding an equal volume of explant IMDM medium (Life Technologies) supplemented with FBS 10% (Life Technologies), β mercaptoethanol 1% (Sigma-Aldrich, St. Louis, MO), Pen/Strep 1%, and L-glutamine 1% (both from BioSera). Samples were collected and pipetted vigorously with a 1 ml tip to release cells from tissue blocks. The dissociated cell suspension was filtered through a 40 μm strainer (Costar, Washington DC, USA) and spun in a conical tube at 200×g for 5 min. The supernatant was removed, and the cell pellet was resuspended in FACS-PBS, made from 1xPBS with 0.5% BSA (Sigma Aldrich) and 2 mM EDTA (Penta, Prague, CZ). Spinning and resuspension were repeated 3 times to ensure enzyme removal and cell separation. Antibodies were finally added to the suspension (CD45-FITC, cl. 30F11; CD117-APC, cl.3C11, all from Miltenyi Biotech, Bergisch Gladbach, DE) and the analysis was run on a BD FACS Canto II (BD Biosciences, New Jersey, NJ-USA). The negative control for FACS was an unlabeled cell suspension. Data were analyzed using FlowJo (FlowJo LLC, Ashland, OR-USA).

Cell migration assay and immunocytochemistry

Samples were cut into 1–2 mm^3 pieces, as described in the previous paragraph. For the migration assay and c-$kit^+/CD45^-$ cell cultivation, the tissue explants were collected in a dissociation solution and incubated for 5 mins at 37 °C. The enzymatic solution was then removed and replaced with a fresh solution. Incubation and enzyme replacement was repeated three times. Dissociation was stopped by adding an equal volume of explant medium. The samples were spun at 200×g for 2 min, then resuspended with explant medium. The tissue explants were distributed evenly on a 0.1% gelatin-treated 6-well plates (TPP), in 5 ml of explant medium. The dishes were not moved for 4 days to allow attachment of the tissue. The medium was changed every 4 days, and photos were taken on the same days using an inverted Olympus IX71 microscope (Tokyo, Japan), and QuickPhoto Camera software (Promicra, Prague, CZ). Pictures were analyzed using ImageJ open-source software to measure migration [40] distance and phase-bright cells. C-kit+ cells were detected using CD117-APC (Miltenyi Biotec, Bergisch Gladbach, DE) dissolved in 1:100 proportion in IMDM + 0.5% BSA. Photos were taken using a Zeiss LSM700 confocal laser scanning microscope (Zeiss, Oberkochen, DE).

Histopathological methods

The heart explants were dissected according to standard procedures, samples were taken from right atrium, tricuspid valve; the anterior and posterior wall, and outflow tract of the right ventricle; the right coronary artery; the right atrium and mitral valve; anterior papillary muscles; multiple samples from the anterior and posterior wall of the left ventricle; the septum and left coronary arteries. For immunehistological identification of dystrophin, formalin-fixed, paraffin-embedded tissue sections were treated with heat antigen retrieval (95 °C for 45 min, pH 9), and then treated with primary antibodies (Dystrophin Mouse Monoclonal Antibody, Leica, clone 34C5) using the avidin-biotin-immunoperoxidase method according to the manufacturer's protocol.

Statistical analysis

Descriptive statistics and comparisons between sample groups were performed using Prism 5.0 software (GraphPad, La Jolla, CA-US). Available normality tests were performed, and the non-parametric Mann-Whitney test was used to estimate statistical differences between samples. A p-value less than 0.05 was considered significant.

Supplementary information

Supplementary information accompanies this paper at https://doi.org/10.1186/s13023-019-1257-4.

Additional file 1. Supplementary materials.
Additional file 2: Video 1. Coronarography – right coronary artery.
Additional file 3: Video 2. Coronarography – left coronary artery.
Additional file 4: Video 3. Echocardiography.

Abbreviations
BMD: Becker muscular dystrophy; DCM: Dilated cardiomyopathy; HTx: Heart transplantation; IVS: Interventricular septum; LV: Left ventricle; PBC: Phase-bright cells; RV: Right ventricle

Acknowledgements
The authors would like to thank geneticist Dr. Gaillyova and attending neurologists Dr. Vohanka and Dr. Peslova for assistance in clarifying the available documentation.

Authors' contributions
MP was responsible for the design of the study and the coordination, conducted clinical follow-up of the patient, and obtained the informed consent as well as the collection of samples. SJ was responsible for the cellular laboratory sample preparation, the cellular experiments, and their evaluation. GC was responsible for results collection, drafting the manuscript, and figures preparation. MH and JK were attending the cardiologists of the patient. PN was responsible for the surgical preparation of the samples during heart transplantation and the surgeon on the case. AK performed part of the ex vivo analysis of the samples. VZ provided the histological examination of the dystrophic heart samples. PD and VR secured funding of the project and supervised the production of the results and the manuscript. All authors read and approved the final manuscript.

Funding
This work was supported by the Ministry of Education, Youth, and Sports of the Czech Republic (7AMB13FR011, No. CZ.02.1.01/0.0/0.0/16_019/0000868, projects no. LQ1605 and no. LQ1601 from the National Program of Sustainability II) and supported by funds from the Faculty of Medicine MU to junior researchers Martin Pesl and Sarka Jelinkova.

Availability of data and materials
The data that support the findings of this study are available from the corresponding author V.R. upon reasonable request.

Ethics approval and consent to participate
This study was carried out in accordance with the recommendations of the Masaryk University Ethics Committee and St. Ann's University Hospital Ethics Committee, issuing approval nr. 51 V/2015 - approved consent for heart tissue sampling and analysis, and genetic information analysis (DNA and circulating free DNA), protocol was approved on 12th August 2015. The "healthy donor" (HD) control samples were obtained from donors diagnosed with brain death. The hearts were brought to the transplantation center for transplantation and were provided for scientific analysis after the anonymization of donor data. Thus, individual information, such as names of donors, was not available to investigators. Samples from deceased donors were not further addressed by the ethics committee since the transplantation system is opt-out according to the law 285/2002 Sb. in the Czech Republic. At the same time, due to anonymization, family members were not reachable.

Consent for publication
The study subject gave written informed consent regarding explanted organ sampling and publication of results.

Competing interests
The authors declare that they have no competing interests.

Author details
[1]Department of Biology, Faculty of Medicine, Masaryk University, Kamenice 5, Brno 62500, Czech Republic. [2]International Clinical Research Center, (ICRC), St. Anne's University Hospital, Pekarska 53, Brno 65691, Czech Republic. [3]1st Department of Cardiovascular Diseases, St. Anne's University Hospital and Masaryk University, Pekarska 53, Brno 65691, Czech Republic. [4]Central European Institute of Technology (CEITEC MU), Nanobiotechnology, Kamenice 5, Brno 62500, Czech Republic. [5]Department of Cardiology, University Hospital Brno, Jihlavska 20, Brno 62500, Czech Republic. [6]Center for Cardiovascular Surgery and Transplantation, Pekarska 53, Brno 65691, Czech Republic. [7]1st Department of Pathology, Faculty of Medicine, Masaryk University and St. Anne's University Hospital in Brno, Pekarska 53, Brno 65691, Czech Republic.

Received: 23 July 2019 Accepted: 19 November 2019
Published online: 05 March 2020

References
1. Ho R, Nguyen M-L, Mather P. Cardiomyopathy in Becker muscular dystrophy: overview. World J Cardiol. 2016;8:356.
2. Yilmaz A, Gdynia H-J, Baccouche H, Mahrholdt H, Meinhardt G, Basso C, et al. Cardiac involvement in patients with Becker muscular dystrophy: new diagnostic and pathophysiological insights by a CMR approach. J Cardiovasc Magn Reson. 2008;10:50.
3. Panovský R, Pešl M, Holeček T, Máchal J, Feitová V, Mrázová L, et al. Cardiac profile of the Czech population of Duchenne muscular dystrophy patients: a cardiovascular magnetic resonance study with T1 mapping. Orphanet J Rare Dis. 2019;14:10.
4. Finsterer J, Stöllberger C. Cardiac involvement in Becker muscular dystrophy. Can J Cardiol. 2008;24:786–92.
5. Papa AA, D'Ambrosio P, Petillo R, Palladino A, Politano L. Heart transplantation in patients with dystrophinopathic cardiomyopathy: review of the literature and personal series. Intractable Rare Dis Res. 2017;6:95–101.
6. Darras BT, Miller DT, Urion DK. Dystrophinopathies. Seattle: University of Washington; 1993. http://www.ncbi.nlm.nih.gov/pubmed/20301298.
7. Furtado MB, Nim HT, Boyd SE, Rosenthal NA. View from the heart: cardiac fibroblasts in development, scarring and regeneration. Development. 2016; 143:387–97.
8. Furtado MB, Costa MW, Pranoto EA, Ekaterina S, Pinto Alexander R, Lam Nicholas T, et al. Cardiogenic genes expressed in cardiac fibroblasts contribute to heart development and repair. Circ Res. 2014;114:1422–34.
9. Lajiness JD, Conway SJ. The dynamic role of cardiac fibroblasts in development and disease. J Cardiovasc Transl Res. 2012;5:739–48.
10. Talman V, Kivelä R. Cardiomyocyte—endothelial cell interactions in cardiac remodeling and regeneration. Front Cardiovasc Med. 2018;5. https://doi.org/10.3389/fcvm.2018.00101.
11. Mathison M, Rosengart TK. Heart regeneration: the endothelial cell comes first. J Thorac Cardiovasc Surg. 2018;155:1128–9.
12. Hui Z, Lui Kathy O, Bin Z. Endocardial cell plasticity in cardiac development, diseases and regeneration. Circ Res. 2018;122:774–89.
13. Gray G, Toor I, Castellan R, Crisan M, Meloni M. Resident cells of the myocardium: more than spectators in cardiac injury, repair and regeneration. Curr Opin Physiol. 2018;1:46–51.
14. Leong YY, Ng WH, Ellison-Hughes GM, Tan JJ. Cardiac stem cells for myocardial regeneration: they are not alone. Front Cardiovasc Med. 2017;4. https://doi.org/10.3389/fcvm.2017.00047.
15. Zhou B, Wu SM. Reassessment of c-kit in cardiac cells: a complex interplay between expression, fate, and function. Circ Res. 2018;123:9–11.
16. Hodgkinson CP, Bareja A, Gomez JA, Dzau VJ. Emerging concepts in paracrine mechanisms in regenerative cardiovascular medicine and biology. Circ Res. 2016;118:95–107.
17. Finan A, Demion M, Sicard P, Guisiano M, Bideaux P, Monceaux K, et al. Prolonged elevated levels of c-kit+ progenitor cells after a myocardial infarction by beta 2 adrenergic receptor priming. J Cell Physiol. 2019;234: 18283–96.
18. Hong KU, Guo Y, Li Q-H, Cao P, Al-Maqtari T, Vajravelu BN, et al. c-kit+ Cardiac stem cells alleviate post-myocardial infarction left ventricular dysfunction despite poor engraftment and negligible retention in the recipient heart. PLoS ONE. 2014;9:e96725.
19. Davis DR. Cardiac stem cells in the post-Anversa era. Eur Heart J. 2019;40: 1039–41.
20. Viklicky O, Fronek J, Trunecka P, Pirk J, Lischke R. Organ transplantation in the Czech Republic. Transplantation. 2017;101:2259.
21. Fajkusová L, Lukáš Z, Tvrdíková M, Kuhrová V, Hájek J, Fajkus J. Novel dystrophin mutations revealed by analysis of dystrophin mRNA: alternative splicing suppresses the phenotypic effect of a nonsense mutation. Neuromuscul Disord. 2001;11:133–8.
22. Messina E, De Angelis L, Frati G, Morrone S, Chimenti S, Fiordaliso F, et al. Isolation and expansion of adult cardiac stem cells from human and murine heart. Circ Res. 2004;95:911–21.
23. Matuszczak S, Czapla J, Jarosz-Biej M, Wiśniewska E, Cichoń T, Smolarczyk R, et al. Characteristic of c-kit+ progenitor cells in explanted human hearts. Clin Res Cardiol Off J Ger Card Soc. 2014;103:711–8.
24. Lombardi R, Chen SN, Ruggiero A, Gurha P, Czernuszewicz GZ, Willerson JT, et al. Cardiac fibro-adipocyte progenitors express desmosome proteins and

preferentially differentiate to adipocytes upon deletion of the desmoplakin gene. Circ Res. 2016;119:41–54.
25. Kazakov A, Laufs U. Healthy and unhealthy cardiac progenitor cells modify the pathogenesis of myocardial diseases. Circ Res. 2016;119:10–2.
26. Jelinkova S, Fojtik P, Kohutova A, Vilotic A, Marková L, Pesl M, et al. Dystrophin deficiency leads to genomic instability in human pluripotent stem cells via NO synthase-induced oxidative stress. Cells. 2019;8(1):53.
27. Dumont NA, Wang YX, von Maltzahn J, Pasut A, Bentzinger CF, Brun CE, et al. Dystrophin expression in muscle stem cells regulates their polarity and asymmetric division. Nat Med. 2015;21:1455–63.
28. Matuszczak S, Czapla J, Jarosz-Biej M, Winiewska E, Cichoń T, et al. Characteristic of c-Kit + progenitor cells in explanted human hearts. Clin Res Cardiol. 2014;103(9):711–8. https://doi.org/10.1007/s00392-014-0705-3.
29. Saheera S, Nair RR. Accelerated decline in cardiac stem cell efficiency in spontaneously hypertensive rat compared to normotensive Wistar rat. PLoS One. 2017;12:e0189129.
30. Rimmelé P, Bigarella CL, Liang R, Izac B, Dieguez-Gonzalez R, Barbet G, et al. Aging-like phenotype and defective lineage specification in SIRT1-deleted hematopoietic stem and progenitor cells. Stem Cell Rep. 2014;3:44–59.
31. Cassano M, Berardi E, Crippa S, Toelen J, Barthelemy I, Micheletti R, et al. Alteration of cardiac progenitor cell potency in GRMD dogs. Cell Transplant. 2012;21:1945–67.
32. Kharraz Y, Guerra J, Pessina P, Serrano AL, Muñoz-Cánoves P. Understanding the process of fibrosis in Duchenne muscular dystrophy. Biomed Res Int. 2014;2014:965631.
33. Mann CJ, Perdiguero E, Kharraz Y, Aguilar S, Pessina P, Serrano AL, et al. Aberrant repair and fibrosis development in skeletal muscle. Skelet Muscle. 2011;1:21.
34. Fan D, Takawale A, Lee J, Kassiri Z. Cardiac fibroblasts, fibrosis and extracellular matrix remodeling in heart disease. Fibrogenesis Tissue Repair. 2012;5:15.
35. Dostal D, Glaser S, Baudino TA. Cardiac fibroblast physiology and pathology. In: Terjung R, editor. Comprehensive physiology. Hoboken: John Wiley & Sons, Inc.; 2015. p. 887–909. https://doi.org/10.1002/cphy.c140053.
36. Li L, Zhao Q, Kong W. Extracellular matrix remodeling and cardiac fibrosis. Matrix Biol. 2018;68–69:490–506.
37. Santiago J-J, Dangerfield AL, Rattan SG, Bathe KL, Cunnington RH, Raizman JE, et al. Cardiac fibroblast to myofibroblast differentiation in vivo and in vitro: expression of focal adhesion components in neonatal and adult rat ventricular myofibroblasts. Dev Dyn. 2010;239:1573–84.
38. Skrbic B, Engebretsen KVT, Strand ME, Lunde IG, Herum KM, Marstein HS, et al. Lack of collagen VIII reduces fibrosis and promotes early mortality and cardiac dilatation in pressure overload in mice. Cardiovasc Res. 2015;106:32–42.
39. Hoit BD, Ohio C. Left atrial size and function role in prognosis. J Am Coll Cardiol. 2014;63:493–505.
40. Treloar KK, Simpson MJ. Sensitivity of edge detection methods for quantifying cell migration assays. PLoS One. 2013;8:e67389.

Publisher's Note

T. Roubíček a kol.

Combination of left ventricular reverse remodeling and brain natriuretic peptide level at one year after cardiac resynchronization therapy predicts long-term clinical outcome
(id 71)

Plos One
Impact Factor: 2,8

‹ rejstřík

PLOS ONE

RESEARCH ARTICLE

Combination of left ventricular reverse remodeling and brain natriuretic peptide level at one year after cardiac resynchronization therapy predicts long-term clinical outcome

Tomas Roubicek[1,2,3]*, **Jan Stros**[1], **Pavel Kucera**[1], **Pavel Nedbal**[1], **Jan Cerny**[1], **Rostislav Polasek**[1,3], **Dan Wichterle**[2,3]

1 Department of Cardiology, Regional Hospital Liberec, Liberec, Czech Republic, **2** Department of Cardiology, Institute for Clinical and Experimental Medicine, Prague, Czech Republic, **3** Faculty of Health Studies, Technical University of Liberec, Liberec, Czech Republic

* tomas.roubicek@nemlib.cz

Citation: Roubicek T, Stros J, Kucera P, Nedbal P, Cerny J, Polasek R, et al. (2019) Combination of left ventricular reverse remodeling and brain natriuretic peptide level at one year after cardiac resynchronization therapy predicts long-term clinical outcome. PLoS ONE 14(7): e0219966. https://doi.org/10.1371/journal.pone.0219966

Editor: Vincenzo Lionetti, Scuola Superiore Sant'Anna, ITALY

Received: March 2, 2019

Accepted: July 6, 2019

Published: July 17, 2019

Data Availability Statement: All relevant data are available from https://osf.io/m2q3h/ (doi:10.17605/OSF.IO/M2Q3H).

Funding: The authors received no specific funding for this work.

Competing interests: The authors have declared that no competing interests exist.

Abstract

Introduction

The aim of this study was to investigate the predictors of long-term clinical outcome of heart failure (HF) patients who survived first year after initiation of cardiac resynchronization therapy (CRT).

Methods

This was a single-center observational cohort study of CRT patients implanted because of symptomatic HF with reduced ejection fraction between 2005 and 2013. Left ventricle (LV) diameters and ejection fraction, New York Heart Association (NYHA) class, and level of N-terminal fragment of pro-brain natriuretic peptide (NT-proBNP) were assessed at baseline and 12 months after CRT implantation. Their predictive power for long-term HF hospitalization and mortality, and cardiac and all-cause mortality was investigated.

Results

A total of 315 patients with left bundle branch block or intraventricular conduction delay who survived >1 year after CRT implantation were analyzed in the current study. During a follow-up period of 4.8±2.1 years from CRT implantation, 35.2% patients died from cardiac (19.3%) or non-cardiac (15.9%) causes. Post-CRT LV ejection fraction and LV end-systolic diameter (either 12-month value or the change from baseline) were equally predictive for clinical events. For NT-proBNP, however, the 12-month level was a stronger predictor than the change from baseline. Both reverse LV remodeling and 12-month level of NT-proBNP were independent and comparable predictors of CRT-related clinical outcome, while NT-proBNP response had the strongest association with all-cause mortality. When post-CRT relative change of LV end-systolic diameter and 12-month level of NT-proBNP

(dichotomized at -12.3% and 1230 ng/L, respectively) were combined, subgroups of very-high and very-low risk patients were identified.

Conclusion

The level of NT-proBNP and reverse LV remodeling at one year after CRT are independent and complementary predictors of future clinical events. Their combination may help to improve the risk stratification of CRT patients.

Introduction

Cardiac resynchronization therapy (CRT) has become an established and important treatment for chronic heart failure (HF) patients with left ventricular (LV) systolic dysfunction and left bundle branch block (LBBB) [1–3]. However, approximately 30% of patients fail to respond to CRT [4]. There is a great interest in the early identification not only of determinants of CRT response but also predictors of future clinical events.

In our previous study [5], we showed that electrical LV lead position at implant assessed by Q-LV ratio (electrical delay from the beginning of the QRS complex to the local LV electrogram/QRS duration) was found to be a significant predictor of mortality in CRT patients. In the same population with prolonged follow up, we investigated the long-term prognostic value of short-term (1-year) CRT response on top of baseline clinical characteristics. Specifically, we focused on endsystolic LV diameter, NYHA class and NT-proBNP, either in absolute 12-month values as well as their relative change compared to baseline. Heart failure hospitalizations, heart failure death, cardiac death and all-cause mortality were pre-specified study endpoints.

Methods

Patient cohort

Similarly, as in our previous study [5], we retrospectively analyzed data from a prospective database of patients in whom de novo biventricular pacemaker (CRT-P) or defibrillator (CRT-D) was implanted at the Regional Hospital Liberec, Czech Republic between June 2005 and December 2013. All patients signed an informed consent with the procedure. CRT was indicated according to current guidelines of the European Society of Cardiology: symptomatic chronic HF despite optimal medical therapy, LV ejection fraction (LVEF) $\leq$35% and QRS duration (QRSd) $\geq$120ms [6]. Only patients with LBBB or intraventricular conduction delay (IVCD) defined according to the Strauss criteria [7] were included. Patients who died prior to 12-month visit were excluded. The study was performed in accordance with the Declaration of Helsinki guidelines and the analysis was approved by the local Ethics Committee.

The right ventricular lead was commonly placed in the midseptum region. The LV lead was inserted transvenously with a preference for lateral followed by posterolateral cardiac veins. Whenever possible, attempts were made to maximize the left ventricular lead electrical delay (Q-LV) at implant. Empirical atrioventricular delay of 120 ms and zero V-V delay were programmed at implant and were not routinely optimized. When no clinical improvement was observed in follow-up visits, patients underwent at least one session of echocardiographic CRT optimization.

Follow-up

All patients were seen in the local outpatient department every 6 months. In the visits, the results of clinical examination, standard ECG, CRT device settings, medical treatment, and echocardiographic findings were recorded. Clinical outcome data were collected from other relevant medical records, by contacting primary care physicians and the National Health Care mortality registry. When the proportion of ventricular pacing in patients with atrial fibrillation was <90% despite medical therapy, atrioventricular junction ablation was performed. The follow up was completed in July 2016.

Laboratory assay

Blood samples in tubes containing serum-separating gel for N-terminal fragment of pro-brain natriuretic peptide (NT-proBNP) analysis were collected at baseline and at 12-months follow-up visit. Samples were taken in the morning (8 a.m.) before CRT implantation and in ambulatory setting (12-months visit). Samples at room temperature (20–25 ˚C) were immediately (< 1 hour) transported for the analysis. Serum / plasma NT-proBNP was measured on a Cobas e411 analyzer (Roche Diagnostics) using the Elecsys proBNP II immunoassay (Roche Diagnostics). The analytical performance of NT-proBNP assay in the reference laboratory of the study was assessed at the level of 140 ng/L (intermediate precision: 2.52%, bias: 2.73%, and combined uncertainty: 5.03%) and at the level of 4810 ng/L (intermediate precision: 1.82%, bias: 2.85%, and combined uncertainty: 3.65%).

Study endpoints

Four study endpoints were defined for the follow up after first year: HF hospitalization, HF mortality, cardiac mortality, and all-cause mortality. HF hospitalization was defined as a hospital admission with overnight stay because of signs or symptoms of HF, with subsequent improvement with medical therapy. All HF hospitalizations within the first year after CRT implantation were disregarded. The cause of death was assessed by the consensus of two physicians. This was done by careful review of clinical, death and autopsy reports, and CRT device memory when available. Heart failure mortality was defined as death following a progressive deterioration of heart failure symptoms over a period of weeks or months, and which did not fulfil criteria for sudden cardiac death. Cardiac mortality was defined as any death due to cardiac causes, including sudden cardiac death, heart failure death and death due to myocardial infarction. Any sudden death of uncertain cause was considered sudden cardiac death.

Statistical analysis

Continuous variables were expressed as a mean ± standard deviation and compared by two-tailed t-test for independent samples or Mann-Whitney U test for non-normally distributed data. Categorical variables were expressed as percentages and compared by Chi-square test. Associations of clinical characteristics (including their change during the first year of follow up) with all study endpoints were investigated by Cox proportional-hazards regression analysis with individual factors as continuous variables whenever possible. The NT-proBNP data were log-transformed prior to this analysis. All factors that were univariably associated ($P<0.20$) with at least one study endpoint were entered into the multivariable Cox regression models and investigated by stepwise-forward method. Predictive power of continuous factors was compared by area under the curve (AUC) by an analysis of receiver-operating characteristics (ROC) curves. Optimum cut-off values were found by the criterion of minimum distance from the [0;1]-point of ROC curve.

In dichotomized population, Kaplan-Meier curves were used to display cumulative event-free survival and the hazard ratios for high-risk subgroups were assessed by Cox proportional-hazards regression analysis. Similarly, combinations of risk factors were investigated. The index of net reclassification improvement was used to quantify the prediction value added by newly proposed risk factors [8]. Starting point for all survival analyses was set at 12-month post-CRT visit. A P-value ≤ 0.05 was considered significant. Statistical analyses were performed using the STATISTICA vers. 12 software (Statsoft, Inc.) and „easyROC" web-tool for ROC curve analysis (ver. 1.3) [9].

Results

A total of 328 consecutive patients with LBBB or IVCD with first-time implantation of CRT pacemaker (n = 79) or defibrillator (n = 249) were included. Thirteen patients died within the first year. These patients did not differ from the rest of the study population except for a higher baseline New York Heart Association (NYHA) class (3.5±0.5 vs. 3.1±0.5, P = 0.007) and higher baseline NT-proBNP levels (9609±7744 vs. 3033±4289 ng/L, P<0.0001).

A total of 315 CRT patients who survived >1 year after CRT implantation were analyzed in the current study. Among those patients, 22 heart failure hospitalizations that occurred before the 12-month visit were disregarded. Patient baseline and 12-month characteristics are shown in Table 1.

Patients were treated with beta-blockers (96%), angiotensin-converting enzyme inhibitors or angiotensin receptor blockers (99%), loop diuretics (91%), and mineralocorticoid-receptor antagonists (89%). Quadripolar LV lead was used only in 11 patients. Only one patient was upgraded

Table 1. Baseline and 12-month characteristics of study population (N = 315).

Variable	Baseline	12 months
Males (%)	76.2	-
Age (years)	67±9	-
Ischemic cardiomyopathy (%)	56.5	-
Left bundle branch block (%)	81.3	-
Atrial fibrillation (%)	15.2	-
Left atrium diameter (mm)	48.7±6.0	-
Creatinine (μmol/L)	103±40	-
Implantable cardioverter-defibrillator (%)	75.9	-
Q-LV (ms)	122±30	-
Q-LV ratio	0.76±0.14	-
Biventricular capture (%)		97.4±4.0
QRS duration (ms)	161±20	138±19
NYHA class	3.1±0.5	2.1±0.7
LV ejection fraction (%)	26.2±5.5	38.8±13.8
LV end-diastolic diameter (mm)	65.7±7.1	60.7±9.0
LV end-systolic diameter (mm)	56.2±8.0	48.4±12.0
Mitral regurgitation (grade)	1.7±1.0	1.3±0.7
NT-proBNP (ng/L)	1672 (871–3603)	952 (423–2519)

The values are percentage, mean ± standard deviation or median (interquartile range). Atrial fibrillation category includes persistent or permanent form of arrhythmia. Left bundle branch block was defined according to criteria by Strauss. Abbreviations: NT-proBNP = N-terminal fragment of pro-brain natriuretic peptide, NYHA = New York Heart Association; LV = left ventricle; Q-LV = left ventricular lead local electrogram delay from the QRS onset; Q-LV ratio = Q-LV / QRS duration.

https://doi.org/10.1371/journal.pone.0219966.t001

from CRT-P to CRT-D due to occurrence of ventricular tachycardia. Ten patients with CRT-D underwent the radiofrequency ablation for ventricular tachycardia during the follow up.

During the mean follow-up period of 4.8±2.1 years (median: 4.6 years) from CRT implantation, 82 patients (26%) were hospitalized for heart failure and 111 (35.2%) patients died of cardiac (n = 61, 19.3%) or non-cardiac (n = 50, 15.9%) causes. Cardiac deaths were due to heart failure (14.2%), sudden cardiac death (4.1%) and other cardiac reasons (1%). The risk of sudden death was higher in patients with CRT-P (7/76 = 9.2%) compared to CRT-D (6/239 = 2.5%), P = 0.02.

Differences between groups of patients defined by clinical outcome after the 12-months visit (HF hospitalization and death, cardiac and all-cause death) can be found in S1 and S2 Tables, and univariate associations between individual factors and clinical events are shown in Tables 2 and 3.

According to the results of multivariate analysis, which are shown in Table 4, the 12-month level of NT-proBNP was an independent predictor of clinical outcome that was consistently associated with all study endpoints. On the other hand, various indices of LV morphology / function (expressed as either the first-year change or final 12-month value) mutually competed and, therefore, did not consistently demonstrate independent association with clinical outcome.

Therefore, we selected NT-proBNP, LV end-systolic diameter (LVESd) and ejection fraction (LVEF) for a direct comparison of their predictive power by the analysis of ROC curves for all clinical endpoints. First, we compared the predictive power of their 12-month values versus the first-year change (Table 5). Except for heart failure hospitalization, survival was predicted significantly better by the 12-month level compared to the relative change in NT-proBNP. On the contrary, the final value and change during the first year were comparably predictive in the case of LVESd and LVEF. Second, we compared NT-proBNP at the 12-month visit and the relative change of LVESd and LVEF. In this more extensive analysis (cross-tabulated results are not shown), the predictive characteristics of all investigated indices were comparable with the exception of NT-proBNP at 12-month visit, which significantly outperformed the relative change of both LVESd and LVEF, but this was only valid for all-cause mortality (Fig 1).

Table 6 shows optimal cut-off values together with predictive characteristics derived from ROC analysis. Cut-offs were rather uniform for individual clinical endpoints, so that the dichotomies that were obtained for cardiac death were subsequently used also for other clinical endpoints.

Finally, dichotomized predictors were investigated by Kaplan-Meier analysis. Knowing the interchangeability of markers of reverse LV remodeling, this was done only for LVESd with the dichotomy of -12.3% for its relative change (Fig 2) and for 12-month level of NT-proBNP with a dichotomy of 1230 ng/L (Fig 3). In multivariate analysis, both factors were statistically independent, and this was preserved even after adjustment for other clinical characteristics, either continuous or dichotomized. Combination of both factors identified subgroups of very-high and very-low risk patients (Fig 4). Inclusion of NT-proBNP to simple LVESd-based risk stratification (when only patients with simultaneous change in LVESd >-12.3% and NT-proBNP >1230 ng/L were considered high-risk) resulted in net reclassification improvement of 10.8%, 14.2%, 13.5%, and 11.5% for HF hospitalization, HF death, cardiac death, and all-cause death, respectively.

Discussion

This single-center study with a long follow up suggested that the level of NT-proBNP and indices of reverse LV remodeling at one year after CRT implantation are replaceable predictors of

Table 2. Univariate association between individual factors and clinical events (hospitalization and death due to heart failure).

	Heart failure hospitalization N = 82			Heart failure death N = 45		
	HR	95% CI	P-value	HR	95% CI	P-value
Male gender (1/0)	1.8	1.01–3.3	0.046	2.2	0.95–5.3	0.06
Age (years)	1.6	0.99–2.4	0.053	1.02	0.99–1.1	0.21
Ischemic cardiomyopathy (1/0)	1.6	0.99–2.4	0.053	2.9	1.5–5.7	0.002
Non-left bundle branch block (1/0)	1.6	0.96–2.7	0.07	1.6	0.83–3.2	0.15
Atrial fibrillation (1/0)	0.76	0.39–1.5	0.41	0.89	0.37–2.1	0.78
Left atrium diameter (mm)	1.1	1.04–1.1	0.00006	1.1	1.1–1.2	0.00002
Creatinine (μmol/L)	1.01	1.00–1.01	0.003	1.00	1.00–1.01	0.42
Biventricular pacemaker only (1/0)	1.2	0.73–1.9	0.53	0.85	0.43–1.7	0.64
Q-LV (ms)	0.99	0.99–1.00	0.07	0.99	0.98–1.00	0.02
Q-LV ratio	0.15	0.03–0.69	0.01	0.06	0.01–0.34	0.002
Biventricular capture (%)	0.95	0.91–0.99	0.03	0.92	0.87–0.97	0.001
QRS duration—baseline (ms)	1.00	0.99–1.01	0.92	1.00	0.99–1.02	0.78
QRS duration—post-CRT (ms)	1.01	1.00–1.02	0.21	1.00	0.99–1.02	0.75
QRS duration—relative change (%)	1.01	0.99–1.03	0.30	1.00	0.98–1.02	0.93
NYHA Class—baseline (2/3/4)	1.8	1.2–2.8	0.005	1.5	0.85–2.6	0.16
NYHA Class—month 12 (2/3/4)	2.0	1.5–2.7	<0.00001	2.1	1.4–3.1	0.0001
NYHA Class—change	1.4	1.03–1.9	0.03	1.7	1.1–2.6	0.009
LV ejection fraction—baseline (%)	0.95	0.91–0.99	0.01	0.95	0.89–1.00	0.047
LV ejection fraction—month 12 (%)	0.95	0.93–0.97	<0.00001	0.93	0.90–0.95	<0.00001
LV ejection fraction—relative change (%)	0.99	0.99–0.99	0.00004	0.98	0.97–0.99	<0.00001
LV end-diastolic diameter—baseline (mm)	1.02	0.99–1.1	0.29	1.02	0.98–1.1	0.32
LV end-diastolic diameter—month 12 (mm)	1.1	1.03–1.1	<0.00001	1.1	1.04–1.1	<0.00001
LV end-diastolic diameter—relative change (%)	1.1	1.04–1.1	<0.00001	1.1	1.1–1.1	<0.00001
LV end-systolic diameter—baseline (mm)	1.02	0.99–1.1	0.15	1.03	0.99–1.1	0.20
LV end-systolic diameter—month 12 (mm)	1.05	1.03–1.1	<0.00001	1.1	1.04–1.1	<0.00001
LV end-systolic diameter—relative change (%)	1.05	1.03–1.1	<0.00001	1.1	1.05–1.1	<0.00001
Mitral regurgitation—baseline (1/2/3/4)	1.1	0.86–1.3	0.54	1.02	0.76–1.4	0.91
Mitral regurgitation—month 12 (1/2/3/4)	1.8	1.5–2.3	<0.00001	1.8	1.4–2.3	0.00003
Mitral regurgitation—change	1.6	1.2–2.1	0.002	1.8	1.2–2.6	0.004
NT-proBNP—baseline (log ng/L)	2.2	1.3–3.5	0.002	3.1	1.6–6.1	0.0009
NT-proBNP—month 12 (log ng/L)	5.2	3.2–8.5	<0.00001	5.8	3.1–10.8	<0.00001
NT-proBNP—change	3.5	2.0–6.0	<0.00001	3.0	1.5–6.2	0.003

CI = confidence interval; HR = hazard ratio; log = decadic logarithm; for other abbreviations see the Table 1.

https://doi.org/10.1371/journal.pone.0219966.t002

future clinical events. Their predictive power was independent, and their combination improved the risk stratification of CRT patients. Another important finding was that the 12-month level of NT-proBNP appeared to be a significantly stronger outcome predictor than its change post-implantation. Conversely, the predictive power of echocardiographic indices (LVESd and LVEF) was comparable for both absolute 12-month values and relative change.

It has been previously demonstrated that uneventful survival of CRT patients is tightly associated with echocardiographic response, and responders have a better prognosis overall [10–17]. It has also been shown that there is considerable disagreement between clinical (NYHA-based) and echocardiographic CRT response [18,19] suggesting that their combination could potentially result in a stronger composite risk predictor. On the other hand, only a single study

Table 3. Univariate association between individual factors and clinical events (cardiac and all-cause mortality).

	Cardiac death N = 61			All-cause death N = 111		
	HR	95% CI	P-value	HR	95% CI	P-value
Male gender (1/0)	2.0	0.98–4.0	0.06	1.5	0.91–2.4	0.11
Age (years)	1.03	1.00–1.1	0.04	1.04	1.02–1.1	0.0004
Ischemic cardiomyopathy (1/0)	2.6	1.5–4.6	0.001	2.3	1.5–3.5	0.00008
Non-left bundle branch block (1/0)	1.4	0.75–2.5	0.31	1.3	0.83–2.1	0.25
Atrial fibrillation (1/0)	0.87	0.41–1.8	0.71	1.2	0.73–2.0	0.49
Left atrium diameter (mm)	1.1	1.1–1.2	<0.00001	1.1	1.04–1.1	0.00001
Creatinine (μmol/L)	1.01	1.00–1.01	0.001	1.00	1.00–1.01	0.002
Biventricular pacemaker only (1/0)	1.3	0.76–2.2	0.34	1.2	0.78–1.8	0.44
Q-LV (ms)	0.99	0.99–1.00	0.17	1.00	0.99–1.00	0.50
Q-LV ratio	0.15	0.03–0.76	0.02	0.33	0.09–1.1	0.08
Biventricular capture (%)	0.91	0.87–0.95	0.00003	0.93	0.90–0.97	0.0001
QRS duration—baseline (ms)	1.00	0.99–1.02	0.53	1.01	1.00–1.02	0.22
QRS duration—post-CRT (ms)	1.00	0.99–1.02	0.79	1.01	1.00–1.02	0.20
QRS duration—relative change (%)	1.00	0.98–1.02	0.73	1.00	0.99–1.02	0.98
NYHA Class—baseline (2/3/4)	1.6	0.98–2.6	0.06	1.1	0.80–1.7	0.46
NYHA Class—month 12 (2/3/4)	1.9	1.3–2.6	0.0002	1.7	1.3–2.1	0.0001
NYHA Class—change	1.5	1.02–2.1	0.04	1.5	1.2–2.0	0.002
LV ejection fraction—baseline (%)	0.98	0.93–1.02	0.33	1.00	0.96–1.03	0.94
LV ejection fraction—month 12 (%)	0.94	0.92–0.96	<0.00001	0.97	0.95–0.98	<0.00001
LV ejection fraction—relative change (%)	0.98	0.98–0.99	<0.00001	0.99	0.99–0.99	<0.00001
LV end-diastolic diameter—baseline (mm)	1.02	0.98–1.1	0.41	1.01	0.98–1.04	0.42
LV end-diastolic diameter—month 12 (mm)	1.1	1.04–1.1	<0.00001	1.05	1.03–1.1	0.00001
LV end-diastolic diameter—relative change (%)	1.1	1.1–1.1	<0.00001	1.1	1.04–1.1	<0.00001
LV end-systolic diameter—baseline (mm)	1.01	0.98–1.04	0.51	1.01	0.99–1.03	0.44
LV end-systolic diameter—month 12 (mm)	1.1	1.03–1.1	<0.00001	1.04	1.02–1.1	<0.00001
LV end-systolic diameter—relative change (%)	1.1	1.04–1.1	<0.00001	1.04	1.02–1.1	<0.00001
Mitral regurgitation—baseline (1/2/3/4)	1.03	0.81–1.3	0.81	1.1	0.89–1.3	0.46
Mitral regurgitation—month 12 (1/2/3/4)	1.6	1.2–2.1	0.0003	1.4	1.2–1.8	0.0004
Mitral regurgitation—change	1.4	1.05–2.0	0.03	1.2	0.96–1.5	0.10
NT-proBNP—baseline (log ng/L)	3.4	1.9–6.1	0.00003	2.6	1.7–4.1	<0.00001
NT-proBNP—month 12 (log ng/L)	6.6	3.9–11.2	<0.00001	4.7	3.2–7.0	<0.00001
NT-proBNP—change	3.2	1.7–6.0	0.0002	2.7	1.7–4.3	0.00002

CI = confidence interval; HR = hazard ratio; log = decadic logarithm; for other abbreviations see the Table 1.

https://doi.org/10.1371/journal.pone.0219966.t003

confirmed the independent predictive power of post-CRT improvement in NYHA class [15], while other studies on the predictive value of clinical CRT response were either negative [10,12] or confirmed that this association was not significant in multivariate analysis when the echocardiographic CRT response was considered [14]. Similarly, our study did not confirm the utility of NYHA class change when adjusted for other predictors.

Having in mind the subjective nature of the assessment of clinical CRT response (without systematic use of 6 minute walking test or a quality life questionnaire in daily practice), natriuretic peptide levels have been suggested for the monitoring of CRT patients in numerous small studies with short follow up [20–27]. Arrigo et al. [28] found that low circulating mid-regional-pro-atrial natriuretic peptide at the time of device implantation is associated with

Table 4. Multivariate predictors of clinical events.

	Heart failure hospitalization N = 82			Heart failure death N = 45			Cardiac death N = 61			All-cause death N = 111		
	Chi-square = 74.6			Chi-square = 64.3			Chi-square = 80.0			Chi-square = 92.2		
	R = 0.37, P <0.0001			R = 0.36, P <0.0001			R = 0.42, P <0.0001			R = 0.47, P <0.0001		
	HR	95% CI	P-value	HR	95% CI	P-value	HR	95% CI	P-value	HR	95% CI	P-value
Age (years)										1.03	1.01–1.1	0.02
Ischemic cardiomyopathy (1/0)				2.5	1.2–4.9	0.01	2.3	1.3–4.1	0.005	2.0	1.3–3.0	0.002
Left atrium diameter (mm)				1.1	1.01–1.1	0.01	1.1	1.01–1.1	0.02	1.04	1.00–1.1	0.04
Biventricular capture (%)										0.96	0.93–1.00	0.045
NYHA Class—baseline (2/3/4)	1.8	1.2–2.7	0.008									
LV ejection fraction—month 12 (%)	0.97	0.95–0.99	0.002									
LV ejection fraction—relative change (%)										1.00	0.99–1.00	0.03
LV end-systolic diameter—relative change (%)				1.05	1.02–1.1	0.0002	1.04	1.02–1.1	0.0005			
Mitral regurgitation—change	1.7	1.3–2.2	0.0001									
NT-proBNP—month 12 (log ng/L)	3.6	2.1–6.2	<0.00001	3.6	1.7–7.7	0.0009	4.6	2.4–8.6	<0.00001	3.3	2.1–5.3	<0.00001

Results are provided only for factors that were significantly associated with at least one clinical endpoint. HR = hazard ratio; CI = confidence interval; log = decadic logarithm; for other abbreviations see the Table 1.

https://doi.org/10.1371/journal.pone.0219966.t004

CRT response and more favorable outcome. An analysis of the CARE-HF study [29] showed that CRT exerts an early and sustained reduction in NT-proBNP [30] and that patients with more severe mitral regurgitation or persistently elevated NT-proBNP despite adequate treatment of heart failure have a higher mortality [31]. In the CRT arm of the MADIT-CRT trial [3], patients in whom 1-year BNP levels were reduced or remained low experienced a significantly lower risk of subsequent HF or death as compared with patients in whom 1-year BNP levels were high [32].

In a study by Hoogslag et al. [33], a left ventricular end-systolic volume (LVESV) and NT-proBNP reduction ≥15% independently predicted the clinical outcome. Bakos et al. [34] proposed a composite score consisting of clinical, echocardiographic (LVESV reduction ≥15%) and humoral response (NT-proBNP reduction ≥25%), which predicted the combined endpoint of mortality and HF events.

In the present study, we did not find any significant value of the clinical response for the prediction of post-CRT risk, whereas the combination of echocardiographic and humoral markers was particularly useful to refine the risk stratification in this context. Indeed, the most divergent survival curves were found for dual responders compared to dual nonresponders. More importantly, our study questioned the utility of relative post-CRT change of individual

Table 5. Receiver-operating characteristics: Comparison of areas under the curve.

	LV ejection fraction			LV end-systolic diameter			NT-proBNP		
	12-month value	relative change	P	12-month value	relative change	P	12-month value	relative change	P
Heart failure hospitalization	0.68±0.05	0.63±0.05	0.34	0.65±0.01	0.66±0.05	0.81	0.68±0.05	0.63±0.05	0.27
Heart failure death	0.75±0.03	0.71±0.05	0.54	0.72±0.03	0.74±0.05	0.57	0.72±0.12	0.59±0.06	0.03
Cardiac death	0.71±0.01	0.70±0.05	0.88	0.68±0.03	0.72±0.05	0.48	0.75±0.14	0.61±0.05	0.006
All-cause death	0.65±0.01	0.63±0.05	0.79	0.65±0.01	0.66±0.04	0.84	0.75±0.12	0.63±0.04	0.005

The values are areas under the curve ± standard error. For abbreviations see the Table 1.

https://doi.org/10.1371/journal.pone.0219966.t005

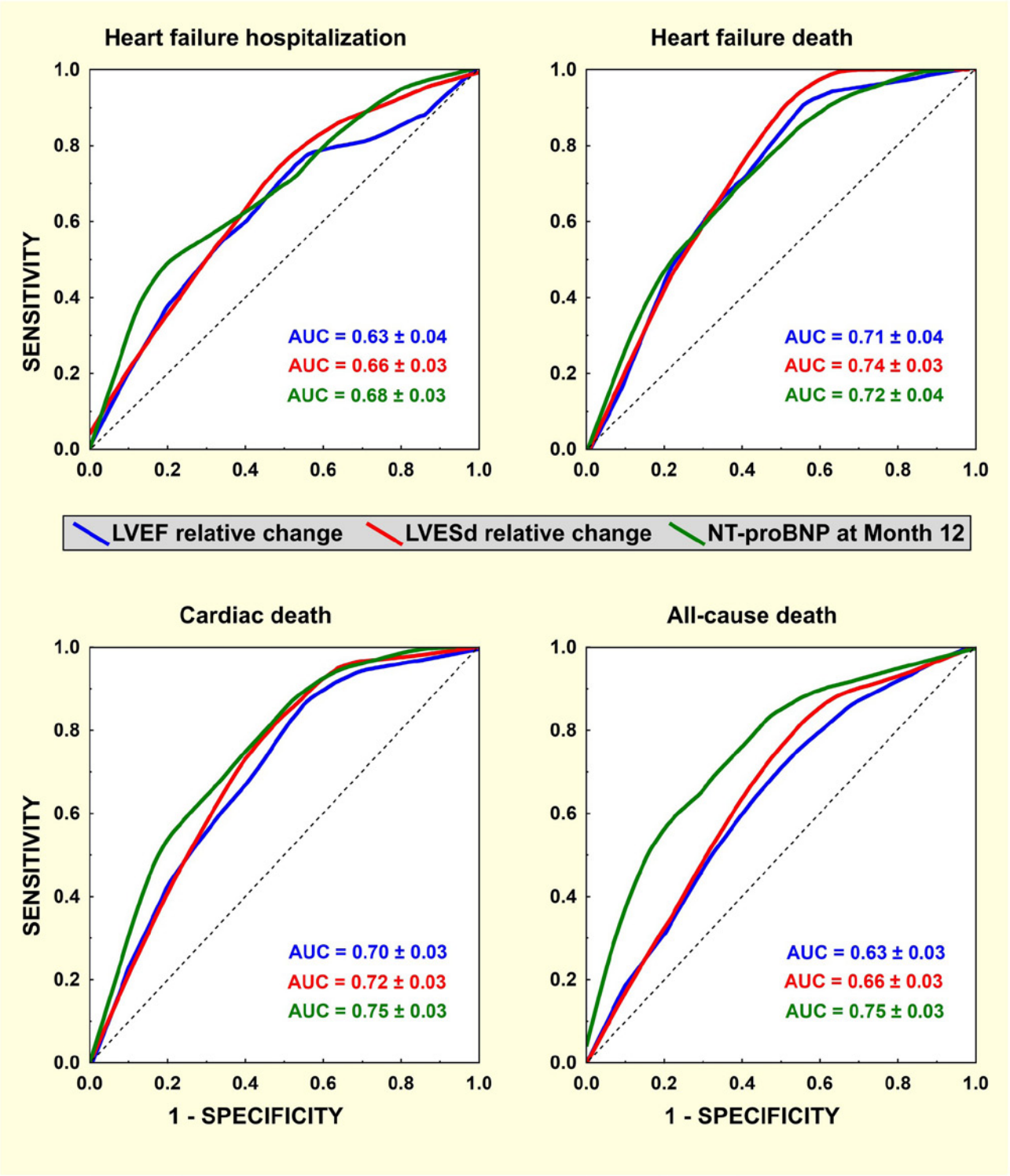

Fig 1. Receiver-operating characteristics for 12-month response to CRT and clinical events. Receiver-operating curves for post-CRT relative change in LV ejection fraction (LVEF, blue), end-systolic diameter (LVESd, red) and 12-month NT-proBNP level (green) and subsequent clinical events (heart failure hospitalization / death and cardiac/ all-cause death). The curves were obtained by locally weighted scatterplot smoothing. Areas under the curve with standard error are shown inside the graphs.

https://doi.org/10.1371/journal.pone.0219966.g001

Table 6. Receiver-operating characteristics: Optimum cut-off values.

	LV ejection fraction (relative change)			LV end-systolic diameter (relative change)			NT-proBNP (at Month 12)		
	Cut-off value	Sensitivity	Specificity	Cut-off value	Sensitivity	Specificity	Cut-off value	Sensitivity	Specificity
Heart failure hospitalization	+33.3%	60%	63%	-12.7%	68%	58%	1170 ng/L	61%	65%
Heart failure death	+33.3%	73%	62%	-12.3%	84%	58%	1184 ng/L	69%	63%
Cardiac death	+34.5%	69%	63%	-12.3%	79%	59%	1230 ng/L	69%	67%
All-cause death	+34.8%	59%	64%	-13.2%	69%	58%	1289 ng/L	63%	75%

Optimum cut-off values were defined by the point with the shortest distance from the [0,1]-point of the receiver-operating graph. For abbreviations see the Table 1.

https://doi.org/10.1371/journal.pone.0219966.t006

markers for the prediction of subsequent clinical outcome, suggesting that the absolute 12-month values of individual indices are equally predictive (or even better predictive in the case of NT-proBNP) when compared to the post-CRT change. Such observation appears logically sound, as the post-CRT change is more applicable for the assessment (or comparison) of early treatment effects, while the 12-month state may be more relevant for subsequent clinical

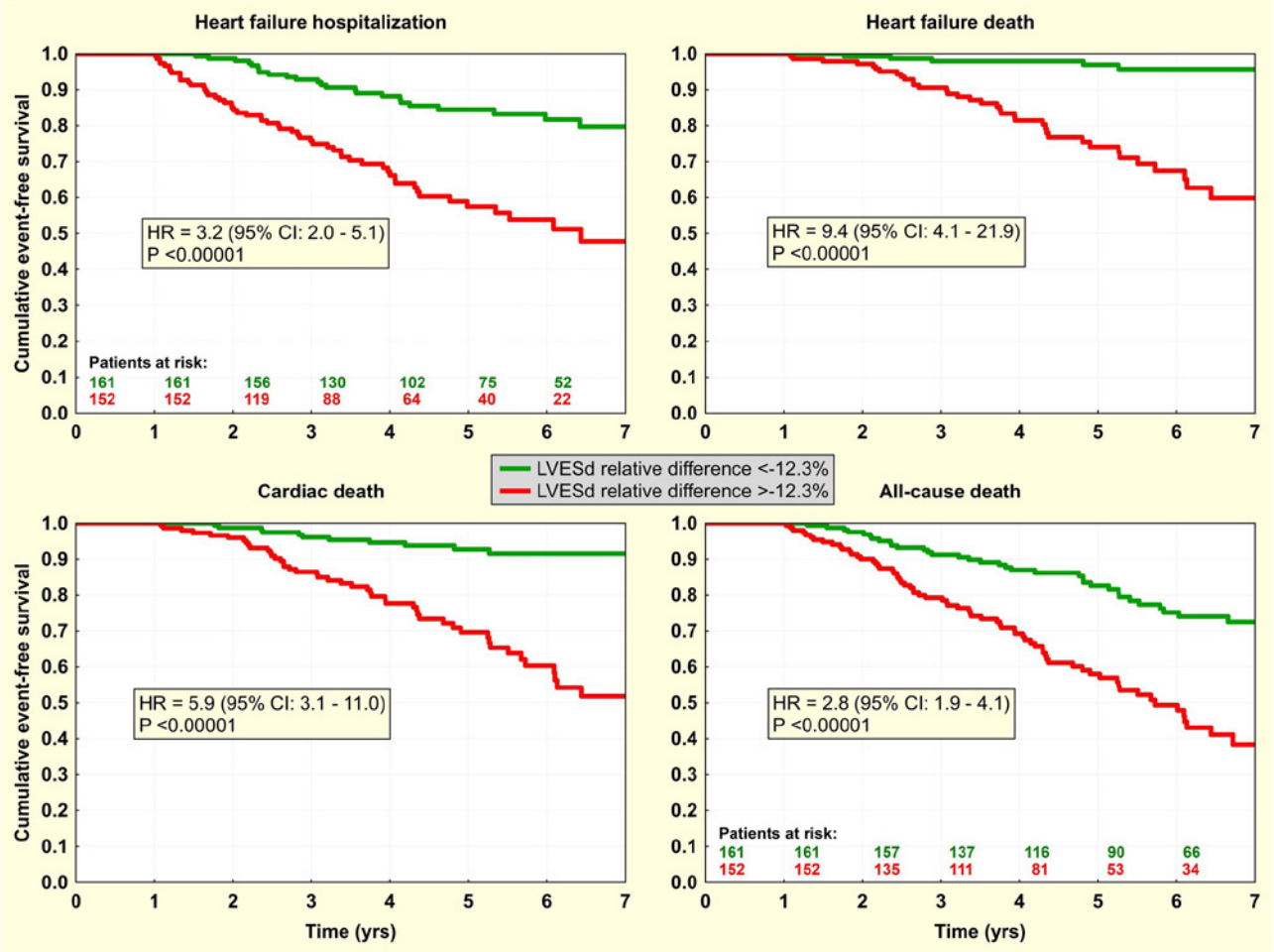

Fig 2. Event-free survival according to post-CRT reverse left ventricular remodeling. Kaplan-Meier curves for the first heart failure hospitalization / death and cardiac / all-cause death according to relative change in left ventricle end-systolic diameter (LVESd) with dichotomy of -12.3% relative change.

https://doi.org/10.1371/journal.pone.0219966.g002

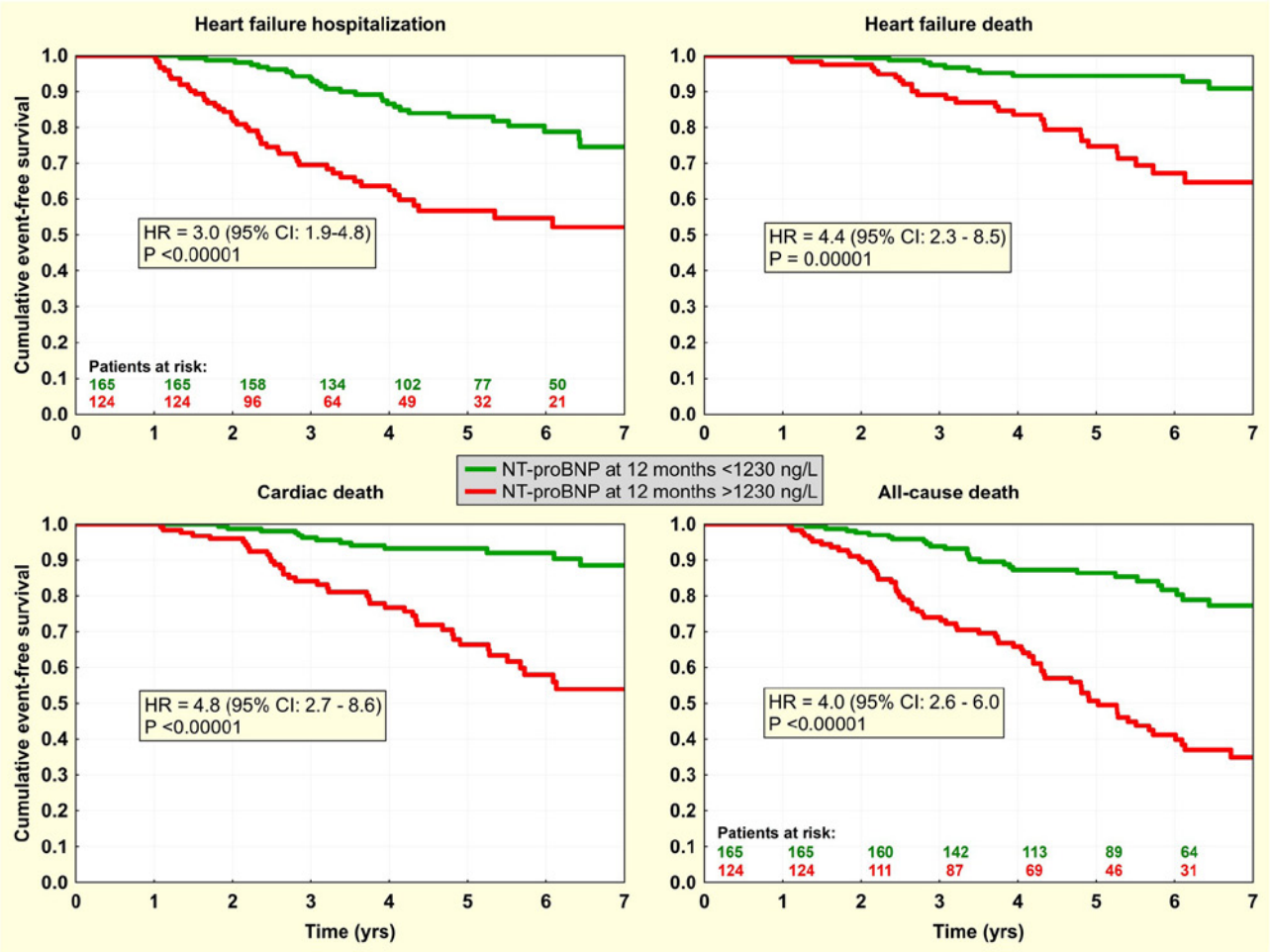

Fig 3. Event-free survival according to post-CRT level of NT-proBNP. Kaplan-Meier curves for the first heart failure hospitalization / death and cardiac / all-cause death according to 12-month NT-proBNP level with dichotomy of 1230 ng/L.

https://doi.org/10.1371/journal.pone.0219966.g003

outcome than any baseline conditions or CRT-induced improvement. The confirmation of these findings with retrospective analyses of randomized studies could provide valuable insight into this matter.

The incidence of sudden death was low in our study (4.1%) which precluded reliable risk stratification. Therefore, corresponding data were not presented as for other study endpoints. The risk of sudden death was higher in CRT-P recipients. However, CRT-P patients were significantly older, had significantly more comorbidities and significantly higher non-sudden mortality. In multivariate analysis, only elevated NT-proBNP was associated with sudden death while absence of ICD was not significant risk factor.

Study implications

This study expands on the current knowledge on the impact of early response to CRT implantation on subsequent clinical events. Clinical response was the weakest predictor of long-term outcome and should be used only when other objective measures are not available. The combination of echocardiographic and humoral response improved the identification of patients at risk. Such patients may benefit from escalated HF therapy, CRT optimization or

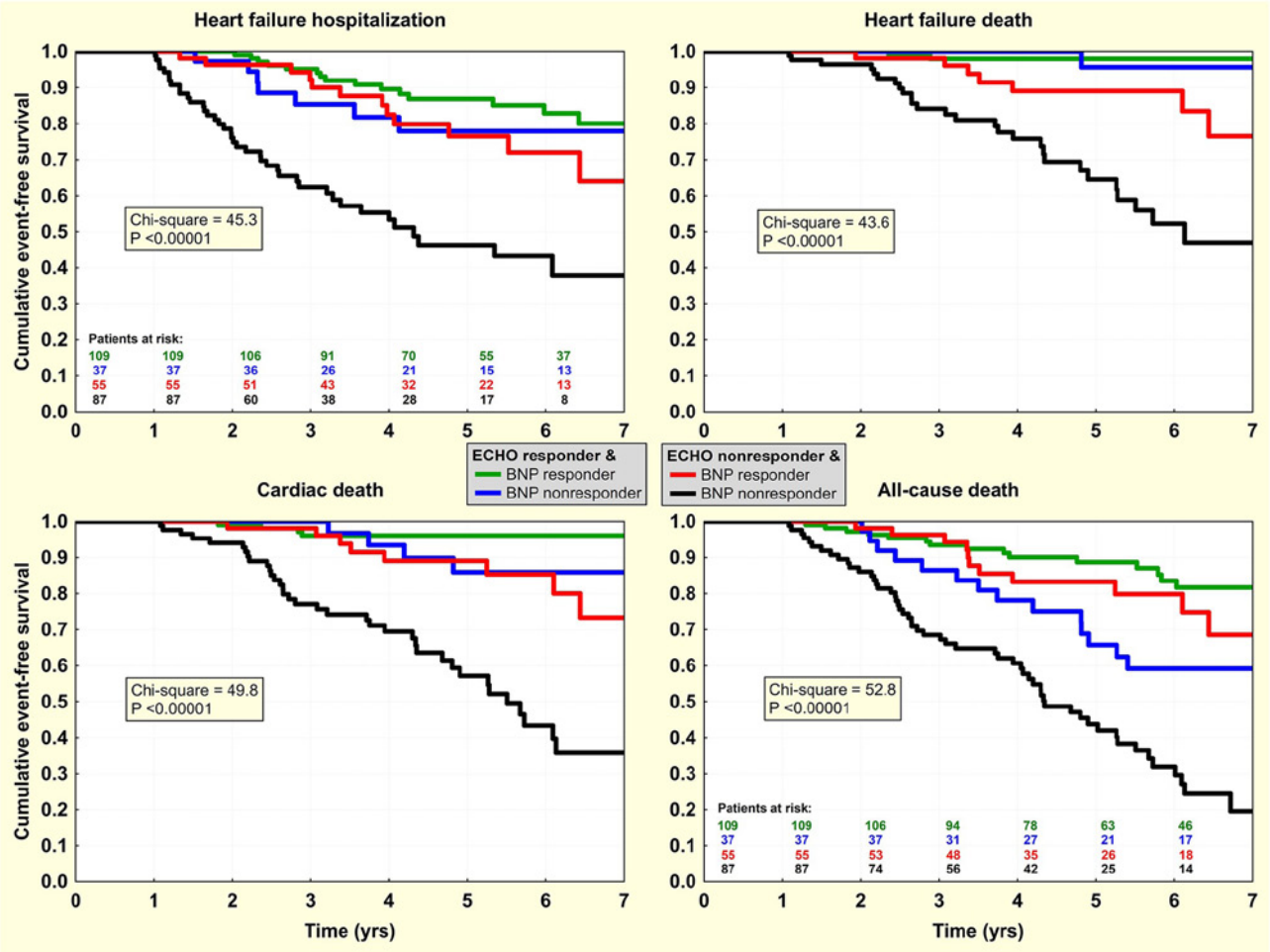

Fig 4. Event-free survival in 4 categories of post-CRT response. Kaplan-Meier curves for the first heart failure hospitalization / death and cardiac / all-cause death according to „ECHO response"(LVESd relative change <-12.3%) and „BNP response"(NT-proBNP <1230 ng/L at Month 12 after CRT).

https://doi.org/10.1371/journal.pone.0219966.g004

reintervention including LV lead reimplant (either transvenously, endocardially or surgically), or the use of multipoint/multisite pacing. Despite the combination of risk factor, their overall predictive power for clinical events is, however, relatively modest and of limited practical utility.

Study limitations

Although the data in our CRT database were collected prospectively, the hypotheses were defined post-hoc and data analyzed retrospectively. Therefore, the results should be interpreted with caution. The cut-off values for risk prediction may not be applicable to different patient populations. Furthermore, the usefulness of the different risk predictors may have been overestimated as cut-off values were optimized for our single-center population. The relative low number of events (especially mortality) found in the study could possibly affect the statistical power of regressions analysis including several variables and subgroups of patients. Finally, we used LVESd as an index of LV reverse remodeling instead of LVESV. However, the lower accuracy of LVESd compared to LVESV may be compensated by its higher reproducibility and ease of access.

Conclusions

Absence of both echocardiographic and humoral response one year after the CRT implant identifies patients at the highest risk of heart failure progression and death. Such patients are good candidates for advanced HF management.

Supporting information

S1 Table. Comparison of baseline and 12-month characteristics in subgroups according to clinical events (hospitalization and death due to heart failure). The values are percentage or mean ± standard deviation. NS = not significant; for other abbreviations see the Table 1.
(DOCX)

S2 Table. Comparison of baseline and 12-month characteristics in subgroups according to clinical events (cardiac and all-cause death). The values are percentage or mean ± standard deviation. NS = not significant; for other abbreviations see the Table 1.
(DOCX)

Author Contributions

Conceptualization: Tomas Roubicek, Jan Cerny, Rostislav Polasek.

Data curation: Tomas Roubicek, Jan Stros, Pavel Nedbal, Rostislav Polasek, Dan Wichterle.

Formal analysis: Dan Wichterle.

Investigation: Tomas Roubicek, Pavel Kucera.

Methodology: Tomas Roubicek, Pavel Nedbal, Dan Wichterle.

Project administration: Jan Stros.

Supervision: Rostislav Polasek.

Validation: Pavel Kucera.

Writing – original draft: Tomas Roubicek, Jan Cerny, Dan Wichterle.

Writing – review & editing: Rostislav Polasek.

References

1. Abraham WT, Fisher WG, Smith AL, Delurgio DB, Leon AR, Loh E, et al. Cardiac resynchronization in chronic heart failure. N Engl J Med. 2002; 346: 1845–1853. https://doi.org/10.1056/NEJMoa013168 PMID: 12063368
2. Bristow MR, Saxon LA, Boehmer J, Krueger S, Kass DA, De Marco T, et al. Cardiac-resynchronization therapy with or without an implantable defibrillator in advanced chronic heart failure. N Engl J Med. 2004; 350: 2140–50. https://doi.org/10.1056/NEJMoa032423 PMID: 15152059
3. Moss AJ, Hall WJ, Cannom DS, Klein H, Brown MW, Daubert JP, et al. Cardiac-Resynchronization Therapy for the Prevention of Heart-Failure Events. N Engl J Med. 2009; 361: 1329–1338. https://doi.org/10.1056/NEJMoa0906431 PMID: 19723701
4. Birnie DH, Tang AS. The problem of non-response to cardiac resynchronization therapy. Curr Opin Cardiol. 2006; 21: 20–26. https://doi.org/10.1097/01.hco.0000198983.93755.99 PMID: 16355025
5. Roubicek T, Wichterle D, Kucera P, Nedbal P, Kupec J, Sedlakova J, et al. Left Ventricular Lead Electrical Delay Is a Predictor of Mortality in Patients with Cardiac Resynchronization Therapy. Circ Arrhythmia Electrophysiol. 2015; 8: 1113–21. https://doi.org/10.1161/CIRCEP.115.003004 PMID: 26338831
6. Ponikowski P, Voors AA, Anker SD, Bueno H, Cleland JGF, Coats AJS, et al. 2016 ESC Guidelines for the diagnosis and treatment of acute and chronic heart failure. Eur Heart J. 2016; 37: 2129–2200. https://doi.org/10.1093/eurheartj/ehw128 PMID: 27206819

7. Strauss DG, Selvester RH, Wagner GS. Defining Left Bundle Branch Block in the Era of Cardiac Resynchronization Therapy. Am J Cardiol. 2011; 107: 927–934. https://doi.org/10.1016/j.amjcard.2010.11.010 PMID: 21376930
8. Wang TJ. Assessing the Role of Circulating, Genetic, and Imaging Biomarkers in Cardiovascular Risk Prediction. Circulation. 2011; 123: 551–565. https://doi.org/10.1161/CIRCULATIONAHA.109.912568 PMID: 21300963
9. Goksuluk D, Korkmaz S, Zararsiz GKA. EasyROC: An interactive web-tool for ROC curve analysis using R language environment. R J. 2016; 8: 213–230.
10. Yu CM, Bleeker GB, Fung JW, Schalij MJ, Zhang Q, van der Wall EE, et al. Left ventricular reverse remodeling but not clinical improvement predicts long-term survival after cardiac resynchronization therapy. Circulation. 2005; 112: 1580–1586. https://doi.org/10.1161/CIRCULATIONAHA.105.538272 PMID: 16144994
11. Solomon SD, Foster E, Bourgoun M, Shah A, Viloria E, Brown MW, et al. Effect of Cardiac Resynchronization Therapy on Reverse Remodeling and Relation to Outcome: Multicenter Automatic Defibrillator Implantation Trial: Cardiac Resynchronization Therapy. Circulation. 2010; 122: 985–992. https://doi.org/10.1161/CIRCULATIONAHA.110.955039 PMID: 20733097
12. Foley PW, Chalil S, Khadjooi K, Irwin N, Smith RE, Leyva F. Left ventricular reverse remodelling, long-term clinical outcome, and mode of death after cardiac resynchronization therapy. Eur J Hear Fail. 2011; 13: 43–51. https://doi.org/10.1093/eurjhf/hfq182 PMID: 21051462
13. Park JH, Negishi K, Grimm RA, Popovic Z, Stanton T, Wilkoff BL, et al. Echocardiographic predictors of reverse remodeling after cardiac resynchronization therapy and subsequent events. Circ Cardiovasc Imaging. 2013; 6: 864–72. https://doi.org/10.1161/CIRCIMAGING.112.000026 PMID: 24084489
14. Bertini M, Höke U, van Bommel RJ, Ng ACT, Shanks M, Nucifora G, et al. Impact of clinical and echocardiographic response to cardiac resynchronization therapy on long-term survival. Eur Heart J Cardiovasc Imaging. 2013; 14: 774–81. https://doi.org/10.1093/ehjci/jes290 PMID: 23221312
15. Boidol J, Średniawa B, Kowalski O, Szulik M, Mazurek M, Sokal A, et al. Many response criteria are poor predictors of outcomes after cardiac resynchronization therapy: validation using data from the randomized trial. Europace. 2013; 15: 835–44. https://doi.org/10.1093/europace/eus390 PMID: 23487543
16. Gold MR, Daubert C, Abraham WT, Ghio S, St. John Sutton M, Hudnall JH, et al. The effect of reverse remodeling on long-term survival in mildly symptomatic patients with heart failure receiving cardiac resynchronization therapy: Results of the REVERSE study. Heart Rhythm. 2015; 12: 524–530. https://doi.org/10.1016/j.hrthm.2014.11.014 PMID: 25460860
17. Menet A, Guyomar Y, Ennezat P-V, Graux P, Castel AL, Delelis F, et al. Prognostic value of left ventricular reverse remodeling and performance improvement after cardiac resynchronization therapy: A prospective study. Int J Cardiol. 2016; 204: 6–11. https://doi.org/10.1016/j.ijcard.2015.11.091 PMID: 26649446
18. Fornwalt BK, Sprague WW, Bedell P, Suever JD, Gerritse B, Merlino JD, et al. Agreement is poor among current criteria used to define response to cardiac resynchronization therapy. Circulation. 2010; 121: 1985–91. https://doi.org/10.1161/CIRCULATIONAHA.109.910778 PMID: 20421518
19. Auger D, Van Bommel RJ, Bertini M, Delgado V, Ng ACT, Ewe SH, et al. Prevalence and characteristics of patients with clinical improvement but not significant left ventricular reverse remodeling after cardiac resynchronization therapy. Am Heart J. 2010; 160: 737–743. https://doi.org/10.1016/j.ahj.2010.07.016 PMID: 20934569
20. Sinha AM, Filzmaier K, Breithardt OA, Kunz D, Graf J, Markus KU, et al. Usefulness of brain natriuretic peptide release as a surrogate marker of the efficacy of long-term cardiac resynchronization therapy in patients with heart failure. Am J Cardiol. 2003; 91: 755–758. https://doi.org/10.1016/s0002-9149(02)03425-2 PMID: 12633819
21. Molhoek SG, Bax JJ, vanErven L, Bootsma M, Steendijk P, Lentjes E, et al. Atrial and brain natriuretic peptides as markers of response to resynchronisation therapy. Heart. 2004; 90: 97–98. https://doi.org/10.1136/heart.90.1.97 PMID: 14676258
22. Erol-Yilmaz A, Verberne HJ, Schrama TA, Hrudova J, De Winter RJ, Van Eck-Smit BLF, et al. Cardiac resynchronization induces favorable neurohumoral changes. PACE—Pacing Clin Electrophysiol. 2005; 28: 304–310. https://doi.org/10.1111/j.1540-8159.2005.09508.x PMID: 15826264
23. Yu C-M, Fung JW-H, Zhang Q, Chan C-K, Chan I, Chan Y-S, et al. Improvement of Serum NT-ProBNP Predicts Improvement in Cardiac Function and Favorable Prognosis After Cardiac Resynchronization Therapy for Heart Failure. J Card Fail. 2005; 11(5 Suppl): S42–46. https://doi.org/10.1016/j.cardfail.2005.04.007 PMID: 15948100
24. Kubanek M, Malek I, Bytesnik J, Fridl P, Riedlbauchova L, Karasova L, et al. Decrease in plasma B-type natriuretic peptide early after initiation of cardiac resynchronization therapy predicts clinical

improvement at 12 months. Eur J Hear Fail. 2006; 8: 832–840. https://doi.org/10.1016/j.ejheart.2006.02.006 PMID: 16546444

25. Pitzalis MV, Iacoviello M, Di Serio F, Romito R, Guida P, De Tommasi E, et al. Prognostic value of brain natriuretic peptide in the management of patients receiving cardiac resynchronization therapy. Eur J Heart Fail. 2006; 8: 509–514. https://doi.org/10.1016/j.ejheart.2005.10.013 PMID: 16503416

26. Delgado RM, Palanichamy N, Radovancevic R, Vrtovec B, Radovancevic B. Brain natriuretic peptide levels and response to cardiac resynchronization therapy in heart failure patients. Congest Hear Fail. 2006; 12: 250–253. https://doi.org/10.1111/j.1527-5299.2006.05469.x

27. Magne J, Dubois M, Champagne J, Dumesnil JG, Pibarot P, Philippon F, et al. Usefulness of NT-pro BNP monitoring to identify echocardiographic responders following cardiac resynchronization therapy. Cardiovasc Ultrasound. 2009; 7: 39. https://doi.org/10.1186/1476-7120-7-39 PMID: 19695099

28. Arrigo M, Truong QA, Szymonifka J, Rivas-Lasarte M, Tolppanen H, Sadoune M, et al. Mid-regional pro-atrial natriuretic peptide to predict clinical course in heart failure patients undergoing cardiac resynchronization therapy. EP Eur. 2017; 19: 1848–1854. https://doi.org/10.1093/europace/euw305 PMID: 28096288

29. Cleland JGF, Daubert J-C, Erdmann E, Freemantle N, Gras D, Kappenberger L, et al. The effect of cardiac resynchronization on morbidity and mortality in heart failure. N Engl J Med. 2005; 352:1539–1549. https://doi.org/10.1056/NEJMoa050496 PMID: 15753115

30. Fruhwald FM, Fahrleitner-Pammer A, Berger R, Leyva F, Freemantle N, Erdmann E, et al. Early and sustained effects of cardiac resynchronization therapy on N-terminal pro-B-type natriuretic peptide in patients with moderate to severe heart failure and cardiac dyssynchrony. Eur Heart J. 2007; 28: 1592–1597. https://doi.org/10.1093/eurheartj/ehl505 PMID: 17298973

31. Cleland J, Freemantle N, Ghio S, Fruhwald F, Shankar A, Marijanowski M, et al. Predicting the long-term effects of cardiac resynchronization therapy on mortality from baseline variables and the early response a report from the CARE-HF (Cardiac Resynchronization in Heart Failure) Trial. J Am Coll Cardiol. 2008; 52: 438–45. https://doi.org/10.1016/j.jacc.2008.04.036 PMID: 18672164

32. Brenyo A, Barsheshet A, Rao M, Huang DT, Zareba W, McNitt S, et al. Brain natriuretic peptide and cardiac resynchronization therapy in patients with mildly symptomatic heart failure. Circ Hear Fail. 2013; 6: 998–1004. https://doi.org/10.1161/CIRCHEARTFAILURE.112.000174 PMID: 23801020

33. Hoogslag GE, Höke U, Thijssen J, Auger D, Marsan NA, Wolterbeek R, et al. Clinical, echocardiographic, and neurohormonal response to cardiac resynchronization therapy: are they interchangeable? Pacing Clin Electrophysiol. 2013: 11: 1391–401. https://doi.org/10.1111/pace.12214 PMID: 23826659

34. Bakos Z, Chatterjee NC, Reitan C, Singh JP, Borgquist R. Prediction of clinical outcome in patients treated with cardiac resynchronization therapy—the role of NT-ProBNP and a combined response score. BMC Cardiovasc Disord. 2018; 18:70. https://doi.org/10.1186/s12872-018-0802-8 PMID: 29699498

M. Hromádka a kol.

Prognostic Value of MicroRNAs in Patients after Myocardial *(id 1333)*

Desease Markers
Impact Factor: 2,76

rejstřík

Research Article

Prognostic Value of MicroRNAs in Patients after Myocardial Infarction: A Substudy of PRAGUE-18

M. Hromádka,[1] V. Černá,[2] M. Pešta,[2] A. Kučerová,[2] J. Jarkovský,[3] D. Rajdl,[4] R. Rokyta,[1] and Z. Moťovská[5]

[1]*Department of Cardiology, University Hospital and Faculty of Medicine of Charles University, Pilsen, Czech Republic*
[2]*Department of Biology, Faculty of Medicine in Pilsen, Charles University, Czech Republic*
[3]*Institute of Biostatistics and Analyses, Faculty of Medicine and the Faculty of Science, Masaryk University, Brno, Czech Republic*
[4]*Department of Clinical Biochemistry and Hematology, University Hospital and Faculty of Medicine in Pilsen, Czech Republic*
[5]*Cardiocentre, Third Faculty of Medicine, Charles University and University Hospital Kralovske Vinohrady, Prague, Czech Republic*

Correspondence should be addressed to V. Černá; vaclava.cerna@lfp.cuni.cz

Received 8 April 2019; Revised 15 August 2019; Accepted 5 September 2019; Published 3 November 2019

Guest Editor: Ioana Mozos

Background. The evaluation of the long-term risk of major adverse cardiovascular events and cardiac death in patients after acute myocardial infarction (AMI) is an established clinical process. Laboratory markers may significantly help with the risk stratification of these patients. Our objective was to find the relation of selected microRNAs to the standard markers of AMI and determine if these microRNAs can be used to identify patients at increased risk. *Methods*. Selected microRNAs (miR-1, miR-133a, and miR-499) were measured in a cohort of 122 patients from the PRAGUE-18 study (ticagrelor vs. prasugrel in AMI treated with primary percutaneous coronary intervention (pPCI)). The cohort was split into two subgroups: 116 patients who did not die (survivors) and 6 patients who died (nonsurvivors) during the 365-day period after AMI. Plasma levels of selected circulating miRNAs were then assessed in combination with high-sensitivity cardiac troponin T (hsTnT) and N-terminal probrain natriuretic peptide (NT-proBNP). *Results*. miR-1, miR-133a, and miR-499 correlated positively with NT-proBNP and hsTnT 24 hours after admission and negatively with left ventricular ejection fraction (LVEF). Both miR-1 and miR-133a positively correlated with hsTnT at admission. Median relative levels of all selected miRNAs were higher in the subgroup of nonsurvivors ($N = 6$) in comparison with survivors ($N = 116$), but the difference did not reach statistical significance. All patients in the nonsurvivor subgroup had miR-499 and NT-proBNP levels above the cut-off values (891.5 ng/L for NT-proBNP and 0.088 for miR-499), whereas in the survivor subgroup, only 28.4% of patients were above the cut-off values ($p = 0.001$). *Conclusions*. Statistically significant correlation was found between miR-1, miR-133a, and miR-499 and hsTnT, NT-proBNP, and LVEF. In addition, this analysis suggests that plasma levels of circulating miR-499 could contribute to the identification of patients at increased risk of death during the first year after AMI, especially when combined with NT-proBNP levels.

1. Introduction

The in-hospital mortality rate for acute myocardial infarction is low, due to efficient antiplatelet treatment and primary percutaneous coronary intervention (pPCI); unfortunately, the risk of cardiac death increases during the chronic phase of ischemic heart disease that follows.

Decreased left ventricular systolic function with left ventricular ejection fraction (LVEF) ≤ 35% and recurrent ventricular tachycardia or ventricular fibrillation, beyond the early phase of myocardial infarction, are connected with a poor prognosis and are a potential indication for cardioverter implantation [1].

Despite the clear benefit of these widely used predictors, they seem to be inadequate for identifying all patients at risk of sudden death, since it fails to identify about 50% of patients who die suddenly [2] after acute myocardial infarction (AMI). Some of the standard laboratory markers associated

with the risk of sudden death can be used in combination with LVEF to improve the risk assessment process, but unfortunately, well-defined cut-off values are still not known.

Among factors that can be used for risk stratification after AMI, the following play an important role: elevated levels of troponin T or I (TnT or TnI) [3, 4] and a combination of (A) increased TnT and CRP plasma levels, (B) increased levels of N-terminal prohormone of brain natriuretic peptide (NT-proBNP) with LVEF < 40% [4–7], and (C) decreased clearance of creatinine (with a reduced LVEF) [8].

A promising group of new biomarkers, released from cells into circulation, is microRNAs (miRNAs), which are small noncoding RNA molecules, 20–22 nucleotides in length, involved in posttranscriptional regulation of gene expression. Mature miRNAs and Ago proteins (Argonaute proteins) form in the cytoplasm RISC complexes (RNA-induced silencing complexes) that interact with protein-coding mRNA molecules. This interaction usually leads to the inhibition of translation or directly to the degradation of mRNA molecules. One particular microRNA can regulate many genes (i.e., interacting with a variety of different protein-coding mRNAs), and one particular gene can be regulated by several different microRNAs. MicroRNAs can act directly within the cells where they are synthesized, or they can be exported, in complexes with proteins or in membrane-bound vesicles (exosomes or microvesicles), to other cells where they can also regulate gene expression. MicroRNAs are involved in the control of many processes in both healthy and infarcted myocardia, including proliferation, differentiation, apoptosis, repair, and revascularization [9]. Additionally, miRNA dysregulation has been strongly implicated in the destabilization and rupture of atherosclerotic plaques [10] as well as being involved in the process of myocardial recovery.

In cardiovascular diseases (CVD), the use of miRNAs as biomarkers for specific disease entities has been successfully investigated in numerous studies [11]. Nonetheless, it is not yet possible to use them in clinical practice [12]. miRNAs also have the potential for clinical use in CVD where protein biomarkers are not available.

More than 2500 mature miRNAs have been identified in humans. Four of them, miR-1, miR-133, miR-208a, and miR-499 have been found to be specific for the myocardium (or the myocardium and skeletal muscle) and are sometimes called "myomiRs" [13].

Many authors have shown that levels of circulating myomiRs increase significantly during the first few hours after the onset of myocardial infarction symptoms. After reaching a peak, myomiRs return to normal after a few hours or a few days [14, 15].

We decided to retrospectively measure the relative levels of circulating miR-1, miR-133a, miR-208a, and miR-499 in a well-described cohort of 122 patients with known one-year mortality, previously involved in the PRAGUE-18 study [16, 17]. The listed miRNAs were assessed alone and in combination with several standard markers in an effort to better characterize the nonsurvivor subgroup, with the goal of finding additional predictors of patients at increased risk of one-year cardiovascular death.

2. Material and Methods

2.1. Patients. The whole cohort of 122 patients was treated in the Department of Cardiology, University Hospital and Faculty of Medicine of Charles University, Pilsen, Czech Republic, which was one of the centers involved in phase IV of a multicenter, open-label, randomized, controlled clinical trial called the PRAGUE-18 study [16, 17].

The PRAGUE-18 study, which compared prasugrel and ticagrelor in the treatment of acute myocardial infarction, was the first randomized head-to-head comparison of these two active substances, with regard to efficacy and safety in patients after AMI undergoing pPCI. One of the outcomes was the combined endpoint of cardiovascular death, MI, or stroke within the first year. Prasugrel and ticagrelor had been similarly effective during the first year after AMI [16, 17]. Plasma samples from 122 patients in the study were used for this retrospective data analysis, where (I) levels of selected circulating microRNAs, (II) standard AMI biomarkers, and (III) LVEF were used to (A) look for correlations between miRNAs and standard AMI markers, (B) identify differences in biomarkers between survivors and nonsurvivors during the first year after AMI, and (C) better characterize the nonsurvivor subgroup relative to measures I, II, and III mentioned above.

2.2. Echocardiography. Two-dimensional, M-mode, and Doppler echocardiograms were acquired using an ultrasound system (Vivid 7, GE Medical Systems, Horton, Norway) using a 3.4 MHz multifrequency transducer. The systolic function of the left ventricle was determined according to the Simpson method from the apical 4-chamber view and the apical 2-chamber view (the biplane Simpson method).

2.3. Levels of Biomarkers. Data for the basic characteristics of all patients involved in the analysis were available from the PRAGUE-18 study. Levels of standard AMI biomarkers were known, including hsTnT, NT-proBNP, cystatin C, myoglobin, growth/differentiation factor 15 (GDF-15), and creatine kinase (CK) at patient admission and hsTnT also after 24 hours.

NT-proBNP was determined using the original analytical kits from Roche on a cobas® 8000 analyzer. NT-proBNP and high-sensitivity cardiac troponin were determined using the original analytical kits from Roche with the electrochemiluminiscence (ECLIA) principle on a cobas e602 analyzer. Imprecission of the hsTnT method on the 99th percentile was below 10% which is the required analytical performance specification. Growth/differentiation factor 15 (GDF-15) (RayBiotech, Norcross, USA) was determined using ELISA kits on a NEXgen Four ELISA reader (Adaltis, Rome, Italy).

Since hsTnT is the most frequently used standard biomarker of AMI and NT-proBNP is a sensitive marker of left ventricular dysfunction, we used them in combination with the potential new microRNA biomarkers, in subsequent analyses.

2.4. MicroRNA Analysis

2.4.1. RNA Isolation. MicroRNA was isolated from plasma samples taken 24 hours after admission (all patients were

already after pPCI at that time) and stored at −80°C. Total cell-free RNA was isolated from 200 μL of plasma using miRNeasy Serum/Plasma Kits (miRNeasy Serum/Plasma Kit (50), Cat no./ID 217184; Qiagen, Hilden, Germany) according to the manufacturer's instructions. Total RNA was eluted in 14 μL of ribonuclease-free water and stored at −80°C until further analyses. MicroRNA-39 (*C. elegans* miR-39) was used as the RNA spike-in control. A fixed volume of 1 μL of this RNA eluate was used for each reverse transcription reaction.

2.4.2. Quantitative Estimation of MicroRNA Expression. For reverse transcriptions and quantitative estimations of selected microRNAs using real-time PCR reactions, TaqMan® MicroRNA Assays and master mixes were used (catalogue number 4440887: hsa-miR-133a-3p—Assay ID 002246, hsa-miR-1-3p—Assay ID 002222, hsa-miR-499a-5p—Assay ID 001352, hsa-miR-208-3p—Assay ID 000511, and cel-miR-39-3p—Assay ID 000200; TaqMan Universal MMIX II: catalogue number 4440049; and TaqMan® MicroRNA RT Kit: catalogue number 4366597). A T100TM thermal cycler (Bio-Rad, California, United States) was used for reverse transcription. The reaction volume was 15 μL. A fixed volume of 2.5 μL from this RT reaction was used into each real-time PCR reaction. Due to either too high or absent Ct values, levels of miR-208a could not be quantified and evaluated.

2.4.3. Processing of Real-Time PCR Data. Samples were assessed in technical duplicate. The Ct values were corrected using calibrators to eliminate differences between individual runs of the Stratagene Mx3000P Real-Time PCR apparatus (Agilent Technologies, CA, United States). In cases where a disagreement between results obtained from both technical duplicates was found, the sample assessment was repeated. Plasma levels for each miRNA were calculated in the form of a relative expression. This relative expression was calculated using the ΔCt method (i.e., the $2^{-\Delta Ct}$ algorithm was $\Delta Ct = Ct_{miR-x} - Ct_{miR-39}$).

2.5. Objectives. Our objectives were to find relationships between selected miRNAs and the standard biomarkers of AMI as well as to find a panel of standard and potential biomarkers that might contribute to the identification of high-risk patients after acute myocardial infarction and post-pPCI treatment. The whole cohort was split according to the primary outcome (death within 365 days after AMI) into two subgroups (survivors and nonsurvivors), and both subgroups were characterized according to their biomarker levels.

2.6. Statistical Analysis. In this analysis, standard descriptive statistics were applied; absolute and relative frequencies were used for categorical variables and medians (supplemented with the 5th and 95th percentiles) were used for continuous variables (mean, SD, and CV were also used for the description of miRs). The statistical significance of differences among groups of patients was tested using Fisher's exact test for categorical variables and the Mann-Whitney test for continuous variables. The Spearman correlation coefficient was used for the analysis of the statistical relationship between miRNAs and the standard markers. Cut-off points (cut-off values) of predictors of all-cause death during 365 days were established by ROC analysis. The point that guarantees the greatest sum of sensitivity and specificity was chosen as the best point. Risk factors for all-cause death during 365 days were analyzed by a Cox regression model of proportional hazards. Analysis was performed in IBM SPSS Statistics 24.0 with 5% level of significance.

3. Results

3.1. Baseline Characteristics. The analysis involved 122 adult patients (78.7% men and 21.3% women) with AMI followed by pPCI; the median age was 61.1 years. All patients used either prasugrel (53.3%) or ticagrelor (46.7%) for antiplatelet therapy. The cohort of patients was split into two subgroups: nonsurvivors ($N = 6$) and survivors ($N = 116$). Only six patients died within one year after AMI (three patients from the prasugrel and three from the ticagrelor group): five died suddenly and one died while in the hospital from an unconfirmed diagnosis of pulmonary embolism. All patients in this subgroup had an LVEF ≥ 40% at their control visit, which was 2–3 months after discharge from the hospital. The baseline characteristics of all patients, and both subgroups, including their comparison, are shown in Table 1.

3.2. Correlation of miRNAs with Standard Biomarkers. The relative levels of all three miRNAs were related to the levels of standard biomarkers: hsTnT (at admission), hsTnT (24 hours after admission), NT-proBNP, GDF-15, cystatin C, and LVEF.

miR-133a and miR-1 weakly positively correlated with hsTnT at admission and strongly positively correlated with hsTnT 24 hours after admission (Figure 1). miR-499 moderately correlated with hsTnT 24 hours after admission. A strong negative correlation was found between all three miRNAs and the LVEF (Figure 1). A strong positive correlation was identified between both miR-133a and miR-499 and NT-proBNP, and a moderate positive correlation was found between miR-1 and NT-proBNP (Figure 1).

No correlation was found between any of the miRNAs and GDP-15 or cystatin C.

3.3. The Relationship between miRNAs and One-Year Mortality. The assessment of the prognostic potential of the selected biomarkers, for the identification of patients at increased risk of death, was based on their peripheral plasma levels and one-year survival.

Median relative levels of miRNAs were higher in the nonsurvivor subgroup. But the total number of patients in this subgroup was small in comparison with that in the group of survivors (six vs. one hundred and sixteen), and the differences found did not reach statistical significance for any of the tested microRNAs (Figure 2).

The calculated cut-off values for miR-1, miR-133a, and miR-499 were 0.031, 0.330, and 0.088, respectively. Relative miRNA concentrations below these cut-off values were described as "low," and those above the value were described as "high."

Table 1: Baseline characteristics.

	All patients	Survivors	Nonsurvivors	p values
	Median (5th-95th percentile)			
Number of patients	122	116	6	
Age (years)	61.1 (40.4–76.8)	61.1 (40.1–76.7)	65.7 (56.1–81.0)	0.166
Men (number, %)	96 (78.7%)	91 (78.4%)	5 (83.3%)	0.999
BMI	27.6 (22.2–34.3)	27.6 (22.1–34.3)	26.7 (24.7–44.1)	0.929
Drug used: prasugrel (number, %)	65 (53.3%)	62 (53.4%)	3 (50.0%)	0.999
Drug used: ticagrelor (number, %)	57 (46.7%)	54 (46.6%)	3 (50.0%)	
STEMI (number, %)	121 (99.2%)	115 (99.1%)	6 (100.0%)	0.999
Left bundle branch block (LBBB) (number, %)	1 (0.8%)	1 (0.9%)	0 (0.0%)	0.999
Right bundle branch block (RBBB) (number, %)	1 (0.8%)	1 (0.9%)	0 (0.0%)	0.999
Hyperlipidaemia (number, %)	36 (29.5%)	35 (30.2%)	1 (16.7%)	0.669
Obesity (number, %)	23 (18.9%)	22 (19.0%)	1 (16.7%)	0.999
Arterial hypertension (number, %)	56 (45.9%)	52 (44.8%)	4 (66.7%)	0.412
Smoking (number, %)	84 (68.9%)	80 (69.0%)	4 (66.7%)	0.999
Diabetes mellitus (number, %)	17 (13.9%)	16 (13.8%)	1 (16.7%)	0.999
Time since the first symptoms to admission (hours)	3.0 (0.5–36.0)	3.0 (0.5–12.0)	6.0 (3.0–72.0)	0.061
Left ventricular ejection fraction (%)	50.0 (30.0–60.0)	55.0 (30.0–60.0)	45.0 (30.0–50.0)	0.054
Laboratory values (median (5th-95th percentile))				
hsTnT (at admission) (ng/L)	86.0 (12.0–1325.0)	84.0 (12.0–1325.0)	201.5 (27.0–4978.0)	0.257
hsTnT (24 hours after admission) (ng/L)	2432.0 (377.0–9651.0)	2324.0 (368.0–9651.0)	4306.5 (1526.0–15114.0)	0.201
Myoglobin (at admission) (μg/L)	198.0 (30.0–1385.0)	176.0 (30.0–1547.0)	652.0 (161.0–1317.0)	0.066
Creatine kinase (at admission) (μkat/L)	3.9 (1.4–23.7)	3.8 (1.3–23.7)	6.4 (2.6–26.8)	0.097
NT-proBNP (at admission) (ng/L)	757.0 (105.0–4142.0)	666.5 (104.0–4285.0)	1373.5 (904.0–3096.0)	0.074
Cystatin C (at admission) (mg/L)	121; 0.99 (0.80–1.47)	1.00 (0.79–1.49)	0.92 (0.85–1.09)	0.417
GDF-15 (at admission) (ng/L)	807.1 (372.8–1827.7)	796.3 (372.8–1827.7)	1044.9 (357.3–1848.8)	0.305

GDF-15 = growth/differentiation factor 15; hsTnT = high-sensitivity troponin T; NT-proBNP = N-terminal prohormone of brain natriuretic peptide; STEMI = acute myocardial infarction with ST-segment elevation.

Comparisons of the number of patients with low and high concentrations of particular miRNAs were made in both subgroups; in the nonsurvivor group, the relative frequency of high concentrations was higher, and in the case of miR-133a and miR-499, this difference reached statistical significance (Table 2, microRNAs). All 6 nonsurvivors had a high concentration of miR-499, whereas, in the survivor subgroup, only 46% of patients had a high concentration.

3.4. Relationship between Standard Biomarkers and One-Year Mortality. For the standard markers hsTnT and NT-proBNP, cut-off values were found in the same way as for miRNAs, and values were then described as either "low" or "high." The cut-off value for hsTnT was 154.5 ng/L, and for NT-proBNP, it was 891.5 ng/L.

The number of patients with low and high concentrations of these two biomarkers was compared in both subgroups, and in the nonsurvivor group, the frequency of high marker levels was higher; in the case of NT-proBNP, this difference was statistically significant (Table 3, standard biomarkers). All patients who died within one year had a high concentration of NT-proBNP, whereas in the survivor group, only 43% had a high concentration of NT-proBNP.

3.5. Combinations of Biomarkers. Using the estimated cut-off values, two or three biomarkers were combined, in an effort to better describe the nonsurvivor subgroup and identify patients at risk of death. Combinations included (A) combinations of different microRNAs, (B) combinations of standard markers, and (C) combinations of microRNAs and standard markers. All tested combinations are shown in Table 3.

Based on a combination of NT-proBNP and miR-499 levels, a test group of 39 "at-risk" patients was created, which was 32% of the entire (survivor+nonsurvivor) cohort. The NT-proBNP and miR-499 combination criteria put all six nonsurvivors in the "at-risk" group, where they represented 15% of the "at-risk" group.

4. Discussion

In patients with a proven increased risk of death based on cardiovascular risk stratification during hospitalization, treatment with ACE inhibitors (or angiotensin AT1 blockers), beta-blocker therapy, and aldosterone antagonists are indicated when EF LK is ≤40% and/or there is heart failure [1]. Implantation of cardioverter-defibrillator (ICD) in a

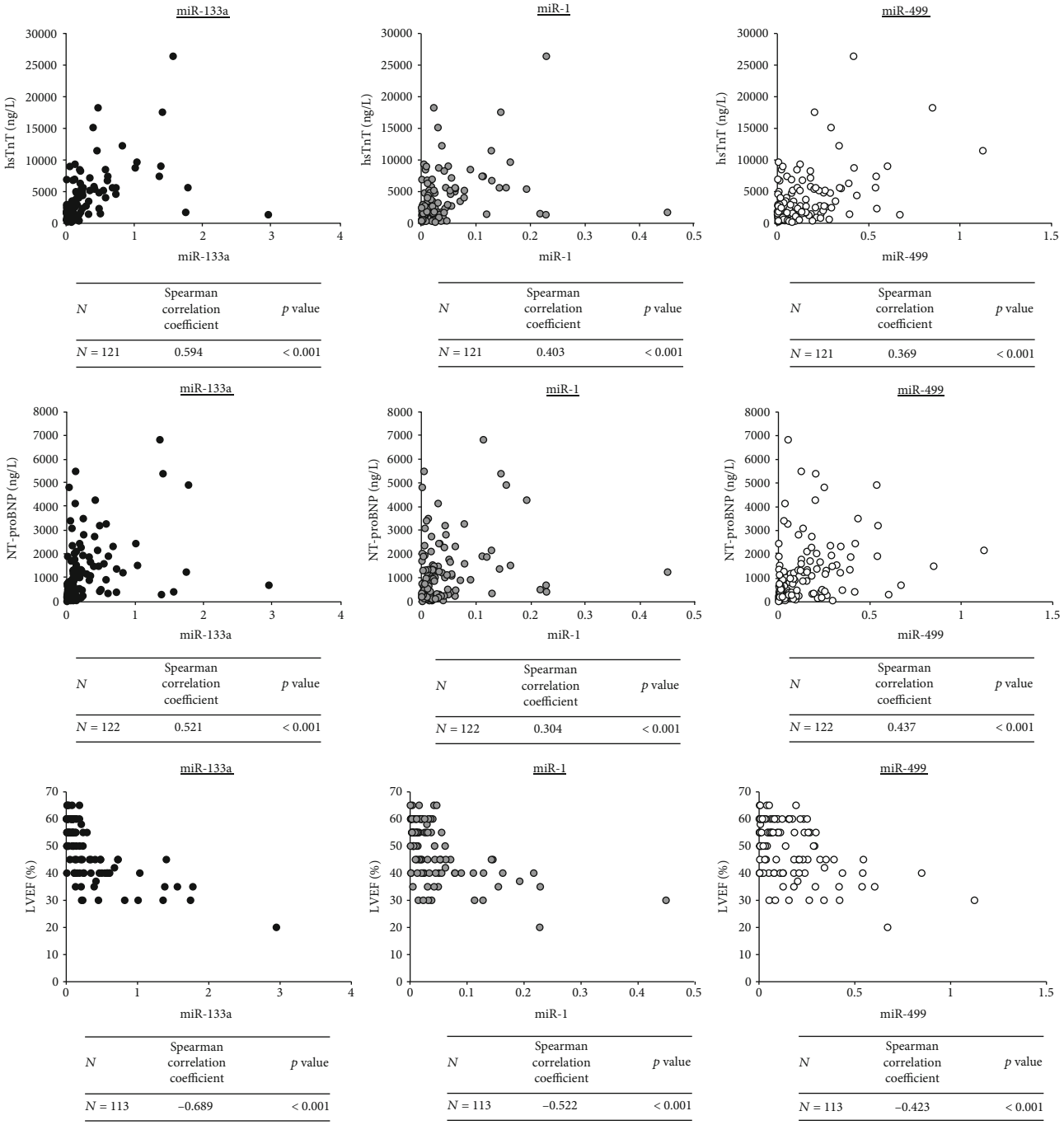

Figure 1: Correlations between particular miRNAs (relative expression) and hsTnT levels 24 hours after admission, NT-proBNP, and LVEF. hsTnT = high-sensitivity troponin T; LVEF = left ventricular ejection fraction; NT-proBNP = N-terminal prohormone of brain natriuretic peptide.

selected patient population is indicated when the indication criteria are met [1].

Despite the risk stratification of patients after myocardial infarction, ischemic complications recur even at low calculated risk, and these events can be fatal. miRNAs, as a group of the potential new markers, could help in the stratification of these patients. Then, if an increased miRNA value and usual risk parameters including LVEF are found without significant pathology, supplementation of the Holter ECG to exclude ventricular arrhythmias and careful follow-up of these patients should be considered.

For this reason, we used a well-defined and very homogeneous cohort of AMI patients after pPCI and tested the prognostic value of three cardiomyo-specific miRNAs (miR-1, miR-133, and miR-499) in one-year cardiovascular mortality and their relation to standard laboratory markers. We proved correlations between levels of miR-1, miR-133, and miR-499 with hsTnT, NT-proBNP, and LVEF in this cohort of

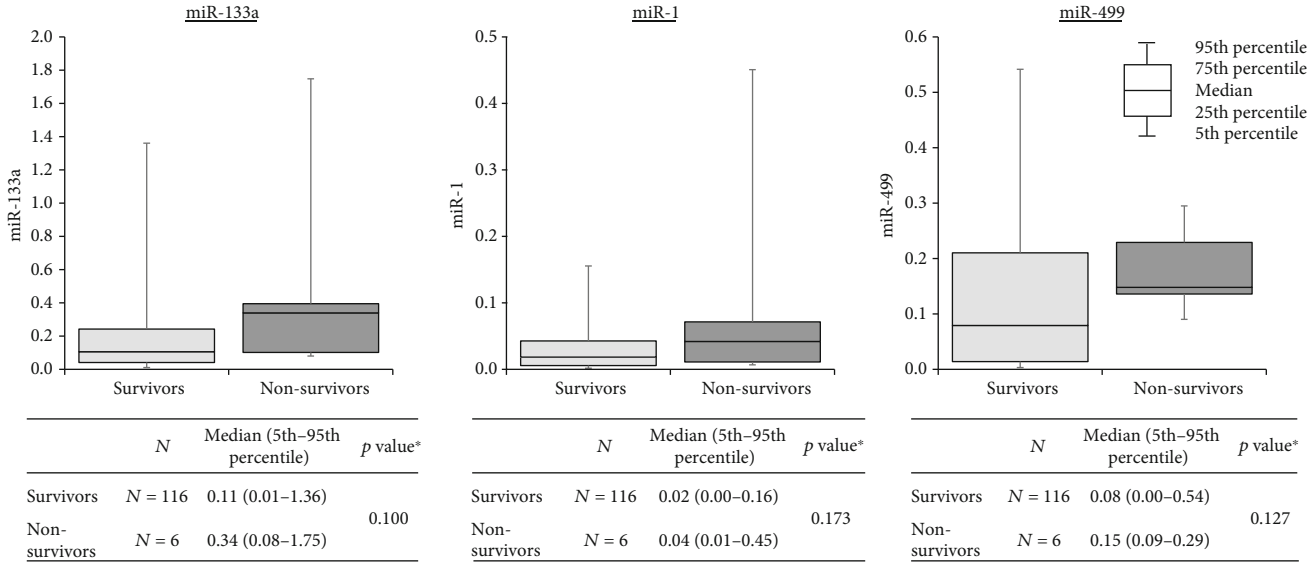

	N	Median (5th–95th percentile)	p value*
Survivors	$N = 116$	0.11 (0.01–1.36)	0.100
Non-survivors	$N = 6$	0.34 (0.08–1.75)	

	N	Median (5th–95th percentile)	p value*
Survivors	$N = 116$	0.02 (0.00–0.16)	0.173
Non-survivors	$N = 6$	0.04 (0.01–0.45)	

	N	Median (5th–95th percentile)	p value*
Survivors	$N = 116$	0.08 (0.00–0.54)	0.127
Non-survivors	$N = 6$	0.15 (0.09–0.29)	

Figure 2: Relationship between miRNAs (relative expression) and one-year mortality. *Mann-Whitney test.

Table 2: Relationship between individual marker levels and one-year mortality.

Marker	Gene Locus (OMIM)	Concentration	Patients, number (%)	Survivors, number (%)	Nonsurvivors, number (%)	p value*
MicroRNAs (relative concentration)						
miR-133a	MIR133A1/MIR133A2	<0.330	93 (76.2)	91 (78.4)	2 (33.3)	**0.028**
	18q11.2/20q13.33	≥0.330	29 (23.8)	25 (21.6)	4 (66.7)	
miR-1	MIR1-1/MIR1-2	<0.031	78 (63.9)	76 (65.5)	2 (33.3)	0.187
	20q13.33/18q11.2	≥0.031	44 (36.1)	40 (34.5)	4 (66.7)	
miR-499	MIR499	<0.088	63 (51.6)	63 (54.3)	0 (0.0)	**0.011**
	20q11.22	≥0.088	59 (48.4)	53 (45.7)	6 (100.0)	
Standard biomarkers (concentration in ng/L)						
hsTnT	TNN2	<154.5	77 (63.6)	75 (65.2)	2 (33.3)	0.189
	1q32.1	≥154.5	44 (36.4)	40 (34.8)	4 (66.7)	
NT-proBNP	NPPB	<891.5	66 (54.1)	66 (56.9)	0 (0.0)	**0.008**
	1p36.22	≥891.5	56 (45.9)	50 (43.1)	6 (100.0)	

*Fisher exact test. NT-proBNP = N-terminal prohormone of brain natriuretic peptide; hsTnT = high-sensitivity troponin.

patients. In addition, we found a possible relationship between combined levels of miR-499 with NT-proBNP and increased one-year mortality risk in these patients on dual antiplatelet therapy that has not been published yet.

4.1. MyomiR Levels after Myocardial Infarction. Many authors focus on miRNA levels during cardiovascular events and their possible contribution to the diagnostics or differential diagnostics [14, 18]. Published papers found that levels of miR-1 and miR-133a/b increase soon after AMI, reaching a peak shortly before TnI and returning to baseline within five days, while miR-499 peaks later, about 12 hours after the onset of the first symptoms [14]. miR-499 levels are naturally very low in healthy people and increase after AMI, with levels being higher in acute myocardial infarction with ST-segment elevation (STEMI) compared to non-STEMI patients [18], and provide a comparable diagnostic value to that of hsTnT [18]. Concentrations of miR-499 are higher in patients after AMI compared to patients with unstable angina [19]. miR-499 remains increased 24 hours after MI and then slowly decreases to original levels over 7 days [19]. Increased levels of circulating miR-499 and miR-208 after AMI reflect the cardiac damage caused by the AMI [19]. miR-208 levels are usually under the limits of detection in healthy individuals but rapidly increase after AMI. The peak is observed 3 hours after reperfusion, which is then followed by a rapid fall in concentration back to initial levels within 24 hours [20]. Since our samples were taken 24 hours after admission to

Table 3: Relationship between various combinations of marker levels and one-year mortality.

Markers and their levels	Patients, number (%)	Survivors, number (%)	Nonsurvivors, number (%)	p value*
MicroRNAs				
miR-133a+miR-1				
Both low	75 (61.5)	73 (62.9)	2 (33.3)	
One low and one high	21 (17.2)	21 (18.1)	0 (0.0)	**0.045**
Both high	26 (21.3)	22 (19.0)	4 (66.7)	
miR-133a+miR-499				
Both low	57 (46.7)	57 (49.1)	0 (0.0)	
One low and one high	42 (34.4)	40 (34.5)	2 (33.3)	**0.004**
Both high	23 (18.9)	19 (16.4)	4 (66.7)	
miR-1+miR-499				
Both low	47 (38.5)	47 (40.5)	0 (0.0)	
One low and one high	47 (38.5)	45 (38.8)	2 (33.3)	**0.019**
Both high	28 (23.0)	24 (20.7)	4 (66.7)	
miR-133a+miR-1+miR-499				
All low	47 (38.5)	47 (40.5)	0 (0.0)	
Minimum one low, minimum one high	55 (45.1)	53 (45.7)	2 (33.3)	**0.003**
All high	20 (16.4)	16 (13.8)	4 (66.7)	
Standard biomarkers				
hsTnT+NT-proBNP				
Both low	42 (34.7)	42 (36.5)	0 (0.0)	
One low and one high	58 (47.9)	56 (48.7)	2 (33.3)	**0.006**
Both high	21 (17.4)	17 (14.8)	4 (66.7)	
MicroRNAs and standard biomarkers				
hsTnT+miR-133a				
Both low	63 (52.1)	62 (53.9)	1 (16.7)	
One low and one high	43 (35.5)	41 (35.7)	2 (33.3)	**0.024**
Both high	15 (12.4)	12 (10.4)	3 (50.0)	
hsTnT+miR-1				
Both low	53 (43.8)	52 (45.2)	1 (16.7)	
One low and one high	48 (39.7)	46 (40.0)	2 (33.3)	0.094
Both high	20 (16.5)	17 (14.8)	3 (50.0)	
hsTnT+miR-499				
Both low	39 (32.2)	39 (33.9)	0 (0.0)	
One low and one high	61 (50.4)	59 (51.3)	2 (33.3)	**0.005**
Both high	21 (17.4)	17 (14.8)	4 (66.7)	
NT-proBNP+miR-133a				
Both low	59 (48.4)	59 (50.9)	0 (0.0)	
One low and one high	41 (33.6)	39 (33.6)	2 (33.3)	**0.003**
Both high	22 (18.0)	18 (15.5)	4 (66.7)	
NT-proBNP+miR-1				
Both low	51 (41.8)	51 (44.0)	0 (0.0)	
One low and one high	42 (34.4)	40 (34.5)	2 (33.3)	**0.014**
Both high	29 (23.8)	25 (21.6)	4 (66.7)	
NT-proBNP+miR-499				
Both low	46 (37.7)	46 (39.7)	0 (0.0)	
One low and one high	37 (30.3)	37 (31.9)	0 (0.0)	**0.001**
Both high	39 (32.0)	33 (28.4)	6 (100.0)	

*Fisher exact test: difference between both subgroups. hsTnT = high-sensitivity troponin T; NT-proBNP = N-terminal prohormone of brain natriuretic peptide.

the hospital, the concentration of miR-208 was either under the detection limit or too low to be quantified, so this miRNA was not included in our analysis, and only levels of miR-1, miR-133a, and miR-499 were measured.

4.2. Correlations of miRNAs with Standard Markers. We focused on the correlation with selected standard biomarkers and found a significant positive correlation of the three microRNAs with hsTnT and NT-proBNP. Our findings agree with other published papers, where levels of miR-499 were found to be positively correlated with levels of troponin T and I [14, 19, 21], despite minor differences in methods, the cohort of MI patients, and time of sampling. A positive correlation ($r = 0.596$, $p < 0.001$) between miR-133a and cTnI was previously published [19, 22] and reported a similar trend in levels of both markers in the early phase of AMI [22]; another work described an early miR-1, miRNA-133a, and miR-133b peak that occurred at a similar time as the TnI peak, whereas miR-499-5p exhibited a slower time course [14]. A correlation was also found between miR-499 and creatinine kinase (CK) [18, 19].

All the three analyzed miRNAs were found to have a moderate or strong positive correlation with NT-proBNP, which was published to be an important independent predictor of poor outcomes [23]. Furthermore, we found a strong negative correlation between all the three miRNAs and LVEF, which is in line with several other authors who found a similar negative correlation of miR-499 with LVEF ($r = -0.36$, $p = 0.008$) [16] or a weak negative correlation of miR-499-5p with LVEF (−0.11, $p = 0.037$) and miR-1 with LVEF ($r = -0.16$, $p = 0.003$) [21].

4.3. miRNAs in One-Year Prognosis. Finally, we looked for differences in the levels of laboratory markers between patients at an increased risk of death (nonsurvivors) and survivors. We found that all nonsurvivors had high levels of NT-proBNP and high levels of miR-499. Levels of NT-proBNP were measured in all AMI patients shortly after admission to the hospital before pPCI; in addition, the levels of microRNAs were also measured as potential new biomarkers. The choice of microRNAs was based on promising assessments for diagnostics or prognostics in recently published literature [14, 21, 22, 24].

Current risk stratification is based primarily on left ventricular dysfunction, measured as left ventricular ejection fraction [1, 2]. Many studies have found a clear relationship between reduced LVEF and mortality, which increases when LVEF falls under 50% and progressively increases when LVEF declines under 40% [2]. Despite this important predictor, about 50% of patients who die suddenly do not meet the abovementioned LVEF criteria [2]. Also, in our cohort, only 2 patients out of 6 in the nonsurvivor subgroup had an LVEF ≤ 35% during hospitalization and none at the time of follow-up. Our goal was to find a combination of laboratory markers that could contribute to the better identification of patients at increased risk of death after myocardial infarction and thus decrease the relatively high post-AMI mortality that reaches 7–20% at one year, 24–38% at five years, and 40–56% at ten years [2].

In our work, we analyzed cardio-enriched microRNAs, measurable 24 hours after patient admission to the hospital, to see if some of them could potentially fit into such a panel of biomarkers. Our results found that miR-499 in combination with NT-proBNP was best able to characterize the nonsurvivor subgroup. The number of papers dealing with myomiRs and AMI patients' prognosis is relatively limited. A recently published work confirms increased levels of cardio-enriched miRNAs (miR-499 and miR-208) in the blood of AMI patients and establishes an association of increased miRNA levels with reduced systolic function after AMI and risk of death or heart failure within 30 days [21]. Another work found that circulating levels of miR-133a and miR-208b were associated with all-cause mortality at 6 months, but this did not add prognostic information to hsTnT, the standard marker of AMI [25]. miR-133 was also studied in the high-risk STEMI patient cohort, where its levels provided prognostic information but do not add independent prognostic information to traditional markers of AMI [26].

In spite of the undeniable advantages of a well-defined and very homogeneous cohort of patients, this analysis was limited by the low number of patients in the nonsurvivor subgroup and by its retrospective character.

5. Conclusion

One-year mortality in patients after AMI treated with pPCI was very low (4.9%). A positive correlation was found between miRNA-1, miR-133a, and miR-499 and hsTnT (24 hours after admission) and NT-proBNP, and a negative correlation with LVEF. Further, this work suggests that plasma levels of circulating miR-499 might contribute to the identification of patients at increased risk of death, especially when combined with NT-proBNP levels. Further analyses are needed to determine if miR-499 or some other miRNAs can be effectively used in practice to better identify at-risk patients, to better understand the roles of these miRNAs in AMI, and to thus improve the clinical management of patients after AMI.

Data Availability

The data (miRNA Ct values and values of hsTnT and NT-proBNP) used to support the findings of this study are available from the corresponding author upon request.

Conflicts of Interest

No potential conflict of interest was reported by the authors.

Acknowledgments

This study was supported by the Ministry of Health of the Czech Republic Conceptual Development of Research Organization (Faculty Hospital in Pilsen (FNPl), 00669806), by the project of Faculty of Medicine in Pilsen (grant no. SVV 2019 260393), and by the Charles University Research Program Q38.

References

[1] B. Ibanez, S. James, S. Agewall et al., "2017 ESC Guidelines for the management of acute myocardial infarction in patients presenting with ST-segment elevation," *European Heart Journal*, vol. 39, no. 2, pp. 119–177, 2017.

[2] J. W. Waks and A. E. Buxton, "Risk stratification for sudden cardiac death after myocardial infarction," *Annual Review of Medicine*, vol. 69, no. 1, pp. 147–164, 2018.

[3] G. Ndrepepa, S. Kufner, M. Hoyos et al., "High sensitivity cardiac troponin T and prognosis in patients with ST-segment elevation myocardial infarction," *Journal of Cardiology*, vol. 72, no. 3, pp. 220–226, 2018.

[4] S. Gupta, G. S. Pressman, and V. M. Figueredo, "Incidence of, predictors for, and mortality associated with malignant ventricular arrhythmias in non-ST elevation myocardial infarction patients," *Coronary Artery Disease*, vol. 21, no. 8, pp. 460–465, 2010.

[5] J. M. Tapanainen, K. S. Lindgren, T. H. Mäkikallio, O. Vuolteenaho, J. Leppäluoto, and H. V. Huikuri, "Natriuretic peptides as predictors of non-sudden and sudden cardiac death after acute myocardial infarction in the beta-blocking era," *Journal of the American College of Cardiology*, vol. 43, no. 5, pp. 757–763, 2004.

[6] M. Grabowski, K. J. Filipiak, L. A. Malek et al., "Admission B-type natriuretic peptide assessment improves early risk stratification by Killip classes and TIMI risk score in patients with acute ST elevation myocardial infarction treated with primary angioplasty," *International Journal of Cardiology*, vol. 115, no. 3, pp. 386–390, 2007.

[7] H. V. Huikuri, J. M. Tapanainen, K. Lindgren et al., "Prediction of sudden cardiac death after myocardial infarction in the beta-blocking era," *Journal of the American College of Cardiology*, vol. 42, no. 4, pp. 652–658, 2003.

[8] L. Savic, I. Mrdovic, J. Perunicic et al., "Impact of the combined left ventricular systolic and renal dysfunction on one-year outcomes after primary percutaneous coronary intervention," *Journal of Interventional Cardiology*, vol. 25, no. 2, pp. 132–139, 2012.

[9] T. Sun, Y. H. Dong, W. Du et al., "The role of microRNAs in myocardial infarction: from molecular mechanism to clinical application," *International Journal of Molecular Sciences*, vol. 18, no. 4, p. 745, 2017.

[10] S. M. J. Welten, E. A. C. Goossens, P. H. A. Quax, and A. Y. Nossent, "The multifactorial nature of microRNAs in vascular remodelling," *Cardiovascular Research*, vol. 110, no. 1, pp. 6–22, 2016.

[11] C. Schulte, M. Karakas, and T. Zeller, "MicroRNAs in cardiovascular disease - clinical application," *Clinical Chemistry and Laboratory Medicine*, vol. 55, no. 5, pp. 687–704, 2017.

[12] E. Cavarretta and G. Frati, "MicroRNAs in coronary heart disease: ready to enter the clinical arena?," *BioMed Research International*, vol. 2016, Article ID 2150763, 10 pages, 2016.

[13] J. J. McCarthy, "The myomiR network in skeletal muscle plasticity," *Exercise and Sport Sciences Reviews*, vol. 39, no. 3, pp. 150–154, 2011.

[14] Y. D'Alessandra, P. Devanna, F. Limana et al., "Circulating microRNAs are new and sensitive biomarkers of myocardial infarction," *European Heart Journal*, vol. 31, no. 22, pp. 2765–2773, 2010.

[15] M. F. Corsten, R. Dennert, S. Jochems et al., "Circulating microRNA-208b and microRNA-499 reflect myocardial damage in cardiovascular disease," *Circulation. Cardiovascular Genetics*, vol. 3, no. 6, pp. 499–506, 2010.

[16] Z. Motovska, O. Hlinomaz, P. Kala et al., "1-year outcomes of patients undergoing primary angioplasty for myocardial infarction treated with prasugrel versus ticagrelor," *Journal of the American College of Cardiology*, vol. 71, no. 4, pp. 371–381, 2018.

[17] Z. Motovska, O. Hlinomaz, R. Miklik et al., "Prasugrel versus ticagrelor in patients with acute myocardial infarction treated with primary percutaneous coronary intervention: multicenter randomized PRAGUE-18 study," *Circulation*, vol. 134, no. 21, pp. 1603–1612, 2016.

[18] Y. Devaux, M. Vausort, E. Goretti et al., "Use of circulating microRNAs to diagnose acute myocardial infarction," *Clinical Chemistry*, vol. 58, no. 3, pp. 559–567, 2012.

[19] X. Chen, L. Zhang, T. Su et al., "Kinetics of plasma microRNA-499 expression in acute myocardial infarction," *Journal of Thoracic Disease*, vol. 7, no. 5, pp. 890–896, 2015.

[20] S. Białek, D. Górko, A. Zajkowska et al., "Release kinetics of circulating miRNA-208a in the early phase of myocardial infarction," *Kardiologia Polska*, vol. 73, no. 8, pp. 613–619, 2015.

[21] O. Gidlöf, J. G. Smith, K. Miyazu et al., "Circulating cardio-enriched microRNAs are associated with long-term prognosis following myocardial infarction," *BMC Cardiovascular Disorders*, vol. 13, no. 1, p. 12, 2013.

[22] F. Wang, G. Long, Z. C et al., "Plasma microRNA-133a is a new marker for both acute myocardial infarction and underlying coronary artery stenosis," *Journal of Translational Medicine*, vol. 11, no. 1, p. 222, 2013.

[23] J. A. Ezekowitz, P. Théroux, W. Chang et al., "N-terminal pro-brain natriuretic peptide and the timing, extent and mortality in ST elevation myocardial infarction," *The Canadian Journal of Cardiology*, vol. 22, no. 5, pp. 393–397, 2006.

[24] L. Zhang, X. Chen, T. Su et al., "Circulating miR-499 are novel and sensitive biomarker of acute myocardial infarction," *Journal of Thoracic Disease*, vol. 7, no. 3, pp. 303–308, 2015.

[25] C. Widera, S. K. Gupta, J. M. Lorenzen et al., "Diagnostic and prognostic impact of six circulating microRNAs in acute coronary syndrome," *Journal of Molecular and Cellular Cardiology*, vol. 51, no. 5, pp. 872–875, 2011.

[26] I. Eitel, V. Adams, P. Dieterich et al., "Relation of circulating microRNA-133a concentrations with myocardial damage and clinical prognosis in ST-elevation myocardial infarction," *American Heart Journal*, vol. 164, no. 5, pp. 706–714, 2012.

D. Jindrová a kol.

Outcome of patients ≥ 60 years of age after alcohol septal ablation for hypertrophic obstructive cardiomyopathy *(id 124)*

Archives of Medical Science
Impact Factor: 2,38

Outcome of patients ≥ 60 years of age after alcohol septal ablation for hypertrophic obstructive cardiomyopathy

Denisa Jahnlová[1], Pavol Tomašov[1], Radka Adlová[1], Jaroslav Januška[2], Jan Krejčí[3], Maciej Dabrowski[4], Josef Veselka[1]

[1]Department of Cardiology, Charles University in Prague, 2nd Faculty of Medicine and Motol University Hospital, Prague, Czech Republic
[2]Department of Cardiology, Heart Centre, Hospital Podlesí a. s., Třinec, Czech Republic
[3]St. Anne's University Hospital, Brno, Czech Republic
[4]National Institute of Cardiology, Warsaw, Poland

Submitted: 25 January 2017
Accepted: 29 May 2017

Arch Med Sci 2019; 15 (3): 650–655
DOI: https://doi.org/10.5114/aoms.2019.84735

Corresponding author:
Denisa Jahnlová MD
Department of Cardiology
University Hospital Motol
V Úvalu 84
150 06 Praha 5
Czech Republic
Phone: +42 0224434901
Fax: +42 0224434920
E-mail: denisajahn@gmail.com

Abstract

Introduction: The outcome of patients ≥ 60 years of age after alcohol septal ablation (ASA) for obstructive hypertrophic cardiomyopathy (HCM) remains unresolved. We sought to determine the long-term survival and the causes of death in this population.
Material and methods: We enrolled 156 consecutive patients (69 ±6 years, 69% women, follow-up: 4.8 ±3.5 years) who underwent ASA at ≥ 60 years of age.
Results: The 30-day mortality rate was 1.3%. At the last check-up, 81% of patients were in New York Heart Association class ≤ 2 and 76% had a left ventricular outflow tract gradient (LVOG) ≤ 30 mm Hg. A total of 39 patients died (51% of cardiovascular causes, 44% of non-cardiovascular causes, 5% of unknown causes) during the 734 patient-years. The annual sudden mortality, the sudden mortality and the all-cause mortality rates were 0.5%, 1.1%, and 4.8%, respectively. The all-cause mortality was higher compared to the age- and sex-matched general population (p = 0.002).
Conclusions: Alcohol septal ablation was safe and effective in the long-term follow-up. We observed a reduced life expectancy compared to the age- and sex-matched general population. Mortality was almost equally due to cardiovascular and non-cardiovascular causes of death.

Key words: hypertrophic cardiomyopathy, sudden cardiac death, survival.

Introduction

Hypertrophic cardiomyopathy (HCM) is a genetic disease defined by the presence of increased left ventricular wall thickness (LVWT) in the absence of abnormal loading conditions sufficient to cause the observed abnormality [1–4]. Patients with HCM are at risk of sudden death (SD), progressive heart failure, and other cardiovascular complications [5]. Recently published data based on an unselected population of HCM patients ≥ 60 years of age suggested that older patients are at low risk of SD and the mortality rate of these patients is mainly influenced by other causes of death [6, 7]. Left ventricular outflow tract (LVOT) obstruction is

an established independent risk factor for progression of heart failure and of cardiac death in HCM patients [8]. In the treatment of symptomatic patients with obstructive HCM who are refractory to medical therapy, alcohol septal ablation (ASA) or surgical myectomy is recommended [1, 2].

Despite early concerns about the potential arrhythmogenicity of the ablation scar, recent studies have shown acceptable periprocedural and long-term results of patients treated with ASA [9–14], comparable to those treated with surgical myectomy [15–18].

Alcohol septal ablation seems to be a preferable therapeutic approach, in patients ≥ 60 years of age with obstructive HCM, because of higher surgical risk [1, 2, 19]. However, the long-term outcome of this specific group of patients remains unresolved. Therefore, in this study, we sought to determine the long-term survival, major causes of death, and the sudden mortality rate in patients ≥ 60 years of age with obstructive HCM after ASA.

Material and methods

Study population

A total of 332 patients with obstructive HCM (58 ±13 years, 55% women) underwent ASA between April 1998 and March 2014 in four European cardiovascular centers and were enrolled into their databases. Within this group, we identified 156 patients aged ≥ 60 years of age at the time of ASA (69 ±6 years, 69% women) who met the inclusion criteria of this study. Some of these patients were included in previous reports.

The diagnosis of obstructive HCM was based on the echocardiographic demonstration of a hypertrophied non-dilated left ventricle (maximum LVWT ≥ 15 mm) and the presence of a maximal left ventricular outflow tract gradient (LVOG) of ≥ 50 mm Hg at rest or during the provocative maneuvers. The baseline LVWT measurement was defined as maximal septal thickness in the basal septum while the post-procedural LVWT was determined by measuring the thinnest part of the intervened basal septum. Alcohol septal ablation was performed only in patients with obstructive HCM that remained highly symptomatic despite maximal tolerated dosage of the optimal medical therapy.

All therapeutic options were discussed with each patient and the decision was made after careful explanation of the risks and benefits of each alternative. Written informed consent was provided by each patient and the local ethics committee approved the study protocol.

Interventional procedure and follow-up

Details of the ASA technique were published previously [20, 21]. Patients were observed in the coronary care unit for ≥ 2 days after the procedure and the temporary pacemaker was removed 2–3 days after ASA if no episode of atrioventricular block occurred. In patients with persistent or recurrent complete heart block, a permanent pacemaker was implanted prior to discharge from the hospital. All patients underwent a clinical, electrocardiographic, and echocardiographic check-up at 3–6 months after ASA and once a year thereafter. In patients with an implanted pacemaker or implantable cardioverter-defibrillator (ICD), the device memory and function were assessed, and the history of appropriate and inappropriate discharges was recorded.

The survival of patients was continuously checked in the National Database of the Departed in each of the participant countries. For the deceased patients who died outside of the study institutions, interviews or mail communication with their next of kin was performed to find out the cause of death.

Definitions

The primary endpoint was all-cause mortality and the secondary endpoint was a composite of all-cause mortality or appropriate ICD discharge. We compared the incidence of all-cause mortality, as well as the all-cause mortality including the first appropriate ICD discharge, with the expected survival of the age- and sex-matched general population.

The causes of death were classified as non-cardiovascular causes of death and cardiovascular causes of death (including heart failure, stroke, procedure-related death, SD, and appropriate ICD discharge). Sudden death was defined as an unexpected natural death within 1 h after a witnessed collapse in a previously stable patient. An appropriate ICD discharge was defined as the first device intervention after ASA triggered by ventricular tachycardia (VT) or ventricular fibrillation (VF). Death within 30 days after ASA at least partially attributable to ASA was considered ASA-related. Any death that could not clearly be attributed to one of these groups was classified as a death of unknown cause.

Statistical analysis

Data are presented as mean ± standard deviation. The χ^2 test, Student's *t*-test, and Kaplan-Meier survival analysis were used as appropriate. Mortality rates were calculated for each individual and combined to form an expected summary curve for the general population. Expected survival was calculated according to age- and gender-specific mortality rates obtained from the Demographic Yearbook of the Czech Republic (http://www.czso.cz/

csu/ 2012edicniplan.nsf/engpubl). Expected and observed mortality rates were compared using the one-sample log-rank test, which provides a standardized mortality ratio and the 95% confidence interval (CI). Cox proportional hazards regression was used to identify the predictors of all-cause mortality, cardiovascular mortality, and SD events. Clinical variables with a potential effect on patient prognosis were chosen for univariable analysis and included age, baseline and residual dyspnea, baseline and residual LVOG, baseline and residual maximum LVWT, and baseline and residual left ventricular end-diastolic diameter (LVEDD). Variables with a $p < 0.15$ were then entered into a multivariable analysis, which was performed using a backward stepwise multiple Cox regression. A $p < 0.05$ was considered statistically significant. The statistical software GraphPad Prism v. 6.05 (GraphPad Software, La Jolla, CA) was used.

Results

Baseline characteristics

A total of 156 patients underwent ASA between 60 and 86 years of age (69 ±6 years); among them, 108 (69%) patients were women. Baseline echocardiographic and clinical characteristics of the study population are summarized in Table I. Of these patients, 141 (90%) suffered from dyspnea of New York Heart Association (NYHA) functional class ≥ 3, while a combination of dyspnea and angina was present in 106 (75%) patients, and 33 (23%) patients experienced repeated syncope. Five patients had been implanted with a permanent pacemaker and 5 patients with an ICD prior to ASA. One patient had experienced an appropriate ICD discharge before ASA.

Mean alcohol injection volumes for the ASA procedure were 1.7 ±0.8 ml with a subsequent CK-MB peak of 3.1 ±2.3 µkat/l (ULN = 0.4 µkat/l). Alcohol septal ablation was combined with percutaneous coronary intervention in 9 (5.8%) patients.

Procedural outcomes

Four (2.6%) patients died during the first 1-month follow-up. Two of them died early after ASA; 1 patient died of cardiac tamponade and 1 patient died of pulmonary embolism. The other 2 patients died of cancer and stroke during the 1-month follow-up after being discharged from the hospital (in-hospital mortality was 1.3%; 30-day ASA-related mortality was 1.3%).

Post-procedural transient complete heart block was identified in 38 (24.4%) patients and a permanent pacemaker for a persistent or recurrent complete heart block was implanted in 18 of these patients (11.5% of total study population). Post-procedural sustained VT or VF requiring urgent cardioversion/defibrillation was observed in 5 (3.2%) patients.

Long-term outcomes

None of the 156 patients were lost to follow-up. The mean duration of follow-up was 4.8 ±3.5 years. Clinical and echocardiographic outcomes are summarized in Table I. At the last clinical check-up, a total of 126 (81%) patients suffered from dyspnea of NYHA class ≤ 2 and a total of 119 (76%) patients had a maximal LVOG ≤ 30 mm Hg at rest or during the provocative maneuvers. During the follow-up, 2 (1.3%) patients underwent myectomy and 6 (3.9%) patients underwent repeated ASA. Eight patients after ASA combined with percutaneous coronary intervention are still alive and 1 patient died of cancer 4 years after the procedure. Eight patients (5.2%, mean follow-up: 4.9 ±2.5 years) underwent an ICD implantation during the follow-up. The decision was based on current guidelines [1, 2]. Two of them experienced an appropriate ICD discharge during the study period. Additionally, another two patients with an ICD implanted before ASA also experienced an appropriate ICD discharge during the follow-up.

Table I. Clinical and echocardiographic characteristics at baseline and follow-up

Parameter	Baseline	Follow-up	*P*-value
Dyspnea, NYHA class	3 ±0.5	1.8 ±0.7	< 0.001
Angina, CCS class	1.4 ±1.2	0.4 ±0.7	< 0.001
Episodes of syncope (%)	21	6	0.002
LVOG [mm Hg]	76 ±44	22 ±22	< 0.001
LVEDD [mm]	43 ±5.5	47 ±5.7	< 0.001
Left ventricular EF (%)	71 ±10	68 ±10	0.025
Baseline maximum LVWT [mm]	20 ±3.6	15 ±4.6	< 0.001

Data are presented as mean ± standard deviation. NYHA – New York Heart Association, CCS – Canadian Cardiovascular Society, LVOG – left ventricular outflow tract gradient, LVEDD – left ventricular end-diastolic diameter, EF – ejection fraction, LVWT – left ventricular wall thickness.

Overall, a total of 4 (2.6%) patients experienced an appropriate ICD discharge during the follow-up. Mean time between ASA and the ICD discharge was 4 ±1.7 years.

Thirty-six (23%) patients died during the 747 patient-years (81% women) and the all-cause mortality rate was 4.8% per year. In these patients, ASA was performed at an average age of 69.7 ±5.8 years, the mean survival was 4.2 ±3.8 years, and the mean age at death was 74 ±6.2 years. Causes of death are summarized in Figure 1. Four (2.6%) other patients experienced an appropriate ICD discharge and 1 (0.6%) patient experienced an appropriate ICD discharge and died later during the follow-up. Considering the first appropriate ICD discharge as an equivalent of SD, 39 (25%) patients died during the 734 patient-years with an all-cause mortality rate of 5.2% per year. The mean survival was 4.1 ±3.6 years and the mean age at death was 74 ±6.1 years. All patients who died were divided into subgroups according to the cause of death. Mortality events from cardiovascular, non-cardiovascular, and unknown causes of death were 51%, 44%, and 5%, respectively.

Cardiovascular mortality events occurred in 20 patients (51% of all mortality events, 13% of all patients, mean age at death: 72.5 ±4.5 years), with an annual mortality rate of 2.7%. Among these 20 patients, 4 patients died of SD, 4 patients experienced an appropriate ICD discharge, 7 patients died of stroke, 3 patients died of heart failure, and 2 patients died of post-procedural complications. The distribution of the causes of death is summarized in Figure 2. Independent predictors of the cardiovascular mortality events were a lower LVEDD at the last check-up (HR = 0.90, 95% CI: 0.82–0.99; $p = 0.027$) and a higher baseline maximum LVWT (HR = 1.3, 95% CI: 1.14–1.49; $p < 0.001$).

Sudden death events (SD, appropriate ICD discharge) occurred in eight patients (5.1%, mean age at death: 74.9 ±3.4 years). The annual sudden mortality rate and the annual sudden mortality rate including the first appropriate ICD discharge were 0.5% and 1.1%, respectively. The only independent predictor of sudden mortality events was a higher baseline maximum LVWT (HR = 1.37, 95% CI: 1.12–1.69; $p < 0.001$).

Non-cardiovascular mortality events occurred in 17 patients (44% of all mortality events, 11% of all patients, mean age at death: 76 ±7 years) with an annual mortality rate of 2.3%. Among these patients, 10 patients died of cancer, 3 patients died of sepsis, 1 patient died of ileus, 1 patient died of pneumonia, one patient died of multiple organ failure, and 1 patient died of renal failure. In 2 patients (5% of all mortality events), the cause of death was unknown.

Survival free of all-cause mortality at 1, 5, and 10 years was 95% (95% CI: 91–98%), 80% (95% CI: 72–86%), and 59% (95% CI: 42–73%), respectively. Compared with the expected mortality in the sex- and age-matched general population, patients ≥ 60 years of age after ASA showed an increased mortality ($p = 0.016$; Figure 3). According to the multivariable analysis, independent predictors of all-cause mortality events were a lower LVEDD at the last check-up (HR = 0.93, 95% CI: 0.87–0.99; $p = 0.017$) and a higher baseline maximum LVWT (HR = 1.16, 95% CI: 1.05–1.29; $p < 0.001$). Survival free of all-cause mortality combined with the first appropriate ICD discharge at 1, 5, and 10 years was 95% (95% CI: 91–98%), 77% (95% CI: 68–84%), and 55% (95% CI: 39–68%), respectively. This observed mortality was higher in comparison with the expected survival of the age- and sex-matched general population ($p < 0.002$; Figure 4).

Discussion

This is the first international study to report the long-term survival and the causes of death in

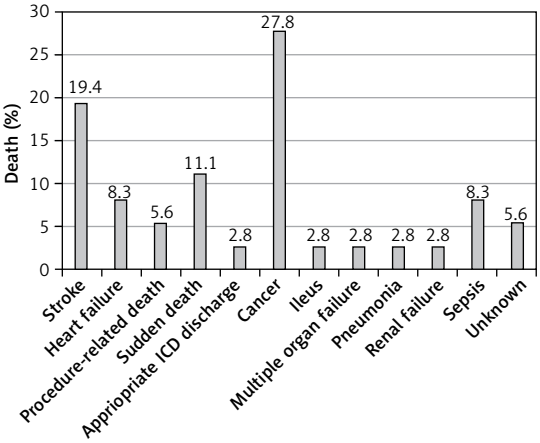

Figure 1. Causes of death

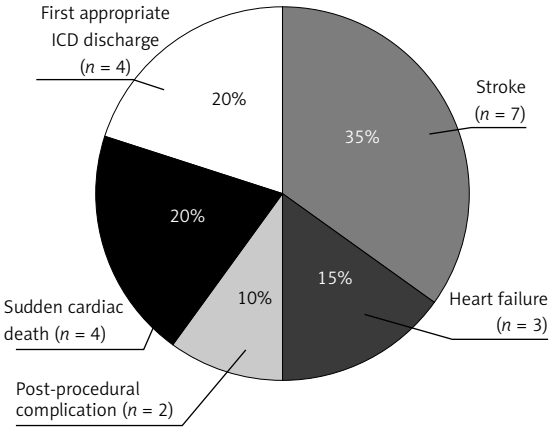

Figure 2. Cardiovascular causes of death

the specific population of patients ≥ 60 years of age with obstructive HCM who underwent ASA. The principal findings of the study are as follows: first, ASA was a safe procedure with low procedure-related mortality and led to an improvement in symptoms and a decrease in LVOG in patients ≥ 60 years of age with obstructive HCM. Second, this study population showed a reduced life expectancy compared with the expected mortality of the age- and sex-matched general population. Third, mortality was almost equally due to cardiovascular and non-cardiovascular causes of death. Fourth, independent predictors of all-cause mortality were a lower LVEDD at the last clinical check-up and a higher baseline maximum LVWT.

In previously published registry data, cardiovascular mortality in HCM patients was predominantly determined by SD, stroke, and heart failure [6, 7, 22–24], and in older patients (≥ 75 years), stroke was the most frequent cardiovascular cause of death [6]. The distribution of cardiovascular causes of death in this study population was similar. The observed annual sudden mortality rate was 1.1%, which is similarly low to the recently published data on ASA patients > 55 years of age described by Liebregts *et al.* [25] and to other previously published studies regarding HCM [15–18, 25, 26]. In addition, the mean time between ASA and the first appropriate ICD discharge was 4 ±1.7 years, which suggests a low arrhythmogenic potential of the resultant myocardial scar. The incidence of death due to heart failure was relatively low, which might suggest a protective effect of ASA. On the other hand, the incidence of stroke-related deaths was similarly high as in the previous reports [6, 7], which reminds us about the importance of the early initiation of anticoagulation therapy when appropriate [1, 2].

Figure 3. Kaplan-Meier survival curve describing all-cause mortality in patients with HCM ≥ 60 years of age after ASA compared with age- and sex-matched general population

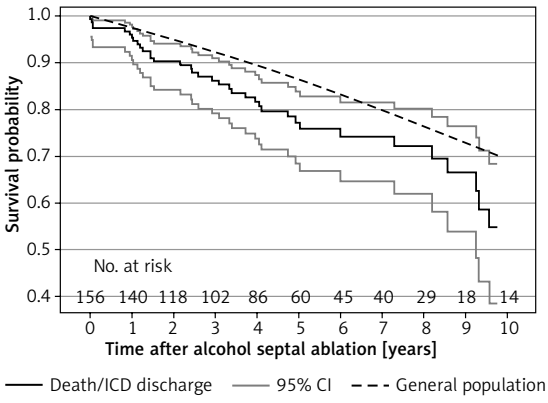

Figure 4. Kaplan-Meier survival curve describing the all-cause mortality and the first appropriate ICD discharge in patients with HCM ≥ 60 years of age after ASA compared with age- and sex-matched general population

Baseline maximum LVWT is one of the established risk factors of SD in patients with HCM [1, 2, 27]. In the present study population, we confirmed the previously described observation that maximum LVWT is an independent predictor of SD mortality and all-cause mortality events [24, 28, 29]. This finding supports the importance of this risk factor in the assessment of the risk of SD. Lower LVEDD at the last check-up was found to be another independent predictor of cardiovascular and all-cause mortality.

The main limitation of this study is its retrospective and observational design.

Also, although this multicenter study was conducted in two neighboring countries, most of the data were obtained in centers within one country, which is why the mortality rate was compared with the mortality data of the age- and sex-matched general population in this more represented country. Even though the mean follow-up in the study population was 4.8 years, the number of patients followed up for more than 5 years was rather small. This may have influenced the reliability of the results. In the present study, we used a common definition of SD as an unexpected natural death within 1 h after witnessed collapse in a previously stable patient. In elderly patients, this definition may potentially yield false-positive results, since the patients may also die suddenly of causes of death not directly related to HCM, such as acute coronary syndrome, stroke, or abdominal aortic aneurysm rupture. Another limitation of our study may be the fact that not all ICD discharges in this setting would have resulted in deaths, which may have led to potential overestimation of risk.

In conclusion, in patients ≥ 60 years of age with obstructive HCM, ASA was a safe and effective procedure in the long-term follow-up. This study population showed a reduced life expectancy compared to the age- and sex-matched general population. Mortality was almost equally due to cardiovascular and non-cardiovascular causes of death.

Acknowledgments

This research was funded by MH CZ - DRO, University Hospital Motol, Prague, Czech Republic 00064203 and SVV-2013-266509 from the Charles University in Prague.

Conflict of interest

The authors declare no conflict of interest.

References

1. Gersh BJ, Maron BJ, Bonow RO, et al. 2011 ACCF/AHA guidelines for the diagnosis and treatment of hypertrophic cardiomyopathy. Circulation 2011; 124: e783-831.
2. Elliott PM, Anastasakis A, Borger MA, et al. 2014 ESC guidelines on diagnosis and management of hypertrophic cardiomyopathy. Eur Heart J 2014; 35: 2733-79.
3. Perrot A, Tomasov P, Villard E, et al. Mutations in NEBL encoding the cardiac Z-disk protein nebulette are associated with various cardiomyopathies. Arch Med Sci 2016; 12: 263-78.
4. Ziółkowska L, Petryka J, Boruc A, Kawalec W. Comparison of echocardiography with tissue Doppler imaging and magnetic resonance imaging with delayed enhancement in the assessment of children with hypertrophic cardiomyopathy. Arch Med Sci 2017; 13: 328-36.
5. Veselka J, Anavekar NS, Charron P. Hypertrophic obstructive cardiomyopathy. Lancet 2017; 389: 1253-67.
6. Maron BJ, Casey SA, Hauser RG, Aeppli DM. Clinical course of hypertrophic cardiomyopathy with survival to advanced age. J Am Coll Cardiol 2003; 42: 882-8.
7. Maron BJ, Rowin EJ, Casey SA, et al. Risk stratification and outcome of patients with hypertrophic cardiomyopathy ≥ 60 years of age. Circulation 2013; 127: 585-93.
8. Maron MS, Olivotto I, Betocchi S, et al. Effect of left ventricular outflow tract obstruction on clinical outcome in hypertrophic cardiomyopathy. N Engl J Med 2003; 348: 295-303.
9. Seggewiss H, Rigopoulos A, Welge D, Ziemssen P, Faber L. Long-term follow-up after percutaneous septal ablation in hypertrophic obstructive cardiomyopathy. Clin Res Cardiol 2007; 96: 856-863.
10. Veselka J, Krejčí J, Tomašov P, Zemánek D. Long-term survival after alcohol septal ablation for hypertrophic obstructive cardiomyopathy: a comparison with general population. Eur Heart J 2014; 35: 2040-5.
11. Kuhn H, Lawrenz T, Lieder F, et al. Survival after transcoronary ablation of septal hypertrophy in hypertrophic obstructive cardiomyopathy (TASH): a 10 year experience. Clin Res Cardiol 2008; 97: 234-43.
12. Jensen MK, Prinz C, Horstkotte D, et al. Alcohol septal ablation in patients with hypertrophic obstructive cardiomyopathy: low incidence of sudden cardiac death and reduced risk profile. Heart 2013; 99: 1012-7.
13. Leonardi RA, Townsend JC, Patel CA, et al. Alcohol septal ablation for obstructive hypertrophic cardiomyopathy: outcomes in young, middle-aged, and elderly patients. Catheter Cardiovasc Interv 2013; 82: 838-45.
14. Nagueh SF, Groves BM, Schwartz L, et al. Alcohol septal ablation for the treatment of hypertrophic obstructive cardiomyopathy. A multicenter North American registry. J Am Coll Cardiol 2011; 58: 2322-8.
15. Sorajja P, Ommen SR, Holmes DR Jr, et al. Survival after alcohol septal ablation for obstructive hypertrophic cardiomyopathy. Circulation 2012; 126: 2374-80.
16. Liebregts M, Vriesendorp PA, Mahmoodi BK, Schinkel AF, Michels M, ten Berg JM. A systematic review and meta-analysis of long-term outcomes after septal reduction therapy in patients with hypertrophic cardiomyopathy. JACC Heart Fail 2015; 3: 896-905.
17. Cooper RM, Shahzad A, Stables RH. Intervention in HCM: patient selection, procedural approach and emerging techniques in alcohol septal ablation. Echo Res Pract 2015; 2: R25-35.
18. Leonardi RA, Kransdorf EP, Simel DL, Wang A. Meta-analyses of septal reduction therapies for obstructive hypertrophic cardiomyopathy: comparative rates of overall mortality and sudden cardiac death after treatment. Circ Cardiovasc Interv 2010; 3: 97-104.
19. Kim LK, Swaminathan RV, Looser P, et al. Hospital volume outcomes after septal myectomy and alcohol septal ablation for treatment of obstructive hypertrophic cardiomyopathy: US Nationwide Inpatient Database, 2003-2011. JAMA Cardiol 2016; 1: 324-32.
20. Cuisset T, Lefèvre T. Contemporary techniques for catheter-based intervention for hypertrophic obstructive cardiomyopathy. EuroIntervention 12 Suppl 2016; X: X44-X47.
21. Veselka J, Zemánek D, Fiedler J, Šváb P. Real-time myocardial contrast echocardiography for echo-guided alcohol septal ablation. Arch Med Sci 2009; 5: 271-2.
22. Veselka J, Krejčí J, Tomašov P, et al. Survival of patients ≤ 50 years of age after alcohol septal ablation for hypertrophic obstructive cardiomyopathy. Can J Cardiol 2014; 30: 634-8.
23. Veselka J, Zemánek D, Jahnlová D, et al. Risk and causes of death in patients after alcohol septal ablation for hypertrophic obstructive cardiomyopathy. Can J Cardiol 2015; 31: 1245-51.
24. Maron BJ, Olivotto I, Spirito P, et al. Epidemiology of hypertrophic cardiomyopathy-related death: revisited in a large non-referral-based patient population. Circulation 2000; 102: 858-64.
25. Liebregts M, Steggerda RC, Vriesendorp PA, et al. Long-term outcome of alcohol septal ablation for obstructive hypertrophic cardiomyopathy in the young and the elderly. JACC Cardiovasc Interv 2016; 9: 463-9.
26. Steggerda RC, Damman K, Balt JC, Liebregts M, ten Berg JM, van den Berg MP. Periprocedural complications and long-term outcome after alcohol septal ablation versus surgical myectomy in hypertrophic obstructive cardiomyopathy: a single-center experience. JACC Cardiovasc Interv 2014; 7: 1227-34.
27. Elliott PM, Poloniecki J, Dickie S, et al. Sudden death in hypertrophic cardiomyopathy: identification of high risk patients. J Am Coll Cardiol 2000; 36: 2212-8.
28. Spirito P, Bellone P, Harris KM, Bernabo P, Bruzzi P, Maron BJ. Magnitude of left ventricular hypertrophy and risk of sudden death in hypertrophic cardiomyopathy. N Engl J Med 2000; 342: 1778-85.
29. Jensen MK, Jacobsson L, Almaas V, et al. Influence of septal thickness on the clinical outcome after alcohol septal ablation in hypertrophic cardiomyopathy. Circ Cardiovasc Interv 2016; 9: e003214.

J. Honěk a kol.

High-Grade Patent foramen Ovale Is a Risk Factor for Unprovoked Decompression Sickness in Recreational Divers
(id 189)

Journal of Cardiology
Impact Factor: 2,289

rejstřík

Journal of Cardiology xxx (2019) xxx–xxx

Contents lists available at ScienceDirect

Journal of Cardiology

journal homepage: www.elsevier.com/locate/jjcc

Original article

High-grade patent foramen ovale is a risk factor of unprovoked decompression sickness in recreational divers

Jakub Honěk (MD, PhD)[a,b,*], Martin Šrámek (MD)[b,c,d], Luděk Šefc (PhD)[b], Jaroslav Januška (MD)[e], Jiří Fiedler (MD)[a], Martin Horváth (MD)[a], Aleš Tomek (MD, PhD)[c], Štěpán Novotný (MD)[f], Tomáš Honěk (MD, PhD)[a], Josef Veselka (MD, PhD)[a]

[a] Department of Cardiology, Charles University in Prague, 2nd Faculty of Medicine and Motol University Hospital, Prague, Czech Republic
[b] Center for Advanced Preclinical Imaging, Charles University in Prague, First Faculty of Medicine, Prague, Czech Republic
[c] Department of Neurology, Charles University in Prague, 2nd Faculty of Medicine and Motol University Hospital, Prague, Czech Republic
[d] Comprehensive Stroke Center, Military University Hospital, Prague, Czech Republic
[e] Cardiocentrum, Hospital Podlesi, Trinec, Czech Republic
[f] Hyperbaric Chamber, Kladno Regional Hospital, Kladno, Czech Republic

ARTICLE INFO

Article history:
Received 3 February 2019
Received in revised form 20 March 2019
Accepted 28 April 2019
Available online xxx

Keywords:
Patent foramen ovale
Decompression sickness
Risk factors

ABSTRACT

Background: Patent foramen ovale (PFO), male sex, age, and body mass index (BMI) were all identified as potential risk factors of decompression sickness (DCS). It has been debated whether PFO might cause unprovoked DCS (i.e. without violation of decompression procedure) due to paradoxical embolization of venous gas emboli. To date, there are no data on the incidence or risk factors of unprovoked DCS. This study sought to evaluate the risk factors of unprovoked DCS in recreational divers.
Methods: A total of 489 consecutive divers were screened for PFO between January 2006 and January 2014 by means of transcranial Doppler. All patients were prospectively included in the study registry. Survival analysis techniques were used to assess for risk factors for unprovoked DCS. Age, sex, BMI, PFO presence, and grade were analyzed. The total sum of dives was used as a measure of time.
Results: The group performed a total of 169,411 dives (mean 346 ± 636). Thirty-six (7%) of the divers suffered from an unprovoked DCS. The frequency of PFO was 97.2% in divers with a history of unprovoked DCS and 35.5% in controls ($p < 0.001$). There was no difference in sex, age, BMI, or total number of dives between the respective groups. In the adjusted Cox proportional hazards model, PFO grade 3 was a major risk factor for unprovoked DCS; there was a slight protective effect of increasing age.
Conclusions: We demonstrated that a high-grade PFO was a major risk factor for unprovoked DCS in recreational scuba divers.

Introduction

Patent foramen ovale (PFO) has been associated with an increased risk of decompression sickness (DCS) in divers due to paradoxical embolization of nitrogen bubbles that form during the diver's ascent [1]. However, this hypothesis has been widely debated. The prevalence of PFO in the general population is high (27%) [2]. Therefore, it remains to be determined whether other factors, such as risky diving behavior, body mass index (BMI), age, or sex, play a more important role [3–6]. On the other hand, reports that nitrogen bubbles can be detected in venous blood, even after a single conservative dive, raised the concern that divers with a right-to-left shunt might suffer from DCS even without violating decompression regimen [7,8]. These unpredictable events have been termed unprovoked DCS and are a potential threat to millions of recreational divers worldwide. Yet, to date, there are no data on the incidence and risk factors for unprovoked DCS. The aim of our study was to assess the risk factors for unprovoked DCS in recreational divers.

* Corresponding author at: Department of Cardiology, University Hospital Motol, V Úvalu 84, 150 06, Praha 5, Czech Republic.
E-mail address: jakub.honek@gmail.com (J. Honěk).

https://doi.org/10.1016/j.jjcc.2019.04.014
0914-5087/

Methods

A total of 489 consecutive divers were screened for PFO at our center between January 2006 and January 2014 by means of transcranial color-coded sonography (TCCS). All patients were prospectively included in the study registry. The screening was offered to all registered Czech diving clubs and was regularly promoted through diving magazines, websites, instructor courses, and diving and hyperbaric medicine meetings. Baseline data (i.e. demographic data, diving experience, and DCS history) were collected from all divers at the time of the screening examination. Divers with a history of DCS filled in a detailed questionnaire in order to reveal any violation of the rules of safe recreational diving. The questions included the number and timing of all preceding dives, maximum depth, bottom time, and any violation of regimen advised by a diving computer or table, such as exceeding the maximum ascent rate or shortening the advised safety stop. The study was approved by the local ethics committee and all study subjects gave written informed consent to participate in the study.

Transcranial color-coded sonography was used for the detection of a right-to-left shunt, as described previously [9]. The shunt was graded according to the International Consensus Criteria: grade 1, 1–10 bubbles; grade 2, >10 bubbles but no curtain (uncountable number of bubbles); and grade 3, curtain [10]. The TCCS was performed by experienced neurologists (MS and AT), blinded to the diver's DCS history. The method used to define the presence of a PFO and its grade in this study was TCCS. In patients considered for catheter-based PFO closure (divers with a history of unprovoked DCS and right-to-left shunt detected on TCCS), a transesophageal echocardiography was performed to assess the anatomy of the interatrial septum and surrounding structures [11,12]. Transesophageal echocardiography was also offered to all other symptomatic divers (provoked and unprovoked DCS regardless of the result of the TCCS examination) and to divers with a high-grade shunt on TCCS and no previous history of DCS.

A history of unprovoked DCS was defined as any DCS symptom that originated less than 24 hours after a dive or series of dives that complied with all the rules advised to recreational divers. For the definition of recreational diving, we reviewed the rules advised by the largest international scuba (self-contained underwater breathing apparatus) diving agencies (Professional Association of Diving Instructors, Confédération Mondiale des Activités Subaquatiques, Scuba Schools International, National Association of Underwater Instructors) at the level of open water diver, and advanced open water diver or their equivalent [13–16]. For the DCS event to be considered unprovoked the divers had to comply with the adopted decompression algorithm [17]. Technical diving, such as diving with mixtures containing helium or decompression diving, was excluded. For an unprovoked DCS, the diver had to perform a non-decompression air dive, according to any commercially available recreational diving table or computer, to a maximum depth of 40 m, with a maximum ascent rate 10 m/min with a safety stop performed as advised by the computer or table. For consecutive dives, a minimum 2 h surface interval between dives and a maximum of 3 consecutive days of diving were required. Also, if the diver reported inadequate hydration or severe exhaustion (e.g. due to technical problems, problems with orientation or strong currents), the DCS was considered provoked.

To assess for risk factors for unprovoked DCS, the association between variables and DCS endpoints was evaluated using survival analysis techniques. We used Cox proportional hazards models to compute a hazard ratio (HR) with a 95% confidence interval (CI), both unadjusted and adjusted, for the potential confounding covariates. The total sum of dives value was used as a measure of time.

We analyzed age, sex, BMI, and PFO (each grade of PFO in a separate analysis compared to divers without PFO). Due to the possibility of numerically unstable estimates and large standard errors, we did not include all available covariates in the final Cox proportional hazards model. Therefore, a backward stepwise elimination algorithm with a likelihood ratio statistic to minimize the exclusion of predictors involved in suppressor effects was used. Variables with a p-value ≤ 0.1 on univariate testing were included in the elimination algorithm. The goodness of fit of the model was tested. Additionally, Kaplan–Meier survival curves were created, and log-rank statistics were calculated. All statistical analyses were carried out using IBM SPSS Statistics 25.0 (IBM, Armonk, NY, USA).

Results

A total of 489 divers were screened for the presence of a right-to-left shunt between January 2006 and January 2014 by means of TCCS. The mean age was 35.5 ± 9.0 years, and 87% were men. A PFO was found in 40% of the divers. Thirty-six (7%) of the divers suffered from an unprovoked DCS. The divers had performed a total of 169,411 dives (mean 346 ± 636) and experienced a total of 54 unprovoked DCS episodes (occurrence rate per dive 0.03%). The prevalence of PFO was 97% in divers with a history of unprovoked DCS and 36% in controls ($p < 0.001$); for PFO grade 3, the prevalence was 86% versus 18%, respectively ($p < 0.001$). There was no difference in sex, age, BMI, or the total number of dives between the respective groups. The results are summarized in Table 1.

PFO presence, age, and sex were included in the final adjusted model (unadjusted HR for unprovoked DCS by individual variables are summarized in Table 2). The adjusted HR for unprovoked DCS in divers with a PFO, compared to divers without a PFO, was 60.0 (95% CI 8.2–438.5, $p < 0.001$). Divers with PFO grade 3 had a higher risk of unprovoked DCS (HR_{adj} = 93.0, 95% CI 12.5–688.7, $p < 0.001$). The adjusted HR for unprovoked DCS in divers with a PFO grade 1, compared to divers without a PFO, was not significant but was numerically higher (HR_{adj} = 10.8, 95% CI 1.0–121.8, $p = 0.054$). Two

Table 1
Results.

Group	All divers (n = 489)	Controls (no unprovoked DCS) (n = 453)	Unprovoked DCS (n = 36)	p-Value
Dives – total, mean (+/-SD)	169,411, 346.4 (635.6)	156,693, 345.9 (647.7)	12,718, 353.3 (463.2)	0.17
Age (years) – mean (+/-SD)	35.6 (9.0)	35.5 (9.1)	36.4 (7.7)	0.22
Male sex, total (%)	423 (86.5%)	393 (86.8%)	30 (83.3%)	0.61
BMI (kg/m^2) – mean (+/-SD)	26.1 (3.2)	26.1 (3.1)	26.2 (3.6)	0.99
PFO	196 (40.1%)	161 (35.5%)	35 (97.2%)	<**0.001**[*]
PFO grade 1	65 (13.3%)	63 (13.9%)	2 (5.6%)	0.21
PFO grade 2	20 (4.1%)	18 (4.0%)	2 (5.6%)	0.65
PFO grade 3	111 (22.7%)	80 (17.7%)	31 (86.1%)	<**0.001**[*]

BMI, body mass index; DCS, decompression sickness; PFO, patent foramen ovale; +/-SD, standard deviation.
[*] Statistically significant difference.

Please cite this article in press as: Honěk J, et al. High-grade patent foramen ovale is a risk factor of unprovoked decompression sickness in recreational divers. J Cardiol (2019), https://doi.org/10.1016/j.jjcc.2019.04.014

Table 2
Hazard ratio for unprovoked decompression sickness by univariate and multivariate analysis.

Variable	Univariate analysis HR (95% CI, p)	Multivariate analysis HR (95% CI, p)
Age (years)	0.955 (0.916–0.995, $p = 0.030$)	0.941 (0.902–0.981, $p = 0.004$)
Sex (male)	0.383 (0.158–0.933, $p = 0.035$)	0.557 (0.223–1.396, $p = 0.212$)
BMI	0.930 (0.824–1.050, $p = 0.243$)	0.970 (0.851–1.105, $p = 0.645$)
PFO	52.371 (7.173–382.382, $p < 0.001$)	59.959 (8.199–438.483, $p < 0.001$)
PFO 1	10.817 (0.978–119.682, $p = 0.052$)	10.806 (0.959–121.772, $p = 0.054$)
PFO 2	28.114 (2.536–311.642, $p = 0.007$)	–
PFO 3	78.124 (10.662–572.418, $p < 0.001$)	92.943 (12.544–688.663, $p < 0.001$)

BMI, body mass index; CI, confidence interval; HR, hazard ratio; PFO, patent foramen ovale.
Final model included adjustments for age, sex, and PFO presence. PFO grades 1–3 were compared to controls, for PFO grade 2 the HR was numerically unstable and not statistically significant.

out of twenty divers with a PFO grade 2 had unprovoked DCS, the HR was numerically unstable and not statistically significant. The results of the multivariant analysis are summarized in Table 2. Also according to the results of the log-rank test of the Kaplan–Meier analysis the risk of unprovoked DCS was significantly higher in divers with a PFO (Fig. 1) and with PFO grade 3 (Fig. 2).

Discussion

We screened a total of 489 divers, who performed a total of 169,411 dives, and found that unprovoked DCS occurred in 7% of the divers, the occurrence rate per dive was 0.03%. The prevalence of PFO and, importantly, PFO grade 3 was high in patients with a history of unprovoked DCS. There was no difference in sex, age, BMI, or the total number of dives between the respective groups. PFO grade 3 was found to be the major risk factor of unprovoked DCS, using the Cox proportional hazards model.

Decompression sickness is caused by nitrogen bubbles that form in supersaturated tissues during the diver's ascent. These bubbles cause either local tissue damage or embolize through venous blood [18]. The clinical manifestation is heterogeneous from severe neurological impairment to a localized skin rash [18]. Clearly, if a diver severely violates the decompression regimen and reaches the surface too early, the bubble load may be massive and cause a fatal pulmonary gas embolism. On the other hand, a small number of venous gas emboli (VGE) might be effectively filtered by pulmonary circulation and, thus, remain subclinical. It is of note, that even after a properly performed recreational dive a small number of VGE may be detected. Ljubkovic et al. found VGE after 80% of single no-decompression air dives [8]. It has been debated whether an unprovoked DCS might occur in some of these divers.

To our knowledge, this is the only study to date to assess for risk factors for unprovoked DCS in recreational divers. However, some previous studies have focused on the risk factors of DCS in general. Traditionally, age, BMI, and repetitive diving were considered risk factors for DCS. Carturan et al. monitored 50 divers after two dive profiles and found ascent rate, age, aerobic fitness, and adiposity to be associated with a higher post-dive VGE occurrence [4]. In a study performed by the Divers Alert Network (DAN), 67 recreational divers were monitored for two years for Doppler-detected VGE. The incidence of high-bubble grade was approximately 20% higher for repetitive dives than for first dives and approximately 20% higher for males than females, which also increased with age (25% in male and 55% in female divers) [7].

In a retrospective observational study, male divers were also at a higher risk of DCS, although this might have been influenced by

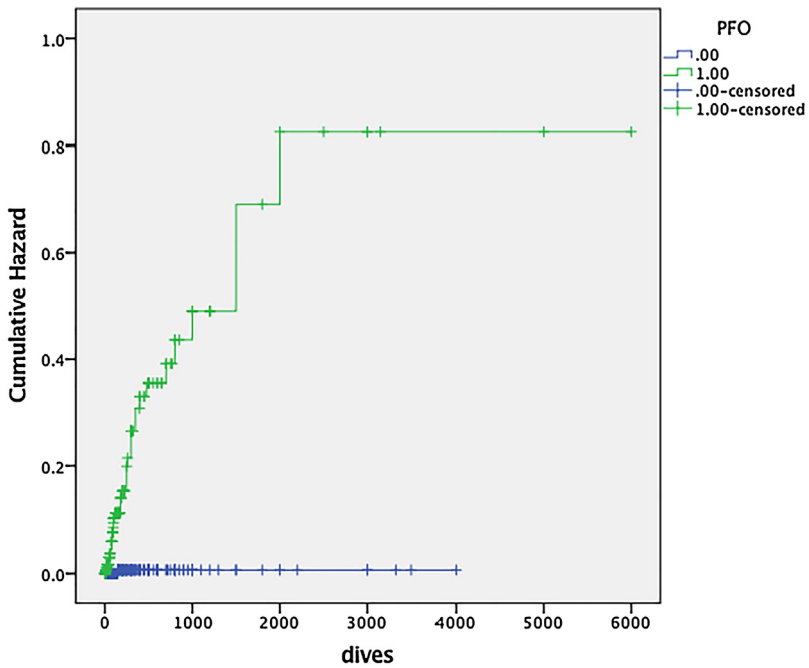

Fig. 1. Kaplan–Meier analysis: cumulative hazard of unprovoked decompression sickness in divers with and without a patent foramen ovale. Log-rank test for equality of survivor function was $\chi^2 = 49.068$, $p < 0.001$. PFO, patent foramen ovale.

Please cite this article in press as: Honěk J, et al. High-grade patent foramen ovale is a risk factor of unprovoked decompression sickness in recreational divers. J Cardiol (2019), https://doi.org/10.1016/j.jjcc.2019.04.014

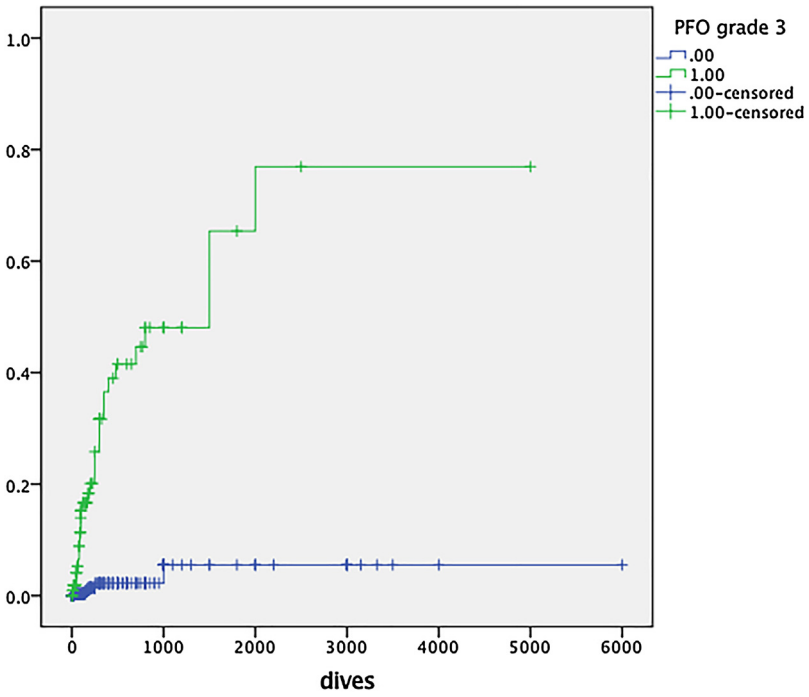

Fig. 2. Kaplan–Meier analysis: cumulative hazard of unprovoked decompression sickness in divers with and without a patent foramen ovale grade 3. Log-rank test for equality of survivor function was $\chi^2 = 76.835$, $p < 0.001$. PFO, patent foramen ovale.

their diving habits [19]. In contrast, Gempp et al. found results similar to ours in a small case-controlled study of divers with recurrent DCS [20]. They found a right-to-left shunt and lack of changes in the way of diving after a prior DCS as the only predictors of neurological DCS recurrence. Age, sex, and diving experience were not associated with recurrent neurological DCS. Together with the results of the present study, this suggests that the presence of a PFO might play a more important role in at least a subset of DCS, such as the neurological form or in unprovoked episodes.

Recreational divers are trained through several international diving organizations with a large emphasis on DCS prevention and diving safety in general. The use of dive computers (or tables) to prevent DCS is recommended for every dive. These devices use a multi-compartment model to calculate nitrogen desaturation in order to prevent bubble formation in all tissues. Furthermore, the divers are advised on other safety measures, such as proper pre-dive hydration or a maximum depth of 40 m [21]. Although recreational diving is generally considered a safe sport, none of the above-mentioned safety measures was ever validated in divers with a high-grade PFO [22]. Furthermore, it is known that, in spite of these preventive measures, small numbers of VGE still occur after a properly performed dive [7]. Theoretically, the paradoxical embolism of these bubbles could be responsible for unprovoked DCS.

The concept, that a small number of bubbles embolizing to the systemic circulation through a PFO could cause DCS, was mentioned already in the 1980s [23,24]. Several retrospective studies confirmed a higher incidence of PFO in symptomatic divers in the two following decades [20,25–28]. However, the role of PFO in the pathophysiology of DCS has been highly debated since then.

In a previous study, it was demonstrated that catheter-based PFO closure eliminated post-dive arterial gas emboli after simulated dives in a hyperbaric chamber [29]. In addition, after PFO closure, DCS was not observed in any of the divers. In another study, a conservative dive profile with a short exposure and a slower ascent rate decreased the occurrence of both venous and arterial gas emboli [30]. Both studies suggest that gas bubbles embolize through the PFO in divers and might be responsible for a higher risk of DCS.

The present study demonstrates that this mechanism might cause unprovoked episodes in recreational scuba divers with a high-grade PFO. In a multivariant analysis, PFO grade 3 was a major risk factor for unprovoked DCS. We also observed a slight protective effect of increasing age. We could speculate that this might be due to more experience or a more conservative approach to diving. However, provocation of DCS by risky behavior was excluded by the strict definition of unprovoked DCS in this study. In the unadjusted analyses of individual variables, an increased risk was also observed for PFO grade 2 and males. However, this was not observed when adjusted to other covariates in the final Cox proportional hazards model.

This retrospective study is subject to inherent limitations, including selection bias. The prevalence of PFO and the incidence of unprovoked DCS might not therefore be generalizable to the overall population of recreational divers. However, the occurrence rate of DCS was comparable to previous reports [31,32]. Although this study is, to our knowledge, the largest available, the number of endpoints is still low. Another limitation is the self-reporting of endpoints, which is due to the fact that the majority of cases were not examined by a specialist at the time of divers' DCS events.

Conclusion

The present study is the first, to our knowledge, to demonstrate that a high-grade PFO is independently associated with unprovoked DCS in recreational scuba divers. The results suggest that the general safety diving recommendations for recreational scuba divers might be less safe for divers with a high-grade PFO.

Funding

Supported by Ministry of Health of the Czech Republic, grant No. 15-34904A. All rights reserved.

Please cite this article in press as: Honěk J, et al. High-grade patent foramen ovale is a risk factor of unprovoked decompression sickness in recreational divers. J Cardiol (2019), https://doi.org/10.1016/j.jjcc.2019.04.014

Conflicts of interest

The authors declare there is no conflict of interest.

Acknowledgments

We would like to acknowledge Eva Hansvenclová for assistance with statistical analysis.

References

[1] Honěk J, Šefc L, Honěk T, Šrámek M, Horváth M, Veselka J. Patent foramen ovale in recreational and professional divers: an important and largely unrecognized problem. Can J Cardiol 2015;31:1061–6.
[2] Hagen PT, Scholz DG, Edwards WD. Incidence and size of patent foramen ovale during the first 10 decades of life: an autopsy study of 965 normal hearts. Mayo Clin Proc 1984;59:17–20.
[3] Bove AA. Risk of decompression sickness with patent foramen ovale. Undersea Hyperb Med 1998;25:175–8.
[4] Carturan D, Boussuges A, Vanuxem P, Bar-Hen A, Burnet H, Gardette B. Ascent rate, age, maximal oxygen uptake, adiposity, and circulating venous bubbles after diving. J Appl Physiol 2002;93:1349–56.
[5] Bove AA. The PFO gets blamed again . . . perhaps this time it is real. J Am Coll Cardiol Interv 2014;7:409–10.
[6] Denoble PJ, Holm JR, editors. Patent foramen ovale and fitness to dive consensus workshop proceedings. Durham: Divers Alert Network; 2015. Available at: https://www.diversalertnetwork.org/research/Conference/2015PFOFTDProceedings/2015-pfo-workshop-proceedings.pdf [accessed 06.12.18].
[7] Dunford RG, Vann RD, Gerth WA, Pieper CF, Huggins K, Wacholtz C, et al. The incidence of venous gas emboli in recreational diving. Undersea Hyperb Med 2002;29:247–59.
[8] Ljubkovic M, Dujic Z, Møllerløkken A, Bakovic D, Obad A, Breskovic T, et al. Venous and arterial bubbles at rest after no-decompression air dives. Med Sci Sports Exerc 2011;43:990–5.
[9] Blersch WK, Draganski BM, Holmer SR, Koch HJ, Schlachetzki F, Bogdahn U, et al. Transcranial duplex sonography in the detection of patent foramen ovale. Radiology 2002;225:693–9.
[10] Jauss M, Zanette E. Detection of right-to-left shunt with ultrasound contrast agent and transcranial Doppler sonography. Cerebrovasc Dis 2000;10:490–6.
[11] Tobe J, Bogiatzi C, Munoz C, Tamayo A, Spence JD. Transcranial Doppler is complementary to echocardiography for detection and risk stratification of patent foramen ovale. Can J Cardiol 2016;32:986.
[12] CaputiL, Carriero MR, Falcone C, Parati E, Piotti P, Materazzo C, et al. Transcranial Doppler and transesophageal echocardiography: comparison of both techniques and prospective clinical relevance of transcranial Doppler in patent foramen ovale detection. J Stroke Cerebrovasc Dis 2009;18:343–8.
[13] Richardson D, editor. PADI open water diver manual. London: Atlantic Books; 2010.
[14] Scuba Schools International. Open water diver manual. Ithaca: Concept Systems; 2002.
[15] Jahns J, Růžička A, Vrbovský V. Přístrojové potápění: Odborné texty pro potápěský výcvik v systému CMAS. Praha: Svaz potápěů České Republiky; 2013.
[16] National Association of Underwater Instructors. NAUI scuba diver. 5th edition, Riverview: National Association of Underwater Instructors; 2000.
[17] Cialoni D, Pieri M, Balestra C, Marroni A. Dive risk factors, gas bubble formation, and decompression illness in recreational SCUBA diving: analysis of DAN Europe DSL data base. Front Psychol 2017;8:1587.
[18] Vann RD, Butler FK, Mitchell SJ, Moon RE. Decompression illness. Lancet 2011;377:153–64.
[19] St Leger Dowse M, Bryson P, Gunby A, Fife W. Comparative data from 2250 male and female sports divers: diving patterns and decompression sickness. Aviat Space Environ Med 2002;73:743–9.
[20] Gempp E, Louge P, Blatteau JE, Hugon M. Risk factors for recurrent neurological decompression sickness in recreational divers: a case–control study. J Sports Med Phys Fitness 2012;52:530–6.
[21] Gempp E, Blatteau JE. Preconditioning methods and mechanisms for preventing the risk of decompression sickness in scuba divers: a review. Res Sports Med 2010;18:205–18.
[22] Vann RD, Freiberger JJ, Caruso JL. Divers Alert Network report on decompression illness, diving fatalities and project dive exploration: 2005 edition (based on 2003 data). DAN technical report; 2005, Available at: http://www.diversalertnetwork.org/medical/report/2005DCIReport.pdf [accessed 06.12.18].
[23] Wilmshurst PT, Ellis PT, Jenkins BS. Paradoxical gas embolism in a scuba diver with an atrial septal defect. Br Med J 1986;293:1277.
[24] Moon RE, Camporesi EM, Kisslo JA. Patent foramen ovale and decompression sickness in divers. Lancet 1989;1:513–4.
[25] Torti SR, Billinger M, Schwerzmann M, Vogel R, Zbinden R, Windecker S, et al. Risk of decompression illness among 230 divers in relation to the presence and size of patent foramen ovale. Eur Heart J 2004;25:1014–20.
[26] Wilmshurst PT, Pearson MJ, Walsh KP, Morrison WL, Bryson P. Relationship between right-to-left shunts and cutaneous decompression illness. Clin Sci 2001;100:539–42.
[27] Germonpré P, Dendale P, Unger P, Balestra C. Patent foramen ovale and decompression sickness in sports divers. J Appl Physiol 1998;84:1622–6.
[28] Cantais E, Louge P, Suppini A, Foster PP, Palmier B. Right-to-left shunt and risk of decompression illness with cochleovestibular and cerebral symptoms in divers: case control study in 101 consecutive dive accidents. Crit Care Med 2003;31:84–8.
[29] Honěk J, Šrámek M, Šefc L, Januška J, Fiedler J, Horváth M, et al. Effect of catheter-based patent foramen ovale closure on the occurrence of arterial bubbles in scuba divers. J Am Coll Cardiol Interv 2014;7:403–8.
[30] Honěk J, Šrámek M, Šefc L, Januška J, Fiedler J, Horváth M, et al. Effect of conservative dive profiles on the occurrence of venous and arterial bubbles in divers with a patent foramen ovale: a pilot study. Int J Cardiol 2014;176:1001–1002.
[31] Ladd G, Stepan V, Stevens L. The Abacus Project: establishing the risk of recreational scuba death and decompression illness. SPUMS J 2002;32:124–8.
[32] Pollock NW. Annual diving report: 2008 edition. Durham: Divers Alert Network; 2008, Available at: https://www.diversalertnetwork.org/medical/report/2008DANDivingReport.pdf [accessed 06.12.18].

Please cite this article in press as: Honěk J, et al. High-grade patent foramen ovale is a risk factor of unprovoked decompression sickness in recreational divers. J Cardiol (2019), https://doi.org/10.1016/j.jjcc.2019.04.014